A research contract report
SEPTEMBER 1988

A RAW-COAL CONCENTRATION SENSOR FOR HYDROTRANSPORT

Contract J0333933
Science Applications International Corporation

BUREAU OF MINES
UNITED STATES DEPARTMENT OF THE INTERIOR

50272 - 101

REPORT DOCUMENTATION PAGE	1. REPORT NO. Bumines OFR 02-90	2.	3. Recipient's Accession No.
4. Title and Subtitle A RAW COAL CONCENTRATION SENSOR FOR HYDROTRANSPORT			5. Report Date September 20, 1988 6.
7. Author(s) Victor V. Verbinski, Costa G. Cassapakis and David deLesdernier			8. Performing Organization Rept. No. SAIC-88/1638
9. Performing Organization Name and Address Science Applications International Corporation 10401 Roselle Street San Diego, California 92121			10. Project/Task/Work Unit No. 11. Contract(C) or Grant(G) No. (C) J0333933 (G)
12. Sponsoring Organization Name and Address U.S. Department of Interior, Bureau of Mines Cochrans Mill Road, PO Box 18070 Pittsburgh, Pennsylvania 15236			13. Type of Report & Period Covered Final Report 6/25/76 to 9/20/88 14.

15. Supplementary Notes

16. Abstract (Limit: 200 words)

This report presents the development of a raw coal concentration sensor for hydrotransport of coal and refuse (rock) from underground mines, and the results of an international test series carried out at the Colorado School of Mines Research Institute in Golden, Colorado, the U.S. Bureau of Mines, Hydraulic Transport Research Facility in Pittsburgh, Pennsylvania, Saskatchewan Research Facility in Saskatoon, Saskatchewan, Canada, and the Steinkohlenbergbauverein Test Facility in Essen, West Germany. Test results are presented for a three-component sensor and also for the more rugged two-component (all nuclear) sensor.

17. Document Analysis a. Descriptors

b. Identifiers/Open-Ended Terms

c. COSATI Field/Group 2

18. Availability Statement	19. Security Class (This Report) Unclassified	21. No. of Pages 265
	20. Security Class (This Page) Unclassified	22. Price

(See ANSI-Z39.18) See Instructions on Reverse OPTIONAL FORM 272 (4-77)
(Formerly NTIS-35)
Department of Commerce

This report was completed under a contract to the United States Department of Energy (D.O.E.). Responsibility for the program to which the report relates has recently been transferred to the Bureau of Mines, United States Department of the Interior, and the report is made public under a Bureau cover.

The views and conclusions contained in this document are those of the authors and should not be interpreted as necessarily representing the official policies or recommendations of the Interior Department's Bureau of Mines or of the U.S. Government.

FORWORD

This report was prepared by Science Applications International Corporation, Instrumentation and Experimental Physics Division, San Diego, California, under USBM Contract number J0333933. The contract was initiated under the Coal Hydrotransport Program. It was administered under the technical direction of Advanced Mining Technology with Richard C. Wang acting as Technical Project Officer. Larry E. Guess was contract administrator for the Bureau of Mines. This report is a summary of the work recently completed as a part of this contract during the period July 25, 1976 to September 20, 1988. This report was submitted by the authors on September 20, 1988.

SUMMARY

A coal slurry concentration sensor was developed by SAIC under contract with the U.S. Bureau of Mines for in-line measurement of coal, rock (refuse) and water content. This sensor was developed to facilitate hydraulic haulage of coal from deep underground mines. Four different sensors were fabricated for the Pittsburgh Research Center. Three were used for testing in an international test series. The 6-inch for tests at the Colorado School of Mines Research Institute (CSMRI) and at the Pittsburgh Research Center's Hydraulic Transport Research Facility (HTRF) when it became completed; the 18-inch for the HTRF test line; a 12-inch sensor for the Saskatchewan Research Council (SRC), Saskatoon, Saskatchewan, Canada, Slurry Transport Facility; and a 10-inch sensor for the Steinkohlenbergbauverein (STBV) test loop in Essen, West Germany. (The 6-inch sensor was used instead, at STBV, because their 10-inch line was disassembled at the time.)

Since the coal/rock/water slurry is a three-component slurry, three gauges are required, each measuring something different about coal, rock and water. Therefore, each of the four (6", 10", 12", and 18") coal-slurry concentration sensors was made with two radiation gauges (a neutron gauge and a gamma-ray gauge) and a conductivity gauge. These three gauges sense different properties of coal, rock and water. The gamma-ray gauge senses density, and is most sensitive to rock, then coal, and least sensitive to water. The neutron gauge is most sensitive to water (hydrogen), then coal (which is hydrogenous), and least sensitive to rock. Both of these are rugged, stable, clamp-on devices, totally non-intrusive. The conductivity gauge measures an electrical current through the slurry along an insulated piece of haulage pipe. The current is proportional to CV(w), where C is the (ever-changing) conductivity of the water and V(w) is the volume fraction of water along the insulated conductivity gauge spoolpiece.

The ever-changing conductivity, C, of the water (C is essentially zero for coal and rock, it was found) is measured by drawing off clear water, free of solids, via a sintered metal filter mounted in the wall of the haulage pipe (the computer uses C to correct the in-line conductivity gauge reading). This

filter worked well with Pittsburgh seam coal and rock, but not with rock at SRC (Canada) and StBV (West Germany), where the clay content was high enough to "poison" the filter, requiring overnight flushing to wash out enough of the clay from the sintered metal filter (where it had become lodged and had erroneously raised the conductivity of the water passing through). We, therefore, reprogrammed the computer to operate with only the two simple clamp-on radiation gauges in Canada and West Germany. However, with a three-component slurry (coal/rock/water), the two-sensor gauge requires added information, namely the density of the coal and of the rock. These are simple measurements that can easily be made on location. The two densities need to be entered into the computer only once for each mine site and geological condition.

As part of the international test series, measurements were carried out at CSMRI with pure Pittsburgh seam coal (density = 1.35 g/cc) and pure rock (density = 2.54 g/cc) obtained from an underground mine in Morgantown, West Virginia. Some of the coal and rock was crushed to fines (-28 mesh) and pumped at speeds of up to 12 ft/sec through both a horizontally oriented and vertically oriented coal slurry concentration sensor, in which case negligible slippage (where the water moves faster than the solids) occurred, and the in-situ concentration measured by the sensor agreed with diversion-tank sample measurements. The coal and rock cross sections were accurately measured by the neutron gauge, and also the gamma-ray gauge, so that the sensor was accurately calibrated (for Pittsburgh seam coal and rock) when we moved the 6-inch sensor to the HTRF in Pittsburgh. The CSMRI tests were reported in Hydrotransport 6 by SAIC and U.S. Bureau of Mines staff members.

The tests in Pittsburgh were conducted with the coal slurry concentration sensor installed in a vertical section of the HTRF lines, so that the hydraulic haulage phenomenon called slippage was at its worst. In addition, no fines (coal or rock) were made available because of HTRF technical and budgetary constraints. Therefore, we could not verify the measured in-situ concentrations. (But these were properly verified at CSMRI.) We could, however, get a measure of the slippage phenomenon in a vertical pipe by comparing line-loading concentrations (i.e., delivered concentrations) with in-situ concentrations measured by the coal slurry concentration sensor. The latter was the order of 50% higher, illustrating the need of an in-situ

concentration sensor for managing efficient haulage of even larger chunks of coal and for avoiding line blockage.

The coal slurry concentration sensor (12") was next tested at SRC in Canada, and was found to be lacking because of the presence of too high a concentration of clay in the coal and rock. We, therefore, reprogrammed the computer to provide a two-component coal slurry concentration sensor. We carefully sampled the coal and rock, obtained the density of each, and entered the densities into the two-component sensor that utilized only the neutron and gamma-ray gauges. The coal slurry concentration sensor worked well in this way, and was received with enthusiasm by the SRC research staff. They were happy to find that a simple, nonintrusive gauge could be clamped onto the haulage pipe and operate in a highly stable and reliable manner. The U.S. Bureau of Mines initially wanted us to develop a coal slurry concentration sensor that would operate accurately on Pittsburgh seam coal without requiring density measurements of coal and rock to be input into the computer. This, indeed, was achieved for Pittsburgh seam coal, where the sintered metal filter for the conductivity gauge could operate without "contamination" by a high concentration of very fine clays. For operation in some other parts of the world, the two-component sensor utilizing only the radiation gauges must be used. This was found to be true at StBV, for the West German coal and rock as well.

1.0 INTRODUCTION

This report presents the development and testing of the coal slurry concentration sensor by Science Applications International Corporation (SAIC) in cooperation with Pittsburgh Research Center (PRC), U.S. Bureau of Mines.

The Bureau of Mines is engaged in a wide variety of programs aimed at increasing productivity and safety within the coal mining industry. Of particular interest is the process of transporting mined material from underground mining faces to appropriate surface locations. One general method which holds promise for improving the efficiency and safety of this haulage process is hydraulic transport through a pressurized piping system. In order to successfully develop such a haulage pipeline system, it is necessary to concurrently develop sensors which are able to measure the concentration of coal/refuse/water in a haulage pipeline. Knowledge of the solids concentration in pipelines is important because of the relation to factors such as quantity of material delivered, pipeline plugging, power requirements, and selection of system equipment.

The contract requirements and preliminary design effort are presented in Section 2 of this report. In the initial contract definition, this was the Phase I effort.

The Phase II effort, presented in Section 3, involved engineering, design and testing of prototype gauge components. These tests were conducted at both the SAIC facilities and at the Colorado School of Mines Research Institute (CSMRI) 6-inch test loop. Tests at CSMRI were carried out with a three-component sensor; a gamma-ray gauge sensitive only to total density of the coal/rock/water (C/R/W) slurry; a neutron gauge selectively sensitive to the different hydrogen content of coal, rock and water; and an electrical conductivity gauge sensitive only to the water-volume fraction of the slurry.

In these preliminary (Phase II) tests at CSMRI, the gamma-ray and neutron gauges worked flawlessly, but the conductivity gauge required constant

correction due to the ever-changing conductivity of the slurry water as it dissolved salts from the coal and rock particles in this closed-loop facility. Initial efforts at drawing off a sample of slurry water at the location of the two radiation (gamma-ray and neutron) gauges failed because of blockage of the sampling line by solids. Some of the slurry was directed to a settling chamber where the slurry water was to be decanted from the top. An additional problem was that of the settling time in the settling tank. It required several hours to obtain a clear liquid because of the micron-sized particles in the slurry. Therefore, the data were corrected a posteriori for the conductivity of the water.

Some of the Phase III effort (fabricate and test a 6-inch sensor) was diverted to Phase II, in order to overcome the problem of obtaining clear slurry water for a conductivity reference cell.

Section 4 of this report presents the tests carried out on the CSMRI 6-inch test loop with an improved conductivity gauge. This gauge utilized a sintered-metal filter to obtain solids-free slurry water for a conductivity reference. Back-flushing was done periodically to clear the surface of the filter of the "filter-cake" buildup. This worked well enough to conduct a complete set of tests on coal/rock/water slurries of known concentration, utilizing Pittsburgh seam coal and rock hauled in from Morgantown, West Virginia. In addition, the nuclear gauges were calibrated on Pittsburgh seam coal in readiness for the tests at the HTRF in Pittsburgh, where the once-through (versus closed test loop) configuration made calibration impractical or totally unfeasible.

After the CSMRI tests, a sensor was designed and fabricated for the HTRF 18-inch pipe test line. This and the 6-inch slurry sensor were installed in the HTRF lines at the Pittsburgh Research Center, and tests were conducted in Pittsburgh in January, 1982, soon after the HTRF first became available for testing. These tests are presented in Section 5 of this report.

The tests at the HTRF, as well as those at CSMRI, were also part of a cooperative international data exchange program. Other tests were carried out

at the Saskatchewan Research Council (SRC) Slurry Transport Facility, Saskatoon, Saskatchewan, Canada (Section 6), and the Steinkohlenbergbauverein (StBV) test loop in Essen, West Germany (Section 7).

2.0 PHASE I WORK: CONCEPT DEFINITION AND DEVELOPMENT

The developmental work carried out in Phase I includes: (1) a survey of literature and manufacturer's product descriptions to identify and evaluate applicable technologies, (2) experimental and theoretical research on several of the more promising technologies, and, most importantly, (3) a description of the conceptual design of sensors to satisfy the design criteria specified in the contract. These criteria are those listed under RESEARCH SENSOR in ARTICLE II and all criteria listed under ARTICLES III, IV and V of the subject contract. For convenience of reference, these criteria are given here in Tables 2.1 and 2.2.

Much of the work within Phase I was conducted concurrently in three categories: a general methods survey, a detailed analysis of nuclear (penetrating radiation) methods, and an analysis of ultrasonic methods. The research was organized in this manner because, based on pre-contract examinations by SAIC scientists and engineers, nuclear and ultrasonic methods appeared to provide the greatest promise as methods on which to base a sensor concept. As it turned out, one other method based on measuring slurry electrical conductivity (which was conceived in the process of the survey of methods) was also examined in the laboratory and, in fact, was formulated into part of the recommended conceptual sensor design.

The latter portion of activity under Phase I has been devoted to formulating a conceptual design based on one or more methods or techniques that must be consolidated into a working coal/rock/water in-situ concentration sensor.

2.1 SURVEY

A survey of literature and sensor manufacturers was carried out. The objective was to determine currently available technologies and component instrumentation having applicability to designing the required concentration sensor. The sensor must accurately measure coal/refuse/water slurry concentrations flowing through pipes of various sizes in an underground pipe

TABLE 2.1 - Concentration sensor design specifications

Factor	Research Sensor	Commercial Sensor	Control Sensor
Accuracy			
Wt. concentration of coal	1.0%	2.0%	3.0%
Wt. Concentration of refuse	1.0%	2.0%	3.0%
Response time, sec.	0.5	1	2
Range			
Ambient temperature, ^{o}F	-20---+120	+20---+80	+20---+80
Water temperature, ^{o}F	+35---+80	+35---+80	+35---+80
Pipeline diameter, in.	6---18	6---24	6---24
Top size of coal, in.	2---6	2---6	2---6
Top size of refuse, in.	2---6	2---8	2---8
Pipeline pressure, psig	50---150	50---1,000	50---1,000
Flow velocity, ft/sec	4---20	4---20	4---20
Water condition, pH	3.5---8	3.5---8	3.5---8
Specific gravity of coal	1.2---1.6	1.2---1.6	1.2---1.6
Specific gravity of refuse	2.3---3.1	2.3---3.1	2.3---3.1
Wt. concentration of coal, %	0---80	5---70	10---60
Wt. concentration of refuse, %	0---80	5---50	10---50
Coal/refuse proportion	0/100---100/0	0/100---100/0	0/100---100/0
Water source	Fresh	Fresh---Brackish	Fresh---Brackish
Cost, desirable, $	7,000---10,000	6,000---9,000	3,000---5,000
Fluctuation (% of Factor)			
Pipeline pressure	20	10	10
Flow velocity	5	5	5
Specific gravity of coal	15	15	15
Specific gravity of refuse	15	15	15

TABLE 2.2 - Coal slurry sensor design criteria

ARTICLE III -- GENERAL CONCEPTS DESIGN CRITERIA

Sec. 3.1 The concentration sensors shall be designed to measure accurately the proportions of coal, mine rock refuse and water in coarse-slurry hydraulic transport pipelines in underground coal mines.

Sec. 3.2 The concentration sensors shall not obstruct the interior of the pipeline, cause flow interference, or cause plugging of the pipeline.

Sec. 3.3 The concentration sensors shall be adaptable to vertical, sloped, and horizontal pipelines and provide instantaneous and continuous measurement without loss of accuracy.

Sec. 3.4 The concentration sensors shall not cause degradation of solids particles, leakage of water from the pipeline or plugging of the line, and they must be able to operate in an underground coal mine environment.

Sec. 3.5 The output signal of the sensors shall be sufficiently simple to be utilized by ordinary readout devices such as millivolt meters and pen-type recorders and sufficiently strong to remain unaffected by small radio frequencies, static charges, moisture, etc.

ARTICLE IV - SERVICE AND ECONOMY REQUIREMENTS

Sec. 4.1 The sensors shall be designed to meet the same service specifications of all underground coal mining machines. All components shall be heavy-duty with minimum maintenance requirements.

Sec. 4.2 Delicate or precision-adjustment mechanisms shall not be easily accessible.

Sec. 4.3 Reliability (in the technical sense) shall be at least 90 percent in an underground coal mine environment.

Sec. 4.4 Provision shall be made for repairs or preventive maintenance in the underground environment. For example, calibration shall be easily accomplished, the use of large or heavy parts shall be minimized, and it shall be possible to change parts with minimum dismantling of the instrument.

Sec. 4.5 Lowest possible costs shall be a primary goal. This can be extended to operator and mechanic skill requirements. It would be useless for the Government to provide an instrument that nobody can afford to buy.

ARTICLE V -- SAFETY REQUIREMENTS

Sec. 5.1 The sensors shall meet the requirements of all applicable Federal legislation, especially permissibility.

Sec. 5.2 The sensors shall fail in a safe manner. That is, upon failure, they should not release a flood of water, electrically charge the pipeline, release radiation or sound waves, or create any new or additional hazard in coal mining.

haulage network. The survey included information on sensors that were commercially available, but required modification, in the developmental stage, or potentially feasible but untried.

Information from the literature survey was obtained from the following main sources:

1. Over 60 contracting firms, governmental and regulatory agencies and other firms involved in coal research projects.
2. Twenty-eight universities involved in coal research.
3. U.S. patent search.
4. SAIC and appropriate Federal and local libraries.
5. Technical journals and periodicals in the areas of mining, coal, pipeline and mining instruments.

For the sensor manufacturer survey, over one hundred and fifty manufacturers of pertinent instruments, including concentration sensors, slurry sensors, flow sensors, etc., were contacted.

2.1.1 Concentration Sensors Currently Available

No existing commercial, prototype, or experimental sensor was found to be capable of adequately measuring the concentration of coal/refuse/water in a slurry pipeline. A variety of sensors, however, is commercially available for measurement of the concentration of one material, but not for two different solids (i.e., coal and rock) in a water slurry.

2.1.2 Sensor Methods Surveyed

A wide variety of sensor methods potentially applicable for measurement of concentration of the coal/refuse/water were considered during the survey. A list of the methods, including reasons for selection or rejection of these methods as candidate sensors concepts, is given in Table 2.3.

TABLE 2.3 DETECTION METHODS SURVEYED FOR COAL/ROCK/WATER CONCENTRATION SENSOR

	Method	Operating Principle	Applicability
1.	Ultrasonic	Ultrasonic transmission/reflection.	None. Particle size dependent.
2.	Pulse Echo	Fourier analysis of reflected pulse.	None. Particle size dependent.
3.	Tomography	Three-dimensional X-ray picture.	None. Much too slow and too complex.
4.	Shadowgrams	Ultrasonic shadowgrams.	None. Particle size dependent. Inaccurate.
5.	Sound Velocimeter	Measures velocity of sound in slurry.	None. Cannot yield coal/rock content.
6.	Energy Absorption	Same as ultrasonic.	None. Particle size dependent.
7.	Electromagnetic	Measure conductivity, dielectric constant or magnetic permeability.	Conductivity measurement is promising: conductivity measures water volume.
8.	Capacitance	Measures dielectric constant.	Promising, but developers were unable to correct for large variations in water conductivity.
9.	Magnetic Field Coil	Coil impedance varies with slurry composition.	None. Unknown relationship to slurry composition. Excessively sensitive to small conducting fragments.
10.	Very Low Frequency Radio Waves	Measure complex change of dielectric constant and conductivity.	None. No one-to-one relationship to coal/rock content.
11.	Optical	Measures reflectivity of slurry.	None. particle size dependent, etc.
12.	Mechanical	Measures slurry density.	Too complex, unreliable. Gamma densitometer is much simpler, more reliable.
13.	Gamma-Ray	Measures total slurry density.	Excellent with neutron gauge. Stable, non-intrusive. Mounts outside pipe.
14.	Dual Gamma-Ray	Measures slurry density and is atomic-weight-sensitive via the lower energy gamma-ray.	Lower energy gamma-ray is almost redundant to higher energy gamma; thin pipe wall is required; finally, it is too sensitive to small variations in iron content in ash rock.
15.	Neutron Gauge	Measures hydrogen content which is very different in coal, rock and water.	Excellent with gamma-ray gauge, non-intrusive. Mounts outside pipe.
16.	Prompt Neutron Activation Analysis	Measures 2.2 MeV gamma from hydrogen, 4.4 MeV from carbon.	Much too slow, cumbersome, expensive, and requires huge neutron source. Otherwise, will work, in principle.
17.	Conventional Activation Analysis	Measures only some selective elements.	Not applicable to coal, rock, water (i.e., H, C, O, Si, Fe don't respond well).
18.	X-ray Resonance Fluoresence Spectrometer	Measures characteristic X-ray lines from elements.	Will not work in a slurry for elements lighter than iron.
19.	Nuclear Magnetic Resonance	Can, in principle, measure hydrogen density point by point in "non-moving slurry".	Much too slow, expensive, unworkable. Neutron gauge does the same fast enough, and is very simple to apply.

2.2 CANDIDATE METHODS

This section discusses the effectiveness of each of the methods that has been selected for study in Phase I of the slurry concentration sensor program. The degree of effort expended on each candidate method depended, in part, on early estimates of probable effectiveness of each type, and in part on the degree of difficulty in obtaining quantitative data.

Evaluation and final selection of the most effective sensor design is presented in Section 2.3.

2.2.1 Nuclear Methods

The study effort of the nuclear probes in Phase I began with a series of neutron and gamma-ray transport calculations. These helped identify neutron and gamma-ray energies useful for the coal slurry sensor. In addition, they were used to determine linear "response functions" that are required for a simple and straightforward solution of the slurry concentrations $M_c/M_r/M_w$ in the coal/refuse/water slurry. The "response function" for the unscattered component of nuclear radiation is a simple exponential. This simplified case is shown schematically in Figure 2.1. For plane-wave attenuation, the response function is

$$I = I_0 \exp - \left(\sum_i \mu_i M_i \right) \qquad (1)$$

where

I_0 = the incident radiation flux

I = the transmitted flux

μ_i = the attenuation coefficient of material i (coal, refuse or water) for the gamma-ray or neutron energy for the particular probe, and

M_i = the product of the average density of material i and the total thickness T.

However, it is not feasible to measure the unscattered component for a sensor, even for the monoenergetic gamma-ray probe. It requires a multichannel analyzer plus a complex peak-area analysis program to subtract out the scattered radiation under the "full energy peak." Also, a collimated source and collimated detector would be required, which would result in prohibitively high radiation source and shielding costs.

Thus, efforts were made to obtain linear responses for a very simple source-detector arrangement, where the source and detector are simply placed on opposite sides of the slurry pipe (against the pipe). This was accomplished by plotting the logarithm of the transmission, or count rate, I_o versus the sum of the $M_i\mu_i$ for properly selected μ_i. The sum $\Sigma M_i\mu_i$ can be regarded as an "effective radiation thickness." In particular, the response function for the complex case of multiple scattering is given by:

$$I = I_0 \exp - \left(\sum_i \mu_i M_i \right) . \qquad (2)$$

For gamma-rays, the best μ_i were obtained by subtracting from the total cross section the in-group scattering cross section.

The case of neutron transmission is far more complex. First, the ^{252}Cf neutron source is not a monoenergetic source, but is continuous in energy. Second, considerable downscattering in neutron energy occurs. Finally, the scattering by hydrogen is a singular case since a hydrogen atom can downscatter a neutron to zero energy in a single collision. Because of this singular behavior, the "transport" cross section of hydrogen is very geometry-dependent. By solving for the hydrogen transport cross section that yielded the best straight-line plot,it was possible to obtain a straight-line "response function" for ^{252}Cf neutrons in the 1-2 MeV and the 2-5 MeV band for the 6-inch haulage pipe. For the 18-inch pipe, 1-5 MeV neutrons were found to be most useful.

An extensive computational effort was carried out to determine the "response function" representation. These calculations were verified with three series of experimental measurements. These involved the use of both slab and cylindrical geometries, and the use of three different approximations to

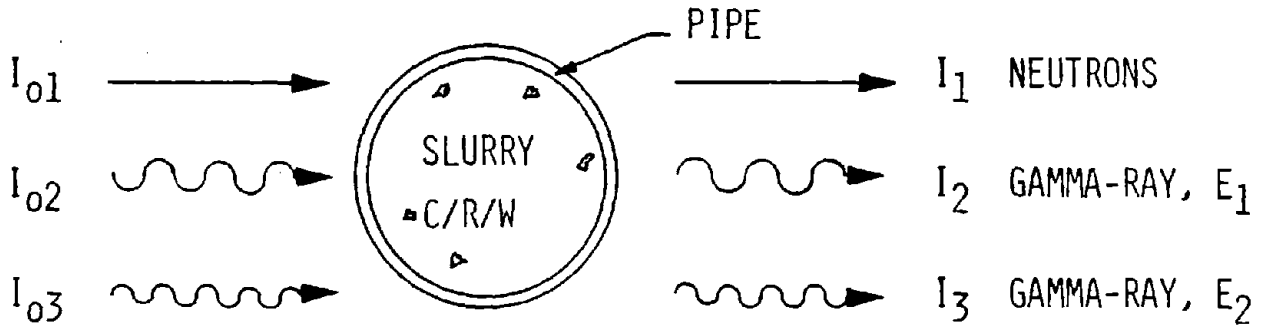

where $$I_i = I_{oi}\, e^{-\{\mu_c M_c + \mu_R M_R + \mu_w M_w\}}$$

$$\ln\left[\frac{I_i}{I_{oi}}\right] = \mu_c M_c + \mu_R M_R + \mu_w M_w$$

μ_i = ATTENUATION COEFFICIENT, cm^{-1}

M_i = DENSITY OF COMPONENT i TIMES SLURRY THICKNESS

FIGURE 2.1 - Illustration of three-sensor probe in which the "unscattered" component is utilized to probe M_c, M_R and M_w.

the materials found in a coal slurry haulage pipe: carbon/glass/lucite, carbon/sand/water, and Eastern bituminous coal/sand/water. In addition, a 1/4-inch wall thickness of iron was used for the 6-inch sensor measurements, and 3/8-inch iron wall for the 18-inch sensor data. The first series of measurements (carbon/glass/lucite) utilized precisely measurable materials in slab geometry, the second (carbon/sand/water) utilized materials almost as precisely measurable but closer in composition to the slurry, also in slab geometry. The third utilized actual Eastern bituminous coal lumps with sand and water, both in slab and 6-inch iron pipe geometry.

Good responses and good sensitivities were obtained with the first two series of measurements. The results for the case of Eastern coal are presented here. The "response function" plots of the transmitted count rate versus the "effective radiation thickness" are shown in Figure 2.2 for 1-2 MeV neutrons transmitted through a 6-inch slurry and 1/2-inch iron (2 x 1/4 in.), and in Figure 2.3 for 2-5 MeV neutrons. The slurry composition in each case is given in the figures as W_c, W_r, W_w, the weight-percentages.

For the same 6-inch case, the experimental "response functions" are shown for ^{137}Cs gamma-rays (662 keV source gamma-ray energy) in Figure 2.4, ^{57}Co (122 keV) in Figure 2.5, and ^{241}Am in Figure 2.6.

The response functions derived from these measurements are given in Table 2.4, along with the "constant density" equation that is useful when the density of coal and refuse is constant within a given mine, and is accurately known (to ~ 2-4%).

To solve for the three mass concentrations M_c, M_r and M_w of the slurry, three equations are selected from Table 2.4. The constants multiplying M_c, M_r and M_w in Eq. 1 are the mass attenuation coefficients, μ_i. Note that if the ratios of the μ_i for two different probes are nearly constant, these two gauges yield poor sensitivity as a pair. For ^{137}Cs, the ratios are .91/.90/1 for C/R/W, while for ^{57}Co, they are .86/.96/1. For the two neutron groups (1-2 and 2-5 MeV), they are .58/.106/1 and .72/.185/1, respectively. Thus, for a three-component gauge, the use of two neutron groups and one gamma group will provide the greater accuracy (for the same statistical accuracy in counting

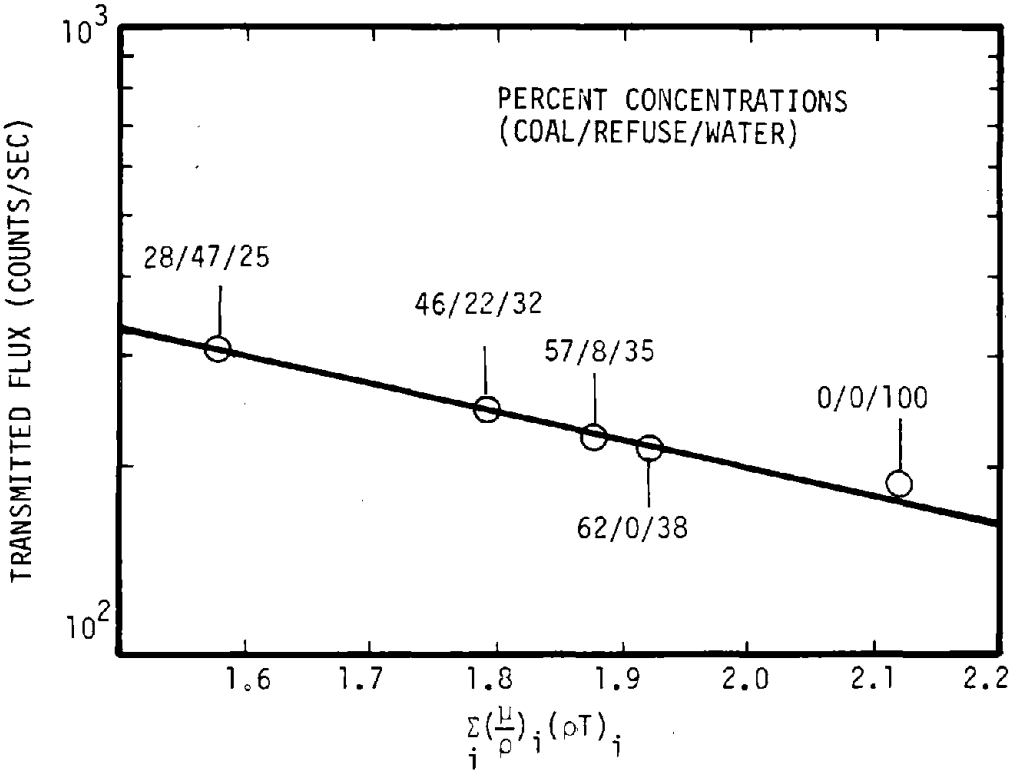

FIGURE 2.2. - Experimental transmission, 6-inch haulage pipe, Cf-252 neutrons, 1-2 MeV. (eastern coal/sand/water).

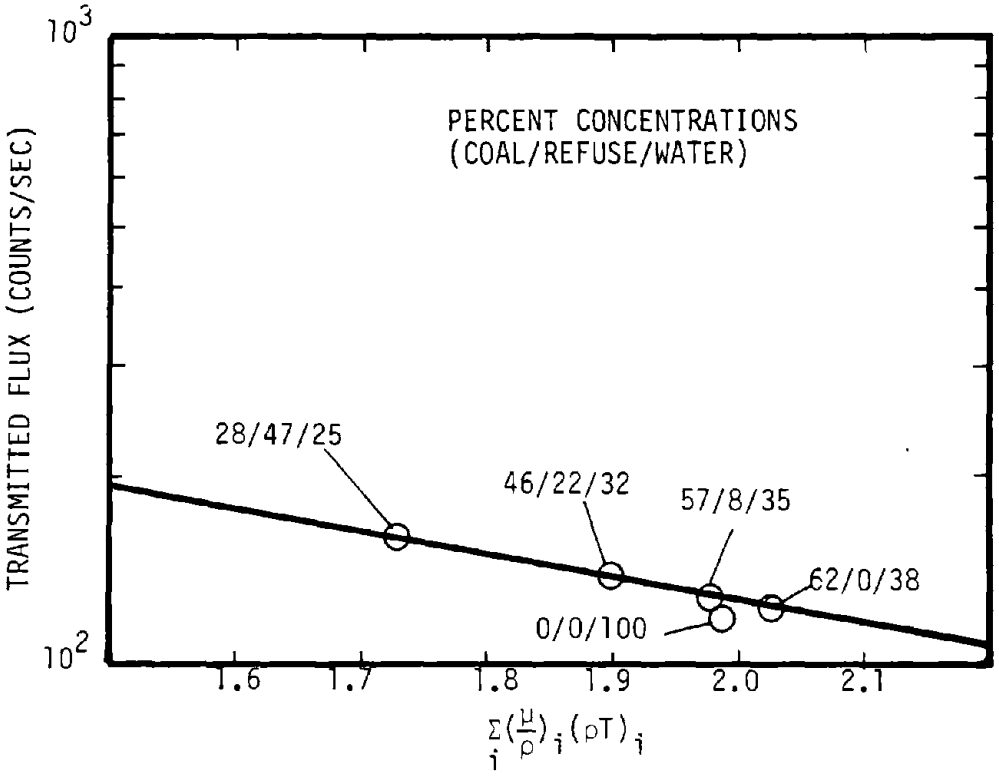

FIGURE 2.3. - Experimental transmission, 6-inch haulage pipe, Cf-252 neutrons, 2-5 MeV. (eastern coal/sand/water).

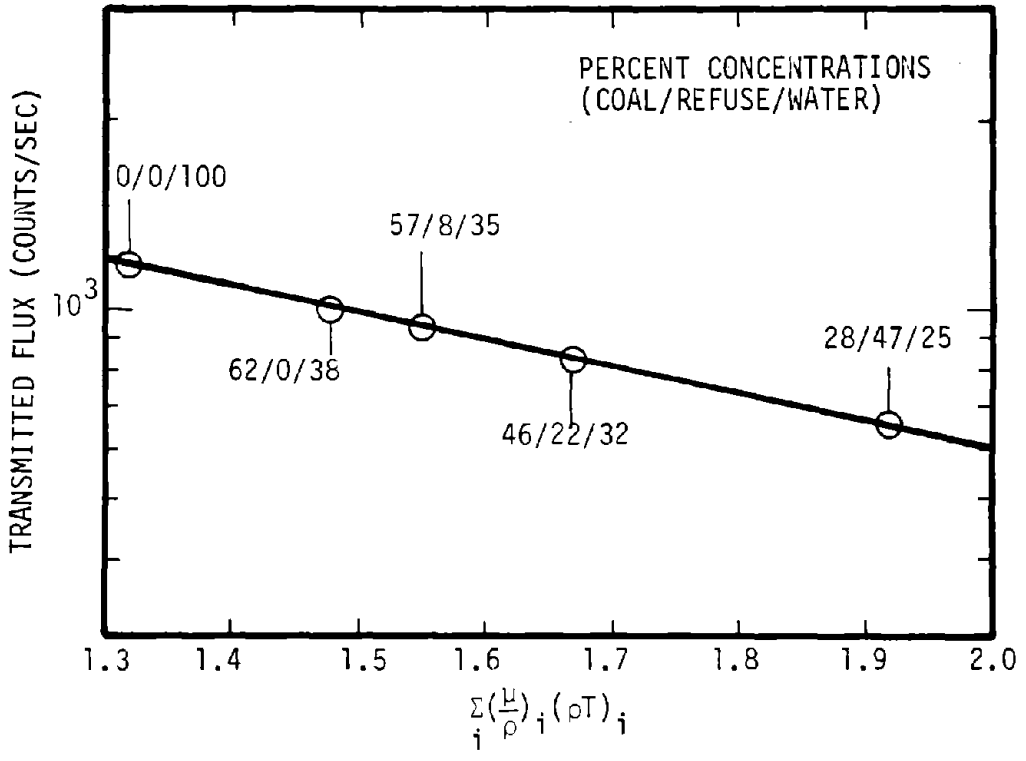

FIGURE 2.4. - Experimental transmission, 6-inch haulage pipe, Cs-137 gamma rays (eastern coal/sand/water).

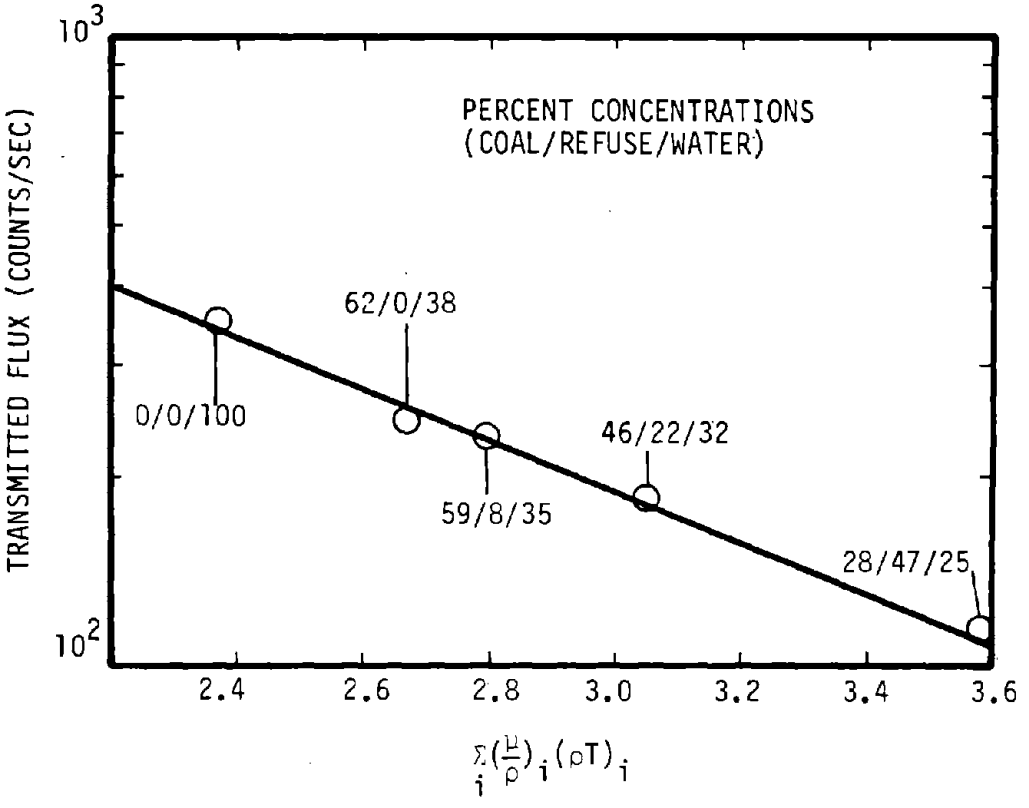

FIGURE 2.5. - Experimental transmission, 6-inch haulage pipe, Co-57 gamma rays. (eastern coal/sand/water).

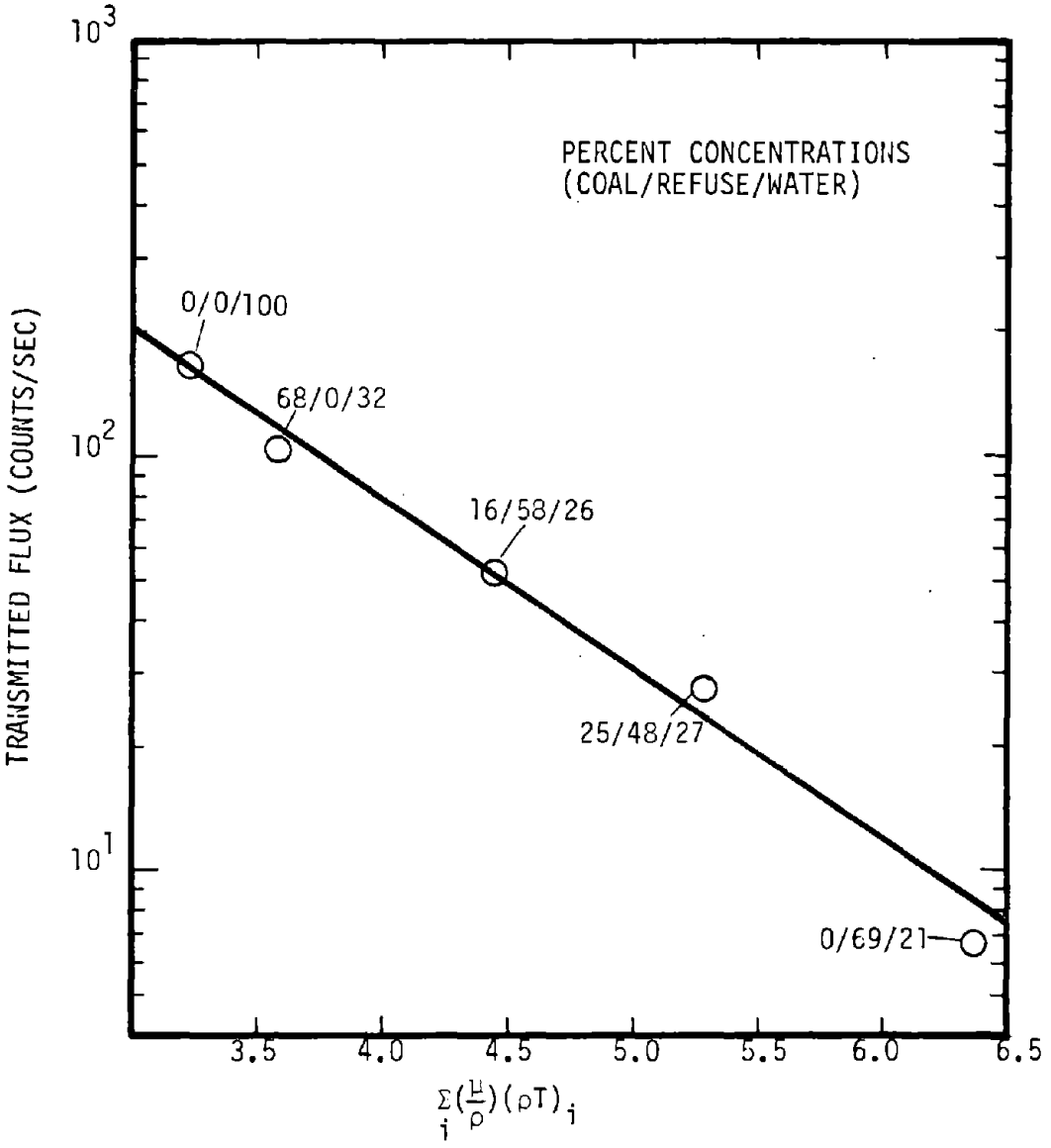

FIGURE 2.6. - Experimental transmission, 6-inch haulage pipe, Am-241 gamma rays (eastern coal/sand/water).

TABLE 2.4 - Linear equations derived from experimental data for eastern coal/refuse/water (6-inch haulage pipe).

^{241}Am $\quad 0.202\ M_c + 0.248\ M_r + 0.212\ M_w = \dfrac{\ln I - 8.288}{-0.982}$

^{57}Co $\quad 0.134\ M_c + 0.149\ M_r + 0.156\ M_w = \dfrac{\ln I - 8.069}{-0.948}$

^{137}Cs $\quad 0.0748\ M_c + 0.0777\ M_r + 0.0862\ M_w = \dfrac{\ln I - 8.323}{-0.954}$

^{252}Cf (1-2 MeV Group) $\quad 0.0806\ M_c + 0.0147\ M_r + 0.139\ M_w = \dfrac{\ln I - 7.360}{-1.038}$

^{252}Cf (2-5 MeV Group) $\quad 0.0937\ M_c + 0.0242\ M_r + 0.131\ M_w = \dfrac{\ln I - 8.166}{-1.021}$

^{252}Cf (1-5 MeV Group) $\quad 0.0848\ M_c + 0.0181\ M_r + 0.135\ M_w = \dfrac{\ln I - 8.166}{-1.021}$

Constant Density Equation: $\dfrac{M_c}{1.43} + \dfrac{M_r}{2.7} + M_w = 15.24$

where: M = component mass in g/cm^2 (c = coal, r = refuse, w = water)

I = transmitted flux in counts/sec.

each of the nuclear "probes") than will the use of one neutron and two gamma probes. This is true only for the 6-inch line. For the 18-inch line, the two neutron groups do not provide independent data. This is related to severe downscattering in energy, and to the lower energy group starting out in the high energy group and being downscattered. For simplicity in gauge design, this mitigates against the use of two neutron energy groups for the 6-inch pipe. The use of one broad-energy group, furthermore, makes possible a much more stable neutron counting configuration, one stable and accurate enough for rugged mine environments.

It should be pointed out that if only two nuclear probes are considered, the neutron and gamma pair have the greatest difference in μ_i ratios and will provide the greatest slurry concentration accuracy and sensitivity for a given statistical precision in count rate measurement. Figure 2.7 illustrates this point. Here, the relative count rate is plotted versus weight percent of water. The gamma-ray probe increases in count rate as W_w increases, while the neutron probe count rate decreases with increasing W_w.

For the 18-inch haulage pipe, the data plots for the experimental "response functions" are presented in Figures 2.8, 2.9 and 2.10 for 1-5 MeV neutrons, ^{137}Cs gamma-rays (E_γ = 662 keV) and ^{133}Ba gammas (E_γ = 356 keV). Note that for the two gamma-ray probes, the relative spacing for the points for the different $W_c/W_r/W_w$ is nearly the same. These two gamma-ray probes cannot give much independent information, except with extremely large sources and extremely high electronic stabilities. This combination of requirements must be avoided in an effective and economic probe design.

The "response functions" derived from the data plotted in Figures 2.8 - 2.10 are shown in Table 2.5 for the 18-inch haulage pipe sensor. The "constant density" equation is also included for the case where the coal density is 1.43 g/cc, as measured, and the refuse density is assumed to be 2.7 g/cc.

The much simpler single neutron plus two gamma sensor is much more sensitive for anthracite, yielding an accuracy of ~4%. For bituminous, the accuracy is probably too poor for the N+2γ gauge to be considered, unless the

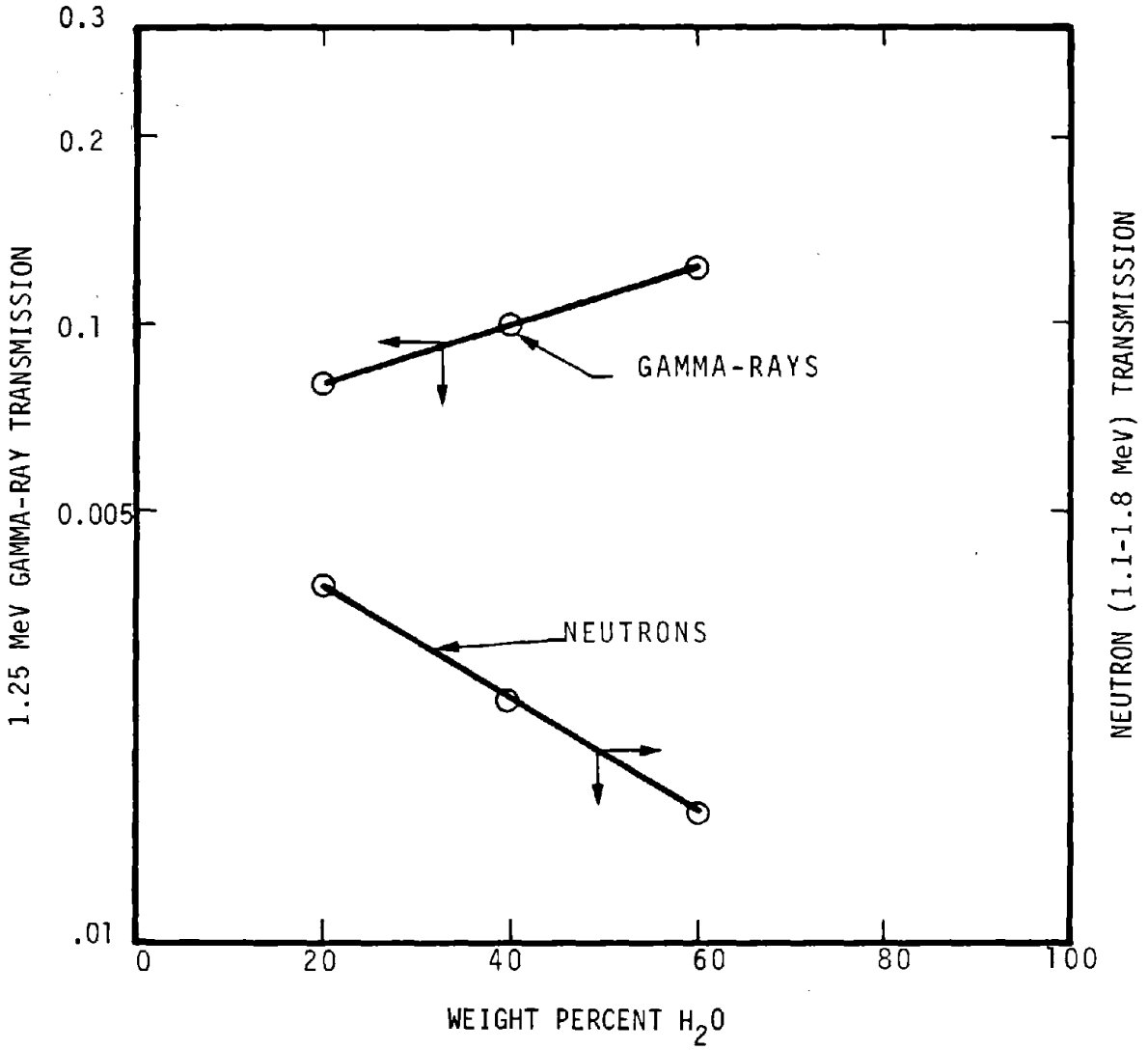

FIGURE 2.7. - Relative sensitivities of neutron and gamma-ray responses to water concentration (6-inch pipe).

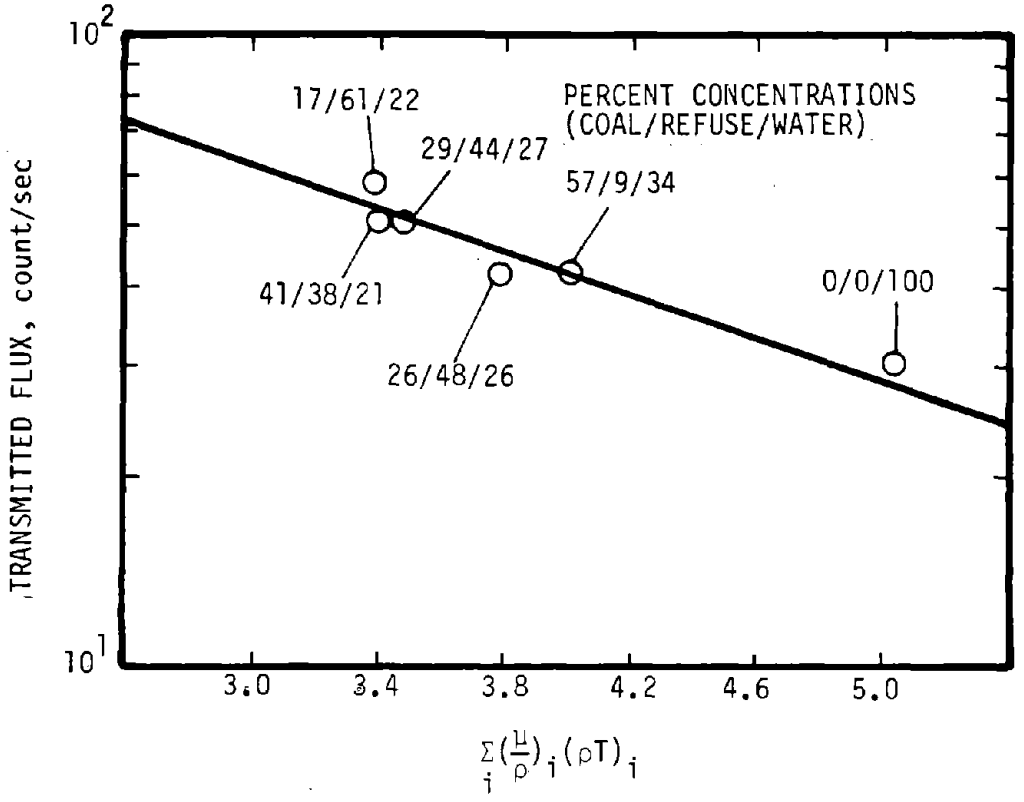

FIGURE 2.8. - Experimental transmission, 18-inch haulage pipe, Cf-252 neutrons, 1-5 MeV. (eastern coal/sand/water)

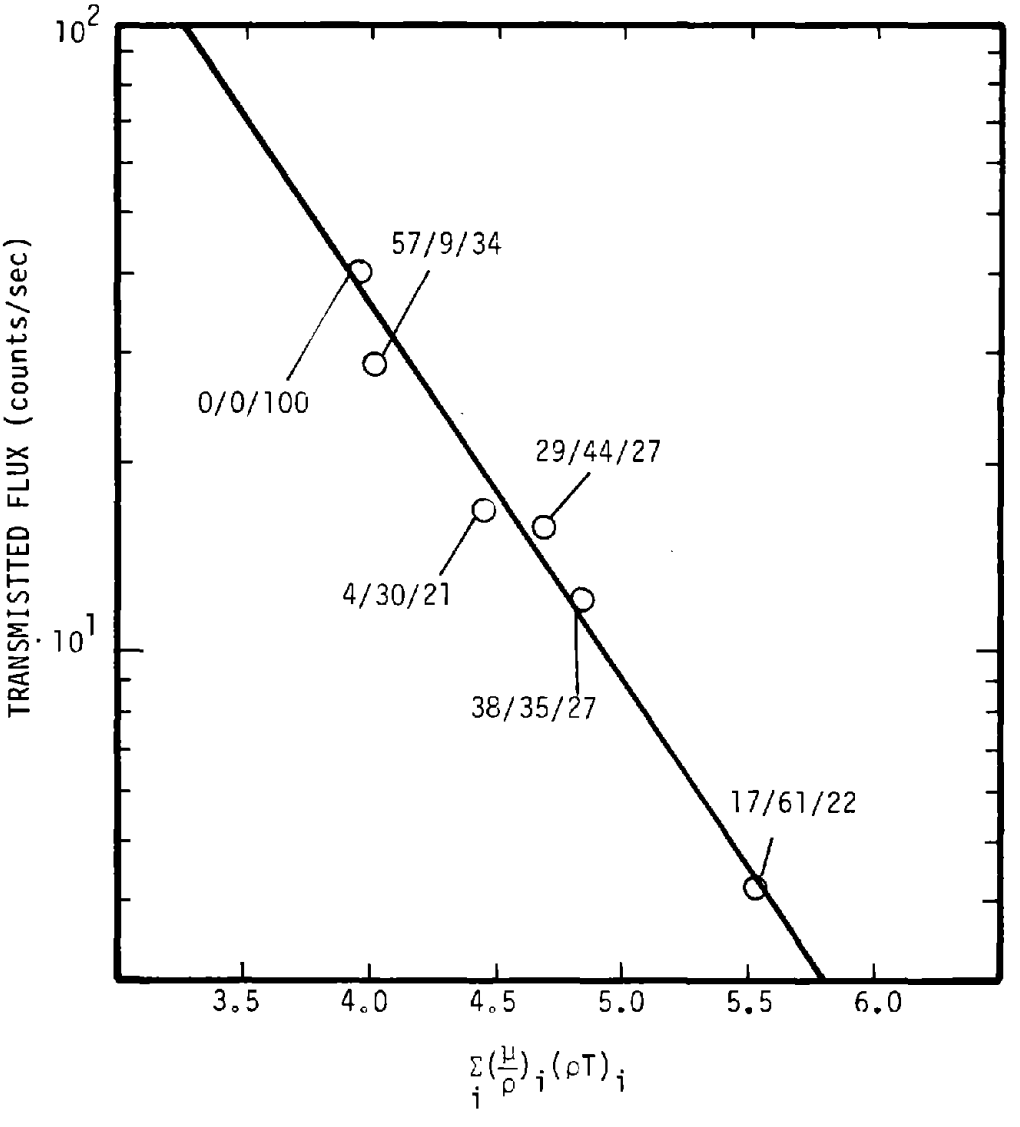

FIGURE 2.9. - Experimental transmission, 18-inch haulage pipe, Cs-137, gamma rays (eastern coal/refuse/water).

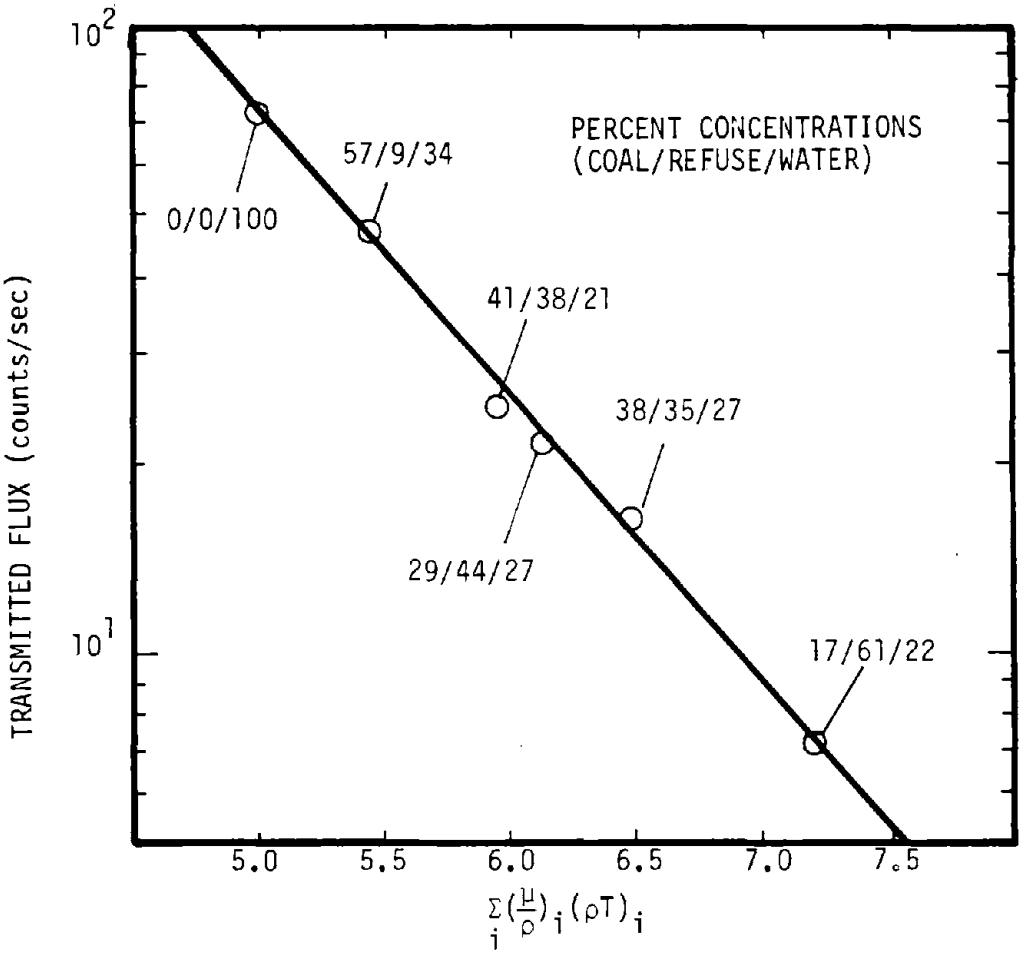

FIGURE 2.10. - Experimental transmission, 18-inch haulage pipe, Ba-133 gamma rays (eastern coal/refuse/water).

TABLE 2.5. - Linear equations derived from experimental data (eastern coal/refuse/water) - 18-inch haulage pipe

$$^{133}Ba \quad 0.108\ M_c + 0.0989\ M_r + 0.109\ M_w = \frac{\ln I - 9.434}{-1.034}$$

$$^{137}Cs \quad 0.0748\ M_c + 0.0777\ M_r + 0.0862\ M_w = \frac{\ln I - 8.659}{-1.285}$$

$$^{252}Cf \quad \text{(1-5 MeV Group)} \quad 0.0735\ M_c + 0.0181\ M_r + 0.110\ M_w = \frac{\ln I - 5.357}{-0.404}$$

Constant Density Equation:

$$\frac{M_c}{1.43} + \frac{M_r}{2.5} + M_w = 45.72$$

where: M = component mass in g/cm^2 (c = coal, r = refuse, w = water)

I = transmitted flux in counts/sec.

^{241}Am 60 keV gamma-ray source is used. Some measurements made with this source showed promise, but were not pursued because of its opacity to the iron pipe. However, if a conductivity gauge is used, a segment of pipe is made with an electrically insulating material that is relatively transparent to ^{241}Am gamma rays. The ^{241}Am source is in this case still a viable candidate as a low-energy gamma-ray probe to be used with a higher energy probe, such as ^{60}Co, ^{137}Cs, or ^{133}Ba, but only for the 6-inch pipe because of the limited range of the 60 keV gamma rays in the coal/refuse (rock)/water slurry.

A schematic diagram for the three-component nuclear sensor is shown in Figure 2.11 for both the two neutron plus gamma and two gamma plus neutron options. The microprocessor can rapidly solve the three equations and three unknowns. The outputs can be shown as mass percentages (W_c, W_r and W_w) plus average density $\bar{\rho}$, as partial densities ρ_c, ρ_r and ρ_w, or as area-mass fractions M_c, M_r and M_w (gm/cm^2 or pounds/in^2).

For the 18-inch haulage pipe, only a single neutron probe and a single gamma-ray probe are viable candidates. The reason for this is that for neutrons, spectral equilibrium is reached at a thickness of 18 inches in a coal/refuse/water slurry, so that the information carried by all neutron groups is nearly the same. Higher energy continuous neutron sources such as Pu-Be source can give more information in two energy groups, but these are prohibitively costly. The Pu-Be source has an abundance of 4.44 MeV gamma-rays and is, therefore, very costly to shield as well as to procure in large sizes.

For the gamma-rays, a low energy gamma-ray source is too opaque to the 18-inch slurry plus 3/4-inch steel (two each 3/8-inch walls of the 18-inch haulage pipe). Thus, only a high-energy gamma-ray source should be considered. The 18-inch sensor, utilizing a single neutron and a single gamma-ray gauge, can either be used with the "constant density equation" or with a non-nuclear probe, as discussed in Section 2.3 below.

2.2.2 Electrical Gauge

The purpose of the conductivity gauge is to determine the percentage of coal and refuse displacing water in a section of slurry pipeline. It has

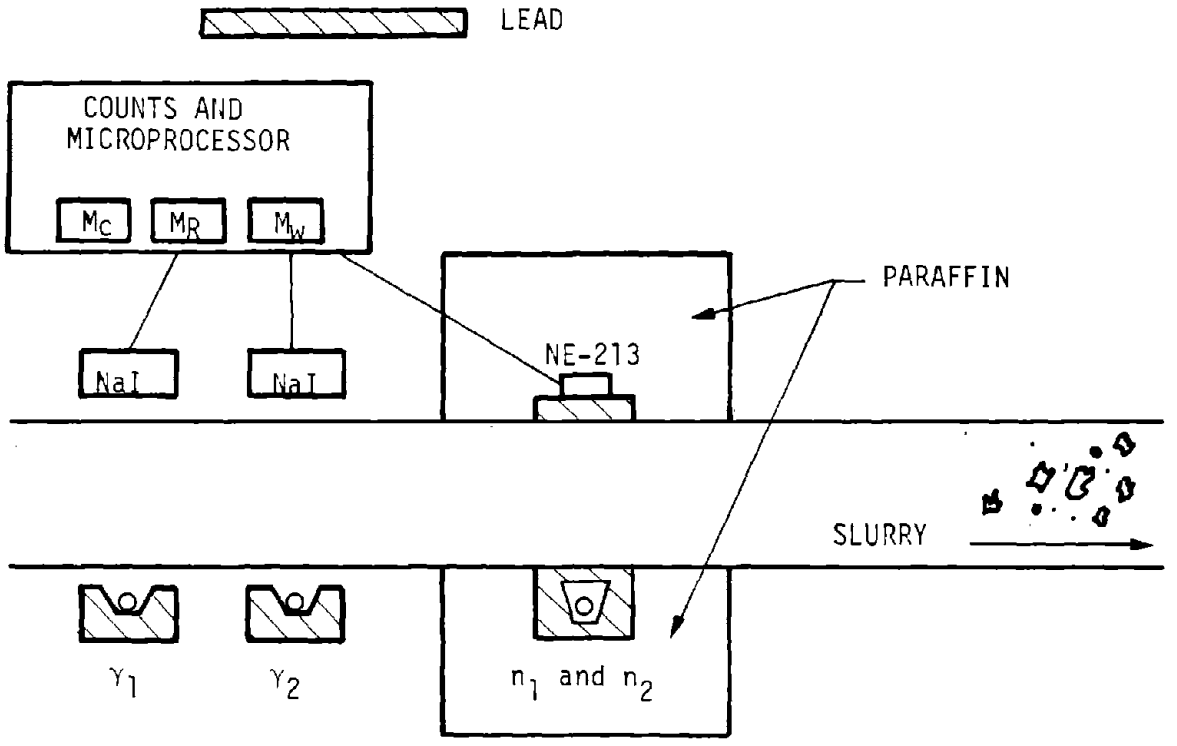

FIGURE 2.11. - Schematic diagram of two gamma probes and two neutron probes omit γ_2 for a γ + 2n sensor and n_2 for a 2γ + n sensor.

been determined that both coal and waste rock are electrical insulators when compared to the water in a slurry. The concept of accurately (within a few percent) determining the percentage of water displaced by insulating material by merely measuring the electrical conductivity of a section of pipe is attractively simple. Verification of the method was accomplished, and is discussed in the following paragraphs.

Preliminary measurements indicated that both coal and rock (shale) are characterized by resistance values in the hundreds of megohm range, which is orders of magnitude above anticipated slurry water resistances. Thus, even relatively large differences in the conductive characteristics of the slurry solids are not likely to significantly affect measurements of the slurry water resistance.

To analyze the effect of the geometry of the haulage, consider a rectangular pipe section 10 units on a side and 50 units long (Figure 2.12). Two simplifying assumptions are made.

1. Although the water is an ionic conductor, its voltage/current relationship is linear for the ranges of voltages encountered.

2. No voltage gradients exist in the water in a plane normal to the haulage flow.

The method of analyzing the effect of geometry consists of removing cubes of water and replacing them with non-conductive cubes in various configurations. Obviously, one extreme would result from removing 100 units normal to the pipe axis at one station. This would insulate the section (resistivity becoming infinite). The same 100 units, if removed along the pipe axis, would only reduce the cross sectional area--and hence the conductivity--by 2%. Fortunately, the dimensions of the materials cannot approach such extremes. It was calculated that if 30 units are removed, the maximum variation in conductivity caused by the shape factor is slightly less than 1/2%. If 50 units are removed, the maximum variation is still less than 2%. This type of analysis, because of the assumptions made, does not constitute proof of validity. Rather than refine the analysis, an experiment was performed. A 24-inch length of 4-inch diameter PVC pipe was slotted

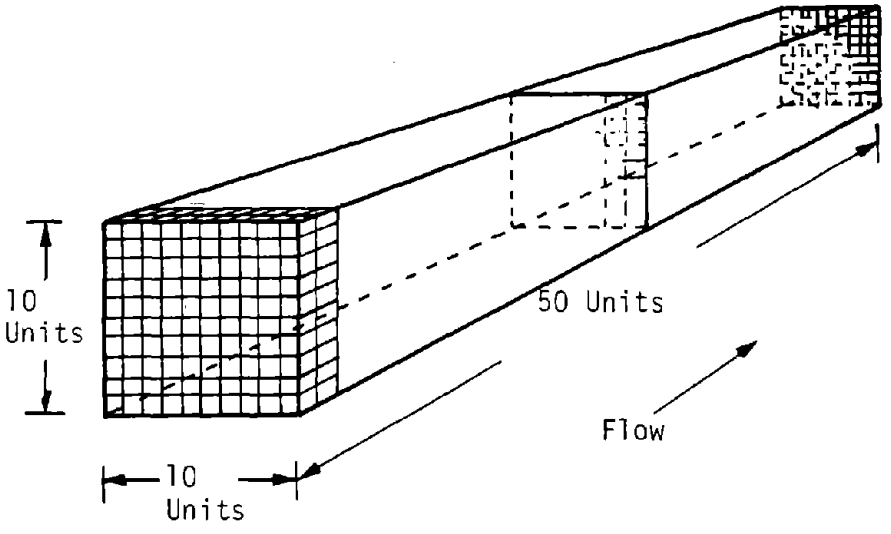

FIGURE 2.12. - Shape factor analysis using unit cubes.

lengthwise to gain access (Figures 2.13 and 2.14). Steel end caps were cemented in place, and an overflow drain was installed. The assembly was leveled and filled with tap water to the overflow drain level. The resistance between the steel end caps was monitored using a low-voltage (2.35 vrms 1 kHz) signal. It is essential that the measurements are made with a-c, because d-c voltages are generated by the electrolytic action of the impure water on the metallic end caps. Rock and coal were placed in the PVC pipe section, and the displaced volume of water (ΔV) was recorded along with the resistance, R. A total of six data point sets (R_i, ΔV_i), i = 1, 6, were taken. It was assumed that the quantitative relationship between the measured resistance R and the effective water volume V was simply VR - K, where K is a constant. However, an accurate calculation or direct measurement of the effective volume of the insulated PVC section could not be made. This is a result of the unknown effect of fringing of the electric field at the ends. The assumption of VR = K was verified as follows. It was assumed that the effective volume V was reduced by the measured displaced volume, i.e., $V_i = V_1 - \Delta V_i$, where V_1 is the effective volume with no water volume displaced. For data point sets 1 and 4, it was assumed that $V_1R_1 = K = V_4R_4$. Using also $V_4 = V_1 - \Delta V_4$, V_1 was computed as

$$V_1 = (V_4 R_4/R_1)/(R_4/R_1 - 1).$$

from whence $K_1 = R_1V_1$ and $V_4 = K/R_4$. The remaining effective volumes were calculated from $V_i = V_1 - \Delta V_i$, and $K_i = R_i\Delta_i$. The results are tabulated below:

Data Set, i	Effective Water Volume, V_i (Liters)	Measured Resistance, R_i (K ohms)	$V_i \times R_i = K_i$ (Liter - K ohms)
1	2.48	1.88	4.67
2	2.32	2.04	4.72
3	2.12	2.21	4.69
4	1.97	2.37	4.67
5	1.74	2.67	4.63
6	1.43	3.25	4.63

The standard deviation for the V x R product is 0.75%, a value well within the accuracy of the experimental technique used. The data shown here

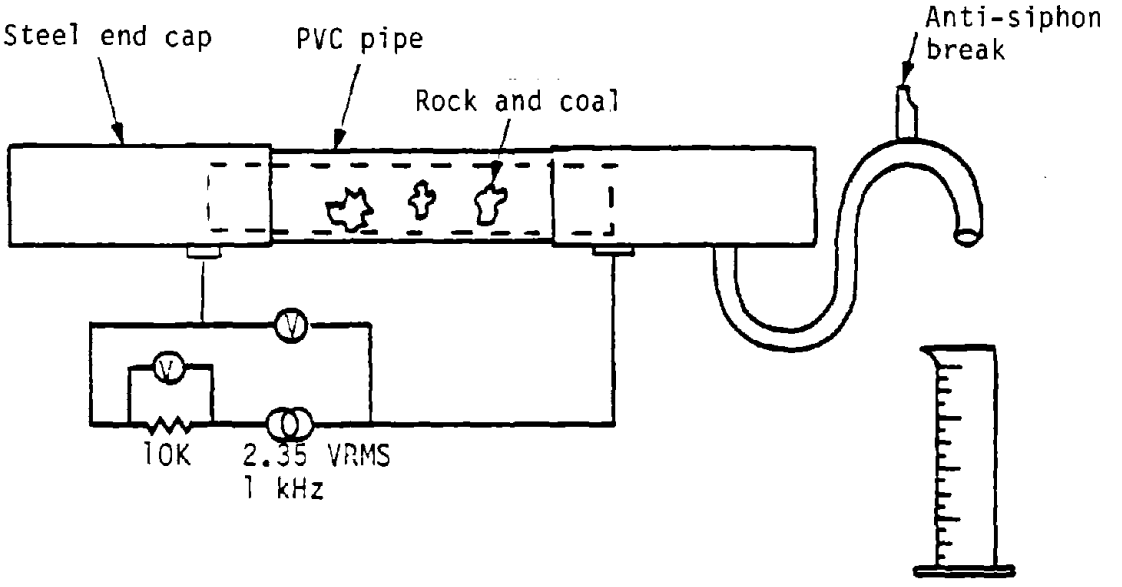

FIGURE 2.13. - Conductivity gauge experiment.

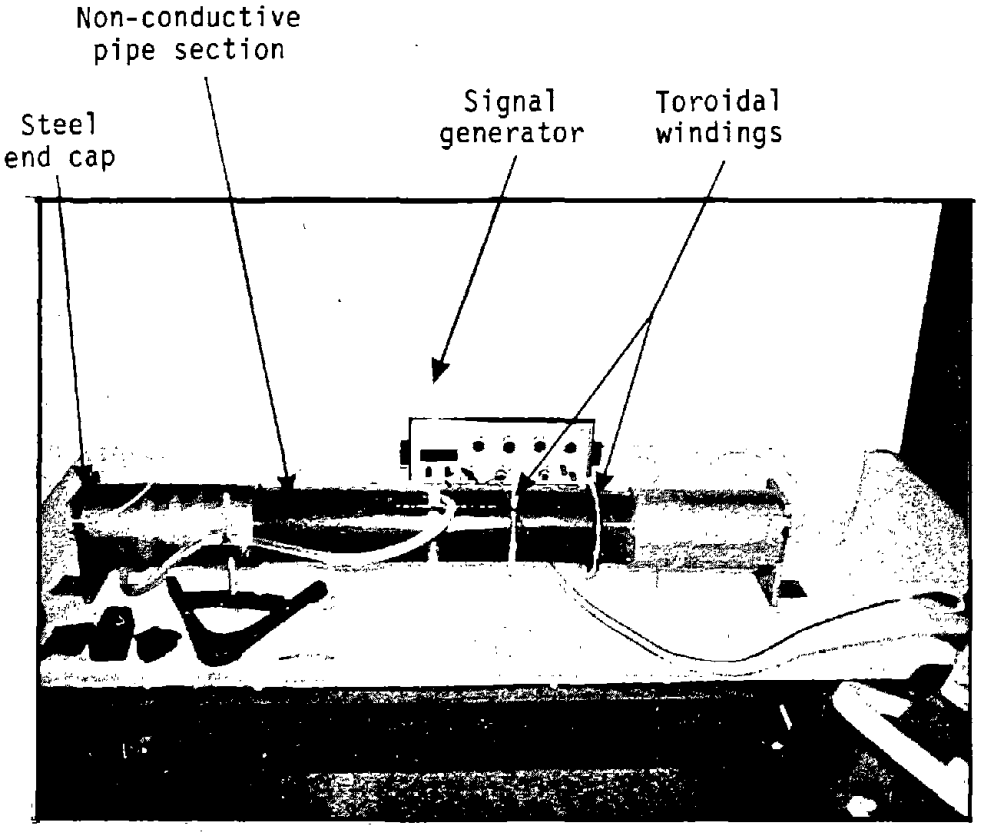

FIGURE 2.14. - Prototype conductivity sensor for measurement of volume of solids (coal/refuse) in a haulage pipeline.

demonstrate the feasibility of inferring the effective water volume from measurements of resistance across a pipeline section.

In a real pipeline application, the resistance across an insulated pipe section cannot be made in the way the experiment was done. In the experiment, it was assured that the slurry formed the only conductive path between the steel ends. In a pipeline installation, supporting structures or the earth itself could form electrical paralleled paths. The parallel path problem can be solved in one of two ways. The more obvious method consists of introducing a conductive ring electrode in the middle of the insulated pipe section (Figure 2.15).

An alternative solution utilizes a single insulated section which becomes part of a single turn variable resistance coupling winding of a toroidal transformer (Figure 2.16). The voltage induced in the secondary is proportional to the conductivity of the slurry in the insulated pipeline section. One advantage of the toroidal transformer system is that for a given length of insulated pipeline, fringing is reduced by a factor of two.

One variable not accounted for in the experiment performed is the variable conductivity of the slurry water. The conductivity will vary with the pH, the dissolved salt content and the temperature. Compensation for the variable conductivity is easily achieved by using a reference. An insulated shunt line with a filter screen would have a toroidal primary and secondary transformer winding (Figure 2.16). Excitation for the main conductivity gauge would be derived from the filtered shunt line. With the excitation proportional to the slurry water conductivity, the conductivity gauge output would be dependent only on the amount of solids contained in the section.

An apparent change in volume of the test section with a change in slurry conductivity may result from increased fringing with decreasing conductivity; that is, solids will be measured beyond the boundaries of the insulated section. This fringing effect can be minimized by using a large length-to-diameter ratio for the insulated pipe section. Apparent volume changes with conductivity changes can also be compensated for with the reference used for conductivity compensation.

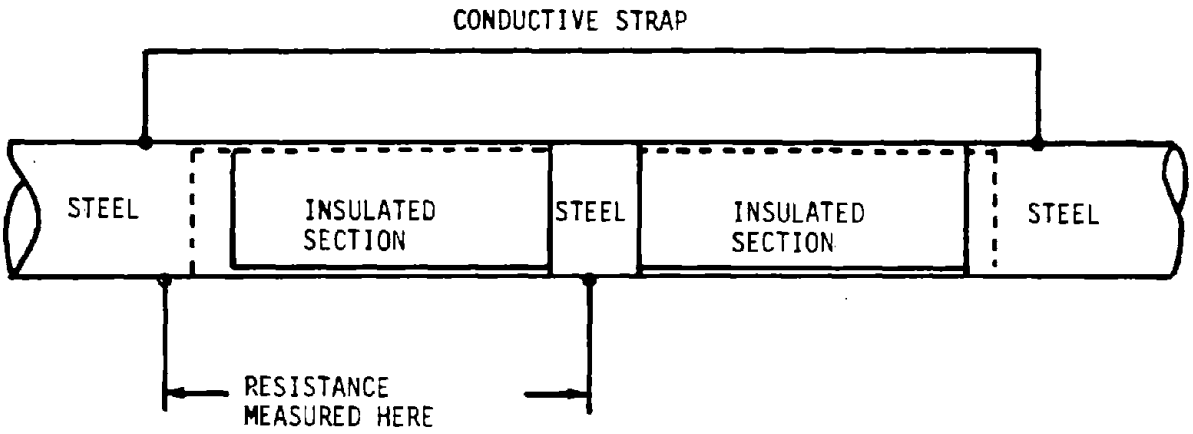

FIGURE 2.15.

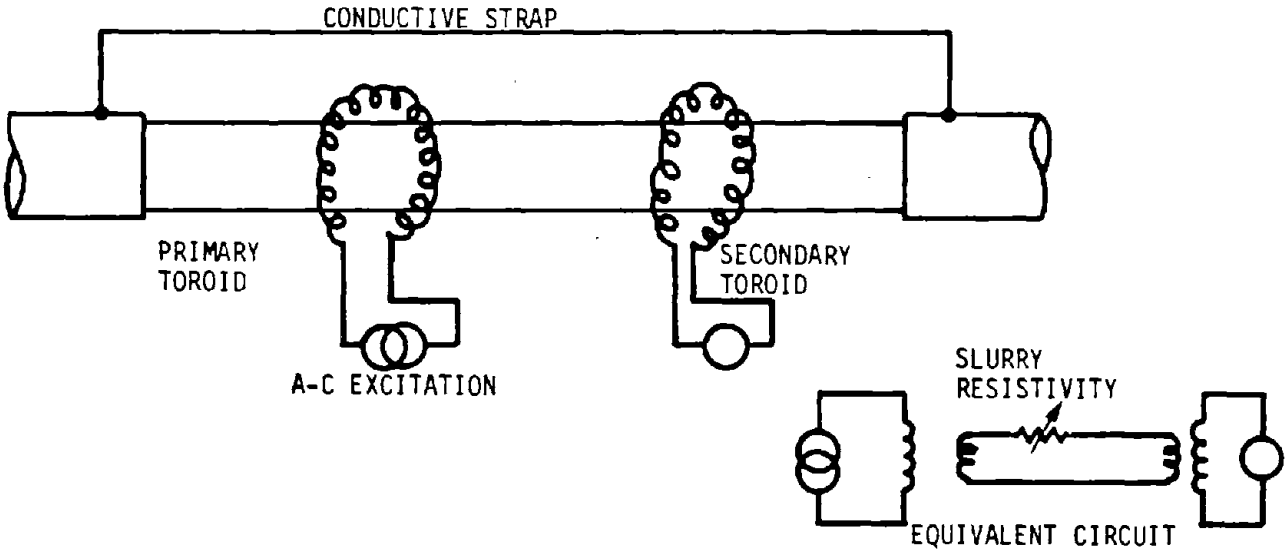

FIGURE 2.16.

2.3 DISCUSSION AND EVALUATION OF CANDIDATE SENSOR CONCEPTS

2.3.1 Prime Candidate Selection

A few of the more promising sensor concepts were selected for further study in Phase I, concepts that initially showed promise of meeting the Bureau of Mines requirements. The study consisted of calculations and feasibility measurements designed to evaluate the performance characteristics. From the data compiled and analyzed, an effort was made to select the candidate sensor concepts that would best meet the Bureau of Mines requirements, as determined by the sensor evaluation guidelines embodied in a recent communication to the SAIC research team. The evaluation criteria included accuracy, range, response time, cost, safety, reliability and maintainability.

The prime candidate that has evolved from the Phase I effort is the combination of a conductivity gauge, a gamma-ray gauge, and a neutron gauge. This combination sensor is feasible for both the small (6-inch) and large (18-24 inch) hydraulic pipelines.

This candidate sensor design does not depend on the density of coal and refuse being constant, and an error analysis presented below indicates that nominal changes in the composition of coal and refuse will not have much of a deleterious effect on the sensor accuracy. After a considerable backlog of experience has been obtained in using the research sensor, it is possible that enough independent data can be compiled in parallel which shows the coal and refuse densities to be nearly constant for a given mine area. At that time, it is possible that the conductivity gauge can be deleted from the control sensor and/or the commercial sensor used for mining operations. For this "constant density" case, the combination neutron plus gamma-ray gauge clearly remains the prime sensor concept (for large and small sensors) according to the data gathered in Phase I. It is stable, rugged and non-obtrusive (i.e., it simply clamps on to the pipe).

The results of a series of error analyses are presented below for the candidate sensor systems.

Section 2.2.1 above presented the response functions for six different nuclear probes and a constant density equation (constraint), should the density be known. In principle, any three of these equations can provide M_c, M_r and M_w. However, the sensitivity or accuracy will vary considerably, so that the best three must be selected for the operational gauge.

The analysis and evaluation of several leading candidates for the final sensor design, for both the 6-inch and 18-inch systems, can most succinctly be presented by including the conductivity gauge as a component of the complete sensor. For this reason, the detailed sensitivity and error analysis are deferred to the next section, "Design and Evaluation of the Combination Nuclear-Conductivity Sensor." The driving reason for this is that only the combination (neutron, gamma-ray, conductivity) sensor appears to meet the Bureau of Mines requirements for the large (18-inch or 24-inch haulage pipe) sensor.

2.3.2 Design and Evaluation of the Combination Nuclear-Conductivity Sensor

An evaluation of five leading sensor candidates is summarized in Table 2.6 for the 6-inch haulage pipe. The first column gives the three compositions, in weight percent, of Eastern coal/refuse/water. The second column lists the areal masses (in gm/cm^2) across the inside diameter of the pipe. The remainder of the table presents the concentrations, as measured by five different sensor concepts, and the fractional error for each measurement, e.g., 0.033 following 7.09 means a 3.3% error in the M_c = 7.09 gm/cm^2 value for Gauge #1. The analysis was carried out using actual nuclear measurements on the 6-inch-thick slurry.

For the combination conductivity-nuclear gauge, it was assumed in the Tables 2.6 and 2.7 data that the water volume is given exactly by the conductivity gauge. A separate error analysis carried out for the combination conductivity-nuclear gauge showed that a 1% error in the water-volume measurement propagates linearly as roughly a 1% additional error in M_c when mostly coal is being hauled, and 1% in M_r when mostly refuse is in the pipe.

TABLE 2.6. - Mass determination from experimentally derived linear equations eastern coal/refuse/water - 6-inch haulage pipe.

% Composition by weight	Actual Mass	Experimentally Determined Mass (g/cm^2)									
		Gauge #1*		Gauge #2*		Gauge #3*		Gauge #4*		Gauge #5*	
Coal/Refuse/Water	g/cm^2	Mass	Error†	Mass	Error†	Mass	Error†	Mass	Error†	Mass	Error†
62/0/38	Coal = 11.61	11.52	(0.008)	11.50	(0.009)	12.41	(0.069)	12.53	(0.079)	9.46	(0.185)
	Refuse = 0.00	0.186	(-)	0.20	(-)	-0.67	(-)	-0.17	(-)	0.846	-
	Water = 7.12	7.12	0	7.12	0	7.21	0.13	6.57	(0.078)	8.32	(0.169)
46/22/32	Coal = 9.64	9.62	(0.002)	9.69	(0.005)			10.51	(0.090)	18.84	(0.950)
	Refuse = 4.66	4.71	(0.010)	4.65	(0.003)			4.45	(0.045)	1.79	(0.616)
	Water = 6.77	6.77	0	6.77	-			6.24	(0.078)	1.40	(0.793)
28/47/25	Coal = 6.87	7.09	(0.033)	6.83	(0.004)	4.80	(0.301)	6.58	(0.042)		
	Refuse = 11.48	11.06	(0.036)	11.31	(0.014)	13.26	(0.155)	11.14	(0.029)		
	Water 6.19	6.19	0	6.19	0	6.19	0	6.51	(0.052)		
0/69/21	Coal = 0.00	0.183	-	0.948	-			1.59	-		
	Refuse = 24.08	23.76	(0.013)	24.89	(0.033)			23.39	(0.029)		
	Water = 6.32	6.32	0	6.32	0			5.37	(0.150)		
65/0/35 (Cylindrical Geometry)	Coal = 12.29	12.74	(0.036)	12.81	(0.043)						
	Refuse = 0.00	-0.80	(-)	-0.92	(-)						
	Water = 6.65	6.65	0	6.65	0						

* Gauge #1 = conductivity + constant density + ^{137}Cs

Gauge #2 = conductivity + ^{137}Cs + ^{252}Cf (1-5 MeV)

Gauge #3 = conductivity + ^{137}Cs + ^{24}Am

Gauge #4 = ^{137}Cs + ^{252}Cf (1-2 MeV) + ^{252}Cf (2-5 MeV)

Gauge #5 = ^{137}Cs + ^{252}Cf (1-5 MeV) + constant density

† Error = $\left|\frac{\text{actual mass - experimentally determined mass}}{\text{actual mass}}\right|$

TABLE 2.7 - Mass determination from experimentally derived linear equations for eastern coal/refuse/water 18-inch haulage pipe

% Composition by weight Coal/Refuse/Water	Actual Mass g/cm²	Experimentally Determined Mass (g/cm²)					
		Gauge #1*		Gauge #2*		Gauge #3*	
		Mass	Error†	Mass	Error†	Mass	Error†
29/44/27	Coal = 17.36	17.17	(0.011)	18.43	(0.061)	25.42	(0.464)
	Refuse = 26.19	26.55	(0.014)	25.18	(0.039)	21.84	(0.167)
	Water = 15.67	15.67	(0.000)	15.67	(0.000)	11.78	(0.248)
57/9/34	Coal = 28.80	29.65	(0.029)	26.70	(0.073)	23.71	(0.200)
	Refuse = 4.63	3.16	(0.317)	6.38	(0.378)	6.58	(0.421)
	Water = 17.20	17.20	(0.000)	17.20	(0.000)	19.98	(0.162)

* Gauge #1 = conductivity + constant density + ^{133}Ba

Gauge #2 = conductivity + ^{133}Ba + ^{252}Cf (1-5 MeV)

Gauge #3 = ^{133}Ba + ^{252}Cf (1-5 MeV) + constant density

† Error = $\left|\frac{\text{actual mass - experimentally determined mass}}{\text{actual mass}}\right|$

This linear propagation of the error in M_w is indeed favorable, since in most other sensor combinations, a 1% error in count rate can result in a much larger error in M_c, M_r and M_w. This is especially true when two of the gauges provide almost the same information, as in the case of the combination of two gamma gauges such as ^{133}Ba (E_γ = 356 keV) and ^{137}Cs (662 keV), or even ^{241}Am (E_γ = 60 keV) and ^{137}Cs. However, it remained to be seen if the conductivity gauge was anywhere near this reliable.

2.3.3 Simplified Analysis and Error Propagation

The error propagation with the combination conductivity-nuclear gauge is small and linear, with essentially no error amplification ("amplification factor" is approximately unity) because the conductivity gauge provides one of the components, M_w, directly. The transmission of the gamma gauge and the neutron gauge through this thickness of water is calculated, the count rate is essentially corrected for this attenuation by water, and the M_c and M_r are then solved for with a simple 2 x 2 determinant; i.e., the equations have the form

$$M_c = \frac{\begin{vmatrix} c_1 & b_1 \\ c_2 & b_2 \end{vmatrix}}{\begin{vmatrix} a_1 & b_1 \\ a_2 & b_2 \end{vmatrix}} = \frac{b_2 c_1 - b_1 c_2}{a_1 b_2 - a_2 b_1}$$

which is easily handled with a small microprocessor.

In the proposed simple calibration scheme, in which the calibration was carried out when the pipe contained only water, the water attenuation data were provided to a high degree of accuracy. Consequently, the simplified analysis was accurate as well as fast, in terms of microprocessor time.

2.3.4 Accuracy of Prime Candidate

Note that the data of Table 2.7 indicate a high degree of accuracy by gauge no. 2, combination conductivity plus gamma-ray plus neutron gauges. This results from the neutron and gamma gauges having a very different sensitivity

for coal (~40% CH_2 + H_2O) and refuse. The maximum gamma transmission, for a given water volume, occurs for high M_c and low M_r, while this is just the opposite for neutron transmission. This is illustrated in Figure 2.1 of Section 2.2.1, where the gamma and neutron transmission are shown for varying concentrations of water.

2.4 CONCLUSIONS AND RECOMMENDATIONS

Under the Phase I survey, no existing commercial prototype or experimental sensor was found to be capable of adequately measuring the concentration of coal/refuse/water in a slurry pipeline.

As a result of the research conducted during this Phase I, SAIC has conceived and recommends a conceptual three-component (σ, γ, n) sensor design which is based on measurement of the slurry electrical conductivity, measurement of transmitted single-energy gamma rays, and measurement of transmitted neutrons from a ^{252}Cf source. This concept, which is described fully in Section 3, is believed promising for development into a sufficiently accurate sensor for measuring coal/refuse/water concentrations in both research and commercial or control applications. Further, the method requires no a priori or additional information regarding slurry characteristics. If, for any reason, difficulties should arise in developing the method of conductivity measurement, SAIC recommends a two-component (γ, n) sensor concept which is based on measurement of transmitted single-energy gamma rays and measurement of transmitted ^{252}Cf neutrons of all energies.

From the practical standpoint of a commercial sensor, it is exceedingly important to determine during Phase II representative variation of the specific gravity of eastern coal and refuse with mining depth into a <u>given seam</u>. If, at a given face, the specific gravity of coal and refuse varies only a few percent over times for which grab sample determinations of specific gravity are practical, then a simpler, two-component (n, γ) sensor is very likely to suffice. Under the contingent finding of slow variation of specific gravity along a given seam, it is specifically recommended that SAIC would modify the conceptual three-component sensor to a two-component (n, γ) sensor,

retaining the neutron and gamma-ray transmission measurements and eliminating the more problematic, more intrusive and less stable conductivity gauge.

Each of the sensor candidates was evaluated as per Bureau of Mines criteria listed in Table 2.8. A qualitative summary of the sensor evaluation study appears in Table 2.9.

TABLE 2.8 - Evaluation criteria

Performance
- Accuracy
- Range
- Response time

Cost

Safety

Reliability

Applicability to larger lines

Environmental specs

Maintainability

Compatible with mine operation

Calibration

Operational inconvenience

Power requirements

Operation by non-technical personnel

TABLE 2.9. - Evaluation criteria for coal slurry concentration sensor: expected performance

CRITERION	SENSOR TYPE				
	6" (σ+n+γ)	18" (σ+n+γ)	6" (σ+γ)	18" (σ+γ)	6" (2n+γ)
Accuracy (Coal)	3% (R, CM, Ct)	8% (R, Cm, Ct)	7% ($\Delta\rho$=3%)	13% ($\Delta\rho$=3%)	6% (R, Cm, Ct)
Accuracy (Refuse)	3% (R, Cm, Ct)	8% (R, Cm, Ct)	7% ($\Delta\rho$=3%)	13% ($\Delta\rho$=3%)	6% (R, Cm, Ct)
Response Time	Determined by source strength, detector: 0.5s, R; 1s, Cm; 2s, Ct.				
Range	0/100% to 100/0% Coal/Refuse Proportion 0-80% Wt. Concentration of Coal, Refuse (Blockage Limited)				
Fluctuation:					
Coal Specific Gravity	±20%	±20%	± 3%	± 3%	±20%
Refuse Specfic Gravity	±20%	±20%	± 3%	± 3%	±20%
Cost	Moderate	High	Low	Moderate	Mod. to High
Safety					
Shield Size Required	Moderate	Large	Small	Small	Mod. to Large
Source Encapsulation					
Fire Proofing	Excellent	Excellent	Excellent	Excellent	Excellent
Explosion Proofing	Excellent	Excellent	Excellent	Excellent	Excellent
Source Shield					
Gamma-ray shield (Fire, explosion) Neutron Shield (Fire, explosion)	Lead may melt: can use tantalum or sintered tungsten. Tantalum or tungsten shield is very explosion proof. Benelex may char. Encase in stainless steel housing for both fireproofing and explosion proofing.				
Reliability:	Good	Good	(Good if $\Delta\rho \leq$ 3%)		Needs engineering
Applicability to larger lines	Good	Good	Good	Good	Not applicable
Environmental Specs	Fair	Fair	Good	Good	Fair
Maintainability	Good	Good	Good	Good	Fair
Compatible with mine operations	Good	Good	Good	Good	Fair
Calibration	Good (100% W)	Good (100% W)	Good (100% W)	Good (100% W)	Poor (Complex)
Operational Convenience	Good	Good	(Must sample ρ_C, ρ_R)		Poor
Power Requirements	Modest	Modest	Modest	Modest	Modest
Operation by non-technical personnel	(Easy calibration)		(Requires careful ρ-sampling)		Difficult

NOTE: (1) 6" (σ+n+γ) means conductivity + neutron + gamma-ray sensor for 6-inch pipe. n = Cf-252 neutron source, γ = Cs-137 gamma-ray source.

(2) 6" (2n + γ) means sensor utilizes two energy bands (1-2 and 2-5 MeV) from Cf-252 neutron source and one energy band from Cs-137 gamma-ray source.

(3) 3% (R, Cm, Ct) in "Accuracy" row, means 3% accuracy for research, commercial and control sensors.

(4) $\Delta\rho \leq 3\%$, in "Reliability" row, means specific gravity (ρ) for both coal and refuse are assumed to vary by 3% or less, as averaged over sampling volume (i.e., 1 sec at 20 ft/sec = 20 ft. sampling "tube").

(5) (100% W), in "Calibration" row, means that the calibration cycle is pushbutton-initiated when it is certain that the pipe contains 100% water.

3.0 SUMMARY OF PHASE II DEVELOPMENTAL WORK

The final design of the nuclear and conductivity gauges at the onset of Phase II followed the preliminary feasibility studies of Phase I. The design of both the gamma-ray and neutron gauges had to be very stable and had to accommodate high count rates because of the following:

- The low density of coal, as immersed in water.
- The requirement of a one-second measurement time.
- The high accuracy called for in the final concentrations ($\pm$ 3%).

A new gauging concept was developed by SAIC to achieve this high required stability and statistical accuracy. The stability was measured to be ~1% over a measuring period of about one month in outdoor use at the Colorado School of Mines Research Institute (CSMRI). The weather conditions varied from hot, sunny afternoons to snow blizzard conditions. This kind of stability (and speed: one-second measuring intervals) will meet hands-off operating conditions in a mining environment.

In addition, a very simple calibration method was developed which, with the microprocessor, will merely consist of pressing a "calibration" button when 100% water is assuredly in the line.

The conductivity gauge, as developed by a laboratory at Santa Ana, California (near Los Angeles) proved to be useless. The water volume, as measured by a flow diversion into an accurate gravimetric tank, was fed into the calculator manually instead of via the runs at CSMRI. These runs proved the nuclear gauges to be adequate for 2-3% accuracy in the concentrations when the water volume is known to 1% or better.

After failure of the conductivity gauge, the SAIC group at La Jolla, California, undertook to develop a workable unit. It was subsequently learned that there was a large number of problems with the conductivity gauge as

developed by the Santa Ana laboratory. These were associated with the following factors:

- Complete removal (99+%) of solids from the slurry liquid routed to the conductivity reference cell.
- Blockage of the clarifier line feeding the reference cell.
- Temperature difference between the slurry water and the reference-cell water (2% conductivity change per $1^{o}C$ was measured for water over a large range of conductivities and temperatures).
- Gain drifts of the conductivity gauge electronics.
- Nonlinearities in the electronics.
- "Tracking" of the reference cell and conductivity gauge cell with 100% water, but with changing conductivities (achieved by adding San Diego tap water to distilled water, and further by adding NaCl).

The SAIC group at La Jolla investigated two slurry-water clarification methods: the cyclone separator and the sintered-metal filter.

The cyclone separator utilized a large-area screen with 160 micron (μ) mesh to separate out the coarser materials and to thus avoid blocking the cyclone. A slurry pump following the 160μ filter provided a 50 psi pressure drop across the cyclone separator. According to the manufacturer's specifications, the cyclone filter should separate out most of the rock (refuse) particles below 5μ size and most of the coal particles above 8μ size with a 50 psi pressure drop. A partial separation of coarse and fine particles was achieved for 10 weight % slurries, but only about 30% removal was achieved: better than 99% removal is required. The cyclone failed for three reasons: (1) it does not appear to work well with a solids concentation much above 1%, above which particle-particle collisions become important in destroying the laminar flow regime; (2) the <u>fines</u> concentration of <u>refuse</u>, after wetting down (our Pittsburgh-seam samples had a high content of what appears to be <u>fine</u> friable rock), contains a large fraction of particle with particle size below 5μ; and the 160μ prefilter blocked up permanently at the high slurry solids concentrations even with a backflush device in use.

Tests were carried out on a sintered-metal filter using both a 0.5 and 5 "mesh" filter. Samples of pulverized coal and pulverized rock were passed through the 1-inch test line at Mott Metallurgical Corp., and clear samples of water were drawn through the Mott sintered-metal filters without permanent blockage after about 1 1/2 shifts (12 hours) of operation. The pulverized-coal (-100 mesh) loading was (22/0/78) and the pulverized-rock (-100 mesh) loading was (0/35/65). Subsequent tests were made at SAIC, as described below, with a test-cell geometry that kept the test cell very near the Mott filter and, therefore, kept the slurry-line to reference-cell temperature difference negligibly small. Gain drifts and nonlinearities in the conductivity gauge electronics were improved dramatically. The blocking of the filter was greatly reduced by backflushing and by periodic cleaning in an ultrasonic bath as discussed below.

With these improvements, a set of successful measurements at the CSMRI 6-inch test loop was completed.

3.1 THE INDIVIDUAL RADIATION GAUGES: DESCRIPTION

In this section, the three individual gauges developed to measure C/R/W concentrations are described. The three-component slurry, with coal and rock of unknown densities, requires three different and very independent datum points (responses) for each concentration. This is achieved with a gamma-ray, a neutron, and a conductivity gauge.

The degree to which very independent data points or responses are achieved with gamma-ray and neutron sensors is illustrated in Figure 3.1, where the straight-line semilogarithmic response of ln (count rate) for neutrons is seen to decrease with increasing water content plotted linearly, while the opposite is true for the gamma-ray behavior. Since the conductivity gauge measures the water volume ($M_w = V_w$ since the specific gravity of water is unity) directly, the two nuclear gauges utilize this data directly to provide the M_c and M_r values used to calculate the C/R/W concentrations.

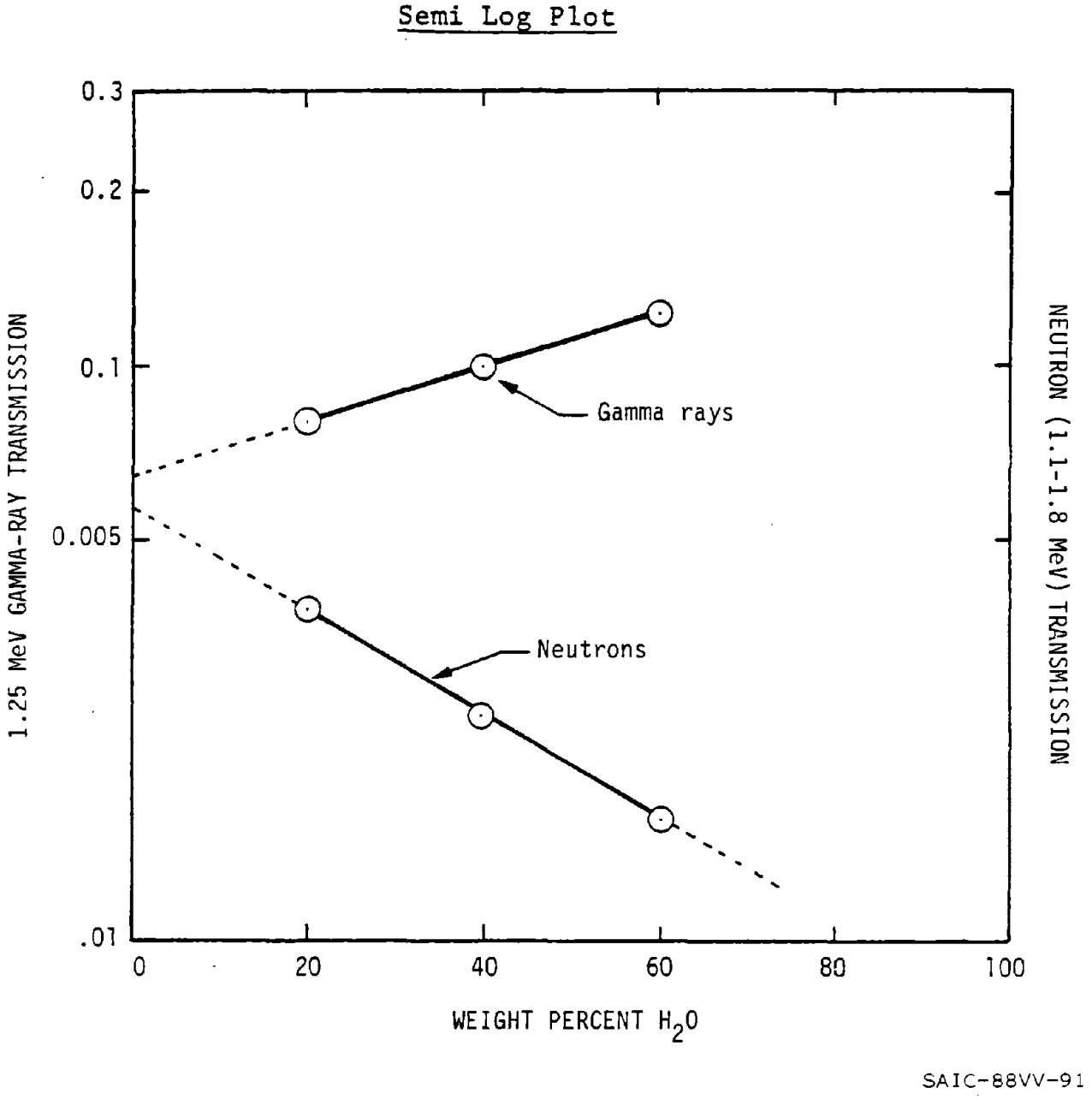

FIGURE 3.1. - Relative sensitivities of neutron and gamma-ray responses to water concentration (6-inch pipe).

As discussed in Section 3.4, the nuclear gauges have the following responses:

$$\sigma_C^{\gamma} M_C + \sigma_R^{\gamma} M_R + \sigma_W^{\gamma} M_W = \frac{\ln N_{\gamma} - I_{\gamma}}{S_{\gamma}} \qquad (2)$$

for gamma rays, and

$$\sigma_C^{n} M_C + \sigma_R^{n} M_R + \sigma_W^{n} M_W = \frac{\ln N_{n} - I_{n}}{S_{n}} \qquad (3)$$

for the neutron gauge.

Here, σ_i^{γ} is the gamma-ray macroscopic cross section for coal, etc., while N_{γ} is the gamma-ray count rate, I_{γ} the intercept of the gamma-ray response obtained from the count rate of the (0/0/100) slurry (100% water), S_{γ} the slope of the response curve, and similarly for the neutron response equation. By inserting M_w into Eq. 2 and Eq. 3, the only two unknowns are M_c and M_r. These are solved with a simple 2 x 2 determinantal equation, as discussed in Section 2.3.3.

3.1.1 The Gamma-Ray Gauge

Figure 3.2 shows the gamma-ray sensor, as clamped onto a 6-inch slurry line with a quick-clamp arrangement. It consists of three cesium-137 gamma-ray sources (0.662 MeV gamma-ray energy, 1.0 millicurie strength each, and 30-year half-life) that penetrate the slurry, and a single 1 1/2-inch diameter x 1 1/2-inch-long NaI (Tl) detector optically coupled to a photomultiplier tube with preamplifier. The heater strip has a miniature, solid-state temperature

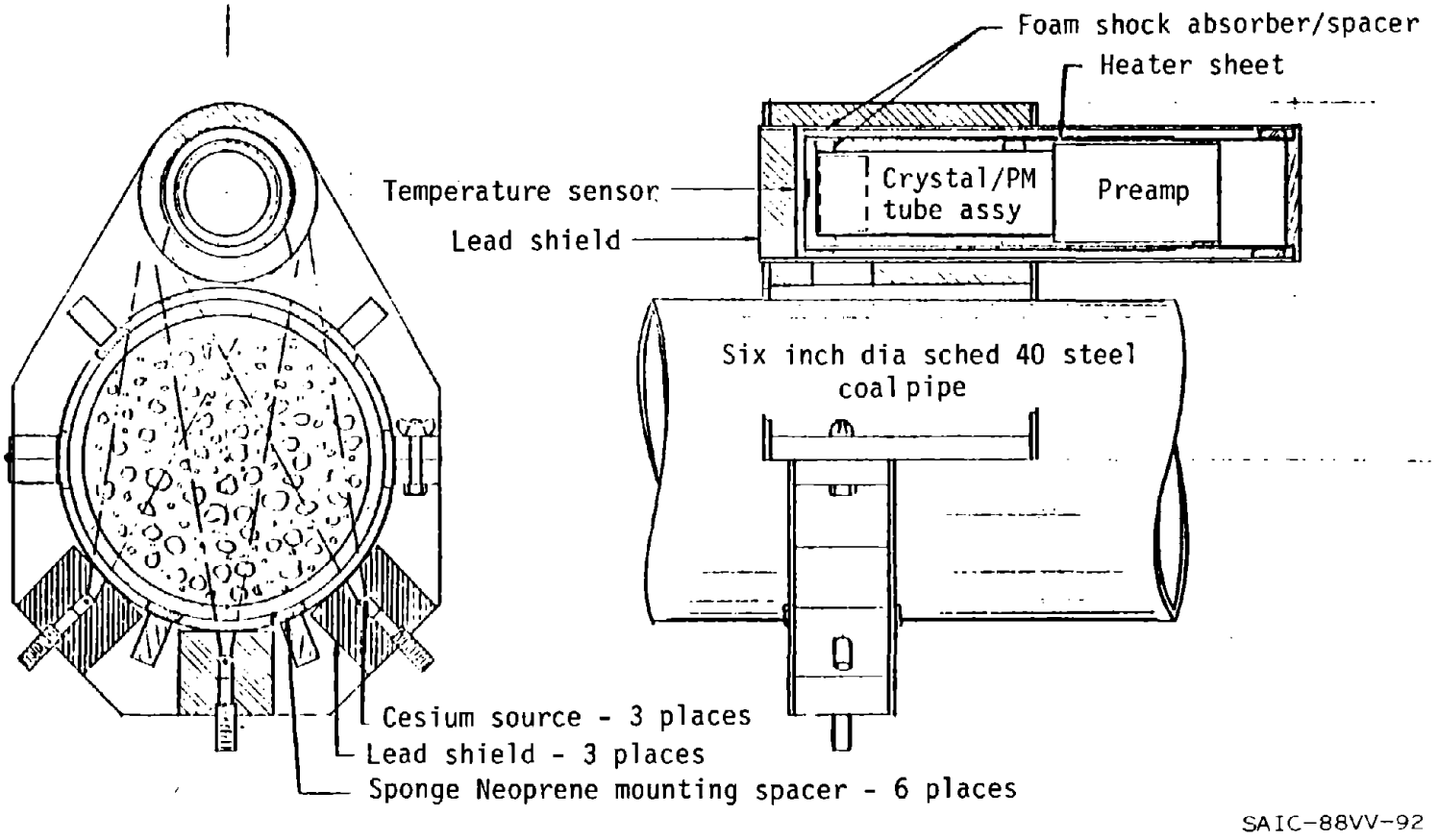

FIGURE 3.2. - Gamma detector assembly coal slurry measurement expt.

controller to keep it at $100^0 \pm 2^0$ F for good gain stability for outdoor use over a large range of weather conditions. Lead shielding around the sources makes them accessible with safe radiation levels nearby.

The response of the gamma-ray gauge, shown in Figure 3.3, is seen to have only a moderately steep slope. This means that a very high stability detector is required. The response is also seen to be linear when plotted as ln (N_γ) versus Mass * Cross Section ($\mu_i \xi_i$). This was achieved with the SAIC high-stability design, which filters out low-energy scattered gamma rays that would otherwise spoil the excellent straight-line response.

The moderately steep slope (versus a desired very steep slope) of the gamma-ray response signifies that a very good counting statistical accuracy is also required to achieve an accurate concentration for a 1-second count rate.

The concentration error associated with a 1% statistical error (10,000 counts per second for a 1-second count time) was seen to be about 2-3% for one standard deviation in concentration. A somewhat smaller statistical error is desired, which means the source strength and/or the detector sensitivity should be doubled over the present value. A correspondingly larger count rate will be designed into any future gauge.

The count rate stability, with the present gamma-ray sensor operated in outdoor environments, was better than 1% in a large variety of weather conditions. This is adequate, considering that the calibration, carried out with 100% water in the line, should be done every few days and can be accomplished with a simple pushbutton operation with microprocessor control to be instituted in the later design.

Note that the present design of gamma-ray gauge only requires about 4% of the gamma-ray source strength of the standard present-day gauges, such as the Ohmart, and yet has 10 to 100 times faster response, a much greater long-term stability, a very linear response in semilogarithmic coordinates, and (consequently) is very easily calibrated. This is the type of gauge needed for blockage measurements, or for coal-mass determinations in a coal-water slurry where little or no rock is present and where the specific gravity, averaged

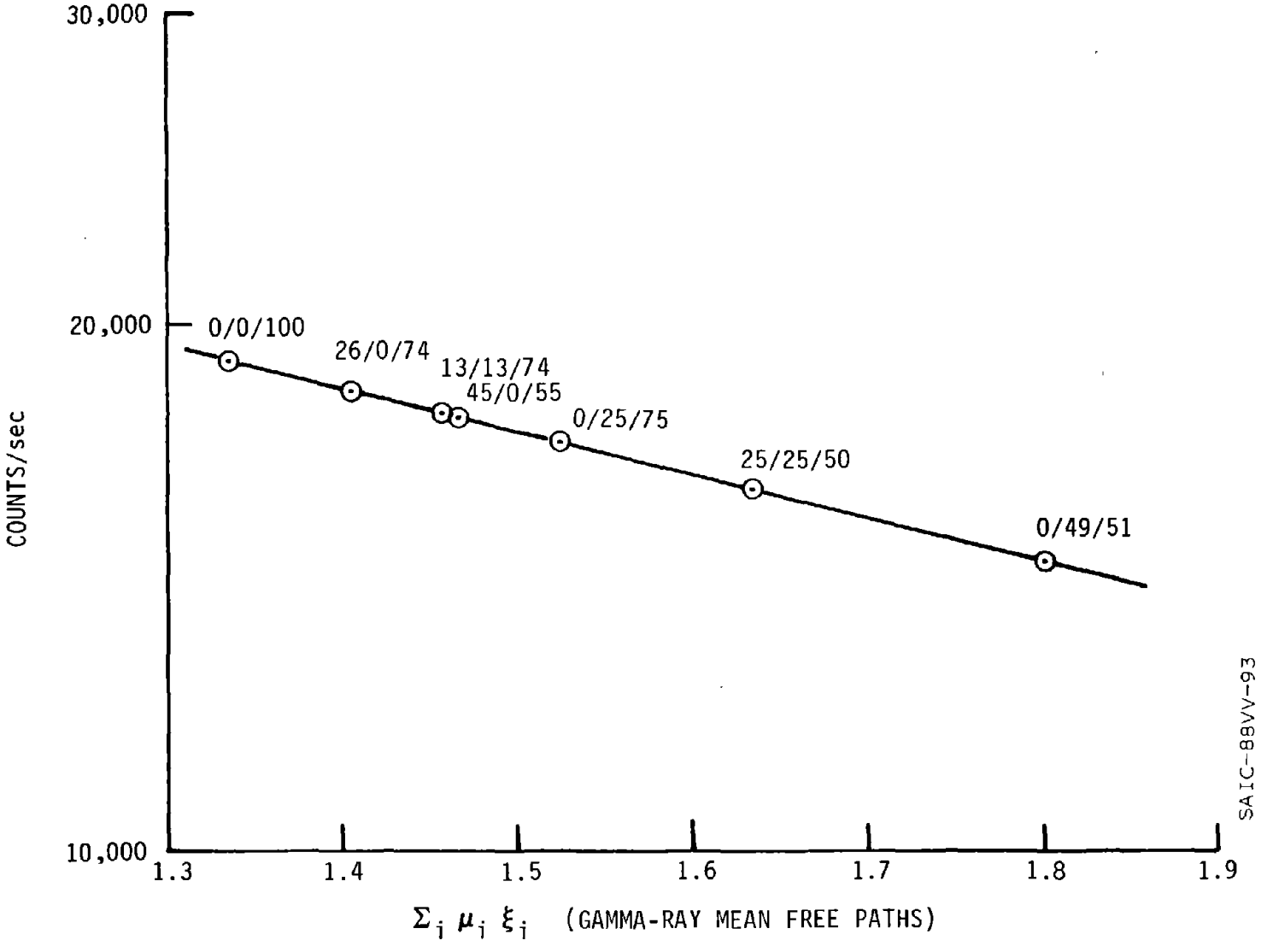

FIGURE 3.3. - Slurry gamma ray (3 mCi ^{137}Cs) response function.

over a 4- to 20-foot length of slurry ("sausage") that is measured every 1-second time interval, is nearly constant from one "sausage" to the next. The high accuracy requirement derives from the low "differential" specific gravity of coal in water (0.35 for coal versus 1.54 for rock for the Pittsburgh seam coal and rock used in the Phase II measurements).

3.1.2 The Neutron Gauge

A drawing of the neutron gauge is shown in Figure 3.4. It consists of a single 5.5 microgram (μgm) Californium-252 source whose neutrons penetrate the haulage pipe, the slurry, and a low-energy cutoff borated-epoxy filter. After the borated filter, the higher energy neutrons that penetrate the filter are moderated in the epoxy moderator where they are then easily detected by ^{3}He-filled neutron detectors. As in the gamma-ray detector, the individual neutron counts are measured and summed up over a counting period of 1 second.

The inherent stability of the SAIC neutron gauge design shown in Figure 3.4 is excellent, being better than 1% per month of operation in an outdoor environment under a large variety of weather conditions. The installation is very simple, since the gauge is of the quick clamp-on configuration.

The neutron-gauge design shown in Figure 3.4 was the result of an extended set of neutron transport calculations and precision measurements carried out in the design phase of this program, Phase I. The resultant counter configuration is not only extremely stable, it yields a straight-line response of $\ln(N_n)$ versus $\mu_i \xi_i$, as shown in Figure 3.5. Here N_n is the neutron count rate and $\mu_i \xi_i$ is the product of the macroscopic cross section μ_i (in units of cm^2/gm) and ξ_i, the thickness of the slurry "column" penetrated by the neutrons (in units of gm/cm^2).

As in the gamma-gauge, the response function is not extremely steep. This requires 1/2% to 1% accuracy in counting statistics for an accuracy in the concentration of 2-3% for a 6-inch haulage pipe. Thus, the counts per 1-second counting time must fall between 10,000 and 40,000. About 20,000 counts per second will be achieved in the delivered gauge.

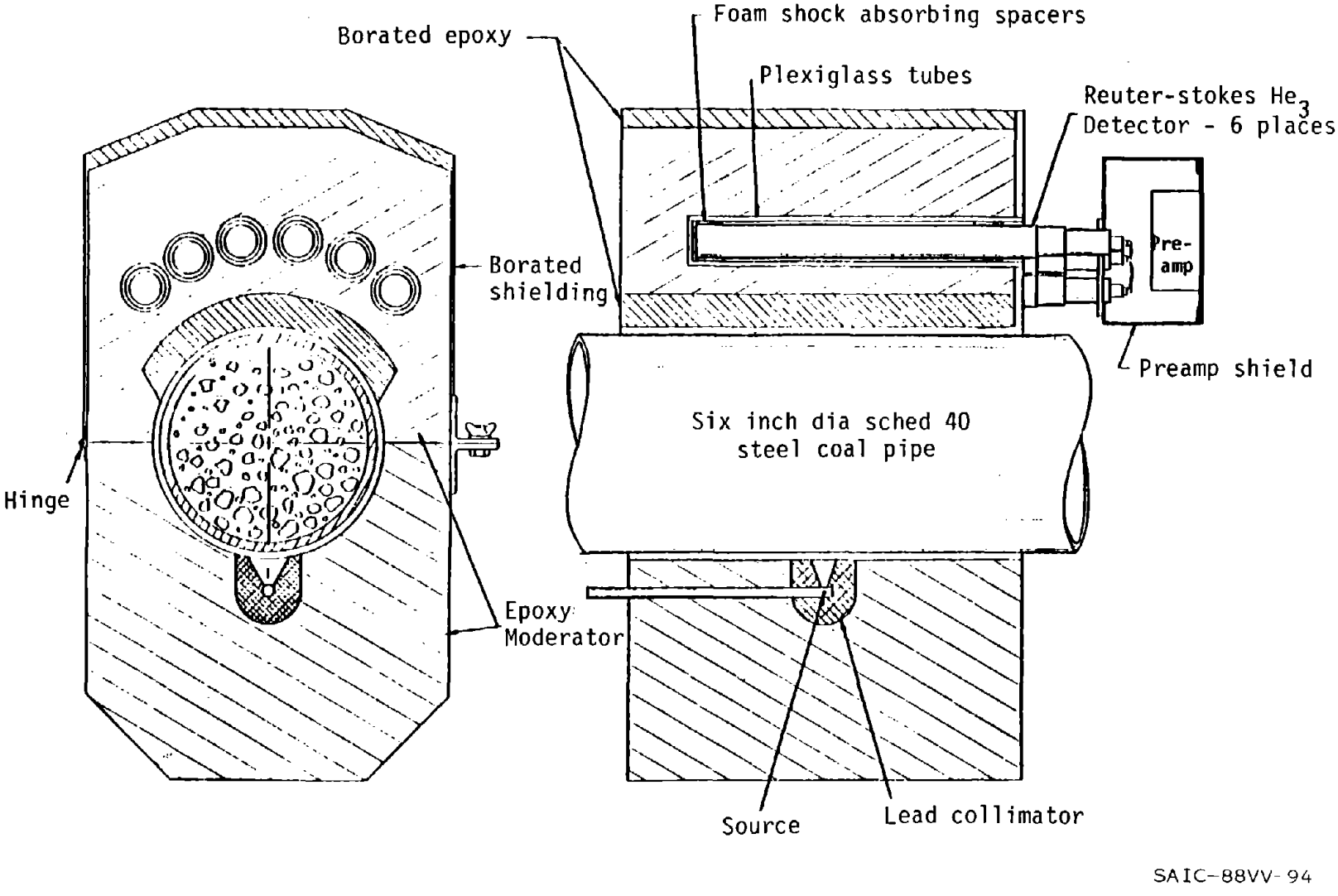

FIGURE 3.4. - Neutron detector assembly coal slurry measurement expt.

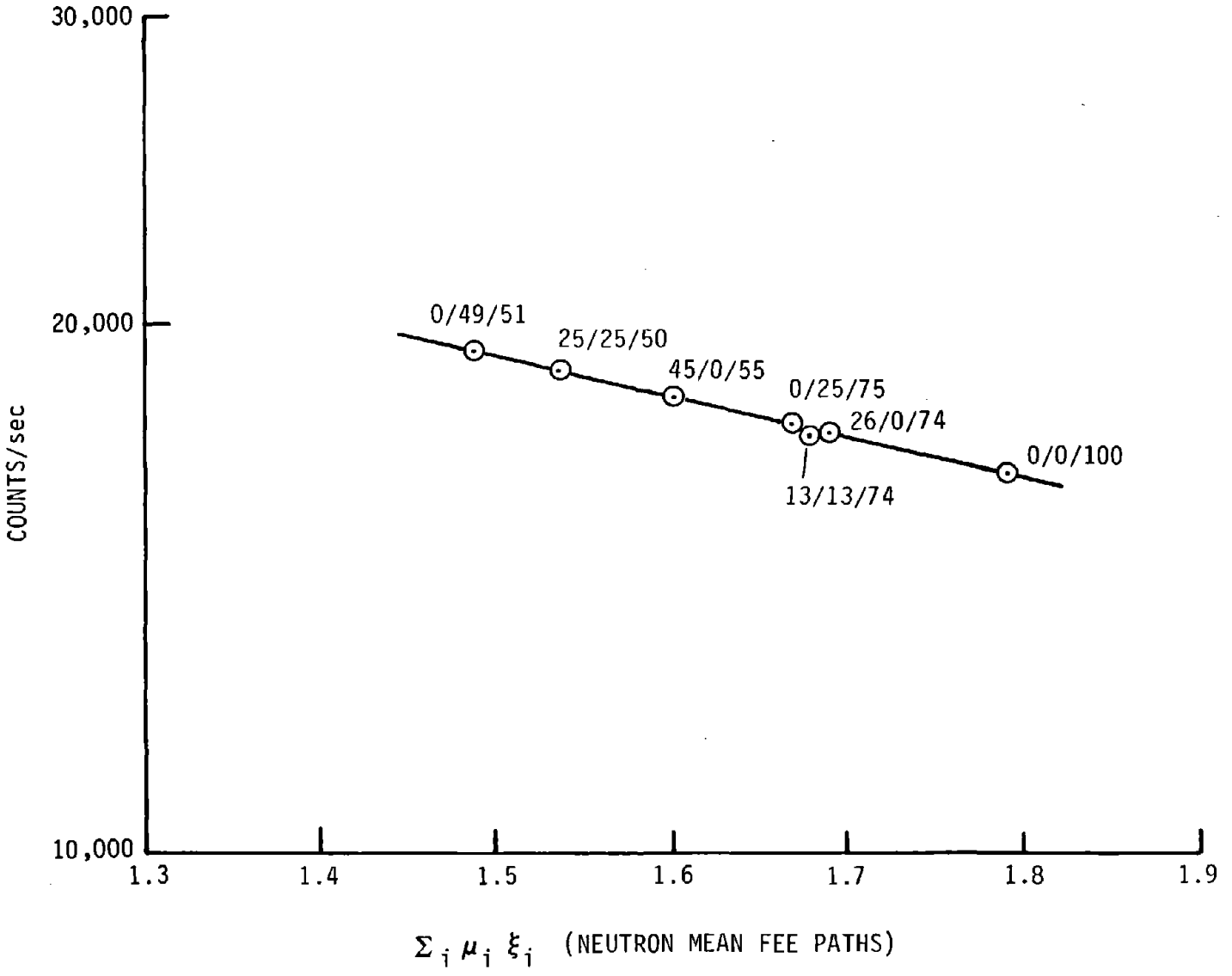

FIGURE 3.5. - Slurry neutron (5 $\mu g^{252}Cf$) response function.

Note that the quick clamp-on neutron and gamma-ray detectors are sufficient for a two-component slurry (such as coal/water or any ore/water) when the densities are not known or vary a lot.

3.2 CONDUCTIVITY SENSOR

3.2.1 Description

By measuring the conductivity of slurry and comparing it to the conductivity of the carrier fluid, the volume ratio of the fluid V_w may be determined. SAIC has designed a sensor that is capable of making such determinations. It consists of three major components--a main gauge, reference gauge and the associated electronics. In principle, a high-frequency AC signal is established between two electrically isolated (except for the fluid) points. An AC signal is required to prevent any voltaic effects. As the resistance of the fluid changes, so does the signal; hence, the output of the circuit. In fact, the output is linearly related to the conductivity. The output from the main gauge is divided by that for the reference gauge to give the fluid volume fraction V_w.

The slurry conductivity is measured between an electrically isolated, conducting ring and the remainder of the piping system. Figure 3.6 depicts the design of the main gauge, which has a stainless steel band centrally mounted in a 36-inch-long PVC spool piece. This design offers the advantage of total electrical isolation of the central conductor, with no chance of grounding the signal. Hence, no special precautions need be taken when mounting this section.

To measure the conductivity of the carrier fluid, a particle-free stream must be withdrawn from the slurry to eliminate these solids. Three systems were designed and tested. One utilized a knockout pot, the second a cyclone, and the third a sintered metal filter. Only the sintered metal filter proved capable of removing the fine particulates expected during operation.

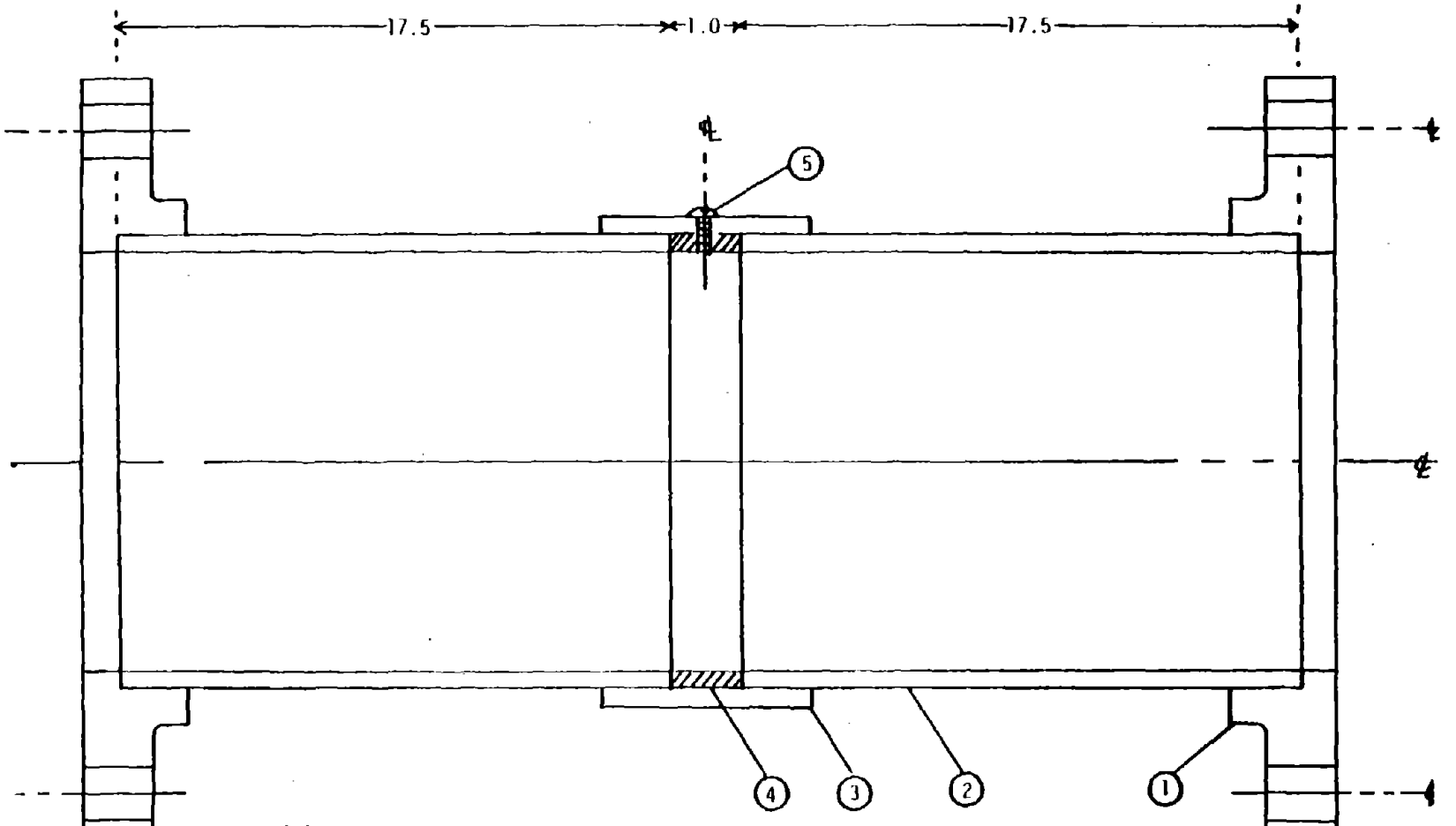

FIGURE 3.6 - Main conductivity gauge.

The electronics have two similar circuits--one for the main gauge and one for the reference gauge--whose output is proportional to the conductivity. To give the volume percent, V_w, the main gauge signal is simply divided by the reference signal. Figure 3.7 details the electrical circuitry used to measure the conductivity. The circuitry consists of an AC oscillator that sends an AC voltage across both main gauge and reference cell. The current passing through each cell is proportional to the conductivity. This current, converted to a voltage by an amplifier (one for each cell), outputs the voltage signal to a voltage-to-frequency converter. The main gauge and reference cell voltage-to-frequency converters (V/F converters), each with a calibration pot (to produce the same output frequency when 100% water is in the slurry line), are counted for one-second time intervals (to produce an averaging of the conductivity over the one-second sampling time) by two scalers of the scaler-timer system attached to the two V/F converters. Two other such scalers are used to count the gamma-ray gauge and the neutron gauge counts. All four scalers input these counts (one-second count intervals) into the programmable calculator (HP 9815) described in Section 3.4 below.

3.2.2 Testing

The conductivity gauge components were tested at three separate locations:

- Mott Laboratories in Connecticut
- SAIC Laboratory in San Diego
- Colorado School of Mines Research Institute in Golden, Colorado

The objective of the tests at the Mott facilities was to confirm the applicability of using a sintered-metal filter on coal and rock slurries. At the SAIC laboratories, the three major components of the gauge were integrated to insure proper functioning. The CSMRI tests confirmed the integration of the conductivity gauge with the multi-component gauge.

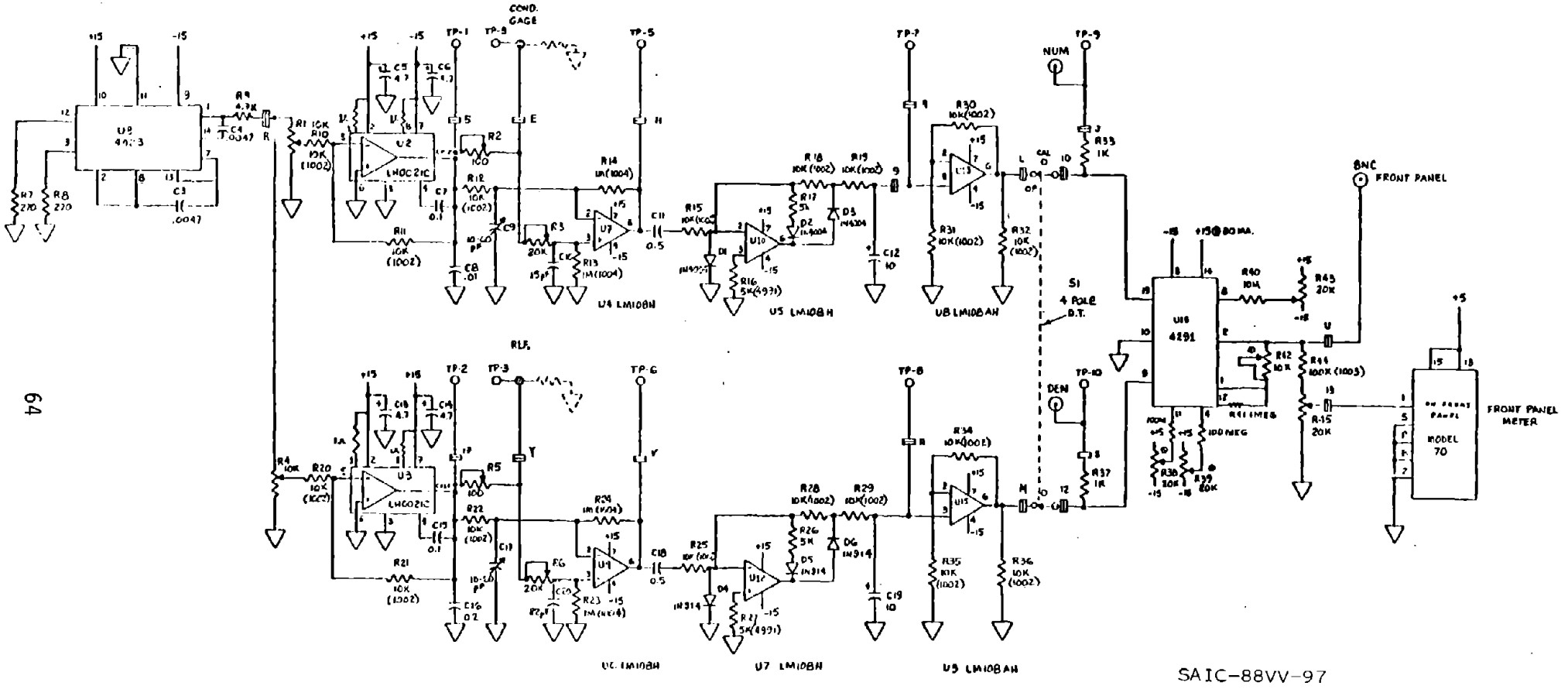

FIGURE 3.7. - Schematic diagram of conductivity gauge electronics.

3.2.2.1 Sintered-Metal Filter Verification Tests

Two sintered-metal-filter elements (Figure 3.8) were tested by their manufacturer, Mott Metallurgical Corp., to determine their operating characteristics in coal and rock slurries. From the resulting operating parameters, an assessment of the filters' ability to provide a particle-free stream to the reference cell could be made.

Figure 3.9 details the test apparatus used, and Table 3.1, the test conditions and results. In all tests, the back-flush was maintained at a constant 3/4-second, 50-psi pulse every 5 or 10 minutes. Additionally, each filter was cleaned after each test.

The clarification results far surpass the maximum turbidity (solids contamination) requirements of 0.1% to 0.5%. The volume flow rate appears limited by the rock to 2 cc/min for the 3/4-inch^2 filters. The blow-back renewed both filters. Based upon these encouraging results, a system utilizing these filters was designed.

3.2.2.2 Reference Gauge Performance and Integrated Tests

A 3/4-inch slurry test loop (Figure 3.10) was assembled at SAIC instrument development laboratory in San Diego to test the performance of two reference gauge designs. The best design was then integrated with the main gauge and the electronics to insure proper performance and linearity at CSMRI, and its response time measured. An additional test was conducted to determine the effect of temperature on conductivity.

3.2.2.3 Mott Sampling System

The Mott sampling system utilizes a spring-loaded cam-driven hydraulic cylinder to withdraw a 40 cc liquid sample through the Mott sintered-metal filter and to backwash the filter. Figure 3.11 gives a schematic of the system, Figure 3.12 details the hydraulic cylinder assembly, and Figure 3.13 details the Mott filter with integral conductivity gauge (first design).

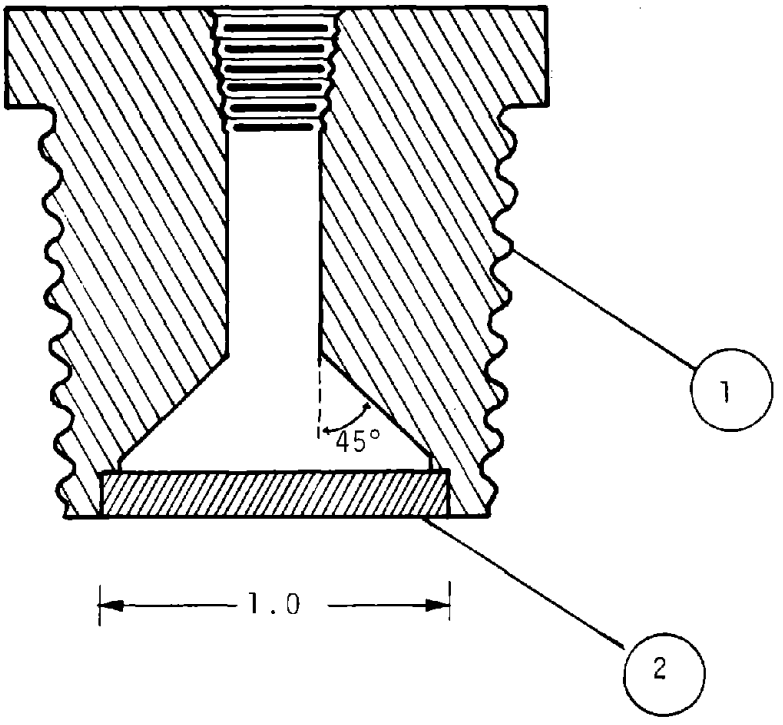

SAIC-88VV-98

1- 1x¼ NPT Bushing 316SS

2- 1/8 x 1 Sintered metal disk 316SS

FIGURE 3.8. - Mott sample filter.

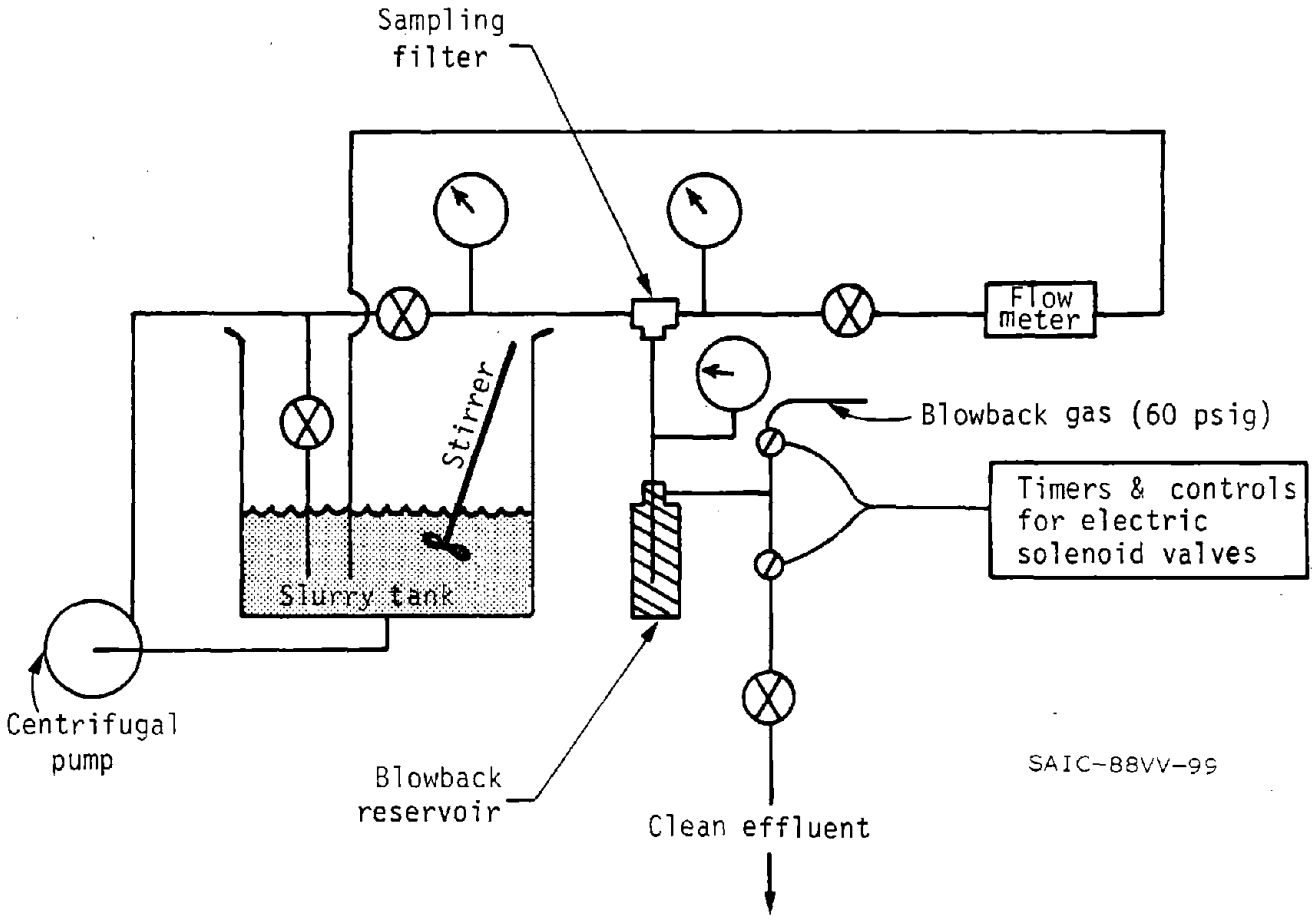

FIGURE 3.9. - Test arrangement for Mott sintered-metal filter clarifier.

TABLE 3.1 - Test conditions and results for the sintered metal filter verification test

Run No.	Particle type	Slurry concentration	Stream Velocity fps	Filter type μ	Filtered flow rate cc/min	Pressure drop across filter psi	Turbidity ppm	Run time hrs.
1	Coal*	20 Vol. %	4	0.5	4.7	13	14	3½
2	Coal	20 Vol. %	4	5.0	4.3	13	10	2
3	Coal	10 Vol. %	10	5.0	7.8	27	14	2½
4	Coal	10 Vol. %	10	0.5	6.5	27	17	2
5	Rock**	20 Vol. %	10	0.5	2.1	30	5	1½
6	Rock	20 Vol. %	10	5.0	2.0	29	5	1½
7	Rock	10 Vol. %	4	5.0	2.0	16	6	1½
8	Rock	10 Vol. %	4	0.5	2.3	16	4	1½

*100 mesh, p=1.34g/cc
**100 mesh, p=2.54g/cc

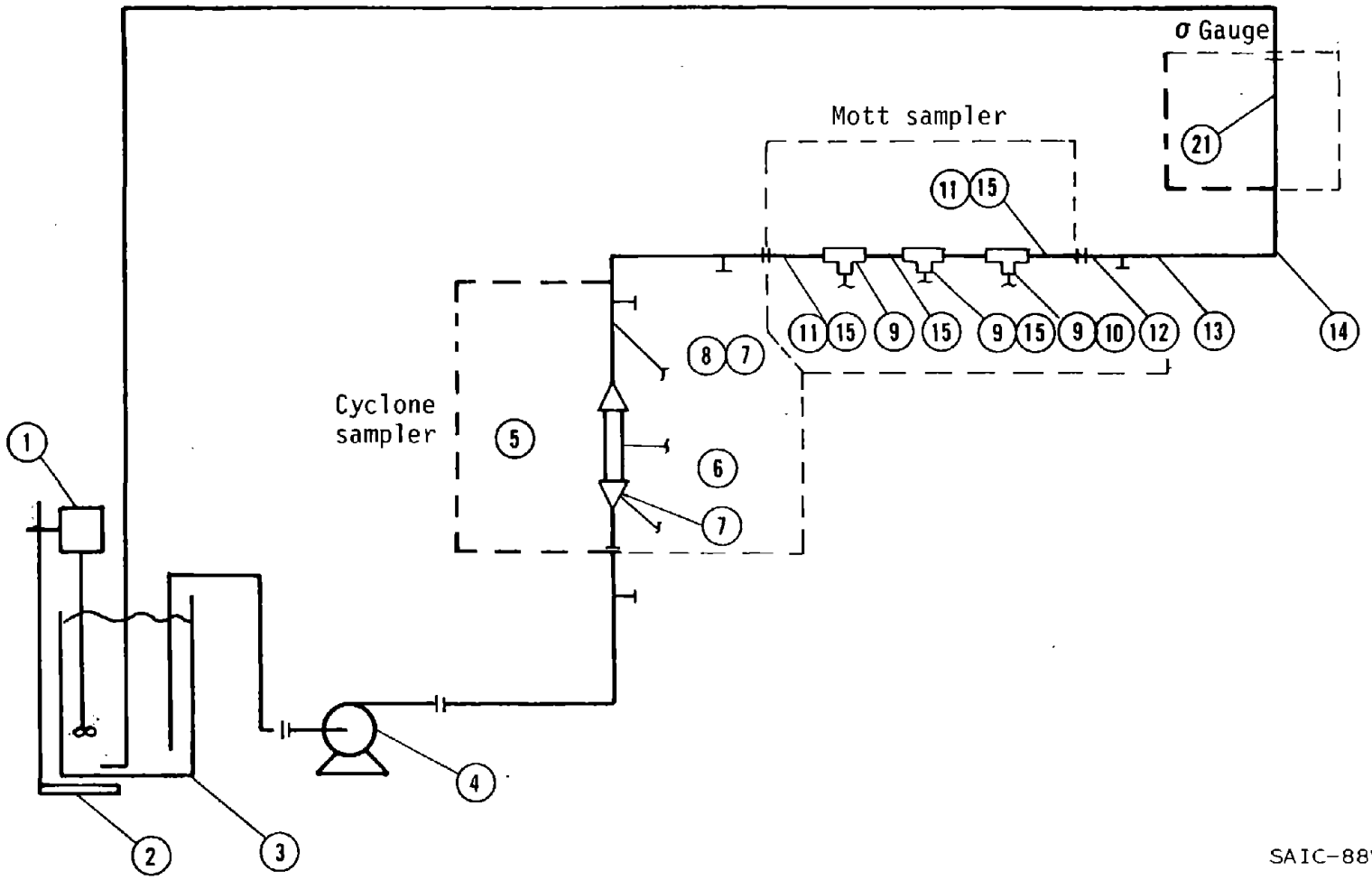

1	Stirrer	6	(2) Male connector	11	(2) Bell reducer 1" x 3/4"
2	Ring stand	7	Male connector	12	(8) Union 3/4"
3	25 gal. can	8	'Y' connector	13	(30') Pipe PVC 3/4"
4	Pump (9 gpm)	9	(3) 'Tee' 1" NPT	14	(15) Elbows PVC 3/4"
5	Screen section	10	Bushing 1" x 1/4"	15	(4) Nipple 1" NPT x 6"

FIGURE 3.10. 3/4" Test loop.

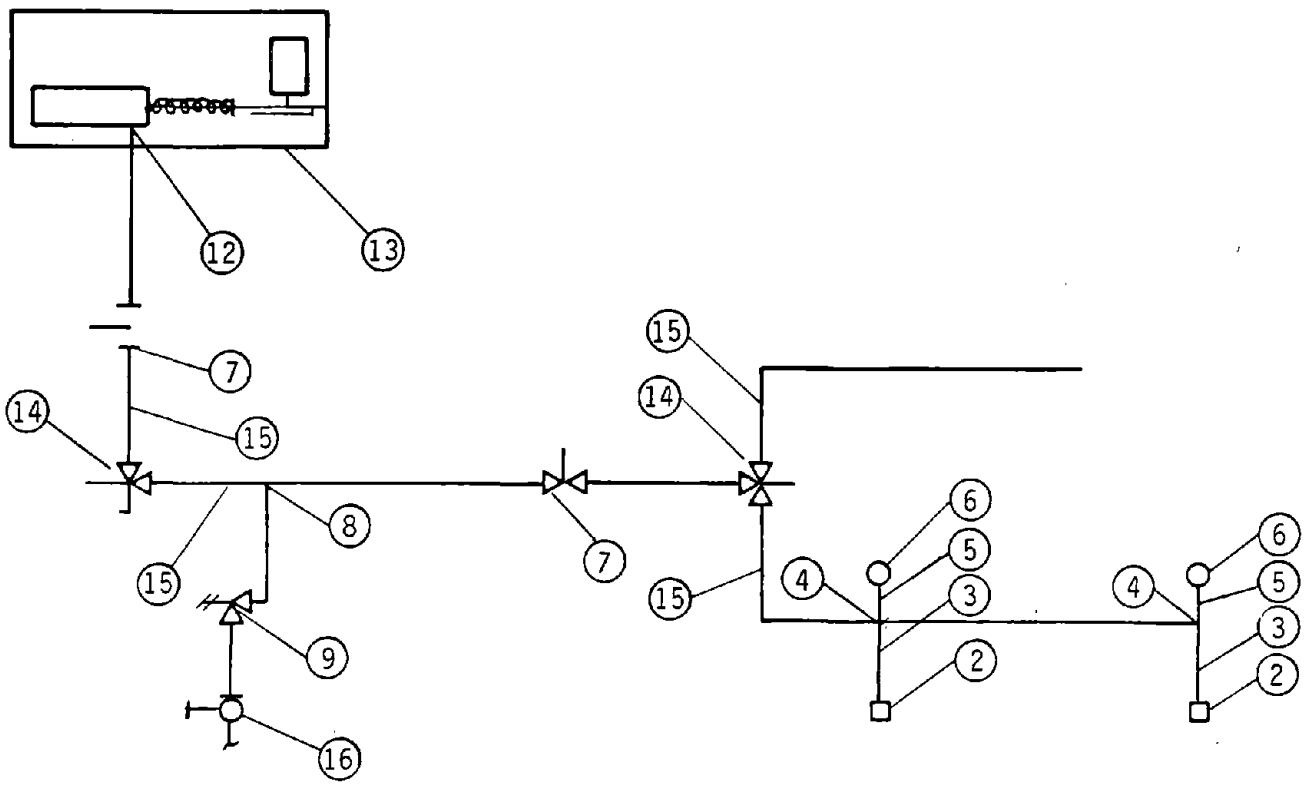

SAIC-88VV-101

1. Not used
2. (2) Mott filter
3. (2) Male run tee
   3/8 x 1/4 NPT 600-3TMT
4. (2) Reducer 1/4 x 3/8
   (2) Reducer 1/8 x 3/8
5. (2) Teflon ferrules
6. (2) Conductivity probe
7. (2) Regulating valve
8. Female branch tee
   1/4" NPT NuPro
   50-15-PSID
10. Not used
11. Not used
12. Male connector 3/8" x 1/2" NPT
13. Pump assembly
14. (2) 3-way ball valve 1/4"
15. (4) Reducing port connector 3/8" x 1/4"
16. Ball valve whitey 1/4" NPT

FIGURE 3.11 - Schematic of reference gauge.

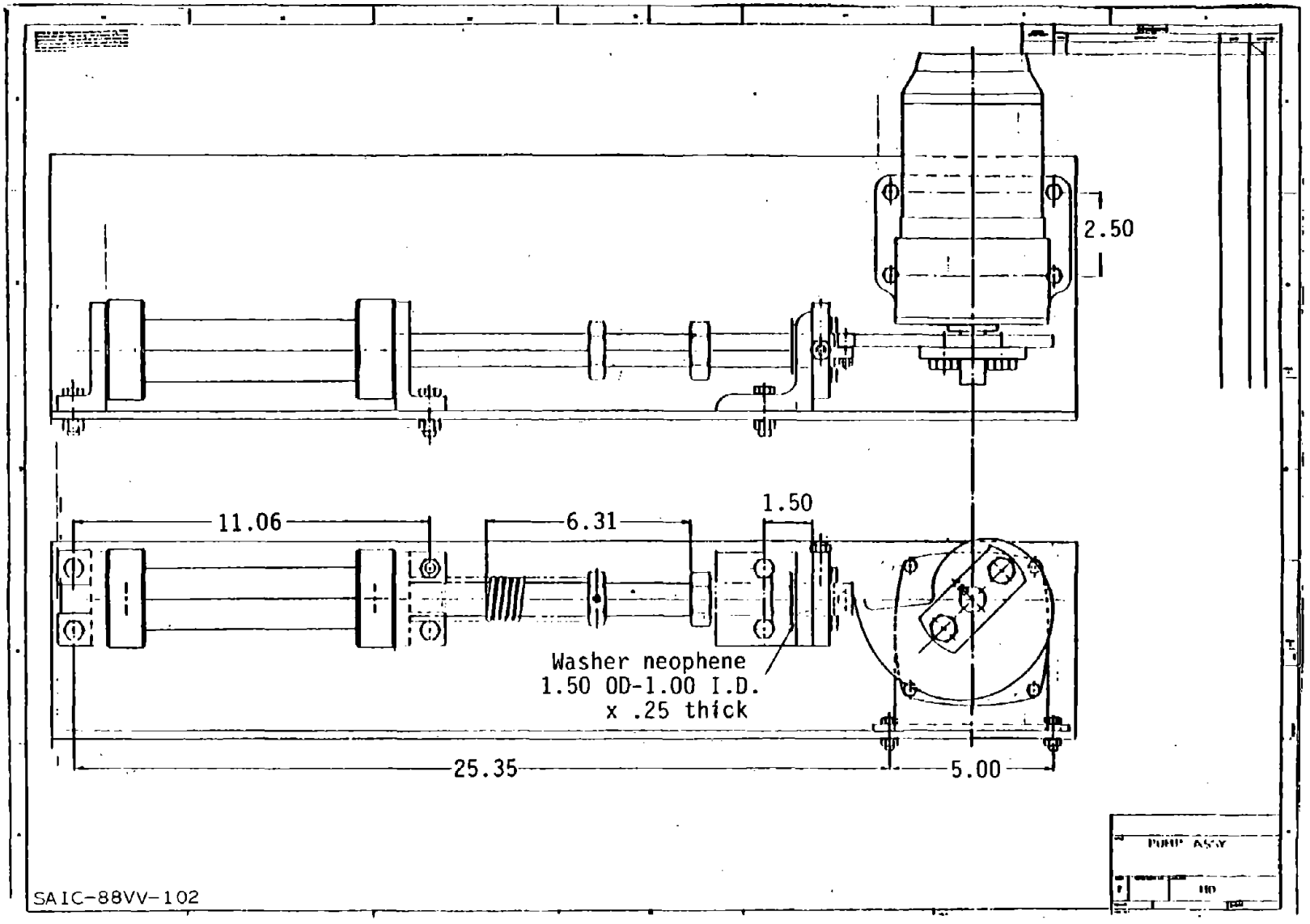

FIGURE 3.12.- Details of the hydraulic cylinder assembly.

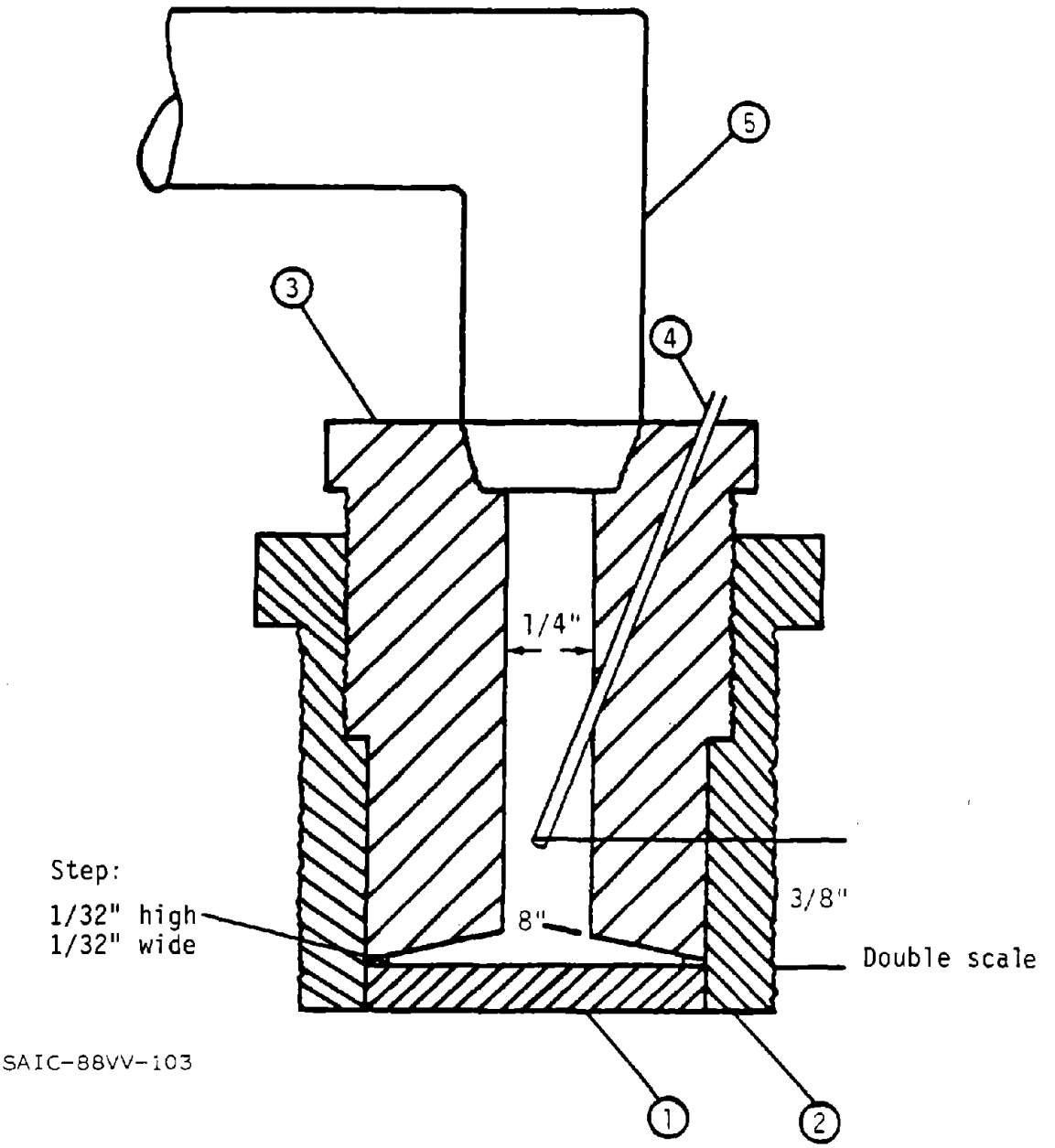

1. Mott 1/8" .5μ sintered metal disk 7/8" dia. (use existing filter).
2. Bushing 1" NPT x 3/4" NPT 316 S.S. (use existing filter).
*2 3. Bushing 3/4" NPT x 1/4" NPT custom (made from PVC "plug" or nylon cylinder).
*2 4. Wire probe 1/32" dia 316 S.S.
*2 5. Male elbow 1/4" NPT x 1/4 400-2-4 Nylon or PVC.

FIGURE 3.13. - Mott filter and reference gauge first design.

The shakedown tests with water provided the following observations:

- Bubbles rising through the conductivity gauge cause erroneous readings. (During the tests at CSMRI, when running with approximately 10 vol. % air in the main line, no air was sucked into the reference system.)
- Cavitation can occur if the flow demand by the cylinder exceeds the rate through the filter. The system was modified as shown in Figure 3.14 to insure that cylinder suction pressure does not fall below 1 psig.
- The response of the cells is less than one minute (Figure 3.15).

To provide the conductivity of the slurry in the 3/4-inch loop for comparison with the reference cell conductivity, a gauge (Figure 3.16) similar to the 6-inch main gauge was installed in the horizontal section. When 10 volume percent coal was added to the system, the gauge indicated 82% on both the 1/2 and 5 cells, as modified per Figure 3.17. To insure that the flow was homogeneous, an identical main gauge was installed in a vertical orientation. The reading remained the same.

To resolve this discrepancy, the output of the main gauge and of the reference gauge were checked against the conductivity of 100% tap water, and 50% tap water and 50% distilled water. A possible non-linear response was noted. To verify this non-linearity and to establish the cause of it, the output of the 6-inch gauge, the 3/4-inch gauge, the Mott gauge (modified to be similar in construction with the main gauge--Figure 3.17), and ten specially constructed gauges (Figure 3.18) were measured for seven ratios of tap and distilled water. All measurements were made on the numerator circuit without adjusting the driving voltage. Figure 3.19 gives the results.

Next, the driving voltage on the 3/4-inch gauge was increased to 9, then to 12, volts with 100% tap water. Figure 3.20 shows this effect.

Finally, the #6 cell voltage with tap water was set equal to the 6-inch gauge voltage (4.33). Their ratio varied from .96 to 1.02, and are shown in Figure 3.21.

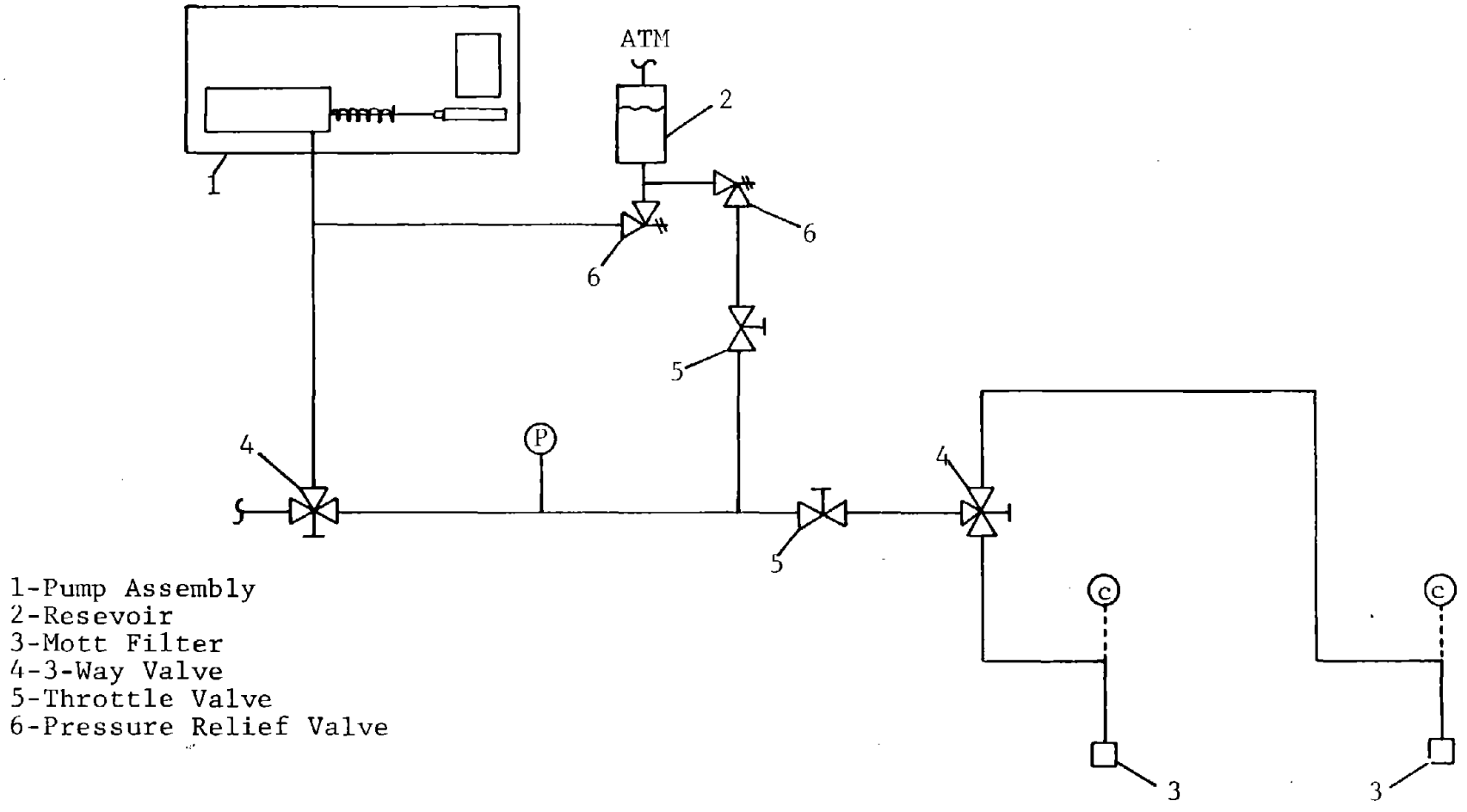

FIGURE 3.14.- Modified hydraulic circuit.

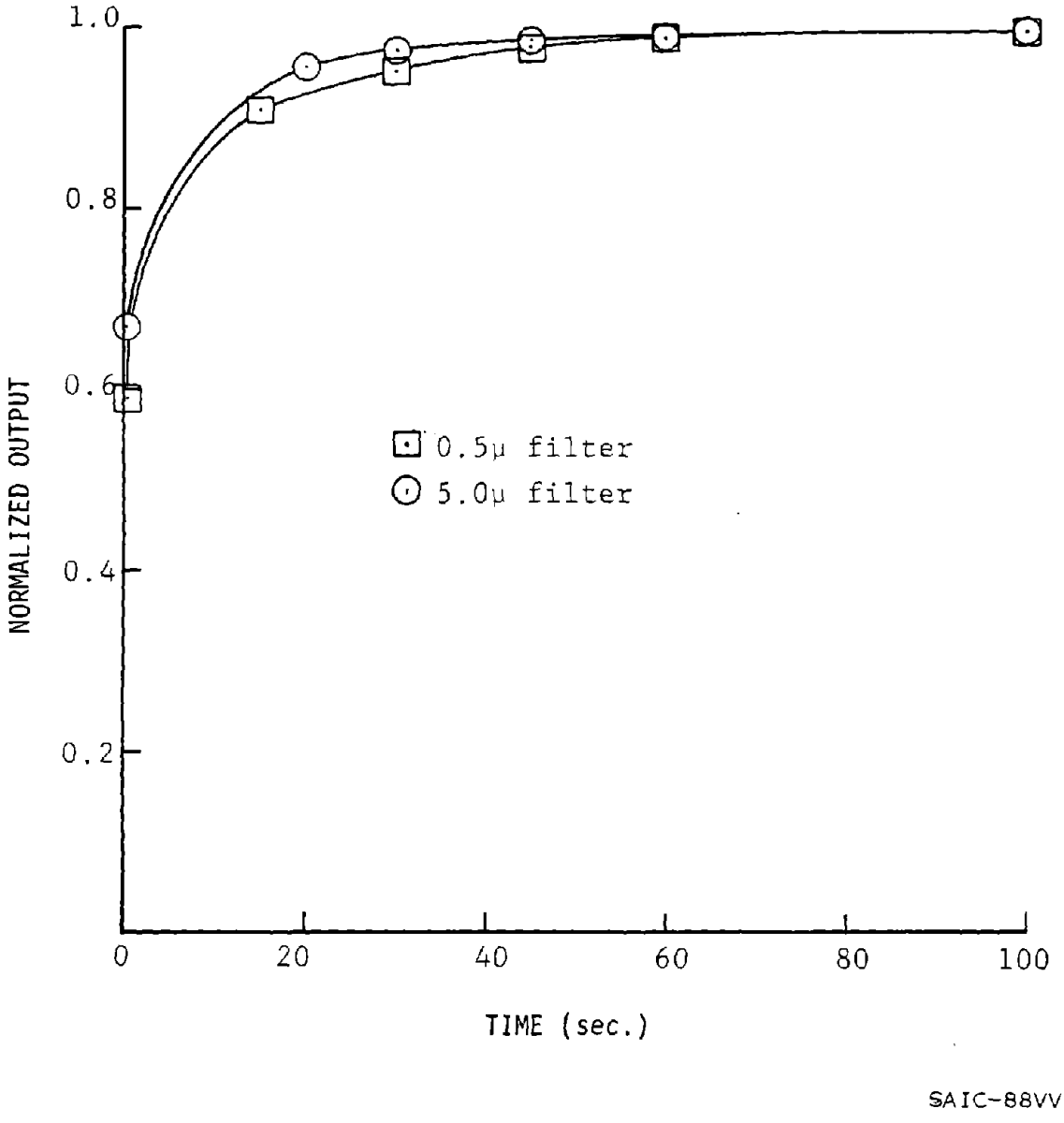

FIGURE 3.15. - Filter response.

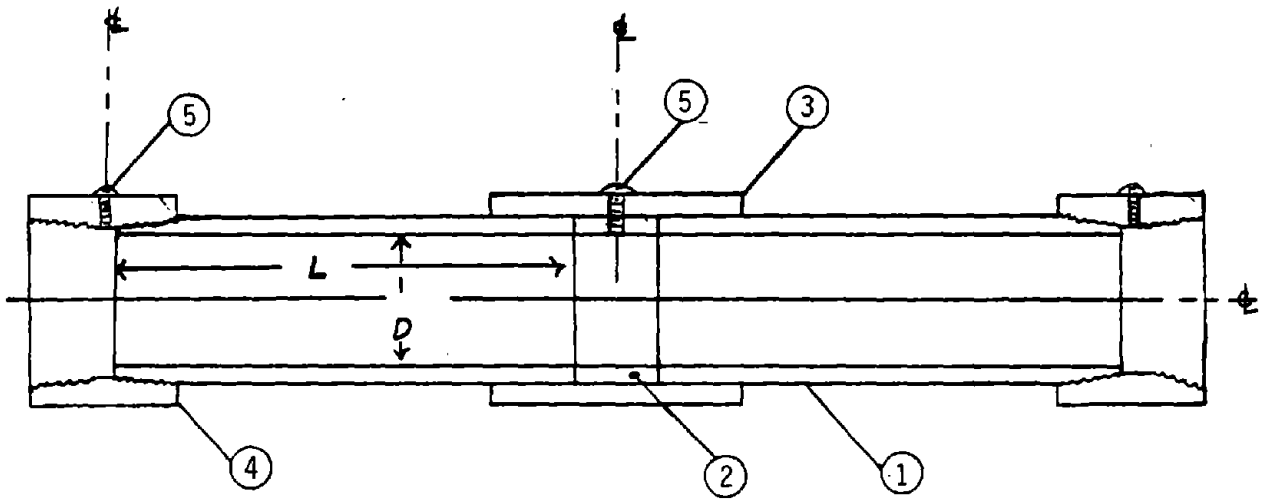

L = 2" FULL SCALE

1 (2) Pipenipple 3/4" NPT ach 40 PVC
2 Pipe section 3/4" NPT sch 40 S.S.
3 Pipe coupling 3/4" PVC
4 (2) Pipe coupling 3/4" NPT S.S.
5 (3) 10-32 Machine screw

FIGURE 3.16. – 3/4" Conductivity gauge.

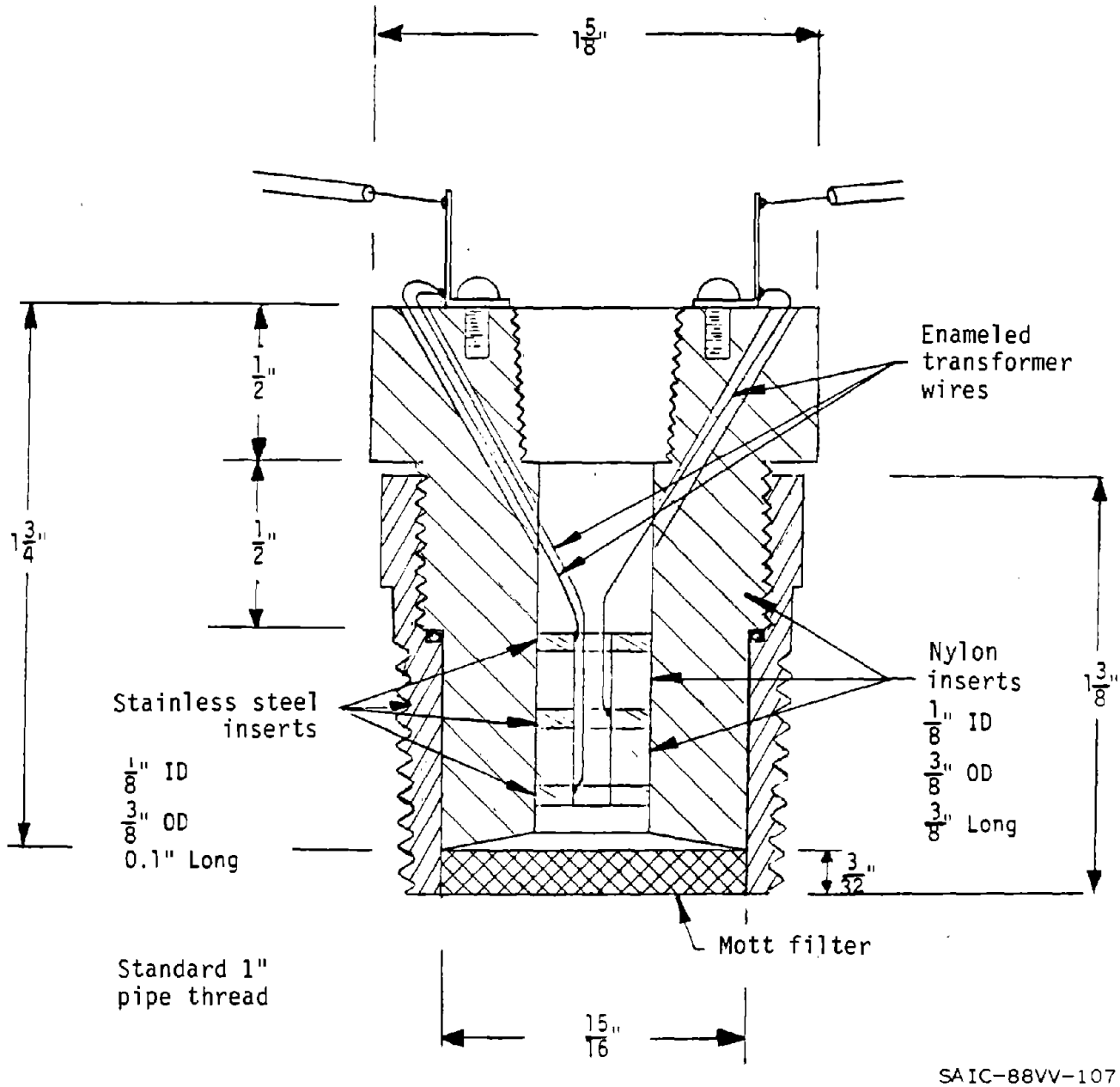

FIGURE 3.17.- SAIC filter and reference cell.

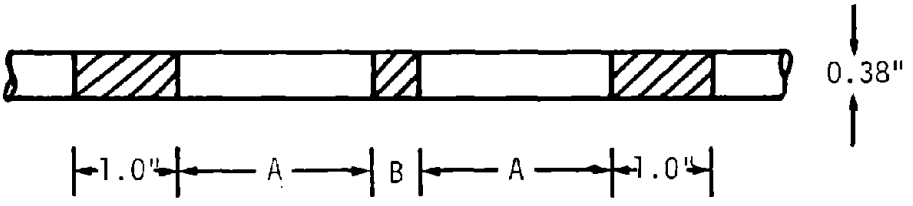

CELL*	A	B
1	2.0	1.0
2	2.0	0.8
3*	2.0	0.6
4*	2.0	0.4
5	2.0	0.2
6	1.0	1.0
7*	0.8	1.0
8	0.6	1.0
9*	0.4	1.0
10	0.2	1.0

*Not Used

SAIC-88VV-108

FIGURE 3.18. - Conductivity gauge.

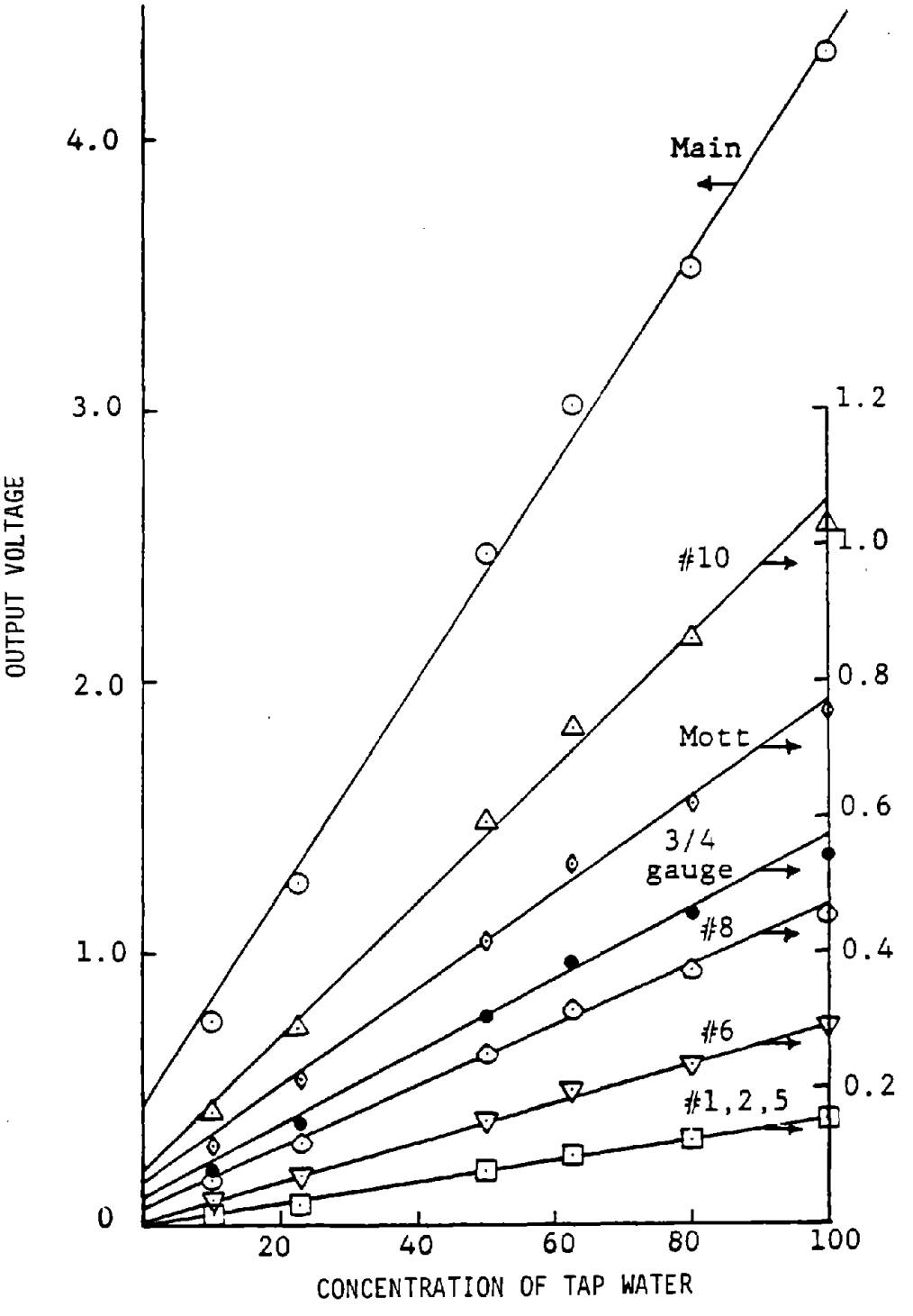

FIGURE 3.19. - Cell linearity results.

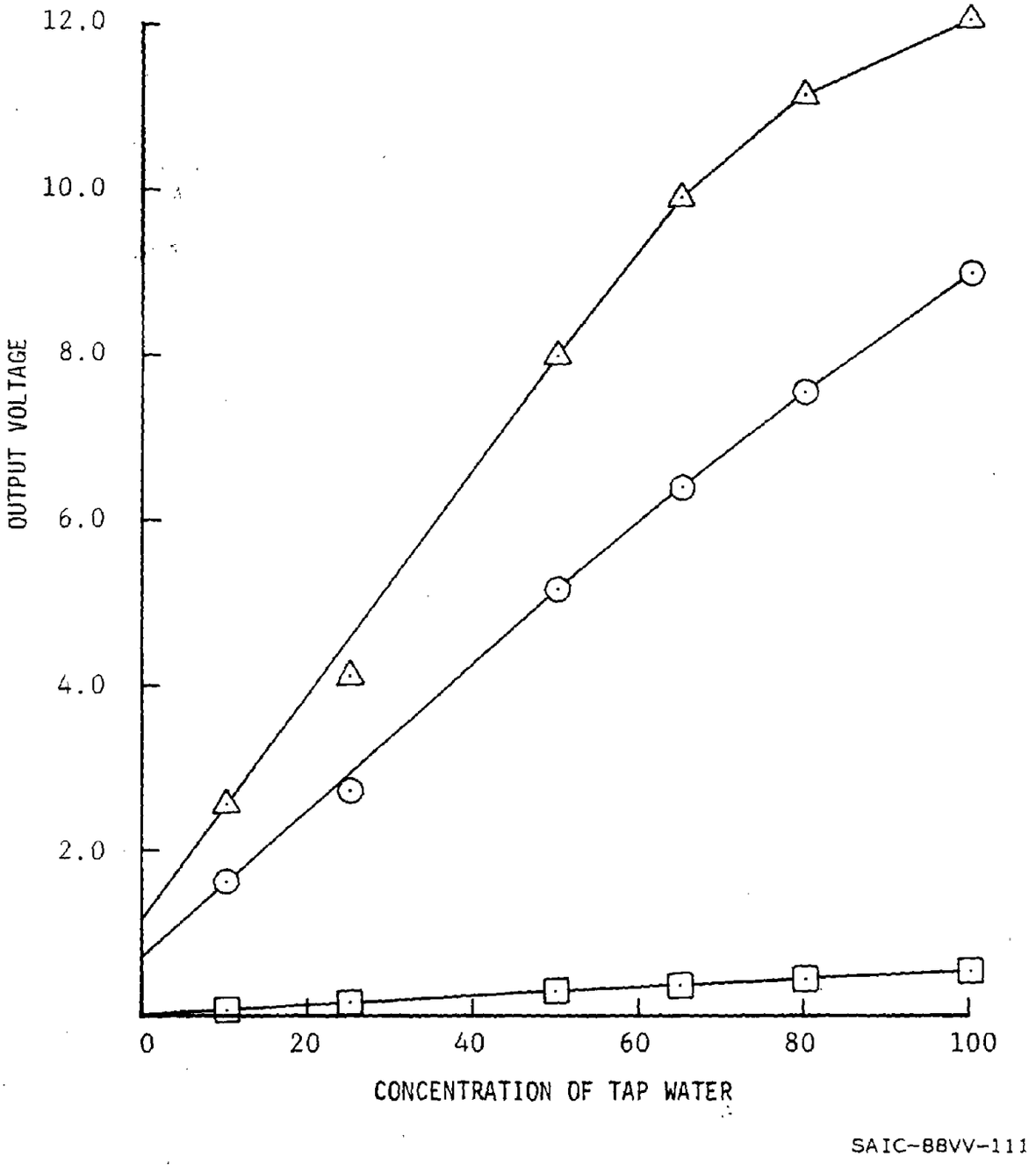

FIGURE 3.20.- 3/4"Cell linearity at 0.5, 9, 12 VDC driving voltage.

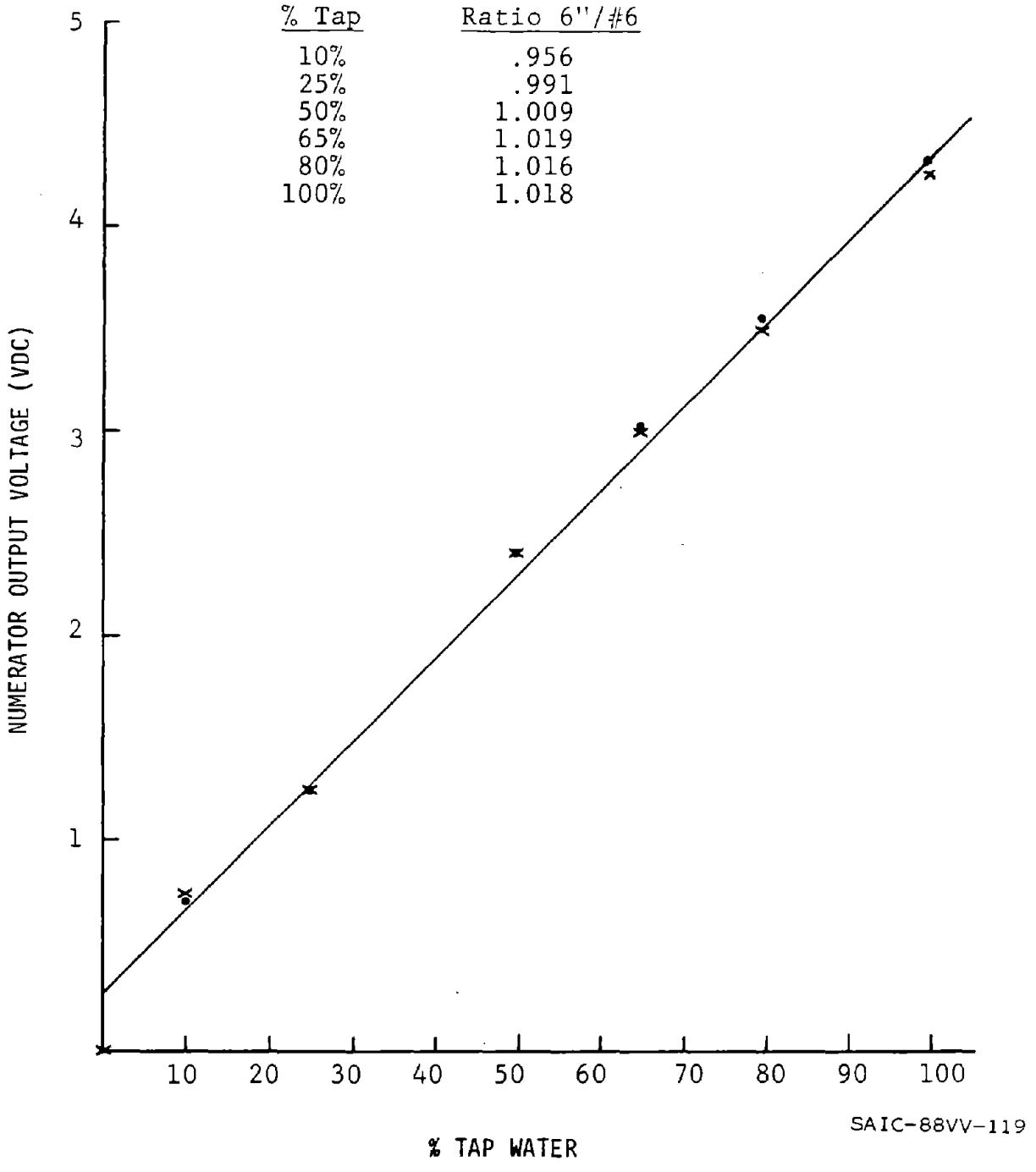

FIGURE 3.21.- Ratio of 6 in. main gauge to #6 cell.

From these tests, we concluded* that:

1. Very little drift occurs in the electronics.
2. The width of the center conducting band is not a factor.
3. The width to diameter of the insulating band below an L/D of 2.6 affects the linearity of the gauge. Therefore, the cell configuration must be scaled.
4. Increases in the driving voltage above approximately 4 VDC give increasing non-linearity with the electronics set as per these tests (see below).

Based upon these conclusions, two cells were made with the exact dimensions of the #6 cell, and two were scaled down to fit into the Mott cell. They were designated M1, M2, Mott 1 and Mott 2 (see Figure 3.17).

Figure 3.22 gives the effect of temperature on conductivity.

3.2.2.4 Conductivity Gauge Performance and Integration
(Tests Conducted at CSMRI, Golden, Colorado)

The integrated conductivity gauge (main gauge, reference gauge and electronics) was taken to CSMRI for testing on a 6-inch IPS loop, along with its companion nuclear gauges. Together the three gauges--conductivity, neutron and gamma--comprise the multi-component gauge. This section will discuss the shakedown and calibration tests for the conductivity gauge.

The gauges were installed in the lower horizontal run, and the test loop was filled with low conductivity tap water and the reference gauge purged. Initial tracking measurements were made between the four reference gauges (Table 3.2). Next, the reference gauges were compared with the main gauge and, based upon these results (Figure 3.23), it was concluded that the numerator electronics were misaligned.

* Based on tests done during the CSMRI test, these effects could have been caused by electronic misalignment.

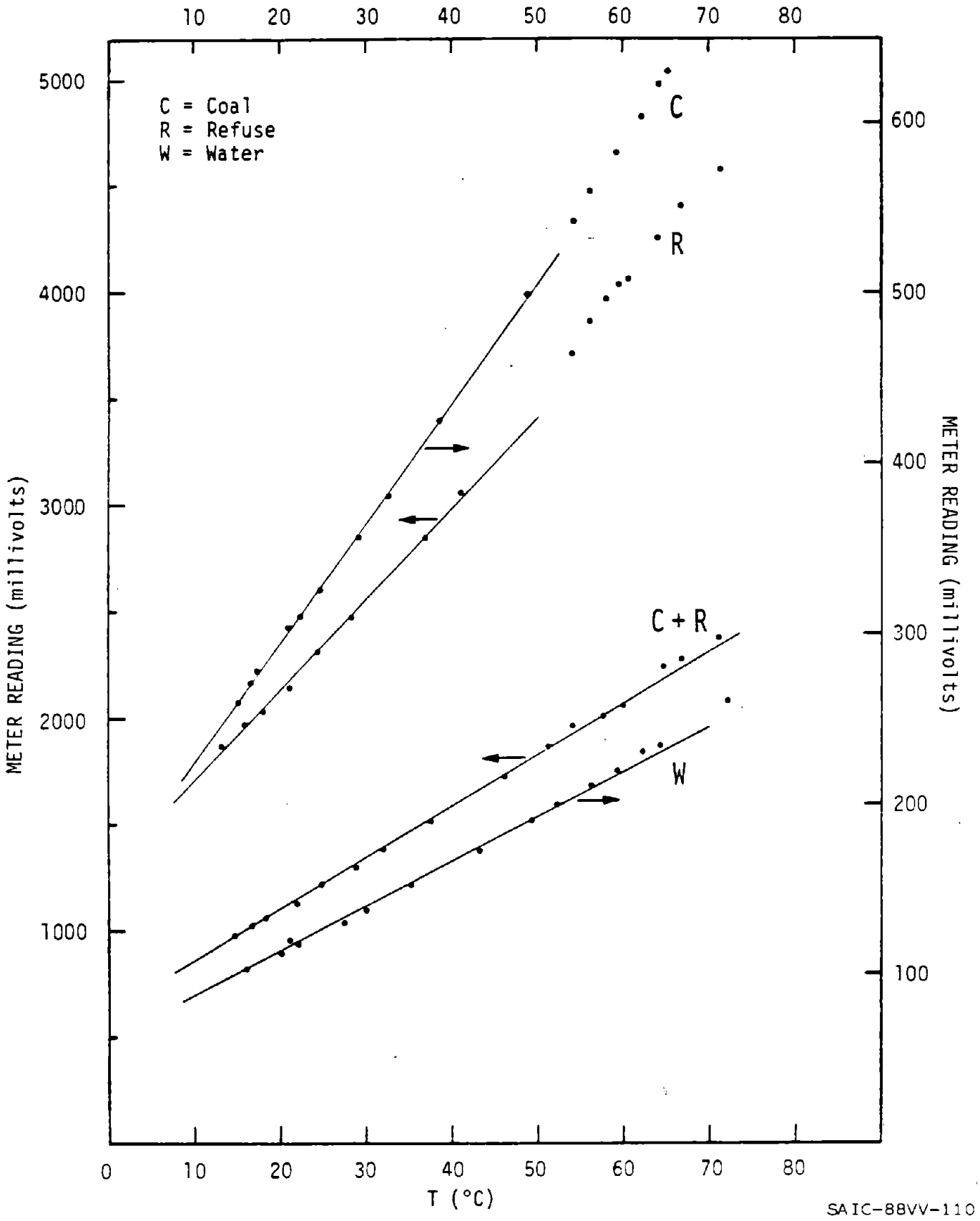

FIGURE 3.22. - Conductivity versus temperature for four different fluids ($\Delta\sigma/\sigma \cong 2\%/°C$ at 5-50°C).

TABLE 3.2 - Reference gauge comparison

Solution	Reference Gauge				
	M1	M2	Mott 1	Mott 2	#6
Tap water	0.314	0.302	0.098	0.89	0.399
Salted water*	2.620	2.630	1.003	0.917	2.984
Decanted saturated rock	5.005	5.005	1.970	1.802	5.670

*1/4 gram NaCl in 300ml water

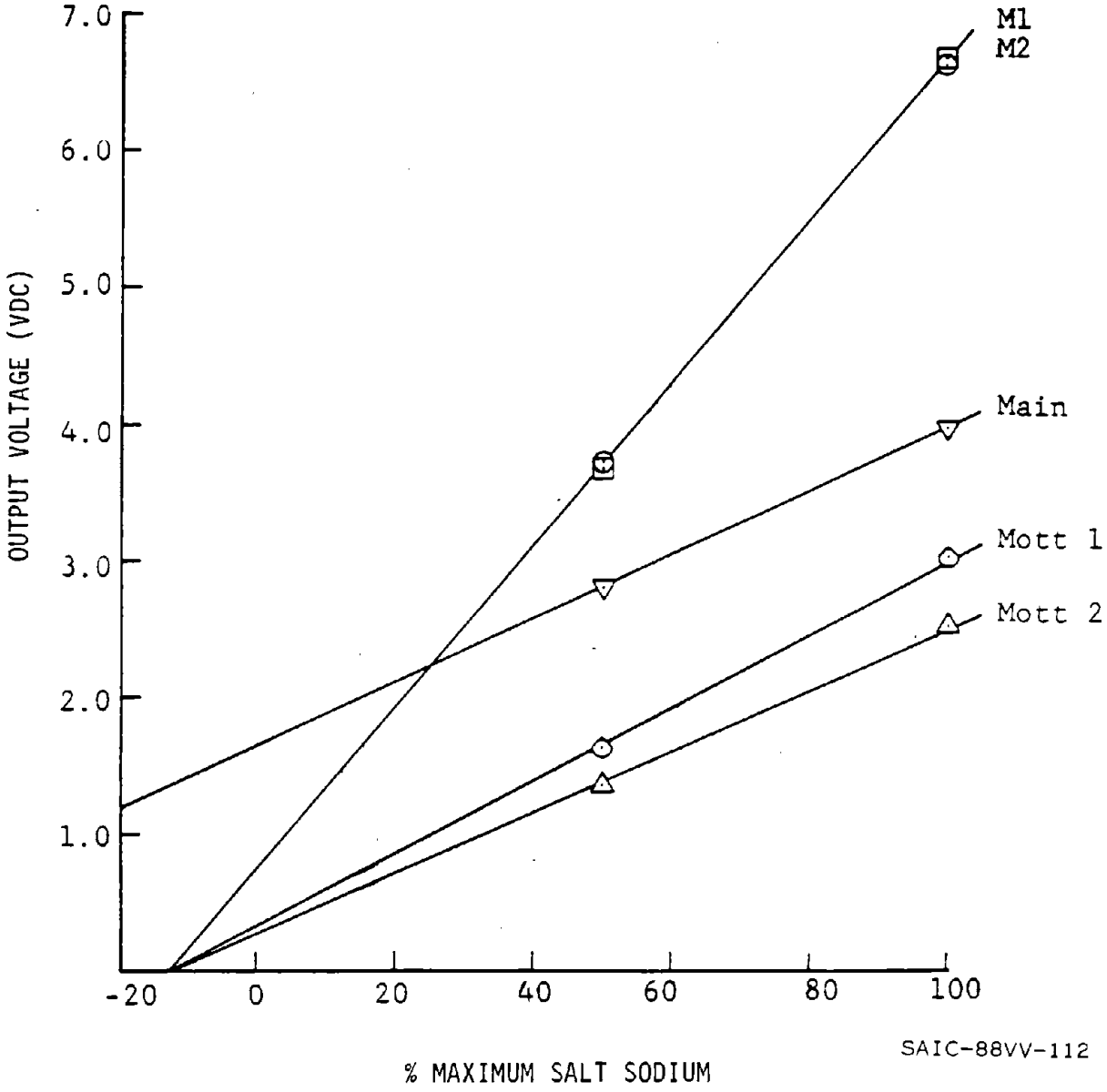

FIGURE 3.23. - Main and reference guage linearity before alignment of electronics.

By substituting resistors for the conductivity gauge, the electronics were recalibrated to give a linear response for the range of conductivity expected. Figures 3.24 and 3.25 give the response of the numerator and denominator circuits, with the peak values expected for the saturated rock solution also indicated. The denominator circuit has a slight zero offset, which will give increasing errors as the conductivity approaches zero.

With the electronics aligned, tracking tests were conducted between the main gauge and the four reference gauges by varying the amount of NaCl added to the low conductivity tap water. With no solids in the system, the gauge reading should return to its initial value since the ratio of two linear responses is constant. As can be seen in Table 3.3, three of the gauges track within $\pm$ 1% over a wide range of conductivity. Only the Mott gauge, which is mounted on the 0.5μ filter, deviated at low concentrations. We feel this is due to high concentration salt solution continuing to diffuse from the filter into the cell a significantly long time after the water was changed to a lower conductivity, which resulted from reducing the concentration in large steps for a very fine mesh filter.

3.3 SUMMARY OF THE CONDUCTIVITY GAUGE PERFORMANCE

With the modifications proposed in the following paragraphs, the conductivity gauge should give performance well within the $\pm$ 1% requirements.

Main Gauge

The main gauge performed flawlessly as expected. No difficulties were experienced in installation or operation. Because it is constructed of PVC, its wear life will probably be less than that for steel pipe, but an estimate is not yet available.

Reference Gauge

While the reference gauge concept proved to be adequate, several design modifications are needed to increase its performance life. First, the filter area must be increased to 4 in.^{2} from 1 in.^{2}, and the motor set to

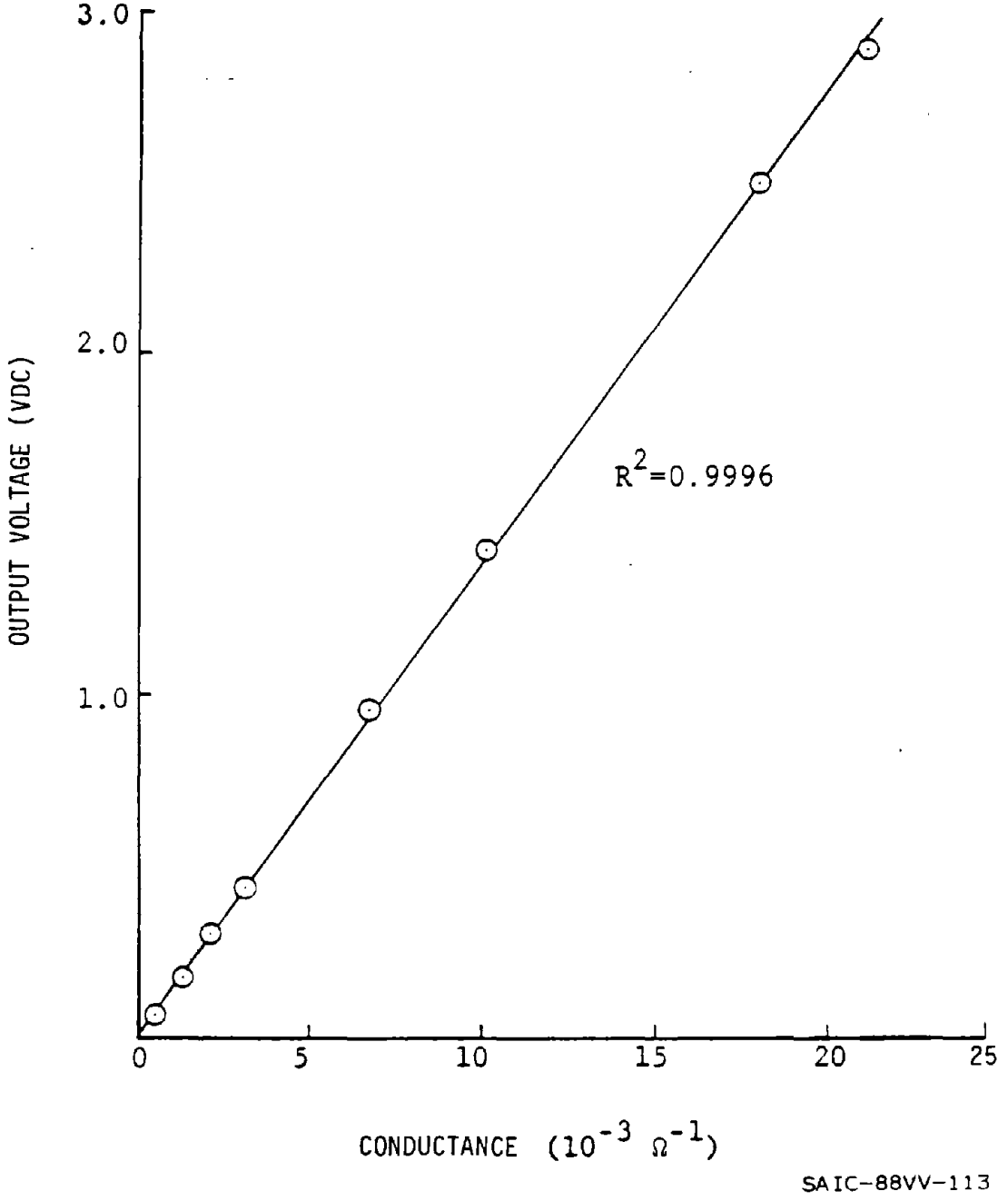

FIGURE 3.24 - Conductance vs. output voltage.

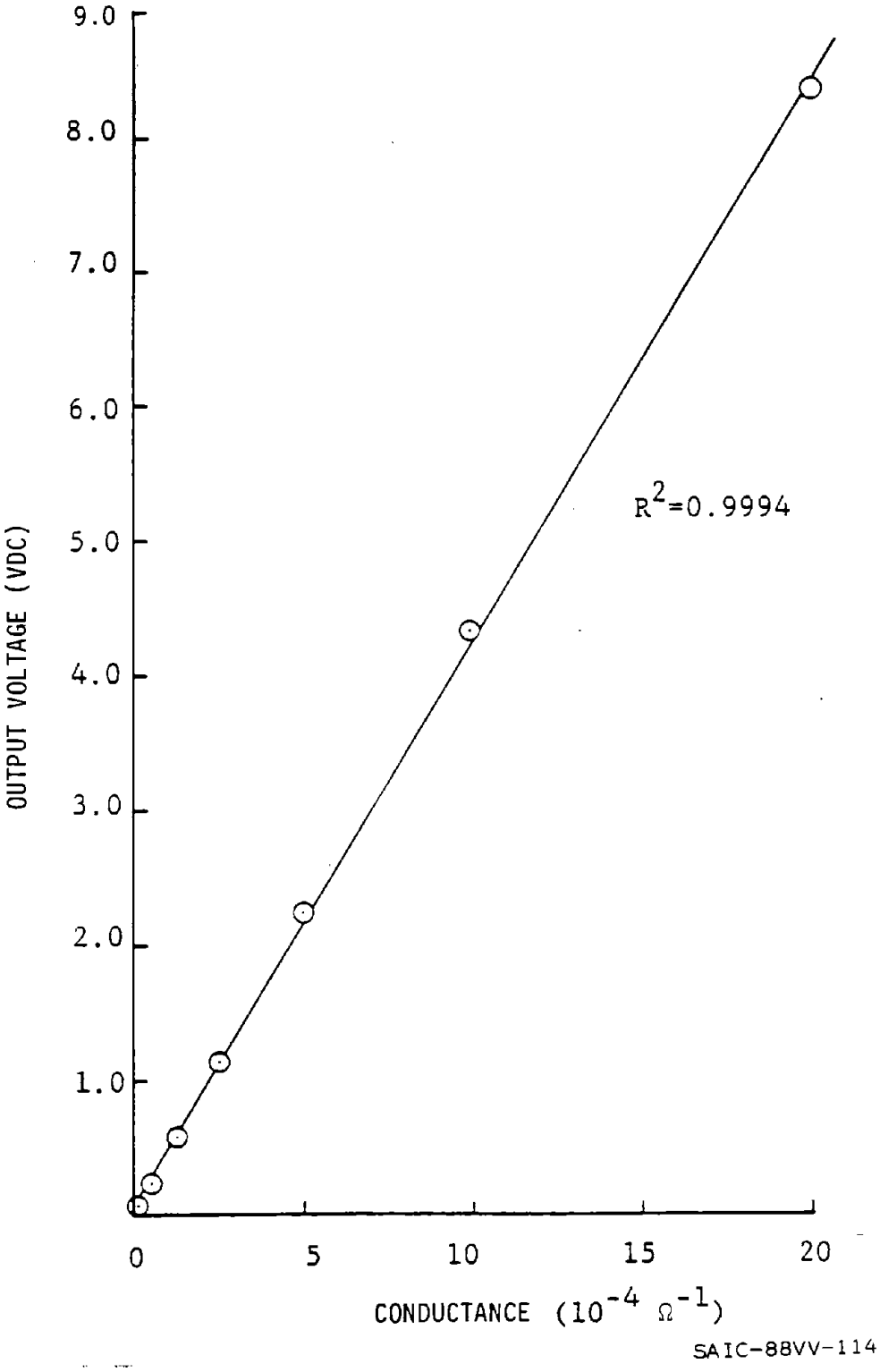

FIGURE 3.25.- Conductance vs. output voltage.

TABLE 3.3 - Main and reference gauge tracking

% Max. Salt Solution* / Gauge (VDC)	100	66 2/3	33 1/3
Main	2.327	1.624	0.888
M1	5.362 (43.4)	3.720 (43.7)	2.043 (43.6)
M2	5.331 (43.7)	3.760 (43.6)	2.108 (42.7)
Mott 1 (0.5 μ)	2.321 (100.5)	1.637 (99.5)	0.936 (94.7)**
Mott 2 (5.0 μ)	1.889 (124.1)	1.315 (124.9)	.725 (123.8)

*17.8 lbs. NaCl in 1500 gal. H_2O

**Rose to 95.9 in 15 minutes

Numbers in ( ) are the gauge reading

10-minute cycles. This will reduce the flow to 2 cc/min per in^2, thereby increasing the time between removals for cleaning from several hours to several shifts or days. Also, this will insure a faster response time (approximately 4x) when operating with fine solids.

The reference conductivity cell will be modified from the design in Figure 3.17 to insure a positive compression between the conducting and insulating bands. This will prevent any drift resulting from changes in cell configurations. The new configuration will be tested to insure linearity and repeatability.

The hydraulic design, as given in Figure 3.12, performs well. Therefore, more permanent fittings should be used in place of the Swageloc fittings that were chosen for flexibility.

Finally, to reduce the envelope of the conductivity gauge, the reference gauge will be mounted on the main gauge. This new configuration will be tested to insure that neither gauge electrically interferes with the other.

Electronics

Once aligned, the electronics performed with little drift. However, the denominator circuit had a small zero offset which must be corrected to increasing the operating range to low conductivities.

The calibration resistors should be changed to reflect the effective resistance of the gauges with a saturated rock solution. This will simplify the calibration procedures and the assessment of drift.

3.4 COAL SLURRY ON-LINE PROGRAM

3.4.1 General Remarks

In its present form, the HP 9815A software is designed to interact

on-line with the necessary hardware through the Tennelec Interface (TC 575) to store the information required by the scalers at the end of each measurement cycle (usually 1 sec) to compute the desired results, and print them in the form specified by the user during the next counting cycle and upon initiation of the latter.

3.4.2 Data Processing Algorithm

The software program is required among other things to calculate the slurry density in g/cm^3, and the coal and refuse concentrations in weight percent. This is accomplished by solving the following three simultaneous equations:

$$M_w = \rho_w V_w D \text{ (conductivity gauge)} \tag{4}$$

$$\sigma_c^{\gamma} M_c + \sigma_r^{\gamma} M_r + \sigma_w^{\gamma} M_w = \frac{\ln N_g - I_g}{S_g} \text{ (gamma gauge)} \tag{5}$$

$$\sigma_c^{n} M_c + \sigma_r^{n} M_r + \sigma_w^{n} M_w = \frac{\ln N_n - I_n}{S_n} \text{ (neutron gauge)} \tag{6}$$

Here, M_c, M_r, and M_w are the masses of coal, refuse and water in g/cm^2;

ρ_w is the water density (1 gm/cm^3);

D is the haulage pipe inside diameter;

$\sigma_c^{\gamma}, \sigma_r^{\gamma}, \sigma_w^{\gamma}$ are the gamma cross sections for coal, refuse, and water;

$\sigma_c^{n}, \sigma_r^{n}, \sigma_w^{n}$ are the neutron cross sections for coal, refuse, and water;

V_w is the volume of water as measured by the conductivity gauge directly. It is input into the main program as the ratio of the second scaler contents (numerator) divided by the first scaler contents (denominator);

N_g and N_n are the accumulated gamma and neutron counts (third and fourth scalers) respectively;

S_g and S_n are the predetermined slopes of the gamma and neutron response curves and, finally;

I_g and I_n are the intercepts of the gamma and neutron response curves. These are determined during calibration with water only from the equations:

$$I_g = {}_wM_wS_g + \ln (NGC) \qquad (7)$$

$$I_n = {}_wM_wS_n + \ln (NNC) \qquad (8)$$

where NGC and NNC are the accumulated gamma and neutron counts per cycle when only water flows through the line.

Now, since M_w is measured directly by the conductivity gauge, the system is reduced to two equations in two unknowns and equations (5') and (6') assume the form:

$$\sigma_c^{\gamma}M_c + \sigma_r^{\gamma}M_r = \left(\frac{\ln N_g - I_g}{S_g}\right) - \sigma_w^{\gamma}M_w \equiv B_g \qquad (5')$$

$$\sigma_c^{n}M_c + \sigma_r^{n}M_r = \left(\frac{\ln N_n - I_n}{S_n}\right) - \sigma_w^{n}M_w \equiv B_n \qquad (6')$$

The solution is given by:

$$M_c = \frac{\begin{vmatrix} B_g & \sigma_r^{\gamma} \\ B_n & \sigma_r^{n} \end{vmatrix}}{\begin{vmatrix} \sigma_c^{\gamma} & \sigma_r^{\gamma} \\ \sigma_c^{n} & \sigma_r^{n} \end{vmatrix}} \ g/cm^2 \qquad (9)$$

$$M_r = \frac{\begin{vmatrix} \sigma_c^\gamma & B_g \\ \sigma_r^n & B_n \end{vmatrix}}{\begin{vmatrix} \sigma_c^\gamma & \sigma_r^\gamma \\ \sigma_c^n & \sigma_r^n \end{vmatrix}} \quad g/cm^2 \qquad (10)$$

with M_w given directly by equation (4). The slurry density can be calculated by the equation

$$\rho_t = \frac{M_c + M_r + M_w}{D} \quad g/cm^3 \qquad (11)$$

and, finally, the coal and refuse concentrations in weight percent are given by:

$$C_c = \frac{M_c * 100}{M_c + M_r + M_w} \% \qquad (12)$$

and

$$C_r = \frac{M_r * 100}{M_c + M_r + M_w} \% \qquad (13)$$

4.0 CONCENTRATION SENSOR TESTS AT THE 6-INCH CSMRI TEST FACILITY

These tests were conducted in two parts: first, a set of diagnostic tests in 1977 to determine the problem areas, and a set of quantitative measurements in 1978 with an upgraded coal slurry concentration sensor.

4.1 1977 TEST SERIES AT CSMRI

A series of tests was carried out at CSMRI in the Fall of 1977 with the high-stability gamma-ray and neutron gauges developed by the SAIC team at San Diego, and the conductivity gauge developed by the Santa Ana laboratory.

Since the conductivity gauge failed because of slurry-water clarification failure, line blocking, temperature differences, and a "non-tracking" reference cell geometry, the nuclear gauges were, nevertheless, tested with the correct water volume input into the computer manually. The correct water volume was deduced from gravimetric diversion-tank measurements. For the coarse-coal and coarse-rock runs, where gravimetric measurements will not yield the correct in-situ concentrations because of slippage (where the water moves faster than the solids in horizontal or uphill pipes), the slurry was pumped a long time to achieve near-equilibrium water conductivity, after which time some of the water was vacuum-assist filtered and placed in the reference cell. However, the results are in question because of improper reference-cell design: the Santa Ana laboratory was unaware of the need for the reference cell geometry to match that of the main gauge (in proportions, but not necessarily in size).

Initial cross section measurements were made with coal fines and also rock fines, where the in-situ concentration was identical to both the loading-inventory concentration and the flow diversion (into the diversion tank) measurement. This was to verify and sharpen the cross section measurements initially carried out with stationary slurries.

The results for the 1977 CSMRI tests, presented in Table 4.1, show that the nuclear gauges perform adequately (to 3% accuracy or better) when the

TABLE 4.1. - Test runs at CSMRI, 1977 Conductivity-guage simulated

Run	P_0 (psi)	P_1 (psi)	P_2 (psi)	V(f/sec)	Nominal Concentr. Wt%			Measured Concentr. Wt%			Difference, wt. % (Mean of Meas. - Nominal		
					Coal	Refuse	Water	Coal	Refuse	Water	Coal	Refuse	Water
VFC1-1	22.5	15.0	12.5	4.4	28.43	0.00	71.57	30.53±1.35	0.0 ±0.0	69.33	+2.10	0	-2.24
VFC1-2	23.0	15.5	13.0	8.5	25.98	0.00	74.02	24.74±1.89	0.39± .66	75.27	-1.24	-0.39	+1.25
VFC1-3	25.5	16.0	13.5	12.5	25.77	0.00	74.23	26.26±1.79	0.0 ±0.0	73.75	+0.49	0	-0.48
VFC2-1	24.0	16.8	13.3	4.5	45.50	0.00	54.50	47.19±1.35	0.0 ±0.0	52.81	+1.69	0	-1.69
VFC2-2	25.0	16.8	13.8	8.6	44.90	0.00	55.10	43.86±2.15	.87±1.56	55.27	-1.04	+0.87	+0.17
VFC2-3	28.0	17.8	15.8	12.7	45.96	0.00	54.04	46.51±1.19	0.0 ±0.0	53.49	+0.55	0	-0.55
VFR1-1	25.0	17.8	15.3	4.7	0.00	26.62	73.38	0.33±0.44	25.87±1.55	73.80	+0.33	-0.75	+0.42
VFR1-2	26.0	18.3	15.5	8.4	0.00	25.34	74.66	.50±1.17	24.96±1.90	74.54	+0.50	-0.38	-0.12
VFR1-3	25.5	20.8	16.8	12.7	0.00	24.44	75.56	0.74±1.01	24.50±1.60	74.76	+0.74	+0.06	-0.80
VFM2-1	30.5	23.5	20.5	4.6	0.00	47.67	52.33	0.88±1.13	48.01±1.46	51.11	+0.88	+0.34	-1.22
VFM2-2	32.5	24.0	20.5	8.4	0.00	49.06	50.94	1.38±1.46	48.45±1.60	50.17	+1.38	-0.61	-0.77
VFM2-3	34.5	25.5	21.0	12.6	0.00	47.44	52.56	0.88±1.02	48.72±1.60	50.40	+0.88	+1.28	-2.16
VFM1-1	23.0	16.3	13.5	4.7	13.13	13.13	73.74	13.74±1.64	14.28±1.60	71.98	+0.61	+1.15	-1.76
VFM1-2	23.8	16.0	13.8	8.4	12.72	12.72	74.56	13.20±1.70	12.18±1.77	74.62	+0.48	-0.54	+0.06
VFM1-3	26.5	16.0	14.0	12.8	12.76	12.76	74.48	12.52±2.03	12.88±1.95	74.60	-0.24	+0.12	+0.12
VFM2-1	27.5	19.3	16.5	4.5	24.28	24.28	51.44	24.71±1.95	24.75±2.03	50.54	+0.43	+0.47	-0.90
VFM2-2	29.5	Inoperative	18.3	8.3	24.54	24.54	50.92	24.86±1.93	24.79±2.11	50.35	+0.32	+0.25	-0.57
VFM2-3	32.0	Inoperative	19.3	12.7	25.16	25.16	49.68	23.96±1.50	25.24±1.65	50.80	-1.20	+0.08	+1.12
VCM1-2	-	-	-	8.5	13.00*	13.00*	74.00	11.89±1.91	15.27±2.09	72.85	--	--	--
HCC2-1	12.5	9.5	9.5	8.8	22.*	0.00	78.	23.24±1.15	0.00±0.00	76.76	--	--	--
HCM1-1	-	-	-	8.8	12.*	12.*	76.	8.43±2.12	14.17±2.75	77.41	--	--	--
HFR1-1	-	-	-	8.4	0.00	47.72	52.28	0.25±0.61	46.96±1.41	52.79	0	-0.76	+0.51
HFR1-2	-	-	-	12.6	0.00	47.72**	52.28	0.46±0.76	47.12±1.46	52.42	--	--	--

*Known only to ±4 wt% because of line-leaking, header tank settling and line slippage. Concentrations deducted from loadings.
**Taken during run HFR1-1, which should be the same as HFR1-2 within ±1%.

correct water volume V_w is measured by the conductivity gauge. The proof of accuracy, of course, is carried by the fines tests (VFR1-1 means vertical test section, fine refuse, composition #1, and speed #1 (~4 ft/sec); HCC2-2 means horizontal test section, coarse coal, composition #2, speed #2 (~8 ft/sec), etc.).

This table shows averaged values of the composition measurements and standard deviation, whereas Figures 4.1 through 4.13 show the point-by-point values for each of the separate test configurations.

4.2 1978 TEST SERIES AT CSMRI

Table 4.2 shows the results of the test series carried out in June, 1978 at CSMRI with a working conductivity gauge, as designed by the SAIC San Diego group.

For the fine coal and refuse slurries, the average agreement between the concentration sensor and the gravimetric measurements is seen to be better than 3% for nearly every case. While the difference between the gravimetric and concentration-sensor results gives an indication of the accuracy of the concentration sensor (for the fines only), it is not an absolutely accurate indication of the error because the gravimetric method is 2-3% uncertain for coal and 1-2% uncertain for rock (refuse).

Note that for the coarse coal slurry, where the particles are large, the slippage is also large and the diversion tank will collect appreciably more water (which is flowing faster) than coarse coal. This explains the large difference (+18%) between the concentration-sensor measurement and the diversion-tank measurement (HCC-1, Table 4.2). The diversion tank provides a measure of delivered concentration, while the concentration sensor gives a direct and accurate measure of in-situ concentration, which is a vital parameter for avoiding line blockage.

Note that after the diversion tank has been filled (it carried 1 1/3 times the volume of the short 6-inch test loop), the coal in situ concentration dropped from 47.3% to 27.7% (HCC-1). This is a result of a large fraction of

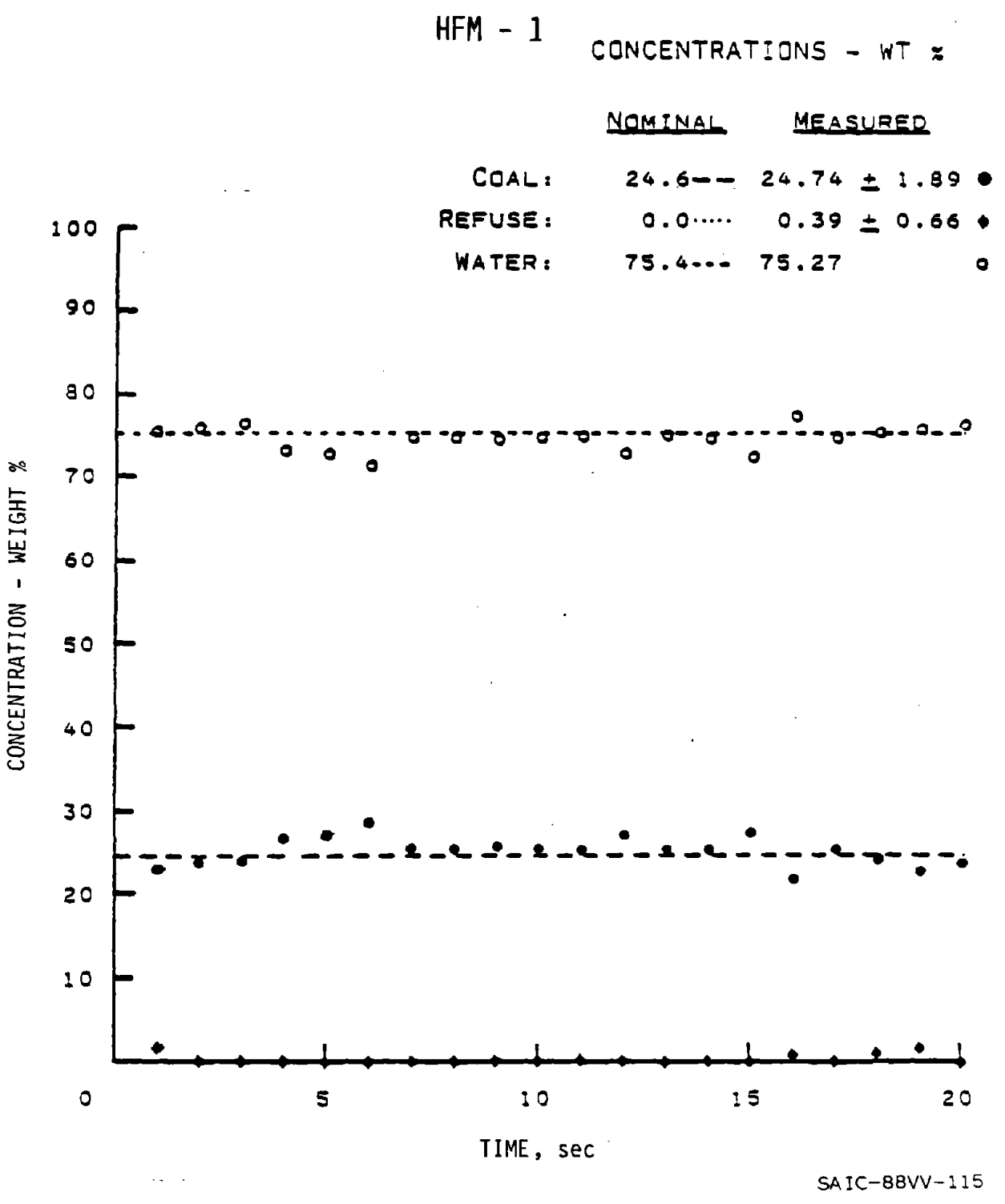
HFM - 1
CONCENTRATIONS - WT %
NOMINAL
MEASURED
COAL: 24.6 24.74 ± 1.89
REFUSE: 0.0 0.39 ± 0.66
WATER: 75.4 75.27
CONCENTRATION - WEIGHT %
100
90
80
70
60
50
40
30
20
10
0
5
10
15
20
TIME, sec
SAIC-88VV-115

FIGURE 4.1.

VFC 2-2

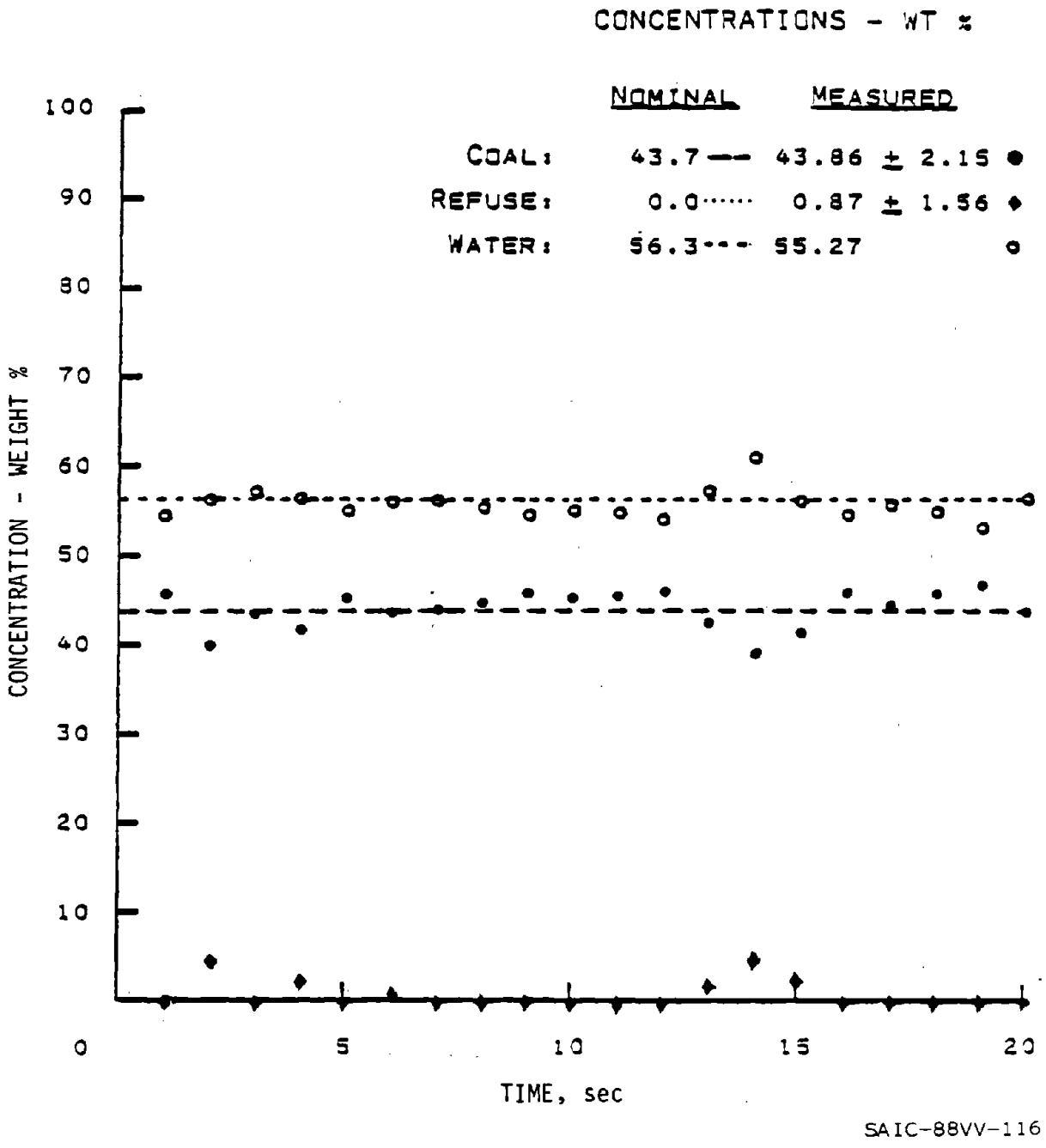

FIGURE 4.2.

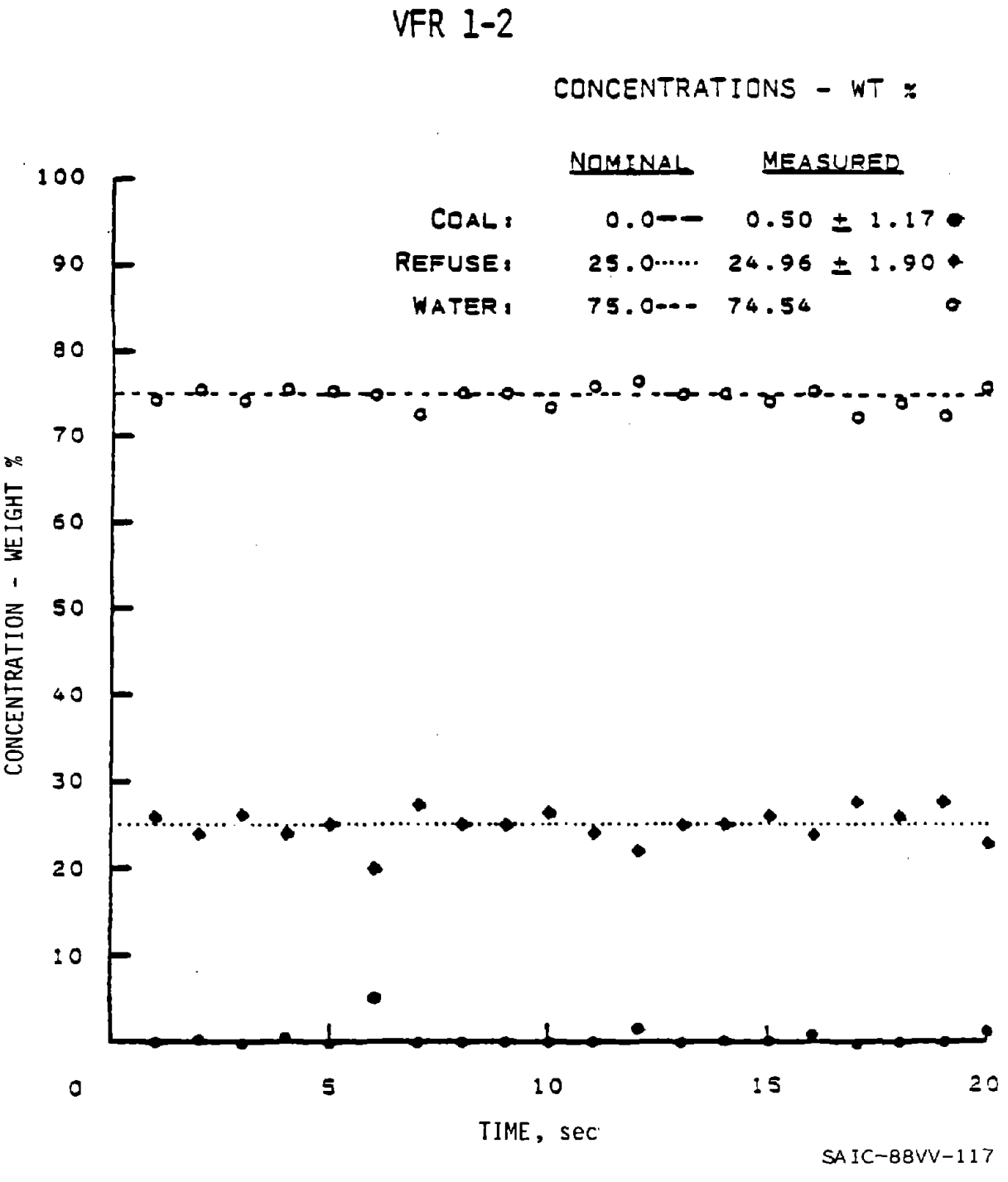
VFR 1-2
CONCENTRATIONS - WT %
NOMINAL
MEASURED
COAL: 0.0 0.50 ± 1.17
REFUSE: 25.0 24.96 ± 1.90
WATER: 75.0 74.54
CONCENTRATION - WEIGHT %
100
90
80
70
60
50
40
30
20
10
0
5
10
15
20
TIME, sec
SAIC-88VV-117

FIGURE 4.3.

VFR 2-2

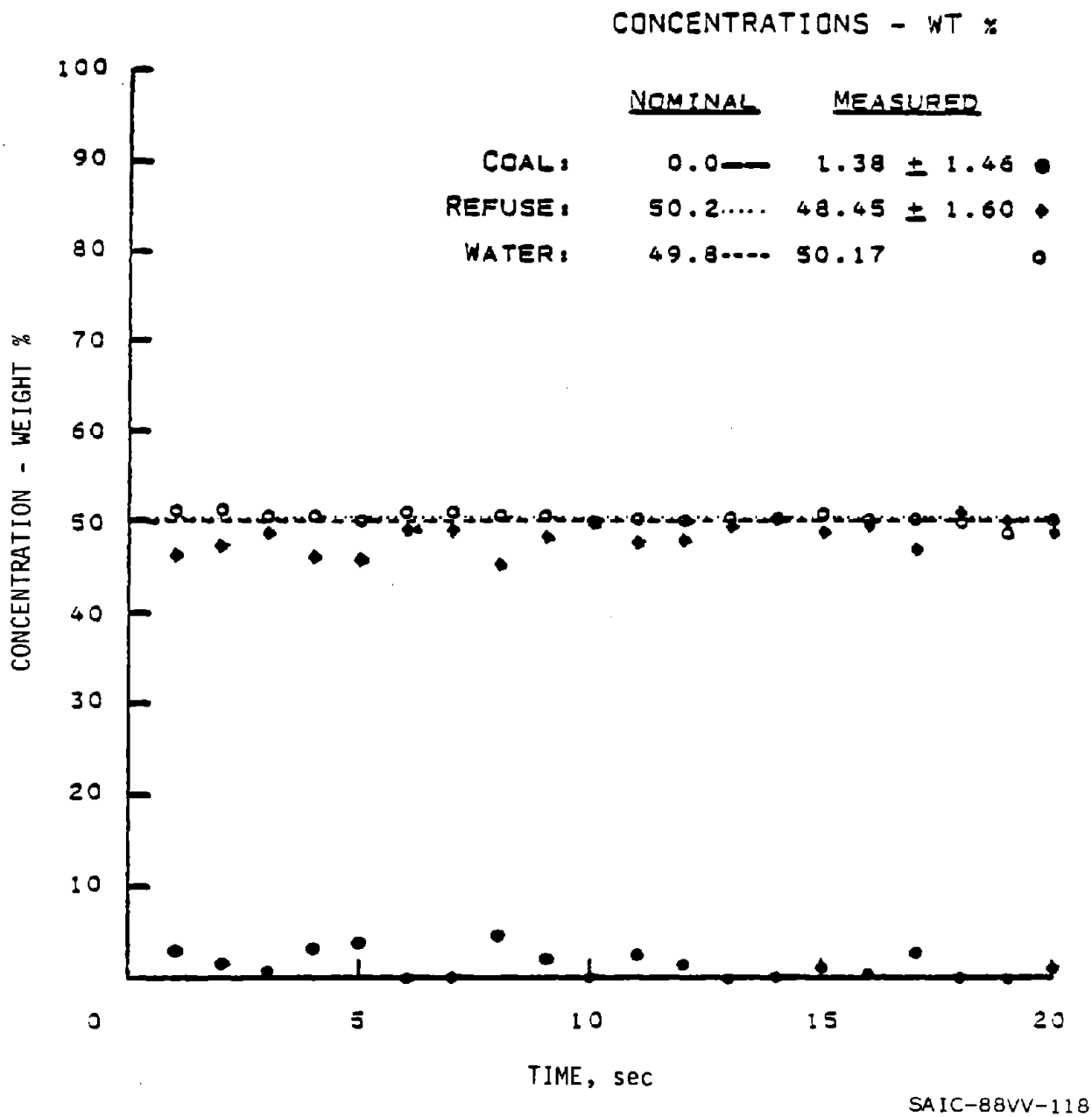

FIGURE 4.4.

VFM 1-1

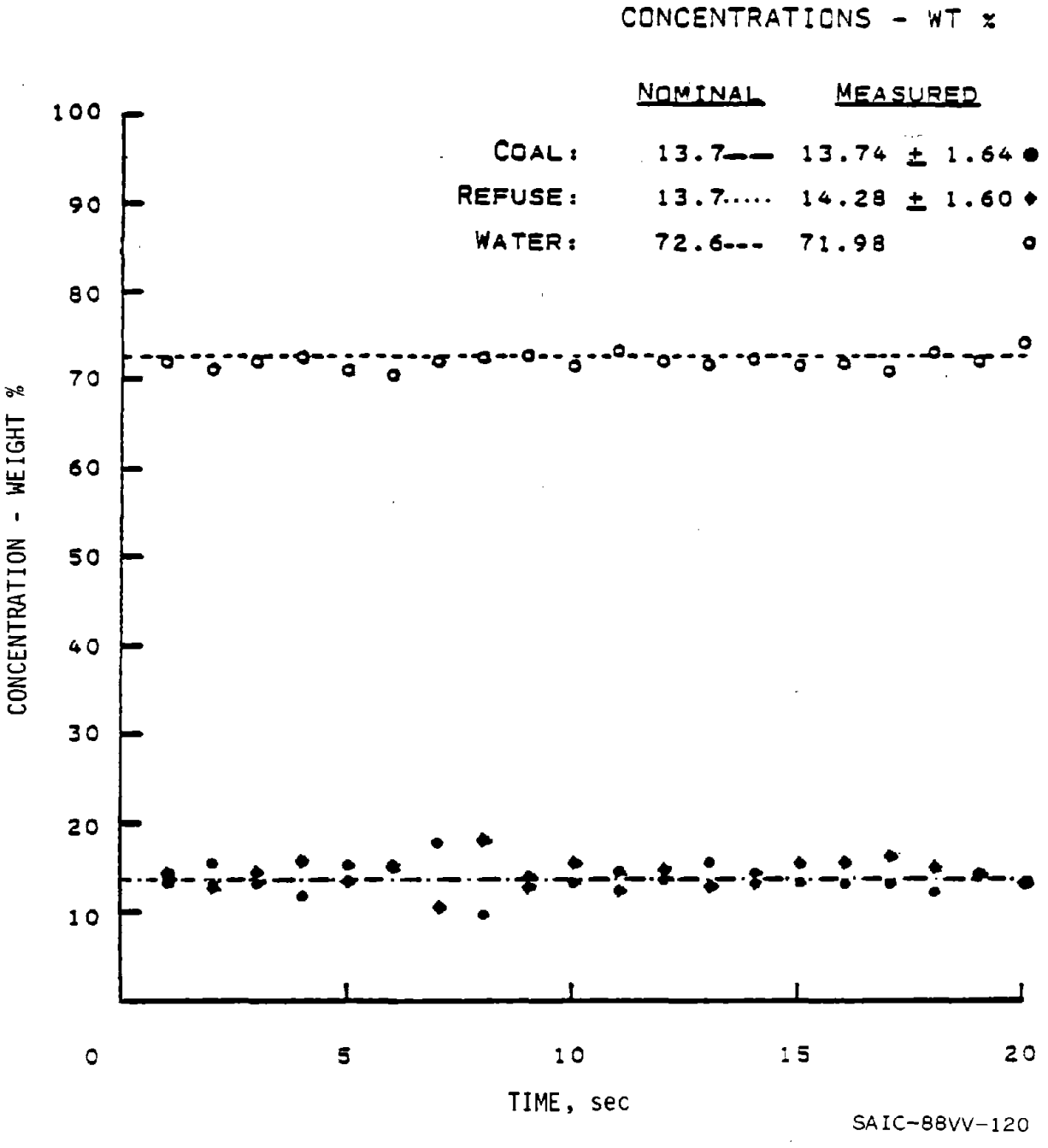

FIGURE 4.5.

VFM 1-2

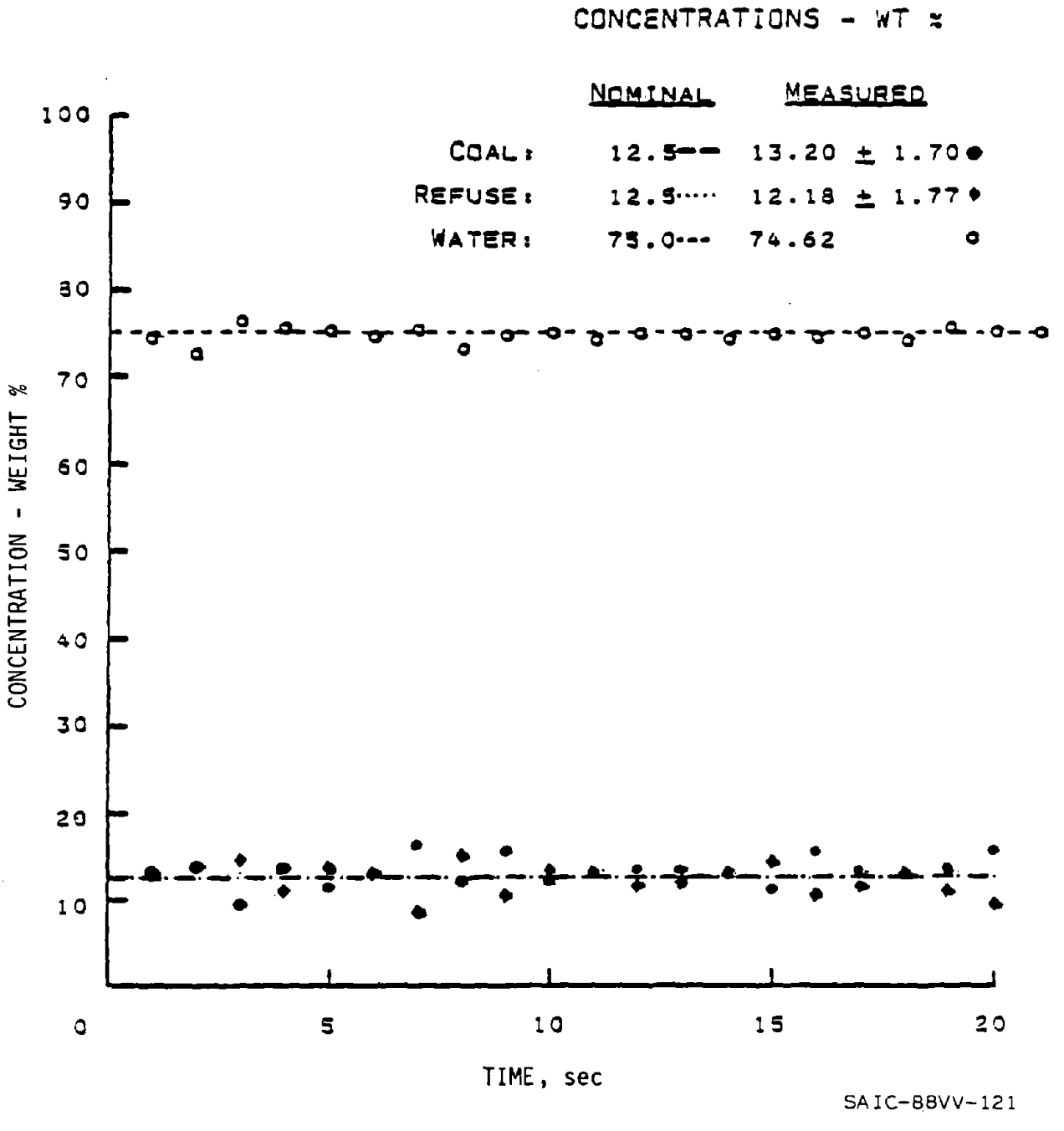

FIGURE 4.6.

VFM 1-3

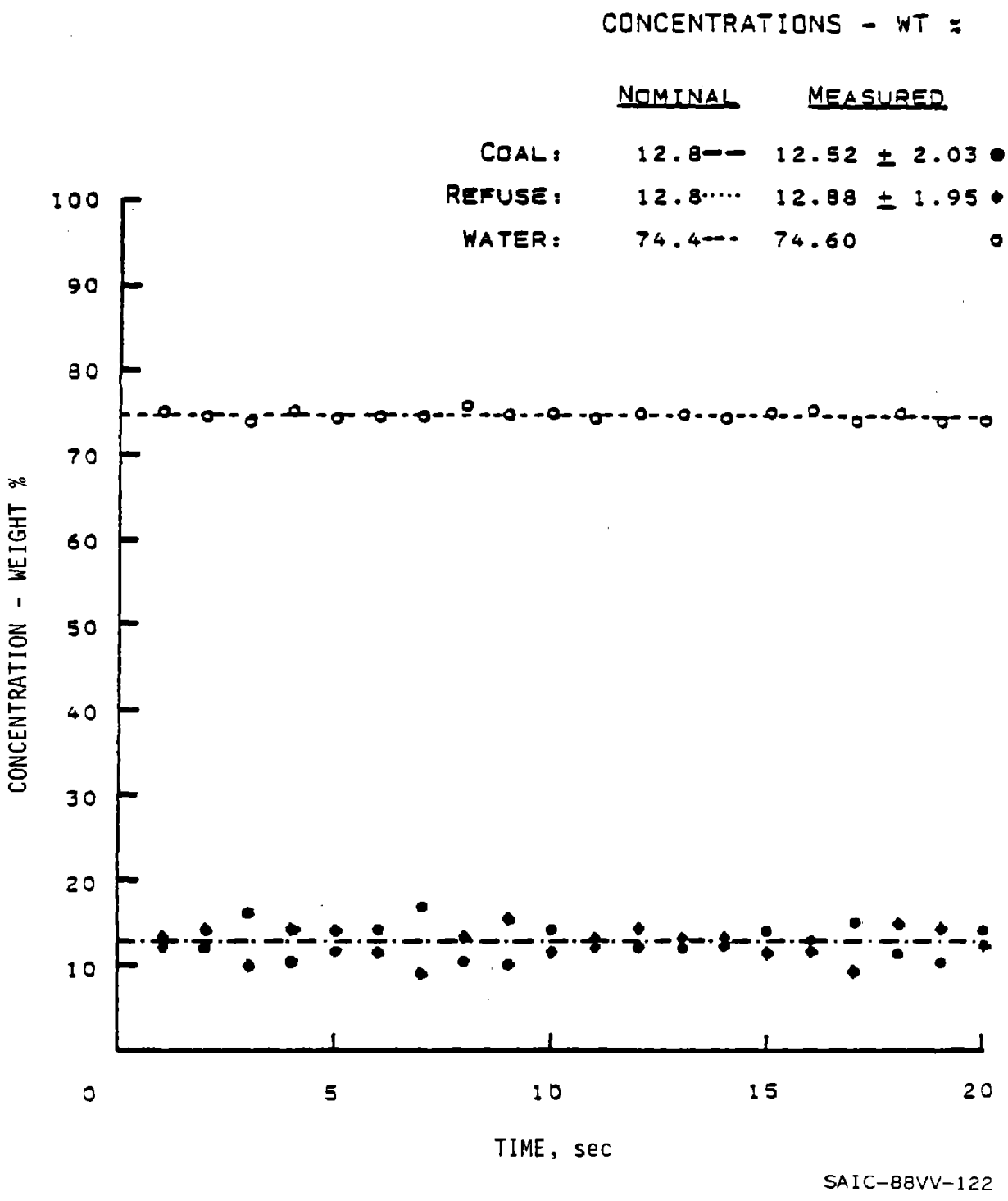

FIGURE 4.7.

VFM 2-2

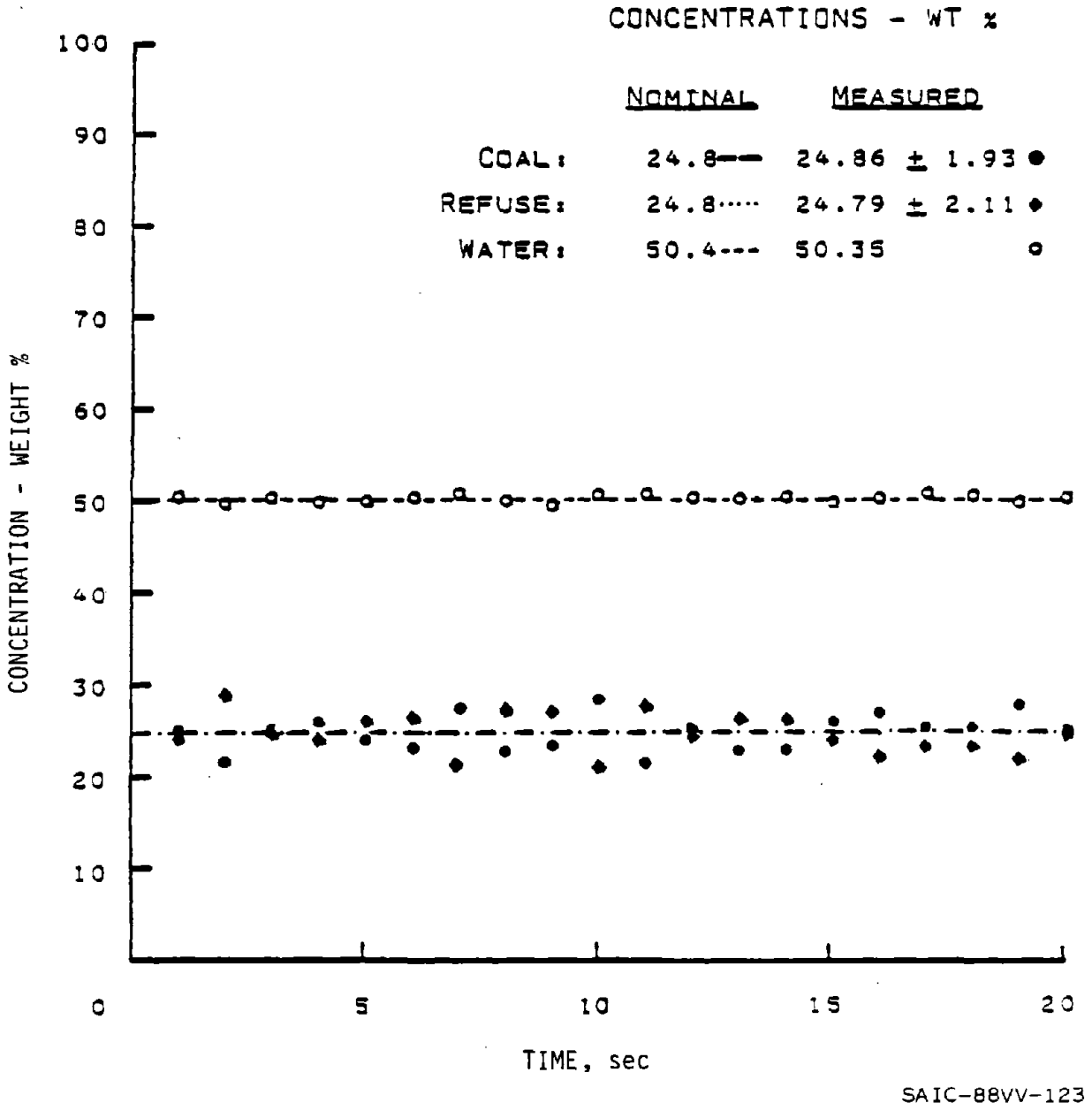

FIGURE 4.8.

VCM 1-2

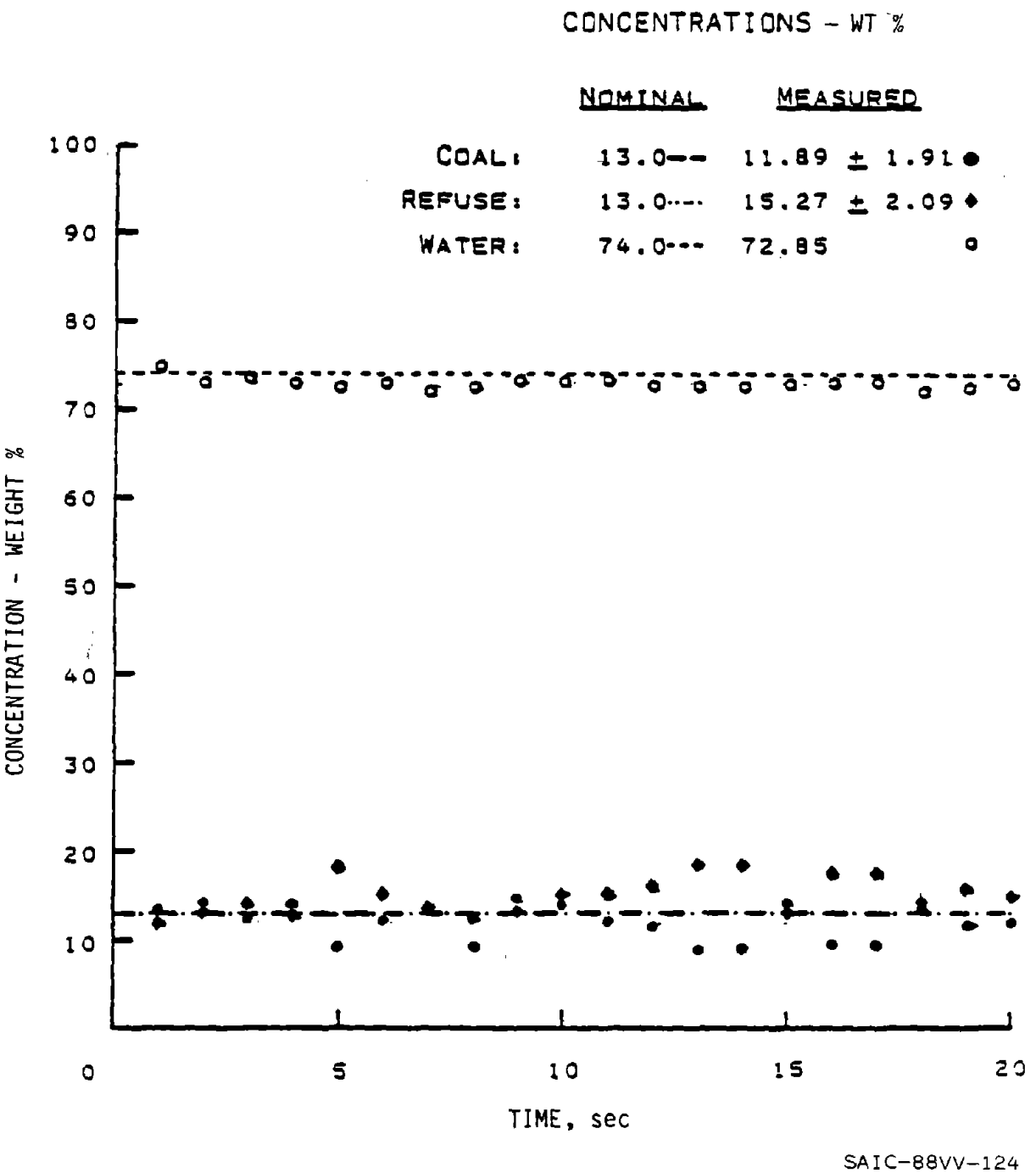

FIGURE 4.9.

HCC 2-1

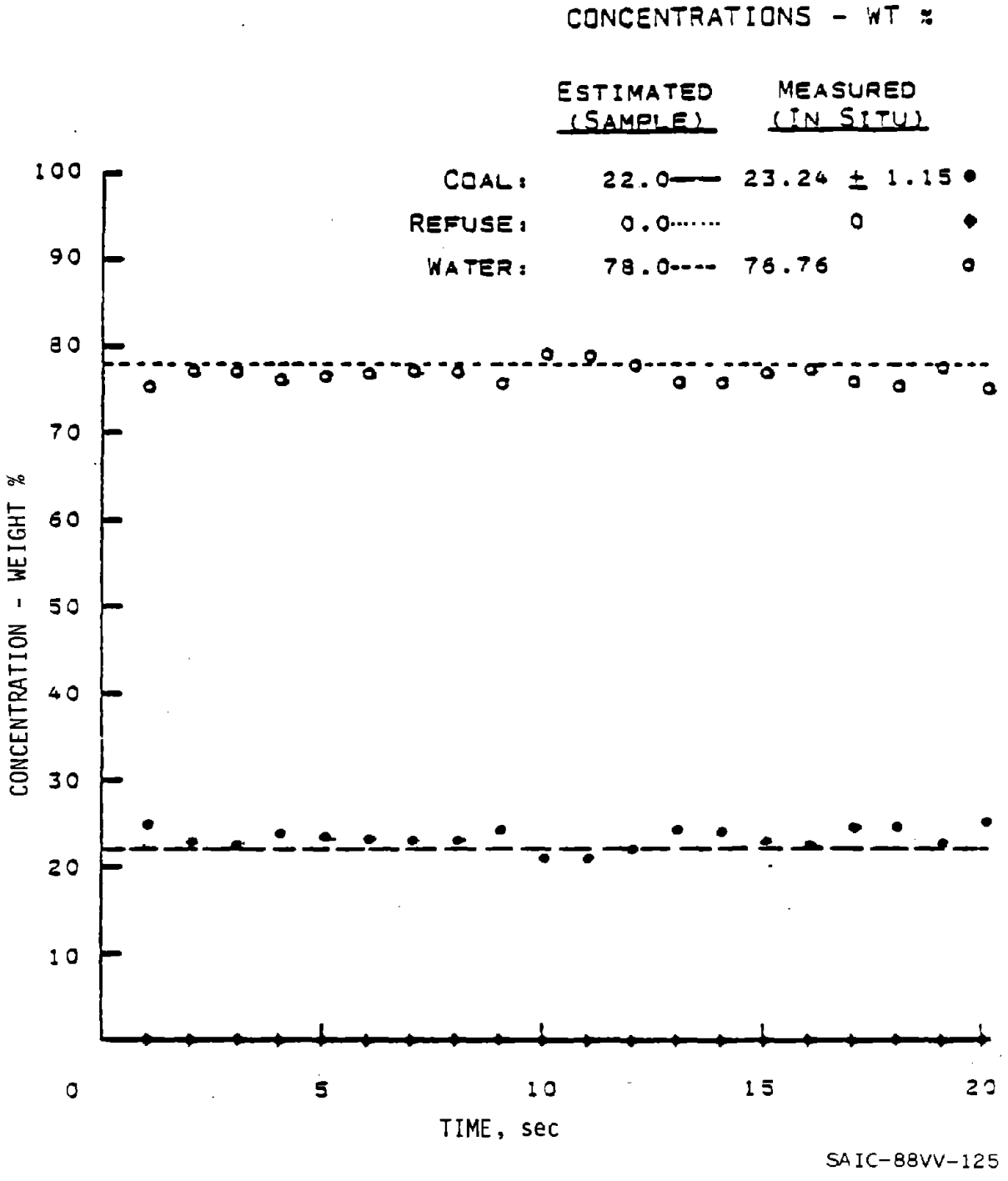

FIGURE 4.10.

HCM 1-1

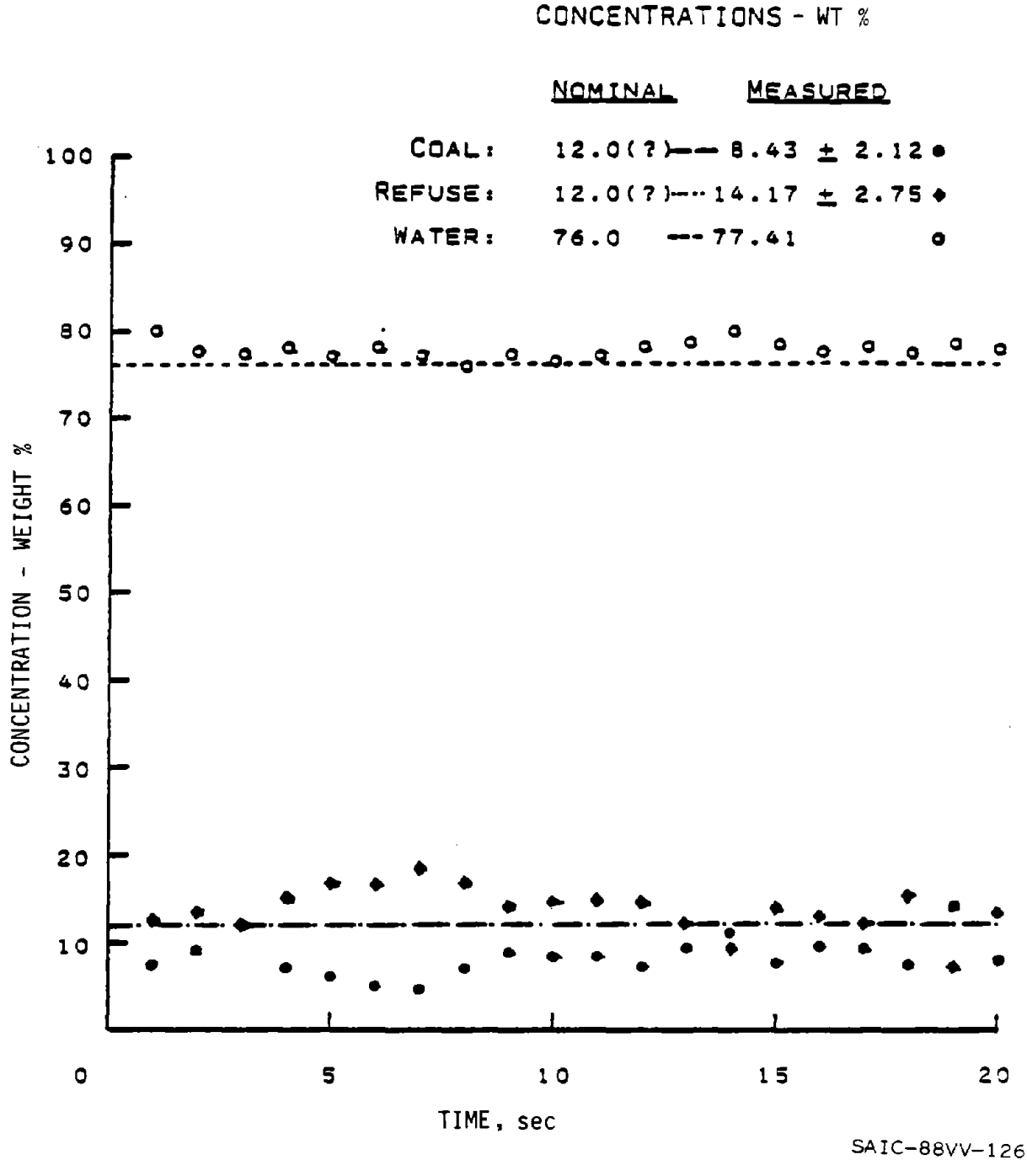

FIGURE 4.11.

HFR 1-1

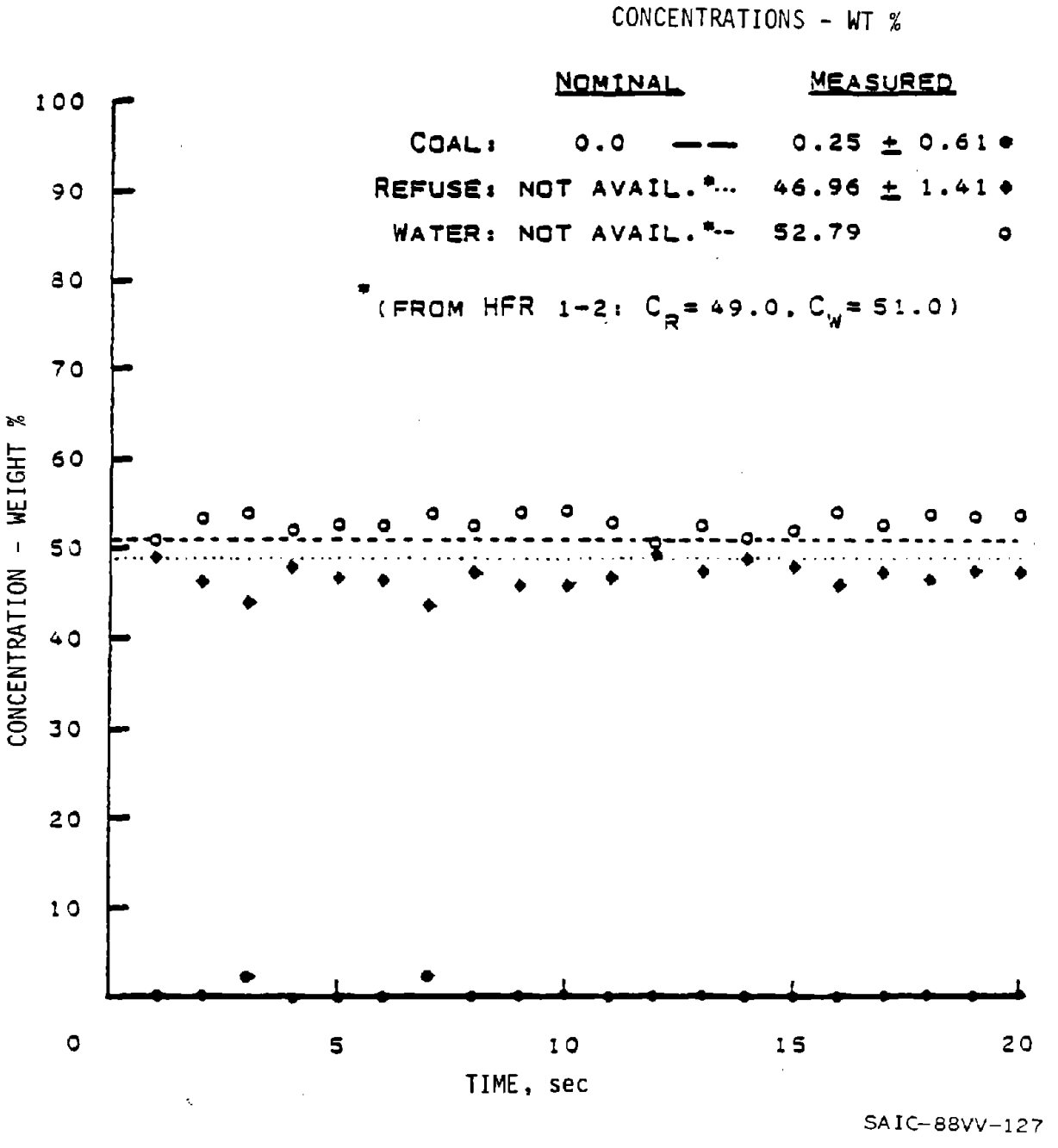

FIGURE 4.12.

HFR 1-2

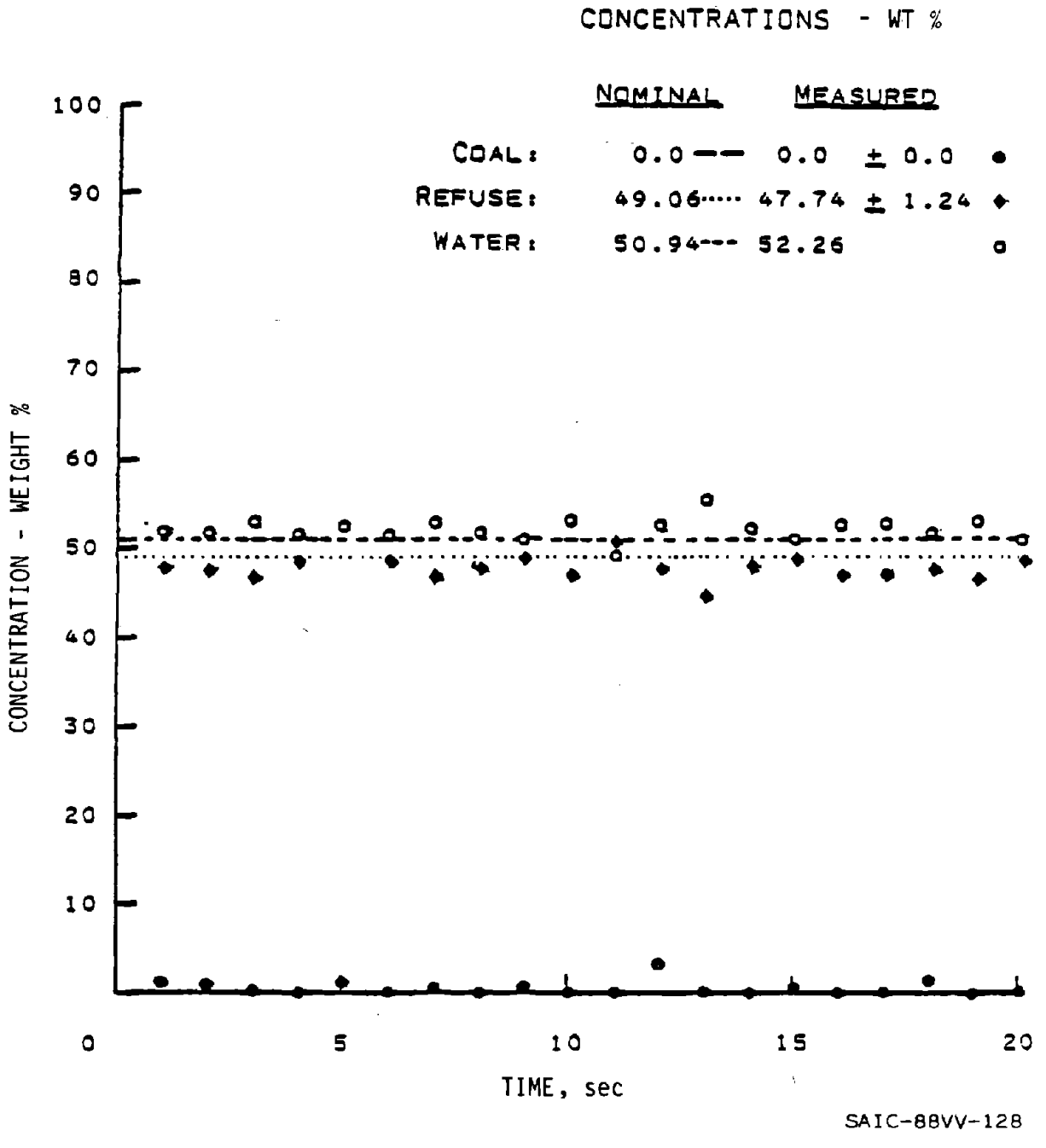

FIGURE 4.13.

TABLE 4.2. - Test runs at CSMRI - June 1978. Complete sensor operation

Run	P_D(psi)	P_1(psi)	P_2(psi)	V(f/sec)	Nominal concentration by diversion,* wt%			Measured concentration wt%			Difference, wt% (mean of meas.-nominal)		
					Coal	Refuse	Water	Coal	Refuse	Water	Coal	Refuse	Water
H_2O	15-20	13-18	6-12	10-11	0.0	0.0	100.0	0.2±0.5	1.4±1.8	100.6±0.3	+0.2	+1.4	+0.6
HFM-1	12-26	10-24	2-15	8.5	16.6	16.6	66.8	15.5±2.3	14.6±2.5	69.9±0.0	-1.1	-2.0	+3.1
HFC-1	25	23	4-15	8.2	34.2	0.0	65.8	36.4±1.0	0.0±0.0	63.6±0.1	-2.2	0.0	-2.2
HFM-2	20	18	1-10	11.	25.3	23.9	50.8	26.6±1.6	20.1±1.7	53.3±0.2	+1.3	-3.8	+2.5
HCC-1**	12	10	2-5	9.	29.1	0.0	70.9	47.3±1.0**	0.0±0.0**	52.7±0.6**	+18.2**	0.0**	-18.2
HCC-1+	12	10	1-4	9.	----	----	----	27.7±1.3+	0.0±0.0+	72.3±0.4+	----	----	----
HCR-1++	14	12	1-5	10.	0.0	18.8	81.2	2.1±1.7++	21.3±2.3++	76.6±0.2++	+2.1++	+2.5++	- 4.6+

*No error has been assigned to the diversion results. This could be as much as 2-3% for Coal and 1-2% for rock, due to their different relative densities.

**Due to slippage in the slurry line, the diversion results are obviously quite lower than the measured in-situ concentration in the case of coarse coal (Cf, next HCC-1 run)

+This is a diagnostic run immediately following the diversion in HCC-1. Observe the dramatic decrease in measured in-situ concentration, as expected.

++Observe that slippage effects are not very drastic here, due to the friability of coarse refuse.

the inventory finding itself in the 6-inch haulage pipe and a correspondingly small fraction in the header tank, where the coarse coal rapidly falls through the large water volume and directly into the slurry pump at the bottom of the header tank.

For the rock (refuse), on the other hand, immediate breakup occurs for at least 90% of the refuse as soon as it becomes wetted because only a small fraction of hard rock is found in the Pittsburgh seam refuse in the deep mine at Morgantown, West Virginia. It rapidly breaks up both from wetting and from the pump and haulage-line mechanical forces.

This accounts for the better agreement between the diversion-tank gravimetric measurement and the concentration-sensor measurement for the coarse refuse, shown in the last row of Table 4.2, than for the coarse coal.

The point-by-point data are shown in Figures 4.14 to 4.18, and correspond to the averaged data of Table 4.2 discussed above. Most of the point-to-point bounce appears to derive from the gamma-ray counter statistical variation (while some very likely derives from haulage line variations), which calls for a larger gamma-ray detector and/or sources. A study of the gamma-ray counter variations in concentrations that have been observed do, indeed, reduce to about one-half their present value, or possibly less, with the gamma-ray counting variations reduced by about a factor of two. A higher gamma-ray count rate will be designed into the next version of the gamma gauge.

The solid lines in the run HCC-1 show the diversion-tank estimates of the in-situ concentration of coarse coal. These diversion-tank measurements are, of course, very far off of the actual in situ concentration for coarse coal, as the figure illustrates, because the water is flowing appreciably faster than the larger chunks of coal. The extent that the two curves disagree gives a measure of the slippage occurring, in that as the coal particle size reduces (or the water velocity increases), the diversion-tank measure of water flow and the concentration gauge measure of in-situ concentration will tend to become one and the same. It is precisely this kind of comparative data that is useful for both direct slippage measurements and line blockage studies. This dramatically illustrates a few of the many uses that the in-situ concentration

HFM-1

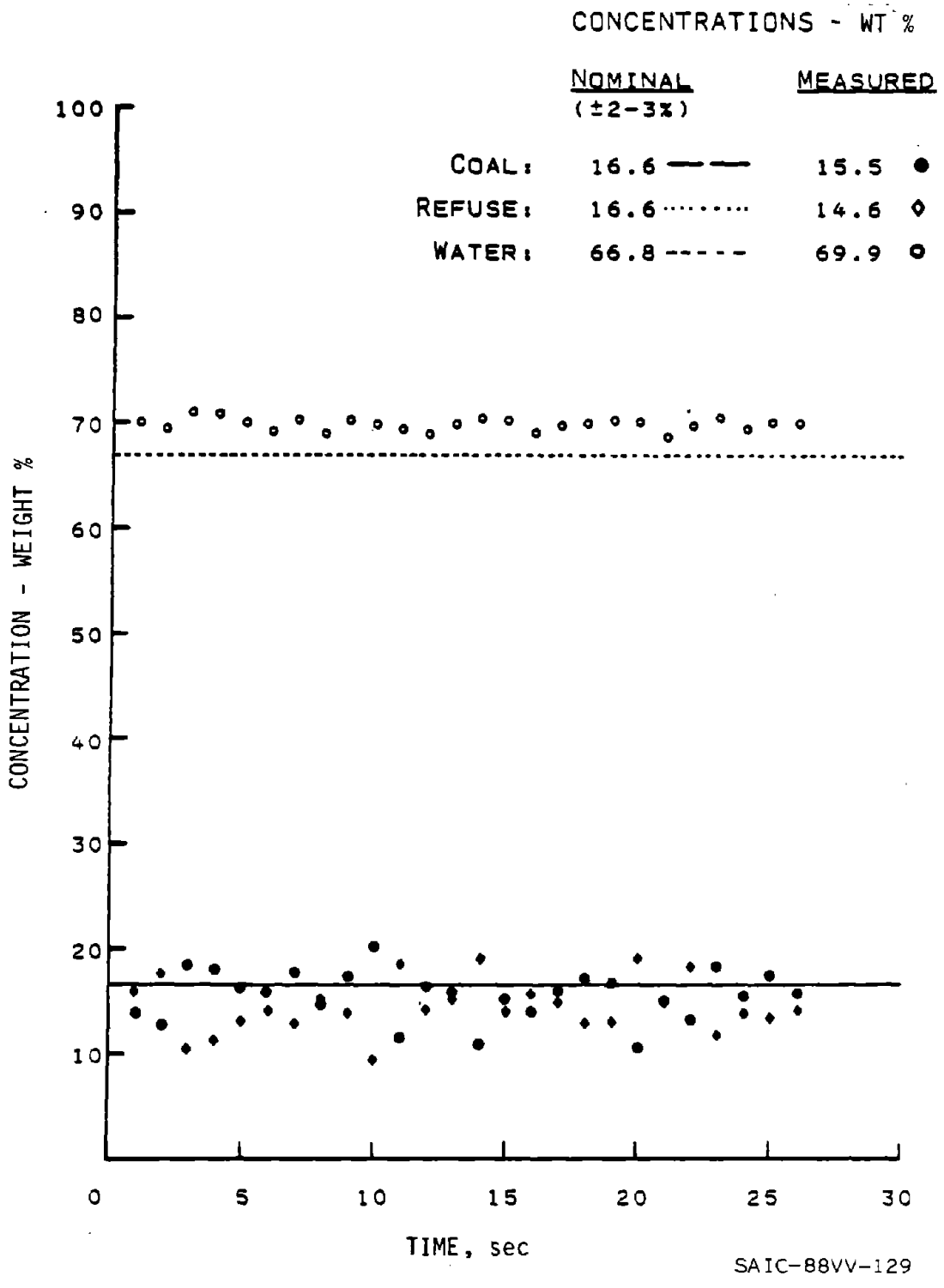

FIGURE 4.14.

HFC-1

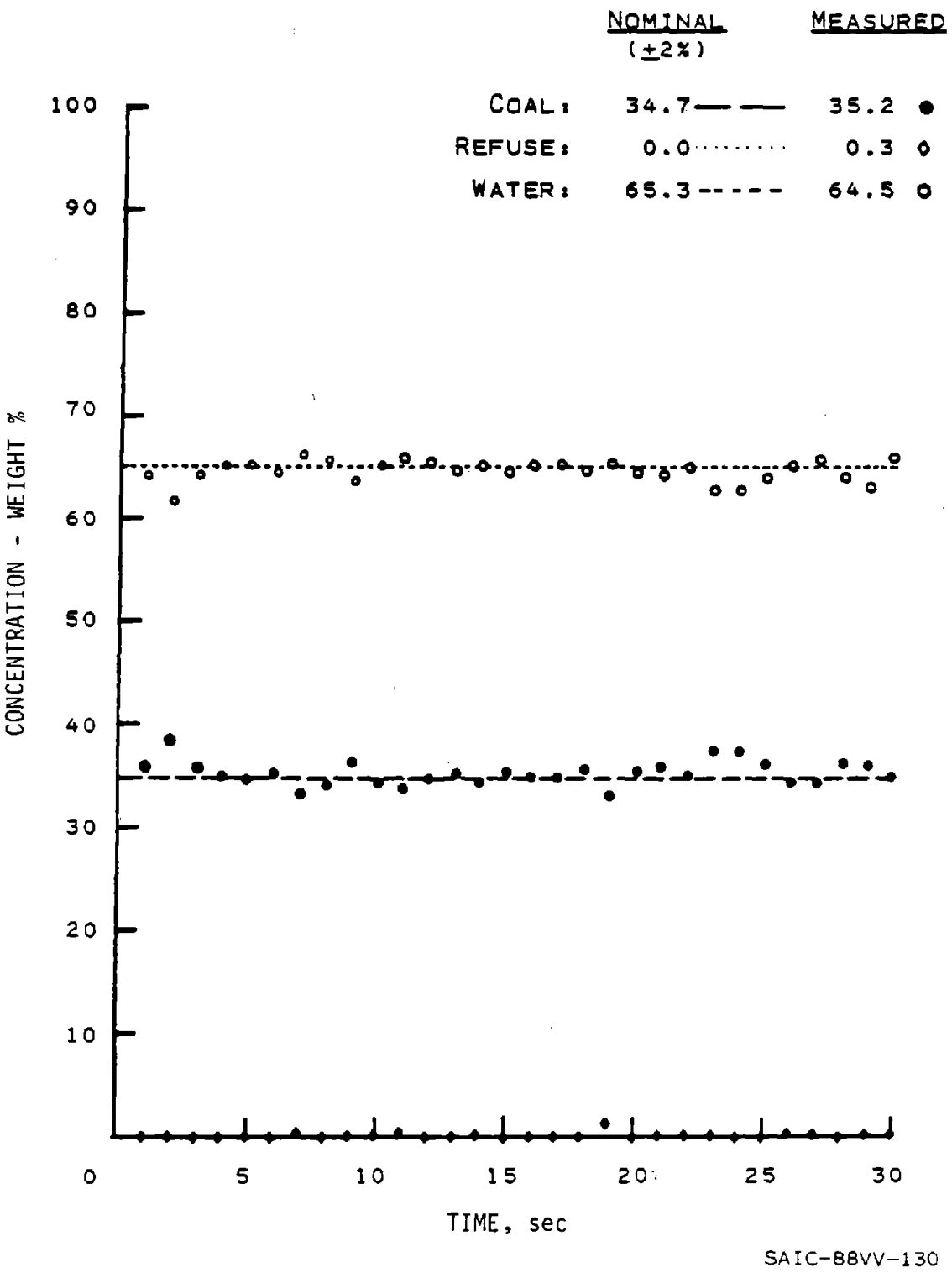

FIGURE 4.15.

HFM-2

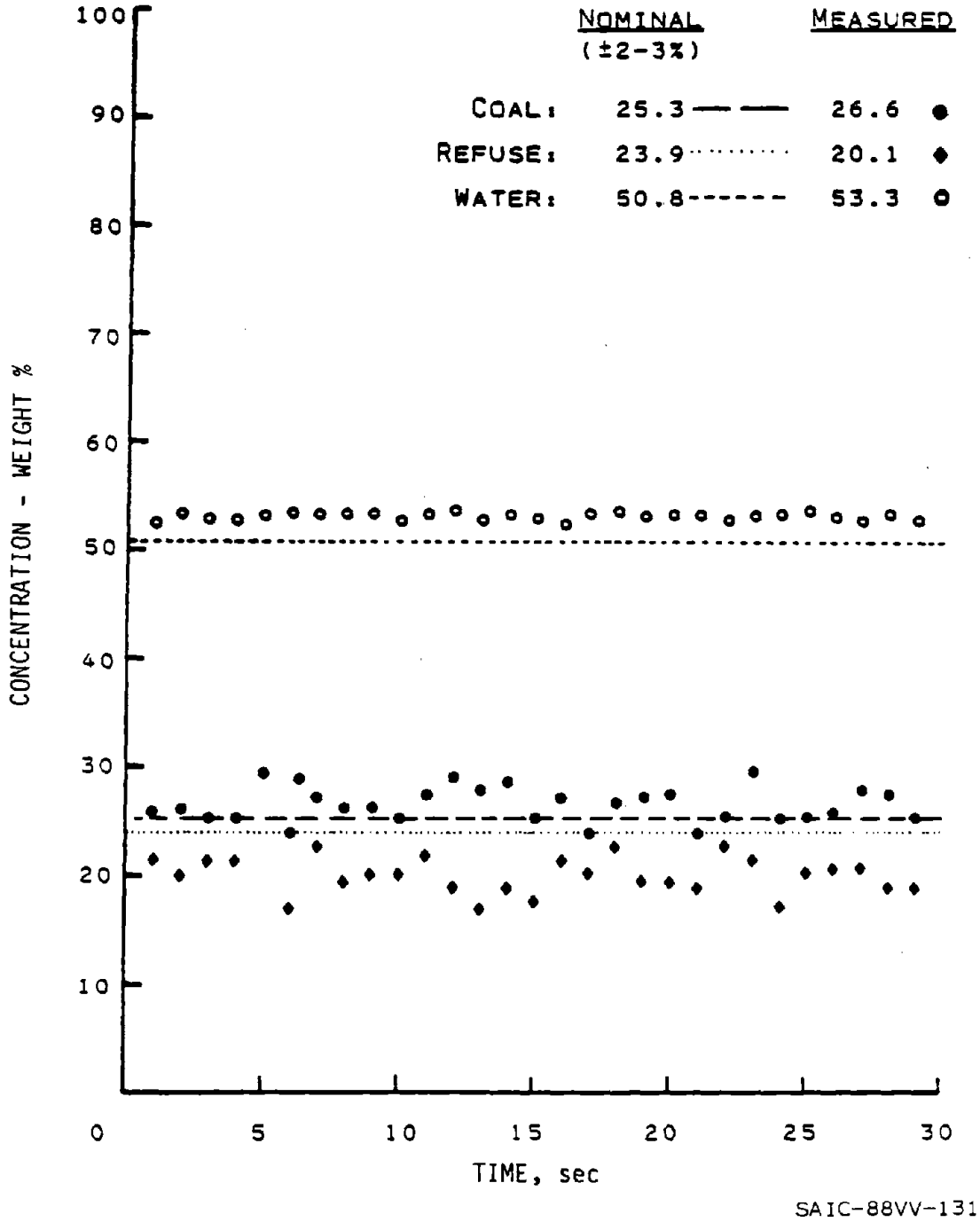

FIGURE 4.16.

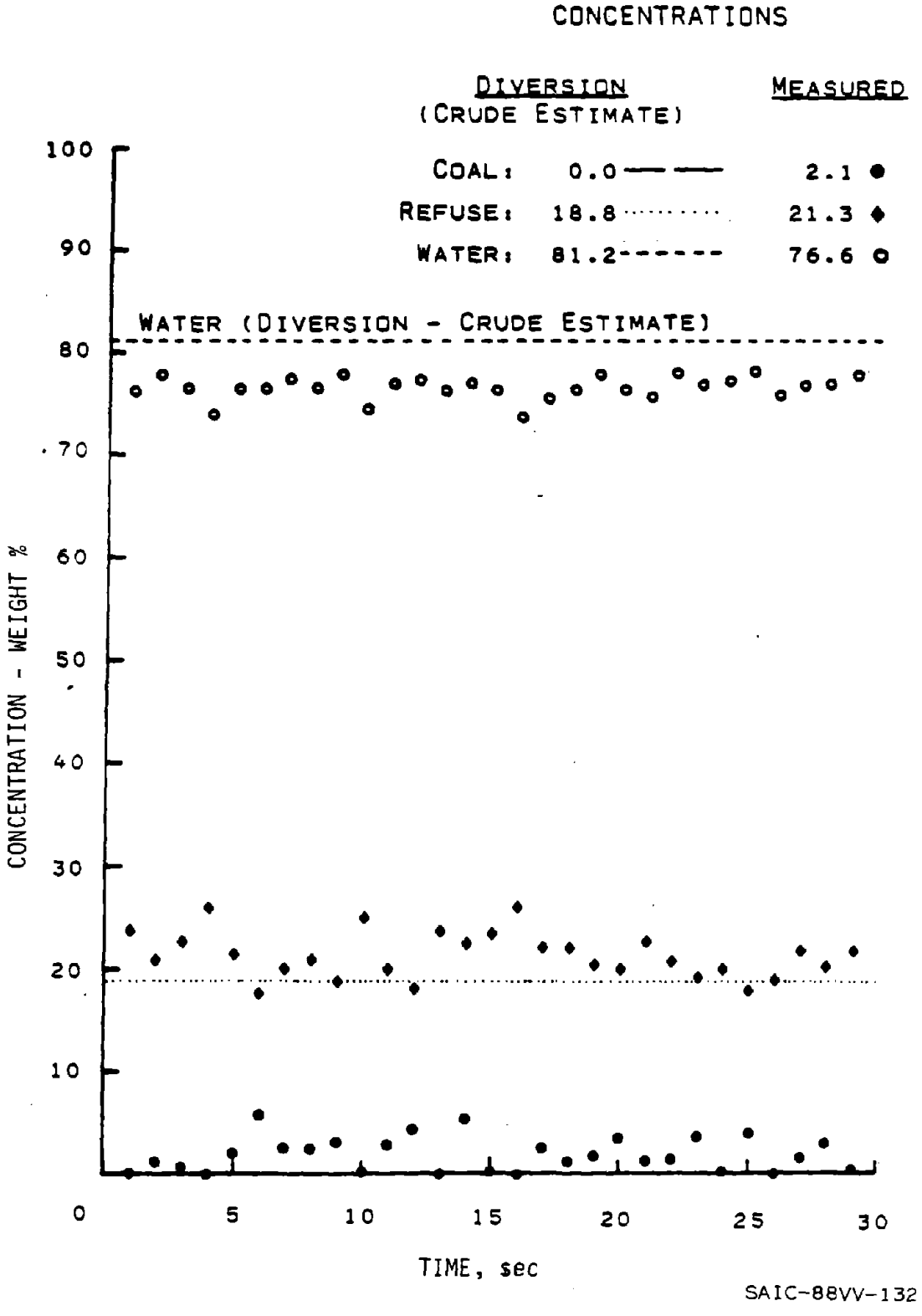
CONCENTRATIONS
DIVERSION (CRUDE ESTIMATE)
MEASURED
COAL: 0.0 2.1
REFUSE: 18.8 21.3
WATER: 81.2 76.6
WATER (DIVERSION - CRUDE ESTIMATE)
CONCENTRATION - WEIGHT %
100
90
80
70
60
50
40
30
20
10
0
5
10
15
20
25
30
TIME, sec
SAIC-88VV-132

FIGURE 4.17.

HCC-1

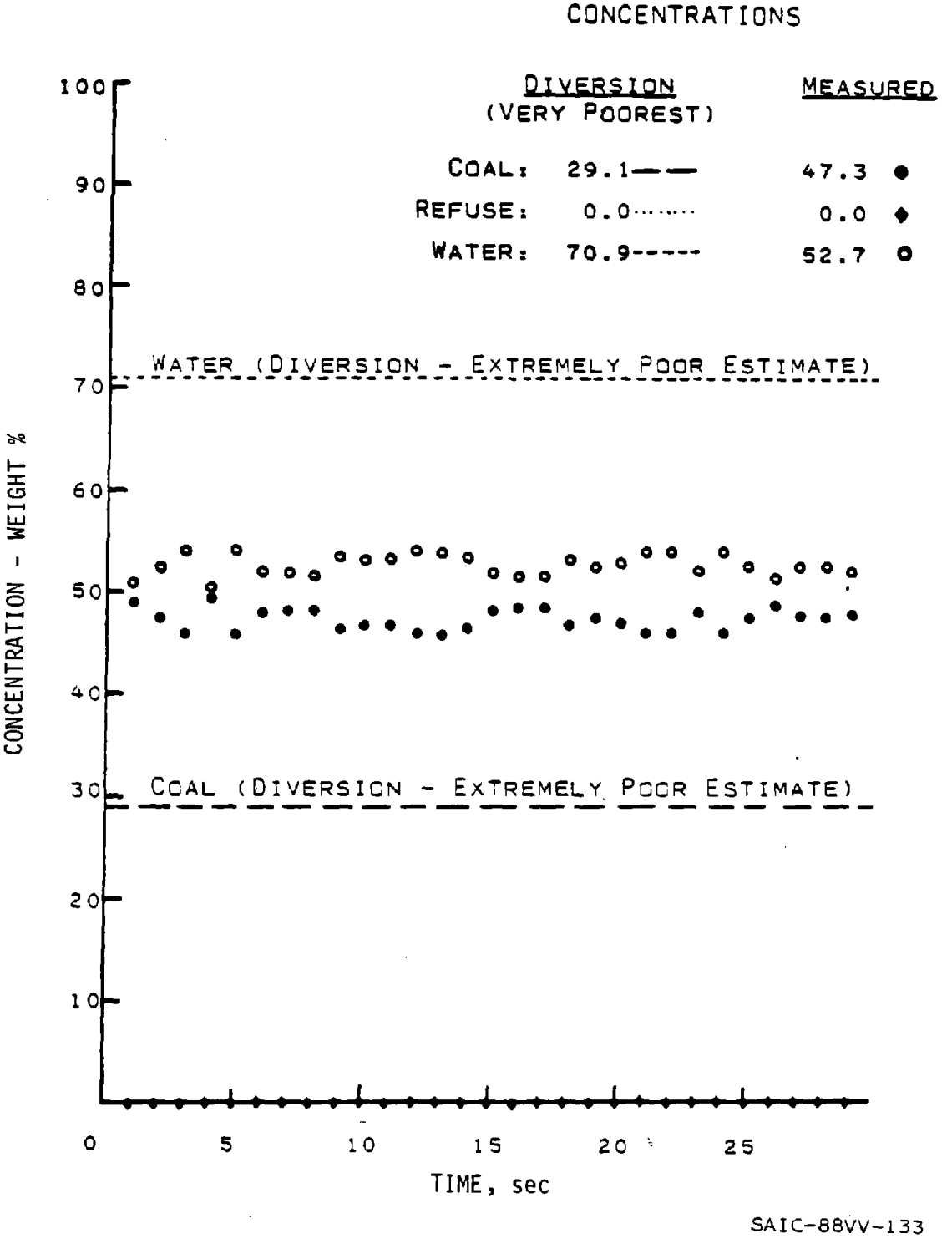

FIGURE 4.18.

gauge, the first ever developed, can be used in coal haulage measurements and in studying the hydraulic flow phenomenon (or phenomena).

The last row in Table 4.2 for HCR-1, the diversion tank measurement, is much closer to the concentration gauge measurement. This agrees with laboratory observations of 90% or more of the "rock" immediately breaking up after being wetted. This is illustrated in Table 4.3 below, by comparing the coarse coal and coarse refuse size distributions before and after pumping. In the case of the coal-refuse mix (pumped), almost 1/3 of the mix is -325 mesh, whereas with pumped coal, less than 1/13th of the mix is -325 mesh. (Very little of either the coal or refuse, unpumped, is -325 mesh.)

4.3 CONCLUSIONS

The test data with fine coal and refuse described in the preceding section show that the concentration sensor measures the in-situ concentration to an accuracy of 1-3%. (The diversion-tank measurements against which the accuracy is measured are no better than that. See Table 4.3 for the solids difference obtained by oven-drying and by the diversion tank gravimetric methods. In some cases, about 3% disagreement is reported.)

In the case of the coarse coal slurry, the test results dramatically illustrate how well the in-situ concentration sensor provides a measure of the hydraulic-haulage slippage phenomenon. A direct measure of the slippage is given by the difference between the diversion-tank measurement of solids and the concentration gauge measure of solids. The difference approaches a factor of two, as seen in Figure 4.18. For times immediately after loading the coal, before any breakup occurs, the in-situ concentrations were even higher. Thus, for coal 1/3 the pipe diameter (or 2 inches) as against the smaller stoker-grade coal (1 5/8 inches), the slippage will be even greater. The coal slurry concentration sensor was developed to measure slurries with coal and rock sizes as large as 1/3 pipe diameter.

This three-component slurry concentration sensor, the first of its kind ever developed, should prove highly useful in line-blockage studies in operating hydraulic haulage equipment to maximum efficiency, and possibly in

TABLE 4.3 - SAIC pipeline test summary for 1977 CSMRI measurements

Run Identification	Date 1977	Time	Samples	Velocity of slurry at Sampling Time(fps)	Weight concentration of solids by Oven drying	Flow diversion
VFC1 (fine coal, vertical pipe)	10-21	11:10	VFC1-1	4.0	28.00	28.85
		12:17	VFC1-2	8.0	27.12	24.84
		14:10	VFC1-3	11.9	25.99	25.55
VFC2	10-22	7:55	VFC2-1	4.1	45.93	45.06
		8:30	VFC2-2	8.2	46.14	43.65
		9:30	VFC2-3	12.3	46.95	44.97
VFR1 (fine refuse, vertical pipe)	10-24	14:10	VFR1-1	4.0	27.62	25.61
		14:38	VFR1-2	8.1	25.73	24.95
		15:05	VFR1-3	12.7	23.93	24.95
VFR2	10-24	16:19	VFR2-1	4.1	46.72	48.61
		16:47	VFR2-2	7.8	47.94	50.18
		17:22	VFR2-3	12.2	45.73	49.15
VFM1 (1265 lb fine coal 1239 lb fine refuse vertical pipe)	10-25	11:41	VFM1-1	4.0	25.07	27.42
		12:25	VFM1-2	8.0	25.97	24.90
		12:58	VFM1-3	12.1	25.48	25.56
VFM2 (3773 lb fine coal 3729 lb fine refuse vertical pipe)	10-25	15:09	VFM2-1	4.1	48.20	48.92
		15:31	VFM2-2	8.1	48.59	49.56
		15:55	VFM2-3	12.5	51.51	49.10
HER1 (fine refuse, horizontal pipe)	11-7	15:58	HFR1-1	12.6	46.38	49.06

providing a direct measure of tonnage delivered when used in conjunction with a flow meter (and with a knowledge of the approximate size distribution of coal/refuse normally used in loading the line).

4.4 PROPERTIES OF COAL AND REFUSE USED IN CSMRI TESTS

4.4.1 Coal and Refuse Source

The coal and refuse used in the concentration gauge tests were obtained from a Pittsburgh seam underground mine. The coal is stoker grade, and the refuse was screened to eliminate chunks larger than 2 inches.

An earlier sample (1976) of about five buckets, five gallons each, was obtained from the Pittsburgh Research Center experimental mine. The analysis of that batch of coal and the Morgantown supply (1977) of coal and refuse is presented in Table 4.4. These analyses were used to calculate the neutron and gamma-ray cross sections for coal and refuse.

Some of the coal and refuse was fine-ground, so that no appreciable slippage would occur in the CSMRI test loop. With their diversion-tank measurements and with oven-drying techniques applied to a separate grab-sample, we were able to determine the in-situ coal concentration to $\pm$ 2-3% and the refuse sample to $\pm$ 1-2% (the difference being due to the large difference in specific gravity of coal and refuse) for direct comparisons with the concentration sensor readings. The results of screening analyses on the fine and coarse coal and refuse are presented in Table 4.5. Table 4.6 gives the size range and the mean particle size for the many test runs carried out in 1977 at CSMRI.

4.4.2 Coal and Rock Conductivity

Careful tests were made of coal and refuse conductivity. Utilizing long plastic trays with electrodes at each end covering the entire cross sectional area so as to give a very accurate parallel electrical-field configuration, conductivity measurements were made on dense coal and rock slurries, and also on the decanted water from the same coal and rock batches

TABLE 4.4 - Chemical analysis of coal and refuse (weight %, deduced from elemental and other analyses).

	COAL		REFUSE
	1976[1]	1977[1]	1977[1]
C	78.6	75.4	5.5
H(combustible)	5.4	5.1	0.9
Moisture	2.5	2.4	2.0
SiO_2	5.5	8.0	52.3
Al_2O_3	3.5	3.7	22.4
$Fe_2(SO_4)_3$ (2)	3.0	3.6	6.2
FeS_2 (2)	1.5	1.8	4.2
FeO_2 (2)	-	-	1.9
TiO_2	-	-	0.8
CaO_2	-	-	3.8
TOTAL	100.0	100.0	100.0

Note: [1] 1976 sample from U.S. Bureau of Mines Bruceton Experimental Mine. 1977 samples from Pittsburgh Seam coal and refuse.

[2] The ratios of $Fe_2(SO_4)_3$, FeS_2 and FeO_2 are only approximate in that they were deduced from a) total ash content minus SiO_2 and Al_2O_3 obtained from Si and Al content, and b) Fe and S content.

TABLE 4.5. - Typical screen-analysis results (weight %)

SAMPLE	SCREEN PRODUCT (TYLER) MESH									
	20/28	28/35	35/48	48/65	65/100	100/150	150/200	200/325	-325	
Coal, Fine, Pumped	1.27	7.29	10.49	12.37	17.42	5.68	13.96	5.77	25.76	
Refuse, Fine, Pumped	0.30	3.45	4.77	6.60	8.33	4.64	7.23	5.84	58.84	
Coal & Refuse Mix,Fine,Pumped	3.46	7.20	9.12	10.97	18.00	4.05	11.31	4.17	31.61	
	1/0.75	0.75/0.5	0.5/3	3/6	6/14	14/28	28/48	48-150	150/325	-325
Coal, Coarse, Pumped	0.00	7.54	24.35	24.70	15.78	6.67	4.95	5.73	2.80	7.48
Coal & Refuse Mix,Coarse,Pumped	0.00	0.00	5.81	17.80	20.70	7.39	4.62	6.88	8.07	28.74
	1.25/1	1/0.75	0.75/0.5	0.5/3	3/6	6/14	14/28	-28	-0.5	
Coal, Coarse, Unpumped	22.68	45.81	29.01	-	-	-	-	-	2.50	
Refuse, Coarse, Unpumped	9.63	8.33	10.00	17.93	12.30	27.68	8.62	4.90	-	

TABLE 4.6.- Science Application International Corporation size distribution analysis summary

Sample	Size Range m.m.	d_{50} (1) μ	Weighted Mean Particle Diameter (2) μ
coarse coal, unpumped	31.8 x 0	21,600	21,400
coarse refuse, unpumped	31.8 x 0	5,800	9,300
fine coal, unpumped	0.82 x 0	190	220
fine refuse, unpumped	0.82 x 0	141	244
VFC1-1	0.82 x 0	190	220
VFC1-2	0.82 x 0	160	180
VFC1-3	0.82 x 0	140	180
VFC2-1	0.82 x 0	160	190
VFC2-2	0.82 x 0	170	200
VFC2-3	0.82 x 0	150	180
VFR1-1	0.82 x 0	40	110
VFR1-2	0.82 x 0	38	97
VFR1-3	0.82 x 0	37	93
VFR2-1	0.82 x 0	42	120
VFR2-2	0.82 x 0	32	98
VFR2-3	0.82 x 0	39	107
VFM1-1	0.82 x 0	155	193
VFM1-2	0.82 x 0	167	202
VFM1-3	0.82 x 0	168	202
VFM2-1	0.82 x 0	160	197
VFM2-2	0.82 x 0	131	180
VFM2-3	0.82 x 0	120	175
VCM1-1	25.4 x 0	3,652	6,135
VCM1-2	25.4 x 0	5,601	7,184
VCM1-3	25.4 x 0	2,743	5,339
VCM1-4	25.4 x 0	541	2,493
VCC1-1	19.0 x 0	4,365	5,229
HCC1-1	12.7 x 0	2,672	3,353
HCC2-1	19.0 x 0	6,318	7,015
HCC2-2	19.0 x 0	3,083	3,886
HCM1-1	12.7 x 0	725	1,980
HFR1-1	0.82 x 0	38	104

(1) diameter at which 50% of the sample by weight is larger in size

(2) Σ(particle diameter "i" x weight fraction of size "i")

(water that had dissolved all the minerals it could after about a one-week soaking with periodic mixing). In each of the dense slurries, the conductivity was measured to be proportional to the water volume to ~1%, as determined by gravimetric methods. Thus, it was concluded that the conductivity gauge, if properly designed with clarification system and a reference cell of "matching" geometry, was a viable candidate for direct measurement of the slurry water fraction, V_w.

4.4.3 Density Variations of Coal and Rock

Table 2.1 (Section 2, above) lists the range of specific gravity for coal as 1.2 to 1.6 and for refuse as 2.3 to 3.1 (for the U.S. Bureau of Mines design specifications). This range is much too great to assume that it is nearly constant. However, if the densities of coal and refuse are nearly constant for a given mine, or even a given seam, and were measured and input to the computer program, the conductivity gauge would not be required as this density data, along with the gamma-ray and neutron gauge data, is all that is needed to yield the concentrations of coal, rock and water. This was not an option in this program, because it was required that for at least one operating configuration of the coal slurry concentration sensor, density measurements would not be required for successful operation of the sensor.

The densities of the Pittsburgh seam coal and refuse, as measured with the ASTM Standard Method, are 1.35 and 2.54 gm/cm^3 respectively for the material used in tests at SAIC and CSMRI.

4.5 SLIPPAGE CALCULATIONS

Calculations of the degree of slippage versus particle size and slurry velocity were carried out for SAIC by George Pouska of CSMRI, as a consultant to SAIC in early 1982. These were needed to determine the maximum particle size (or the size distribution) that would cause no greater than 1%, and also 2%, error when utilizing flow-diversion measurements (into a diversion tank) to obtain a check on the in-situ concentration sensor; i.e., the coal/rock/water concentration sensor. These calculations are presented as Appendix B of this report.

5.0 HTRF TESTS

These tests were carried out with the 6" sensor mounted on the 6" test line and the 18" sensor (on the 18" line), each mounted in a vertical section of the HTRF test facility. The cross sections for coal and rock for the 6" sensor were determined with great accuracy at CSMRI (Colorado School of Mines Research Institute) for Pittsburgh seam coal (100%) and rock (100%) shipped in from a deep seam from Morgantown, West Virginia. These neutron and gamma-ray cross sections were rechecked at the HTRF in October, 1982 and found to be the same for the coal supplied by PRC. They were also measured for the 18" sensor and were found to be only slightly different, the difference being attributed solely to the differences in geometry of the 6" and 18" sensors, as well as the different pipe diameters (different penetration thicknesses).

In October, 1982, two runs were carried out for the 18" sensor, one with coarse coal and the other with coarse rock. The data are presented in Figures 5.1 and 5.2 The in-situ concentration of the solids was, in each case, about a factor of two higher than that calculated from loading concentrations. This was, of course, as expected, especially for a vertical flow, relatively large particle size, and a low fluid velocity of only 10 ft/sec. The two small 12" pumps feeding an 18" line were under-rated by about a factor of 4-1/2. See Appendix B for some slippage calculations relating to these test results.

For the 6" concentration sensor in the vertical 6" line, the slippage was less (the order of 25-35%, depending on whether the finer or coarser coal was used) for coal. (See Figures 5.3 through 5.10.) For coarse rock, that is 100% rock, the in-situ concentration was 60% to 100% above the loading-inventory concentration. These data are presented in Figure 5.11. For all other runs (see Figures 5.12 through 5.16), the "rock" or "refuse" contained varying percentages of coal. The submerged (in water) density for rock is about a factor of 3 1/2 greater than for coal. Table 5.1 presents the densities for 100% coal (first row), 100% rock (second row), and various rock/coal ratios for the "refuse" supplied by PRC for these tests. The % (C+H) is also given for each batch. Here C+H = carbon and hydrogen content. By plotting the % (C+H) for 100% coal and 100% rock, as in Figure 5.17, and

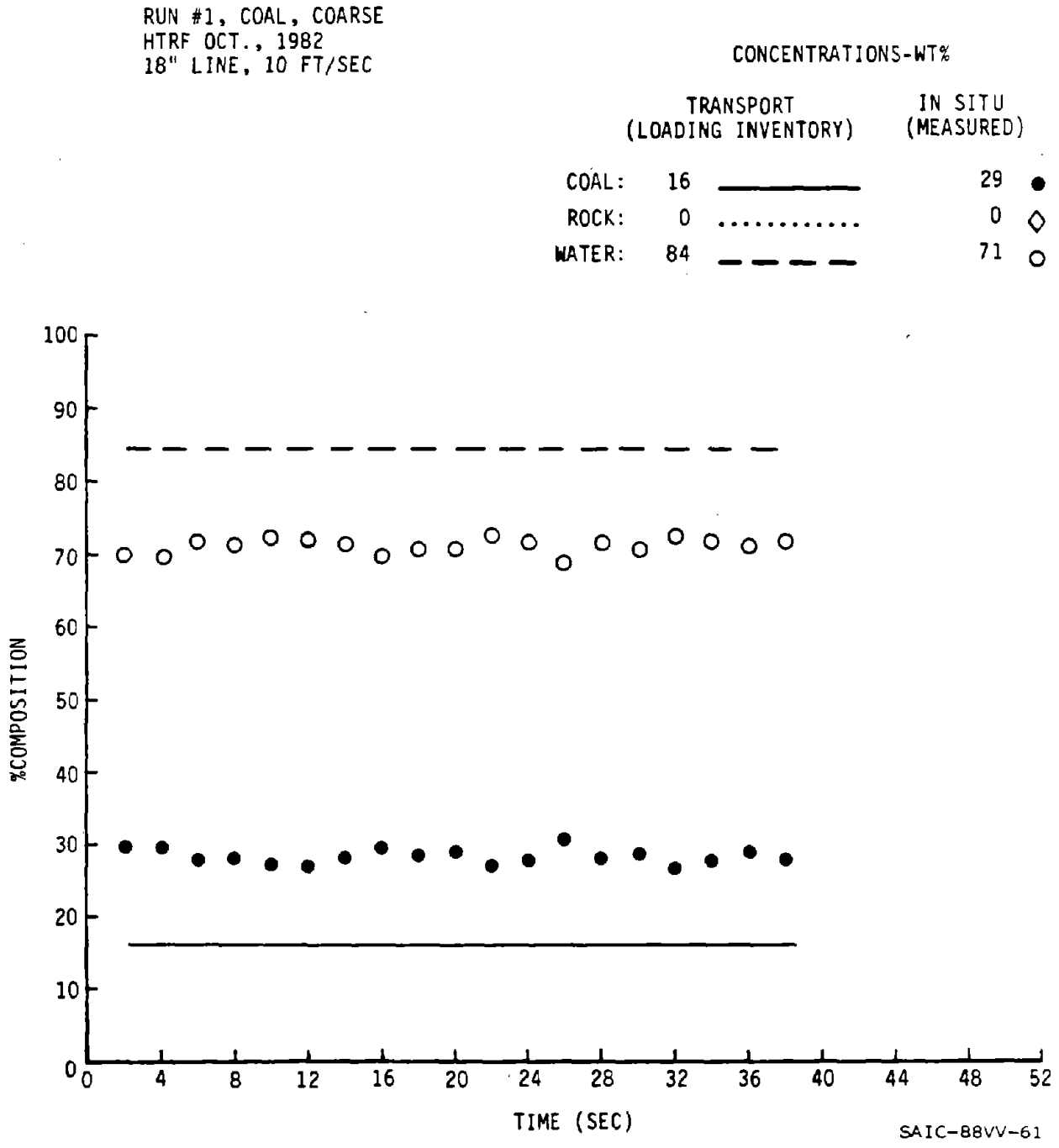
RUN #1, COAL, COARSE
HTRF OCT., 1982
18" LINE, 10 FT/SEC
CONCENTRATIONS-WT%
TRANSPORT (LOADING INVENTORY)
IN SITU (MEASURED)
COAL: 16 29
ROCK: 0 0
WATER: 84 71
%COMPOSITION
TIME (SEC)
SAIC-88VV-61

FIGURE 5.1.

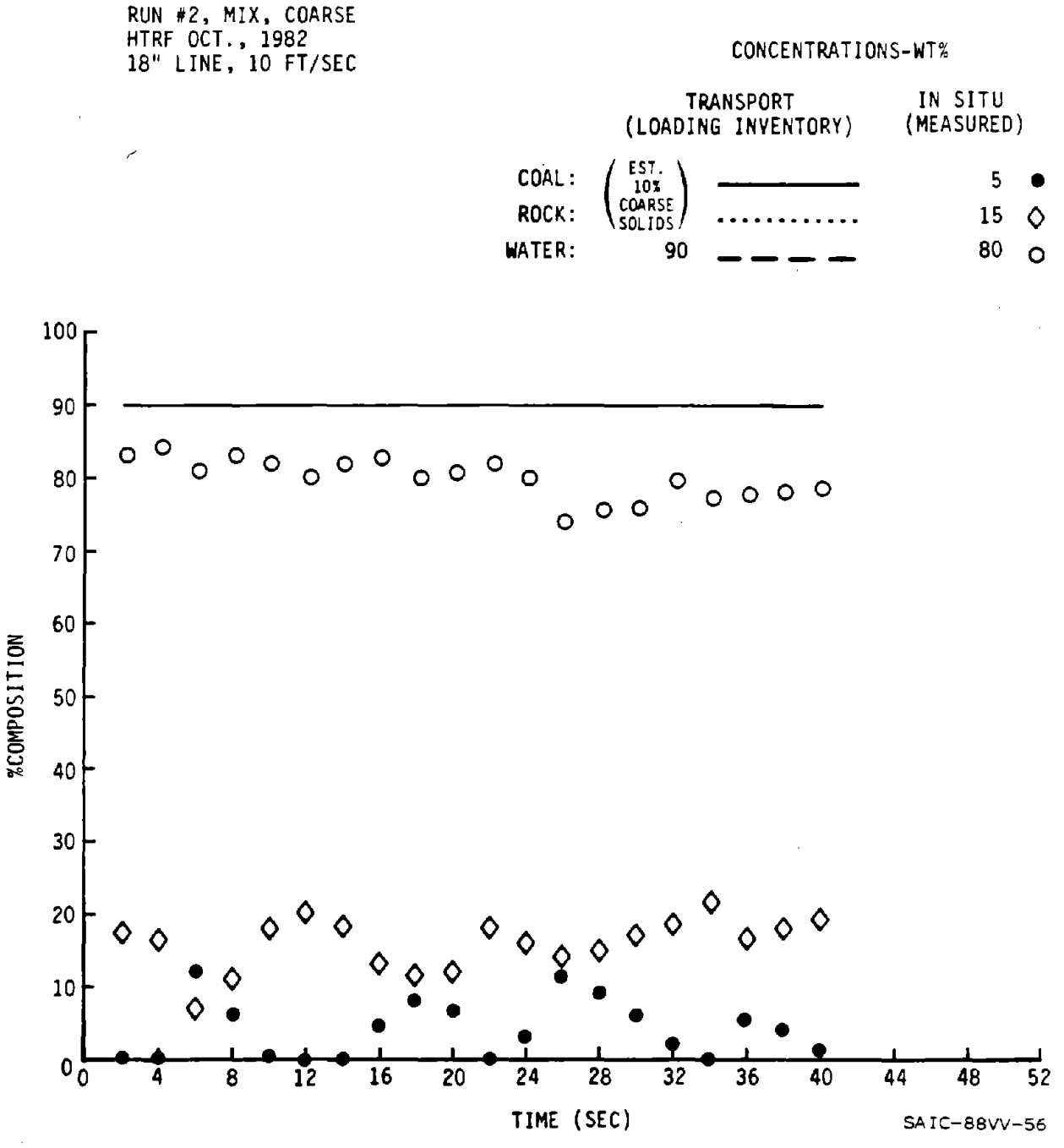
RUN #2, MIX, COARSE
HTRF OCT., 1982
18" LINE, 10 FT/SEC
CONCENTRATIONS-WT%
TRANSPORT (LOADING INVENTORY)
IN SITU (MEASURED)
COAL: (EST. 10% COARSE SOLIDS) 5
ROCK: 15
WATER: 90 80
%COMPOSITION
TIME (SEC)
SAIC-88VV-56

FIGURE 5.2.

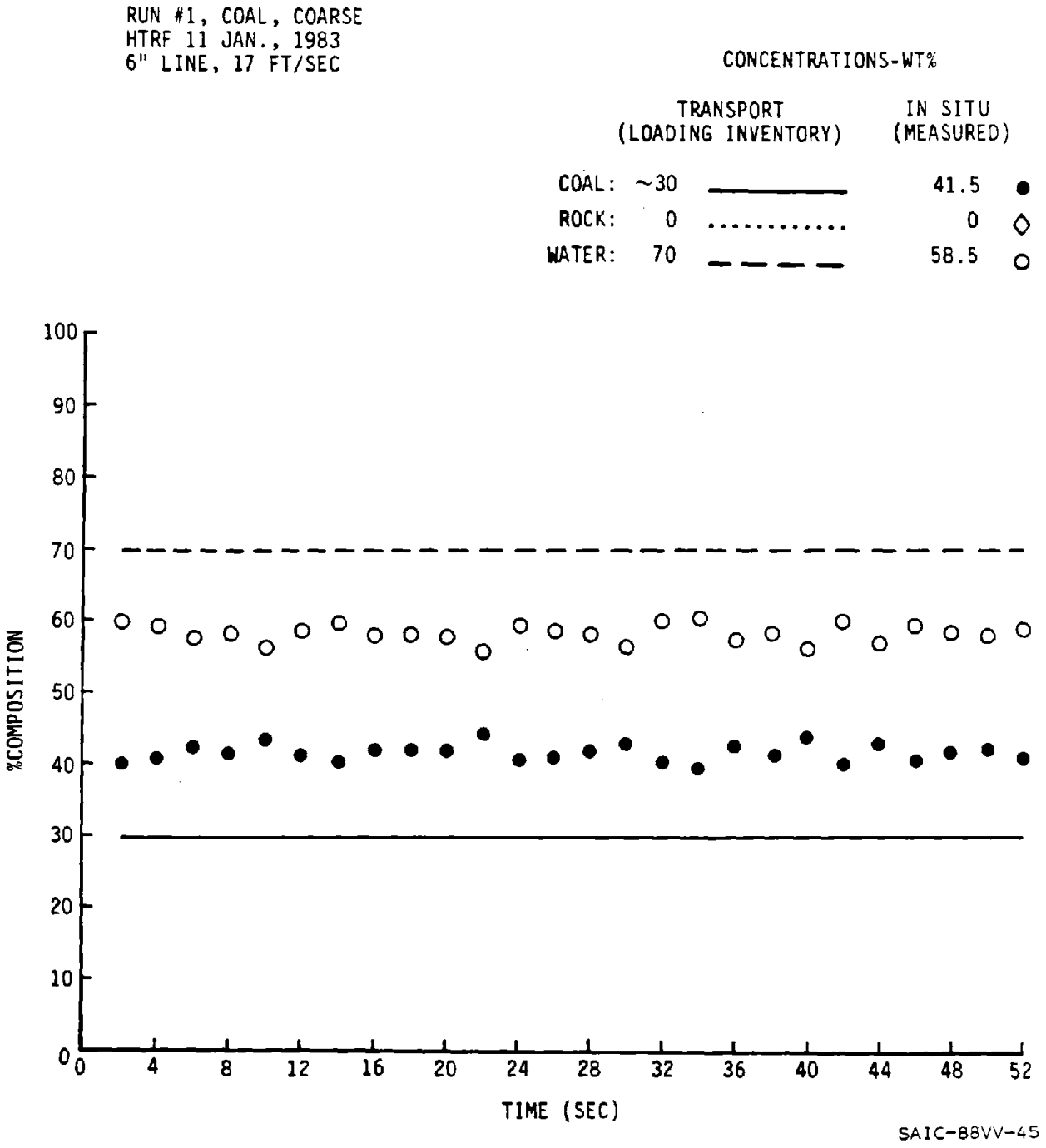
RUN #1, COAL, COARSE
HTRF 11 JAN., 1983
6" LINE, 17 FT/SEC
CONCENTRATIONS-WT%
TRANSPORT (LOADING INVENTORY)
IN SITU (MEASURED)
COAL: ~30
41.5
ROCK: 0
0
WATER: 70
58.5
%COMPOSITION
TIME (SEC)
SAIC-88VV-45

FIGURE 5.3.

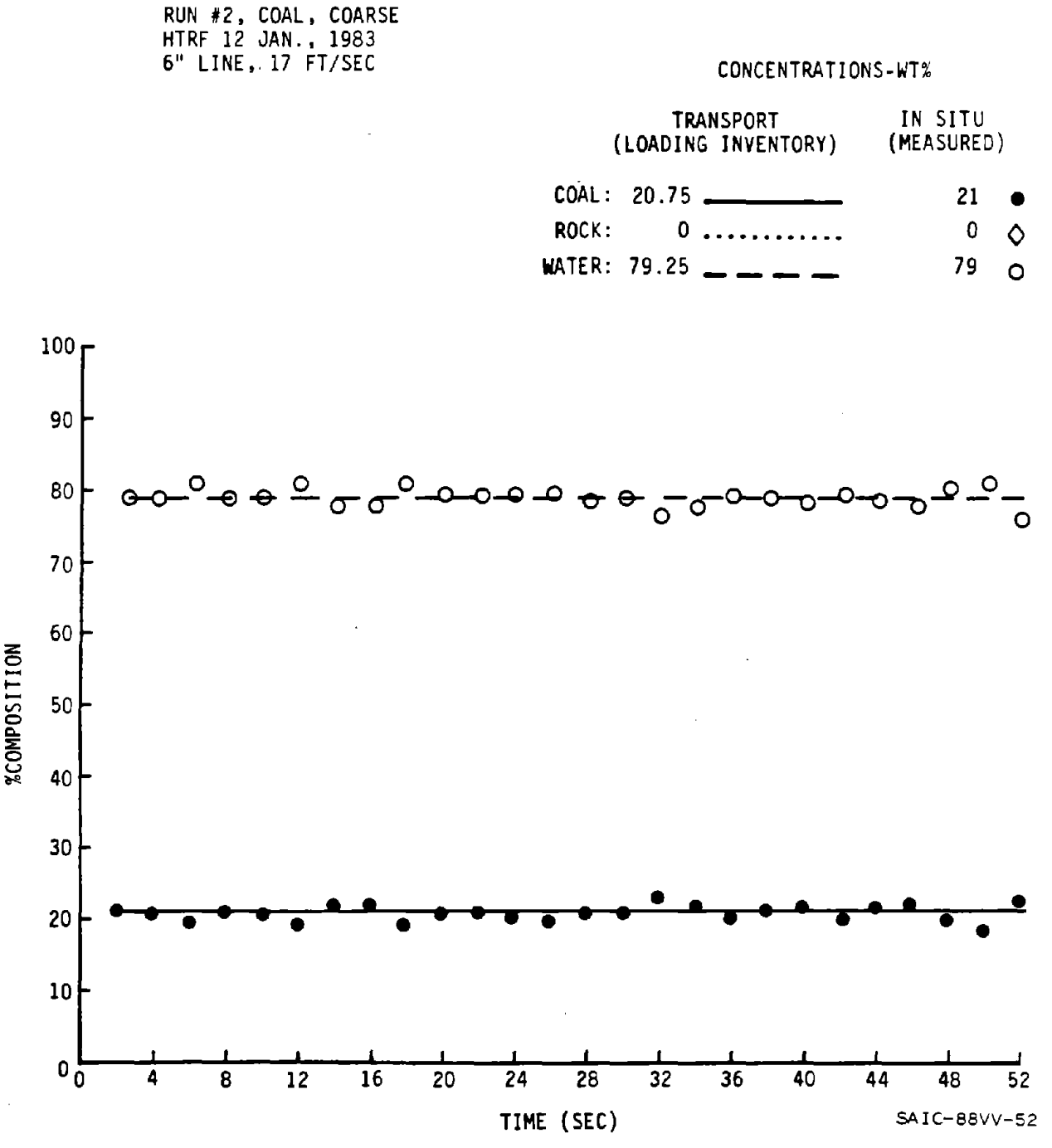
RUN #2, COAL, COARSE
HTRF 12 JAN., 1983
6" LINE, 17 FT/SEC
CONCENTRATIONS-WT%
TRANSPORT (LOADING INVENTORY)
IN SITU (MEASURED)
COAL: 20.75
21
ROCK: 0
0
WATER: 79.25
79
%COMPOSITION
TIME (SEC)
SAIC-88VV-52

FIGURE 5.4.

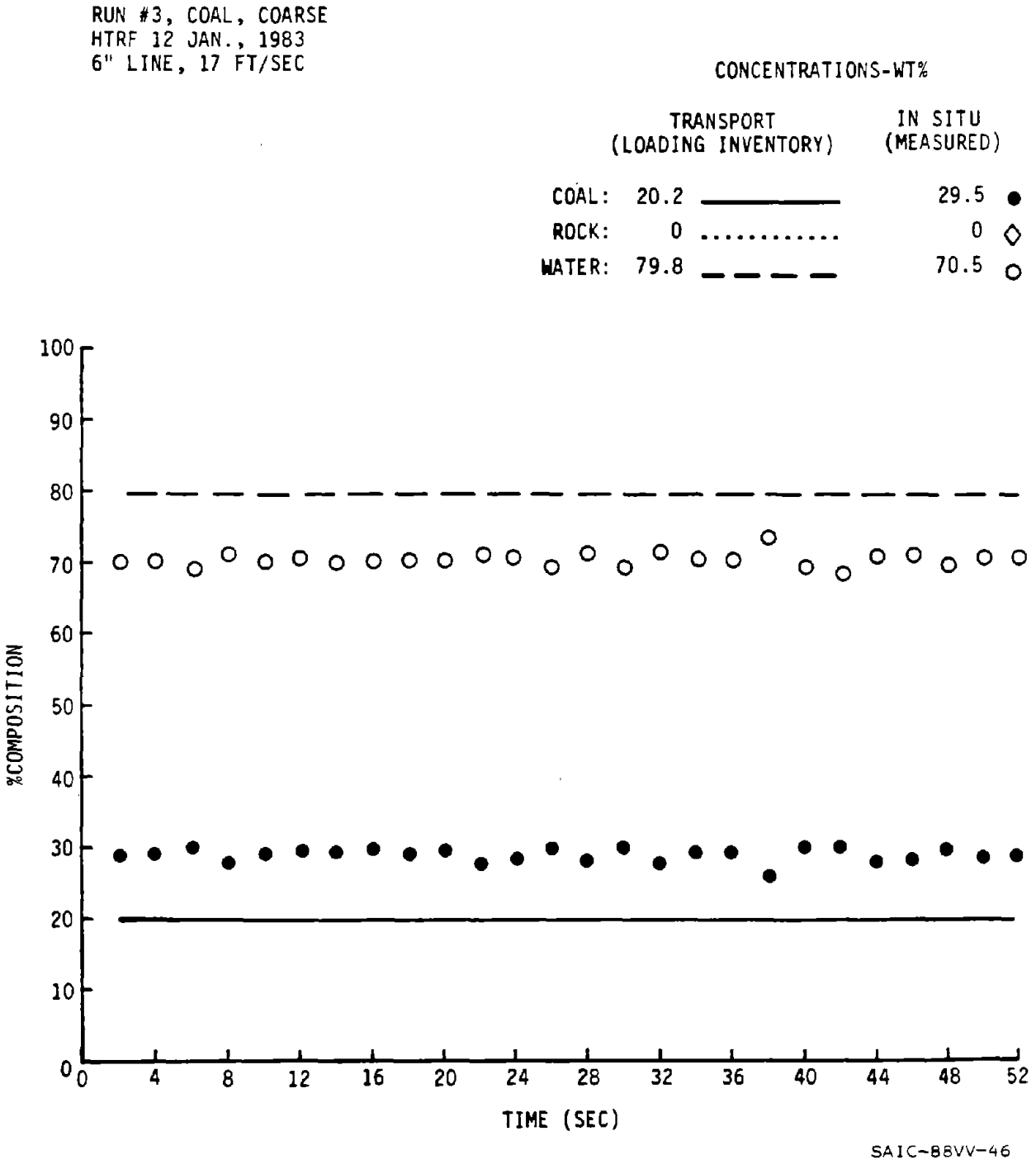
RUN #3, COAL, COARSE
HTRF 12 JAN., 1983
6" LINE, 17 FT/SEC
CONCENTRATIONS-WT%
TRANSPORT (LOADING INVENTORY)
IN SITU (MEASURED)
COAL: 20.2
29.5
ROCK: 0
0
WATER: 79.8
70.5
%COMPOSITION
TIME (SEC)
0
10
20
30
40
50
60
70
80
90
100
0
4
8
12
16
20
24
28
32
36
40
44
48
52
SAIC-88VV-46

FIGURE 5.5.

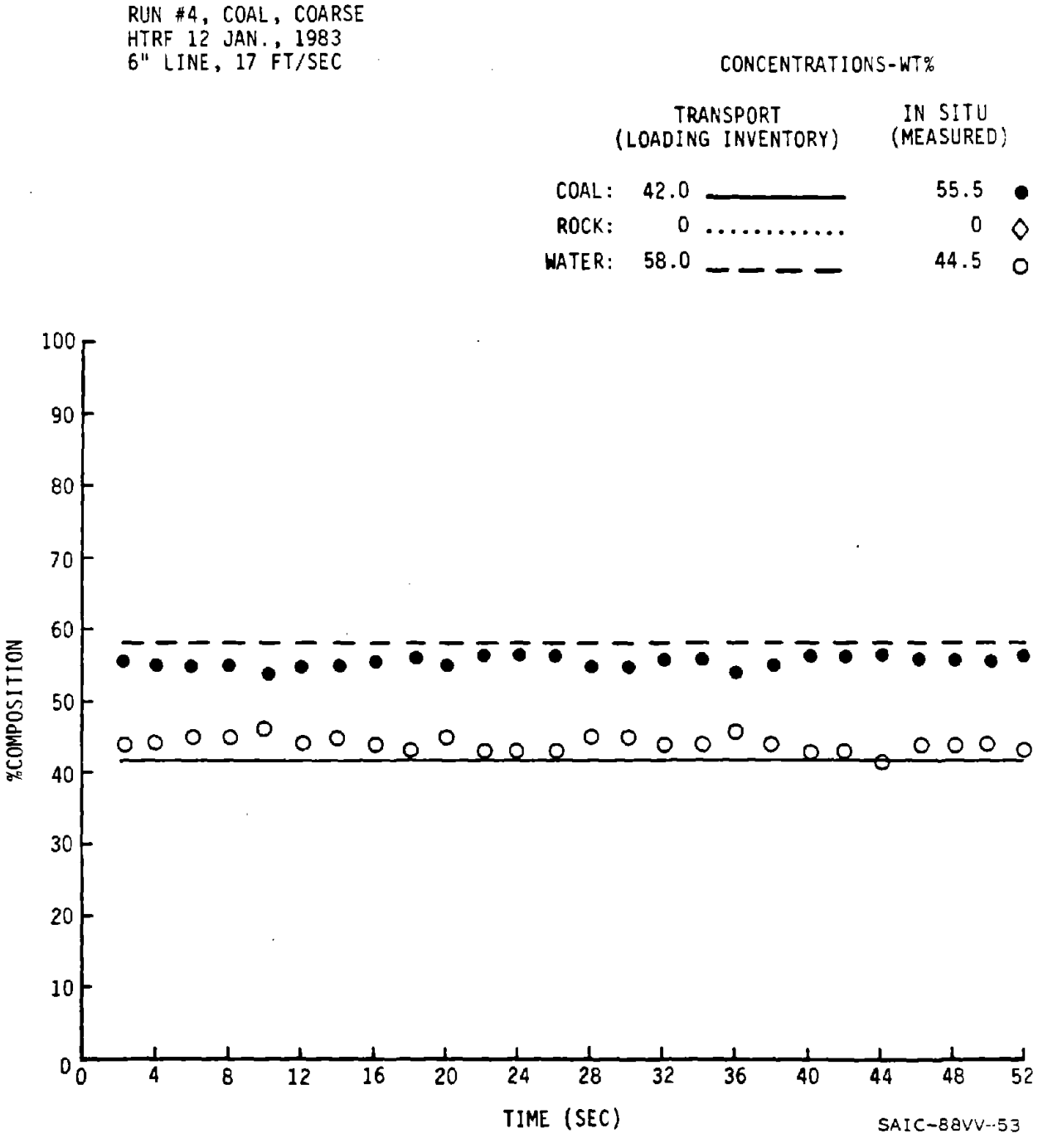
RUN #4, COAL, COARSE
HTRF 12 JAN., 1983
6" LINE, 17 FT/SEC
CONCENTRATIONS-WT%
TRANSPORT (LOADING INVENTORY)
IN SITU (MEASURED)
COAL: 42.0
55.5
ROCK: 0
0
WATER: 58.0
44.5
%COMPOSITION
TIME (SEC)
SAIC-88VV-53

FIGURE 5.6.

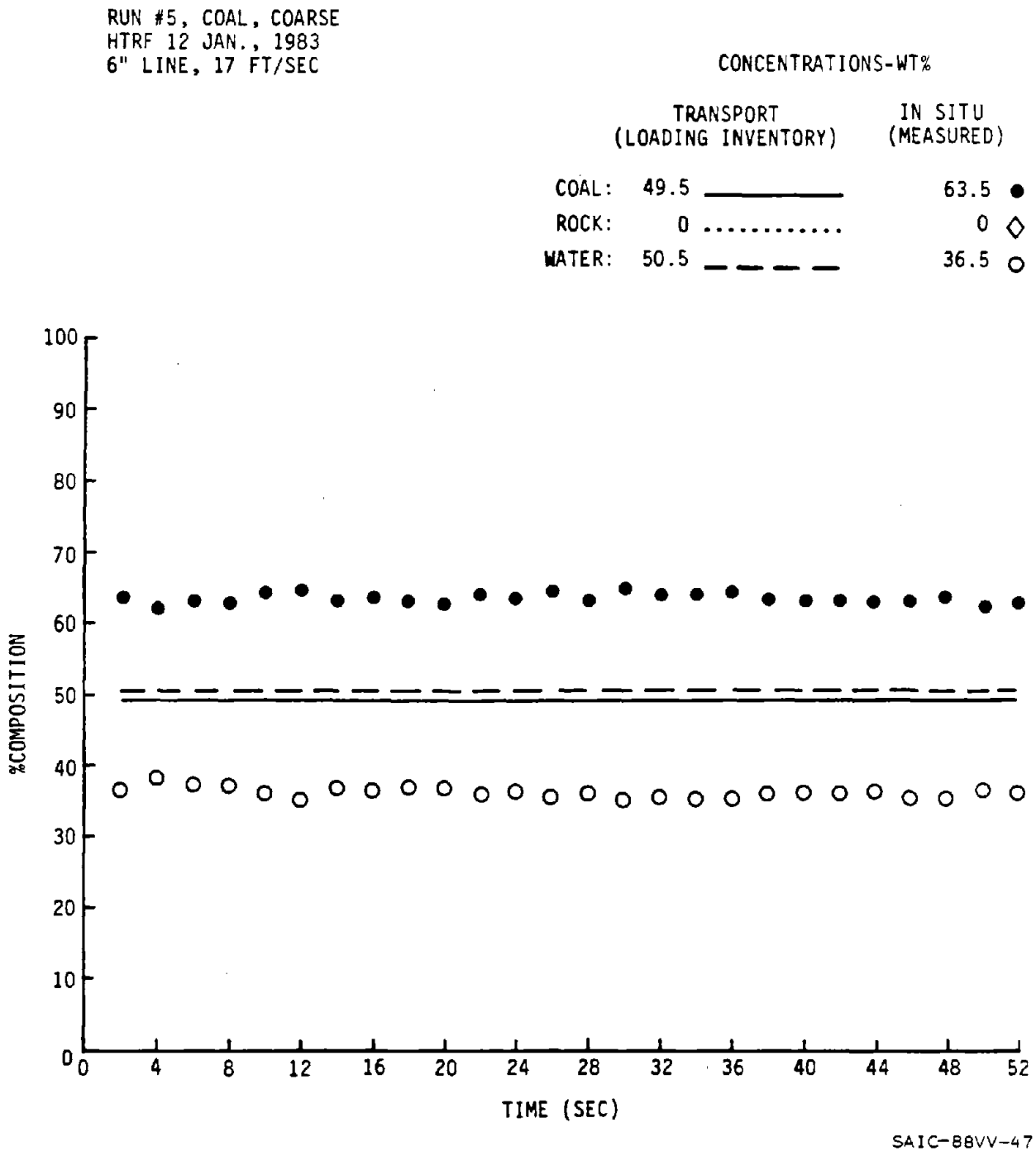
RUN #5, COAL, COARSE
HTRF 12 JAN., 1983
6" LINE, 17 FT/SEC
CONCENTRATIONS-WT%
TRANSPORT (LOADING INVENTORY)
IN SITU (MEASURED)
COAL: 49.5
63.5
ROCK: 0
0
WATER: 50.5
36.5
%COMPOSITION
TIME (SEC)
0
10
20
30
40
50
60
70
80
90
100
0
4
8
12
16
20
24
28
32
36
40
44
48
52
SAIC-88VV-47

FIGURE 5.7.

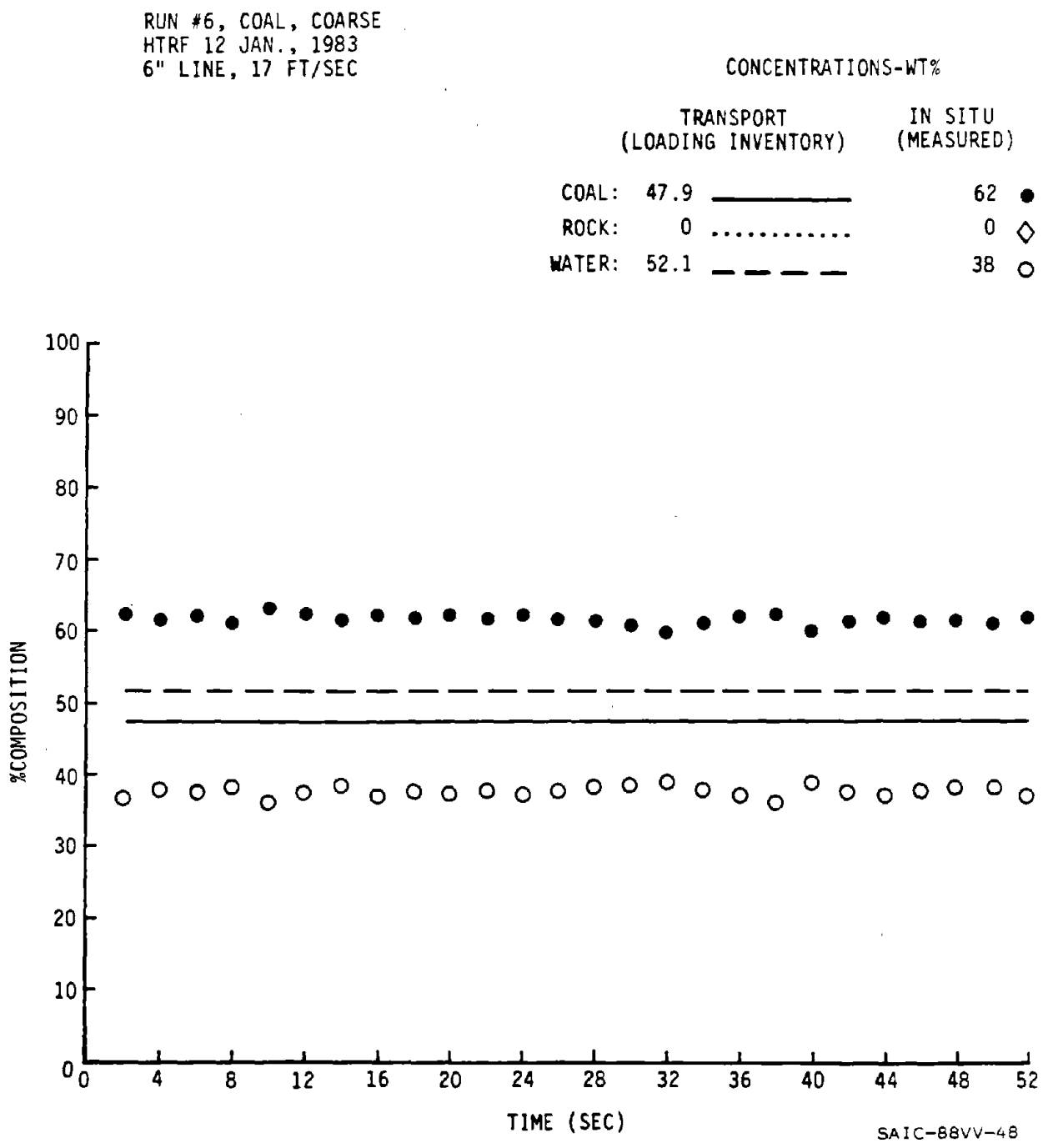
RUN #6, COAL, COARSE
HTRF 12 JAN., 1983
6" LINE, 17 FT/SEC
CONCENTRATIONS-WT%
TRANSPORT (LOADING INVENTORY)
IN SITU (MEASURED)
COAL: 47.9
62
ROCK: 0
0
WATER: 52.1
38
%COMPOSITION
TIME (SEC)
0
10
20
30
40
50
60
70
80
90
100
0
4
8
12
16
20
24
28
32
36
40
44
48
52
SAIC-88VV-48

FIGURE 5.8.

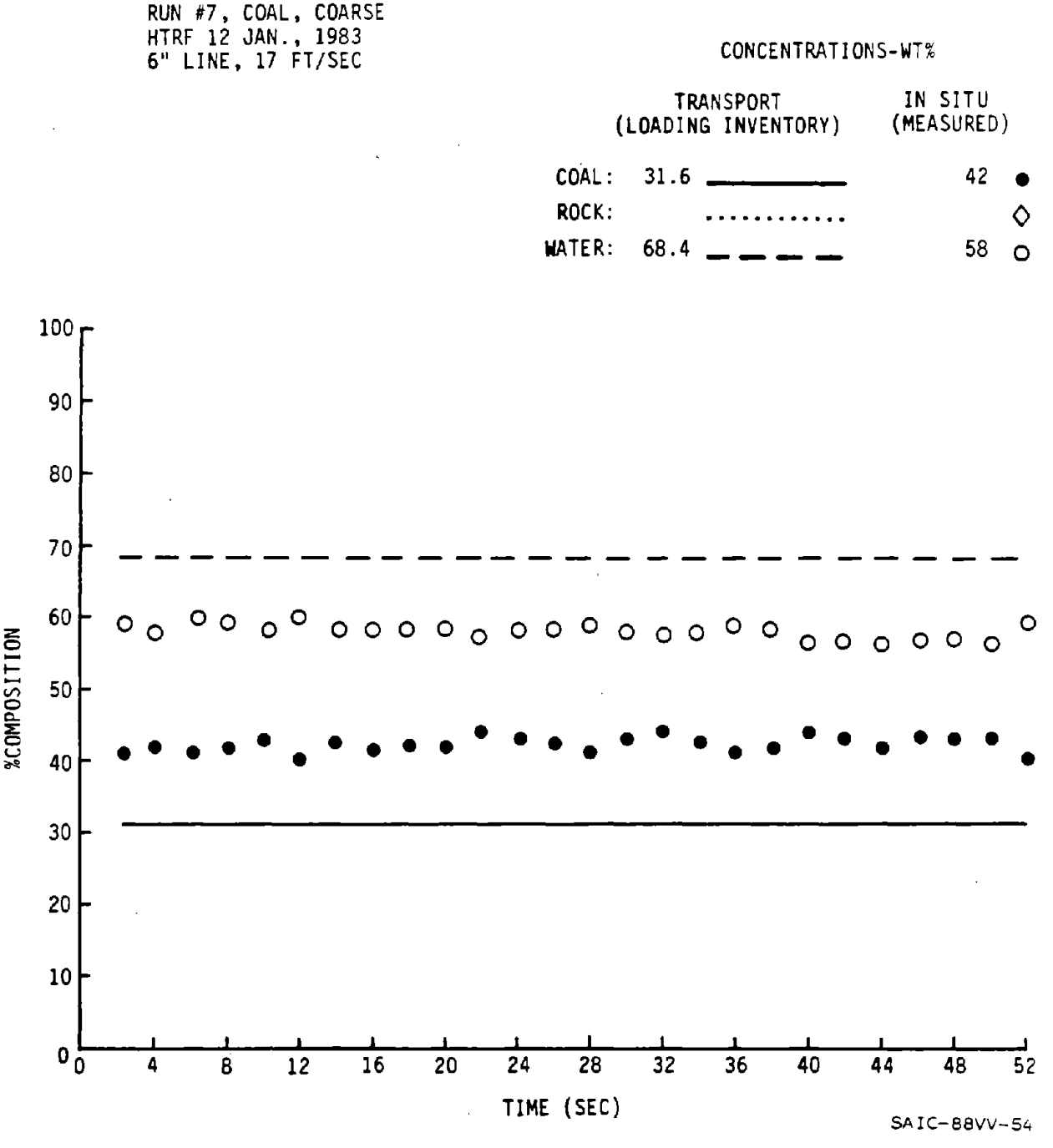
RUN #7, COAL, COARSE
HTRF 12 JAN., 1983
6" LINE, 17 FT/SEC
CONCENTRATIONS-WT%
TRANSPORT (LOADING INVENTORY)
IN SITU (MEASURED)
COAL: 31.6
42
ROCK:
WATER: 68.4
58
%COMPOSITION
TIME (SEC)
0
10
20
30
40
50
60
70
80
90
100
0
4
8
12
16
20
24
28
32
36
40
44
48
52
SAIC-88VV-54

FIGURE 5.9.

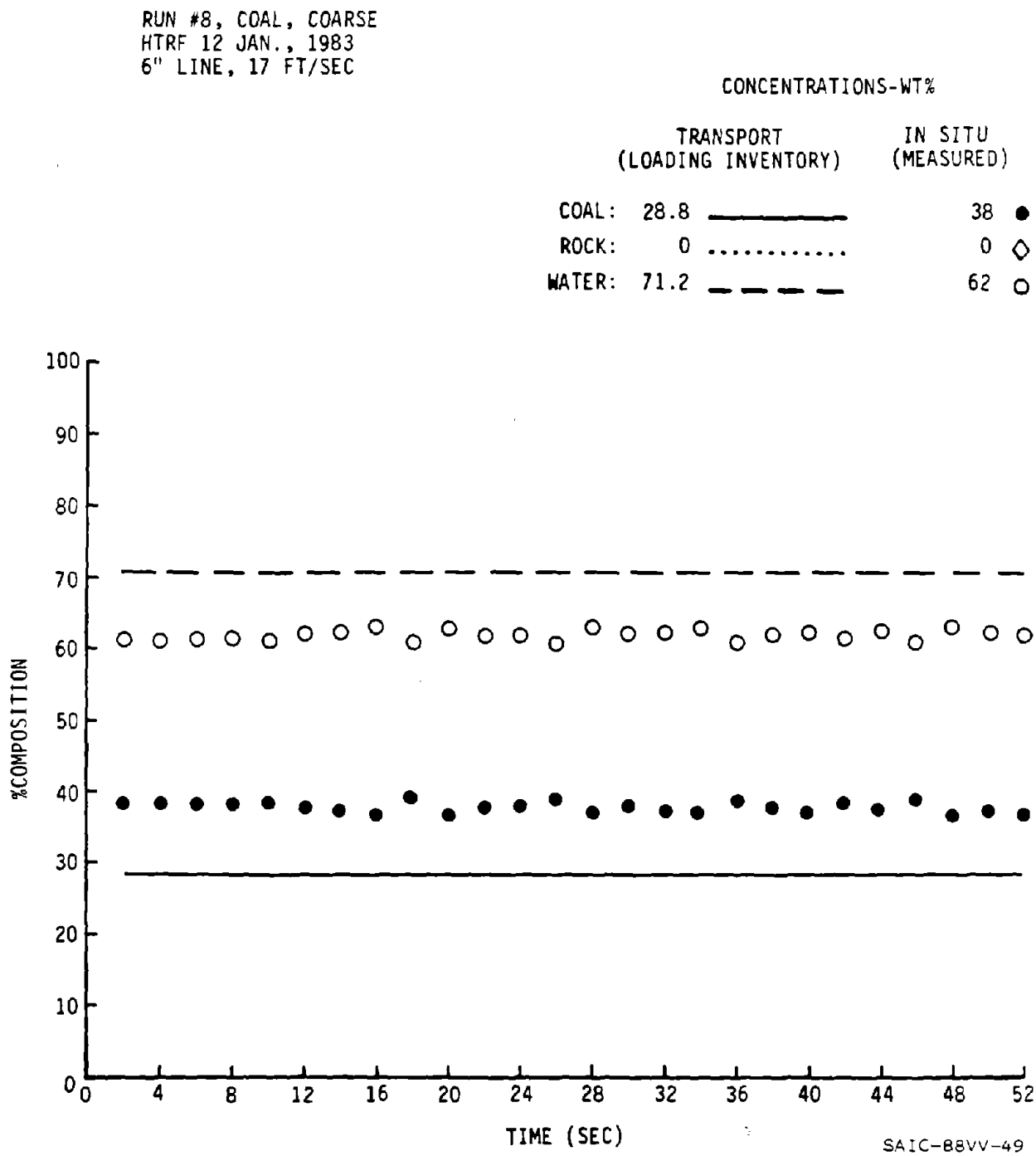
RUN #8, COAL, COARSE
HTRF 12 JAN., 1983
6" LINE, 17 FT/SEC
CONCENTRATIONS-WT%
TRANSPORT (LOADING INVENTORY)
IN SITU (MEASURED)
COAL: 28.8
38
ROCK: 0
0
WATER: 71.2
62
%COMPOSITION
TIME (SEC)
SAIC-88VV-49

FIGURE 5.10.

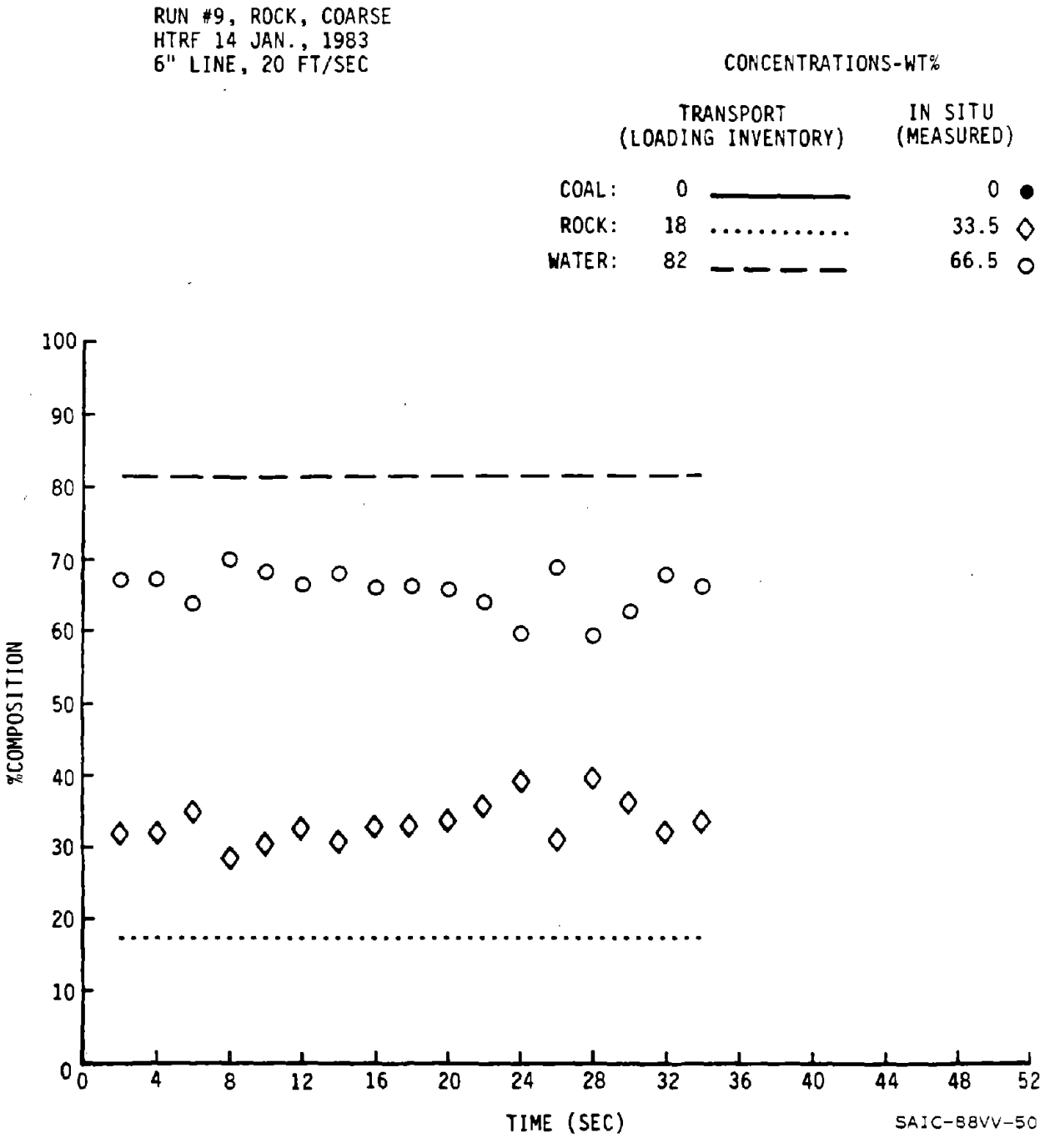
RUN #9, ROCK, COARSE
HTRF 14 JAN., 1983
6" LINE, 20 FT/SEC
CONCENTRATIONS-WT%
TRANSPORT (LOADING INVENTORY)
IN SITU (MEASURED)
COAL: 0 0
ROCK: 18 33.5
WATER: 82 66.5
%COMPOSITION
TIME (SEC)
0 10 20 30 40 50 60 70 80 90 100
0 4 8 12 16 20 24 28 32 36 40 44 48 52
SAIC-88VV-50

FIGURE 5.11.

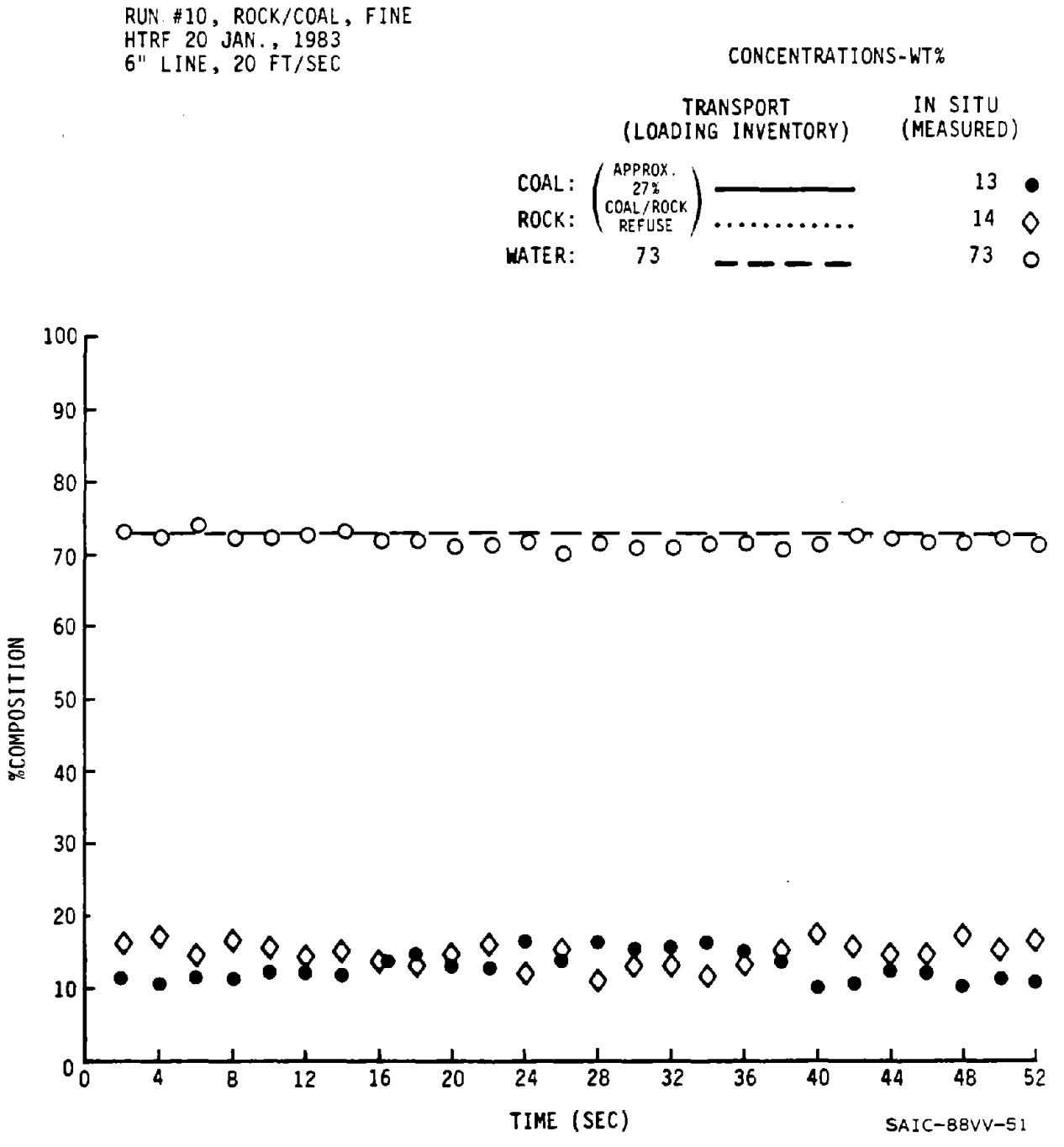
RUN #10, ROCK/COAL, FINE
HTRF 20 JAN., 1983
6" LINE, 20 FT/SEC
CONCENTRATIONS-WT%
TRANSPORT (LOADING INVENTORY)
IN SITU (MEASURED)
COAL: (APPROX. 27% COAL/ROCK REFUSE)
ROCK:
WATER: 73
13
14
73
%COMPOSITION
TIME (SEC)
0
4
8
12
16
20
24
28
32
36
40
44
48
52
10
20
30
40
50
60
70
80
90
100
SAIC-88VV-51

FIGURE 5.12.

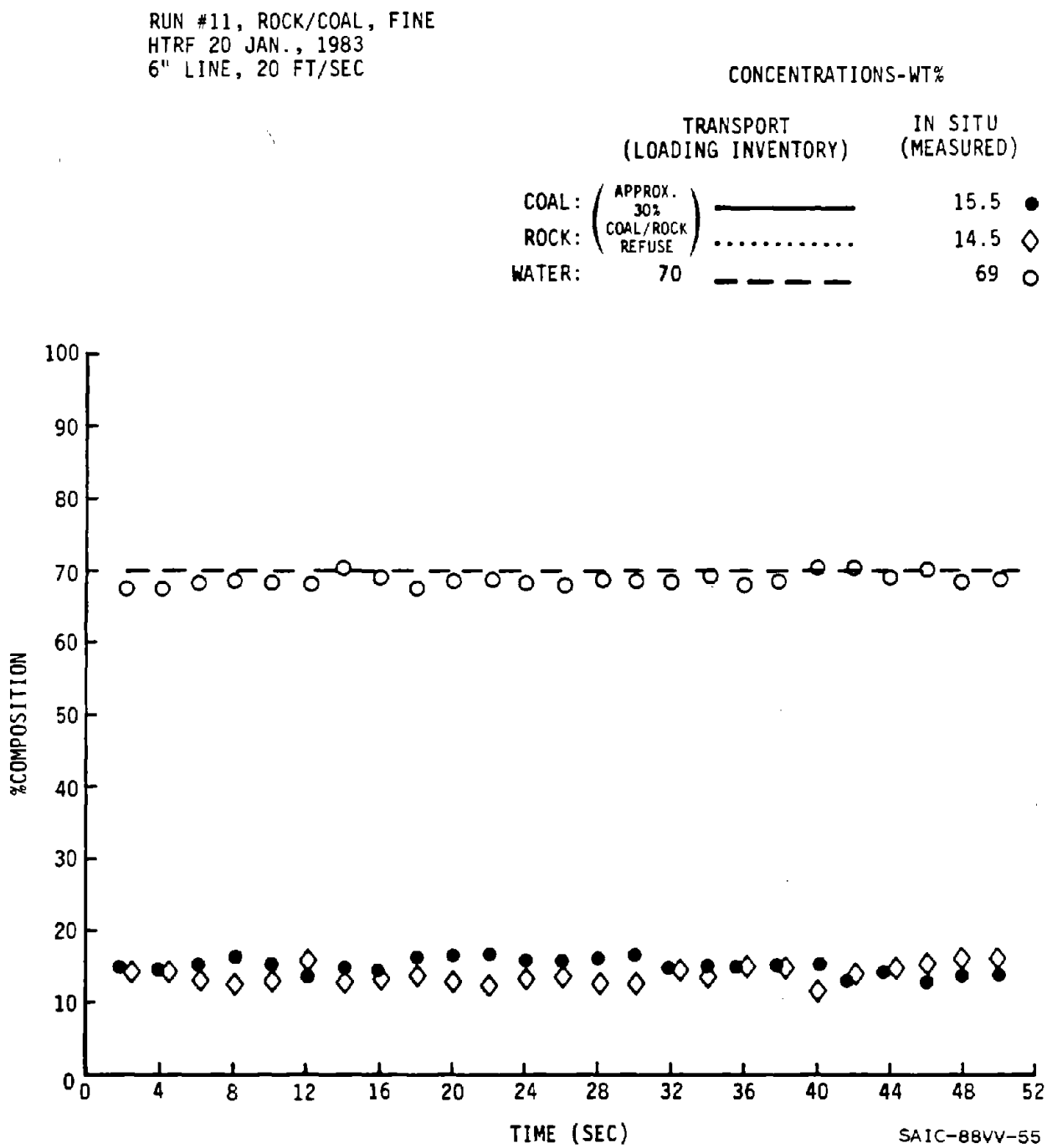
RUN #11, ROCK/COAL, FINE
HTRF 20 JAN., 1983
6" LINE, 20 FT/SEC
CONCENTRATIONS-WT%
TRANSPORT (LOADING INVENTORY)
IN SITU (MEASURED)
COAL: (APPROX. 30% COAL/ROCK REFUSE)
ROCK:
WATER: 70
15.5
14.5
69
%COMPOSITION
TIME (SEC)
0
10
20
30
40
50
60
70
80
90
100
0
4
8
12
16
20
24
28
32
36
40
44
48
52
SAIC-88VV-55

FIGURE 5.13

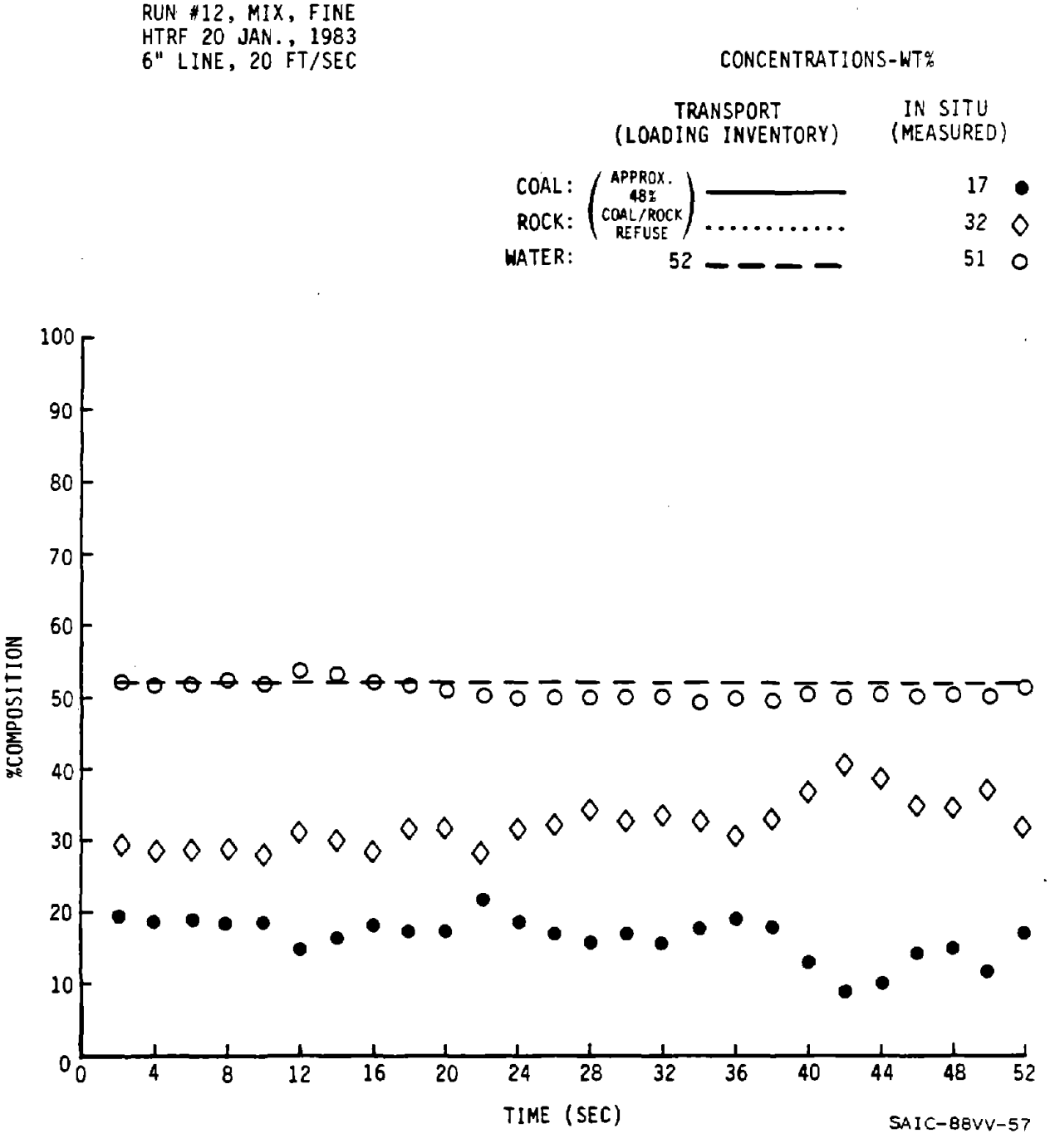
RUN #12, MIX, FINE
HTRF 20 JAN., 1983
6" LINE, 20 FT/SEC
CONCENTRATIONS-WT%
TRANSPORT (LOADING INVENTORY)
IN SITU (MEASURED)
COAL: (APPROX. 48% COAL/ROCK REFUSE)
ROCK:
WATER: 52
17
32
51
%COMPOSITION
TIME (SEC)
0
10
20
30
40
50
60
70
80
90
100
0
4
8
12
16
20
24
28
32
36
40
44
48
52
SAIC-88VV-57

FIGURE 5.14.

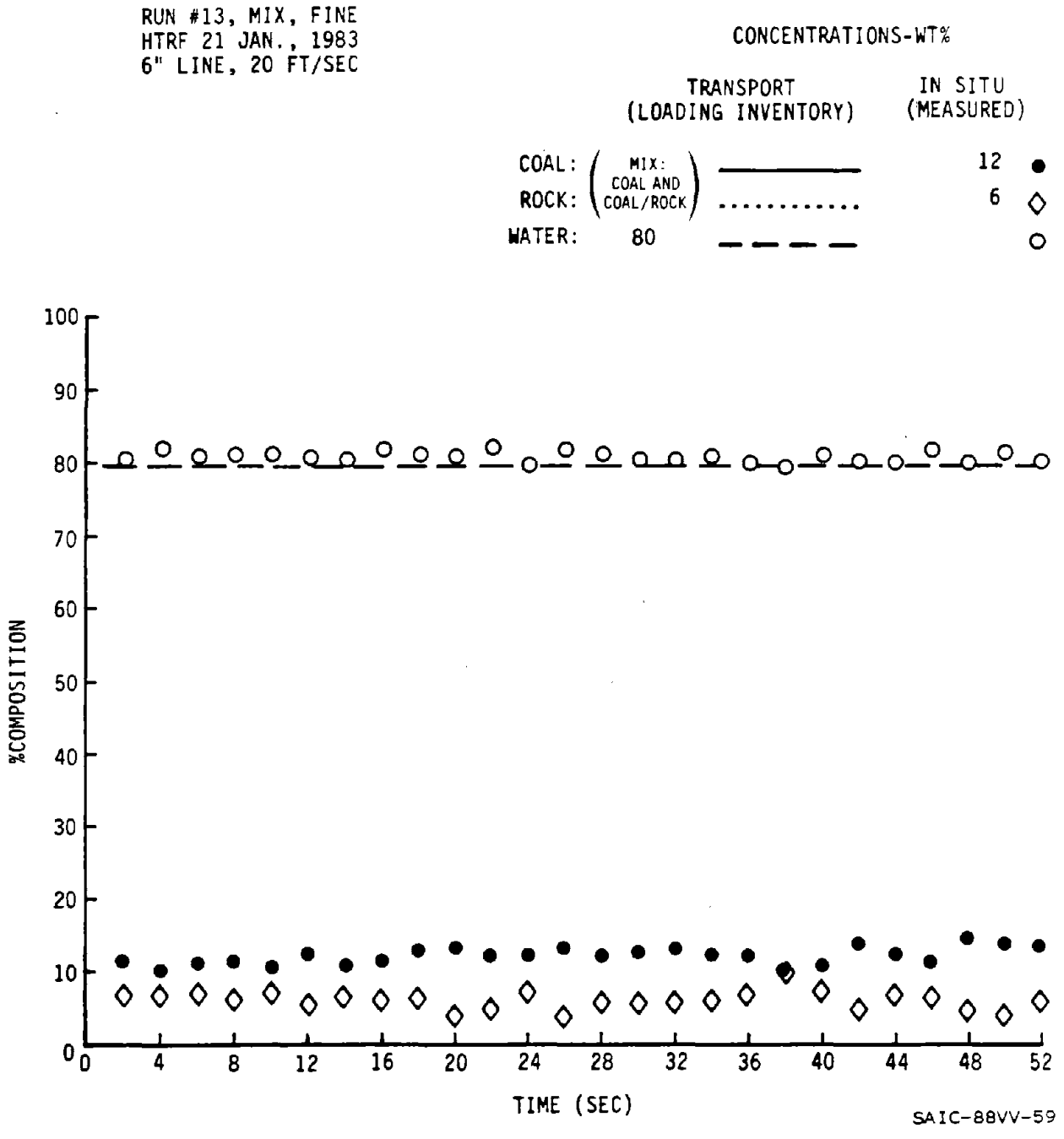
RUN #13, MIX, FINE
HTRF 21 JAN., 1983
6" LINE, 20 FT/SEC
CONCENTRATIONS-WT%
TRANSPORT (LOADING INVENTORY)
IN SITU (MEASURED)
COAL:
ROCK:
MIX: COAL AND COAL/ROCK
WATER: 80
12
6
%COMPOSITION
TIME (SEC)
0
10
20
30
40
50
60
70
80
90
100
0
4
8
12
16
20
24
28
32
36
40
44
48
52
SAIC-88VV-59

FIGURE 5.15.

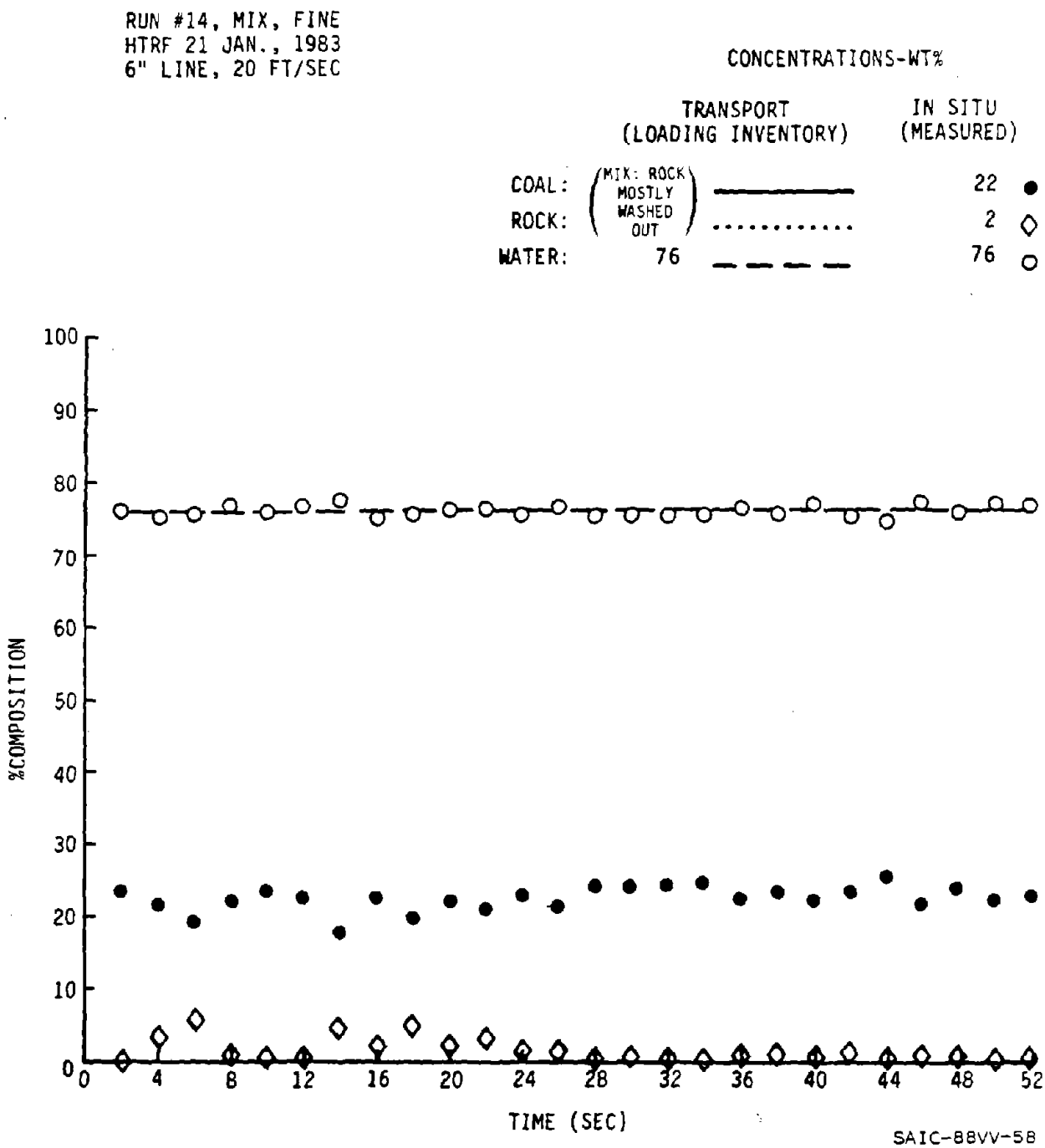
RUN #14, MIX, FINE
HTRF 21 JAN., 1983
6" LINE, 20 FT/SEC
CONCENTRATIONS-WT%
TRANSPORT (LOADING INVENTORY)
IN SITU (MEASURED)
COAL: (MIX: ROCK MOSTLY WASHED OUT)
22
ROCK:
2
WATER: 76
76
%COMPOSITION
100
90
80
70
60
50
40
30
20
10
0
0
4
8
12
16
20
24
28
32
36
40
44
48
52
TIME (SEC)
SAIC-88VV-58

FIGURE 5.16.

TABLE 5.1

Material	ρ	% Coal	% C+H
ρ Coal	1.42	100	77
ρ Rock	2.46	0	14
Coal/Rock	2.44	13	22
Coal/Rock	2.29	23	28
Coal/Rock	1.98	50	45
Coal/Rock	1.94	52	46
Coal/Rock	1.90	50	45
Coal/Rock	2.02	40	39
Coal/Rock	2.09	37	37
Coal/Rock	1.90	42	41
Coal/Rock	1.87	47	43
Coal/Rock	1.98	47	43
Coal/Rock	1.70	71	58
Coal/Rock	1.81	64	54
Coal/Rock	1.63	85	68
Coal/Rock	1.65	78	63
Coal/Rock	1.70	72	59

Coal, rock and rock/coal provided for HTRF tests. All but the high-density (14% C+H) rock showed up as 100% rock on coal slurry concentration sensor because it was calibrated for rock of high density (and low C+H content). C and H are carbon and hydrogen concentrations (combustibles).

drawing a straight line between these two points, one can determine the % coal in each batch of refuse supplied by reading off that value for the % (C+H) given from the chemical analysis of each batch. This somewhat arbitrary determination of % coal in refuse was made, and the results are given in the next-to-last column of Table 5.1. The % coal varies from 13% to 85% in the different batches of refuse supplied.

Figures 5.12 through 5.16 present the results of measurements made with finer refuse. The results are also summarized in Table 5.2 for the 6" sensor and Table 5.3 for the 18" sensor. Here, the in-situ concentration, as measured by the coal slurry concentration sensor, agreed well with the total solids (with relative percentages of coal and rock unknown) concentrations. The run presented in Figure 5.16 represents a loading of coal added to "recycled" rock. However, most of the "recycled" rock disintegrated, turning into mud, whereupon it fell through the "loading screen" in vain attempts to recycle it. This can be seen in the near 0% rock concentration. As can be seen, a "test loop," wherein nothing leaves the pipe system in recycling, would have been more useful for testing the coal slurry concentration sensor. However, having calibrated the sensor at CSMRI and at the HTRF, there was no point in recirculating the coarse particles until they degraded into fines, at which time the slippage would have reduced to a negligible level. This is what occurred in tests at the SRC "test loop" in Canada, and the STBV "test loop" in West Germany. These tests, all four (CSMRI and HTRF included), are all part of the international test series. The international ones are presented in Sections 6 and 7 below.

The tests performed with coarse particles at the HTRF provided a unique opportunity to observe the coal and rock haulage directly after loading the dry solids into the pump. The slippage was observed to qualitatively agree with the calculations carried out for SAIC/PRC by George Pouska and presented in Appendix B. The HTRF is the only test facility in which this slippage has been measured, because it is the only test facility wherein coarse particles were loaded, pumped vertically, and measured with a three-component coal/rock/water concentration sensor.

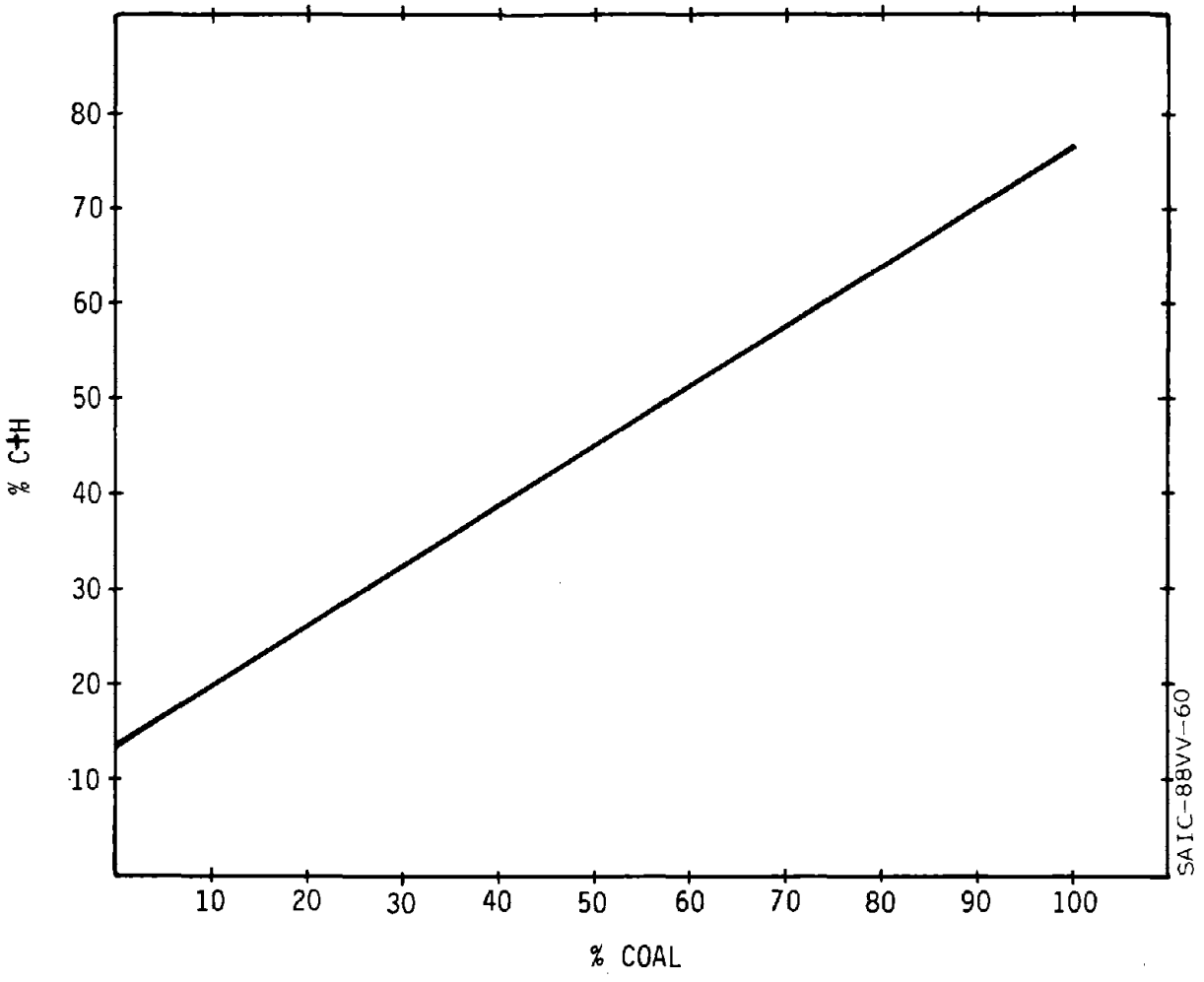

FIGURE 5.17. - Percent coal determination for rock/coal refuse (via % C+H content).

TABLE 5.2. - 6" HTRF

Run #	Date	Type Solids	Velocity	Loading/Sampling Concentration	In-Situ Concentration
1	1/11/83	coal, coarse	17 f/s	30/0/70	42/0/58
2	1/12/83	coal, coarse	17 f/s	20.75/0/79.25	30/0/70
3	1/12/83	coal, coarse	17 f/s	20.2/0/78.5	29/0/71
4	1/12/83	coal, coarse	17 f/s	42.0/0/58.0	57/0/43
5	1/12/83	coal, coarse	17 f/s	49.5/0/50.5	63/0/37
6	1/12/83	coal, coarse	17 f/s	47.9/0/52.1	62/0/38
7	1/12/83	coal, coarse	17 f/s	31.6/0/68.4	42/0/42
8	1/12/83	coal, coarse	17 f/s	28.8/0/71.2	38/0/62
9	1/14/83	rock, coarse	20 f/s	0/18/82	0/33/67
10	1/14/83	rock/coal, fine	20 f/s	?/?/73	13/14/73
11	1/20/83	rock/coal, fine	20 f/s	?/?/70	16/15/69
12	1/20/83	rock/coal+coal, fine	20 f/s	?/?/52	17/32/51
13	1/21/83	rock/coal+coal, fine	20 f/s	?/?/82	12/6/82
14	1/21/83	fine mix with rock washed out	20 f/s	?/?/76	22/2/76

TABLE 5.3. - 18" HTRF

1	10/82	coal, coarse	10 f/s	16/0/84	29/0/71
2	10/82	rock/coal, coarse	10 f/s	?/?/90	5/15/80

6.0 SRC TESTS: SASKATOON, SASKATCHEWAN, CANADA

6.1 INTRODUCTION

The 12-inch coal slurry concentration sensor was shipped to SRC (Saskatchewan Research Council) and put through a series of blind tests as part of an international test effort funded in part by the U.S. Bureau of Mines (Department of Interior) and coordinated by the Canadian Centre for Mineral and Energy Technology. Prior to conducting the tests, the electronic signal processing and transmitting system, the computer interface, the HP85 computer, and software were given a shakedown test at SAIC. After this, the apparatus was shipped to SRC, installed and given a shakedown test at SRC.

The coal and rock were prepared and weighed out in amounts known only to the SRC Slurry Transport Facility staff for conducting the gauge calibrations and, subsequent to this, the blind tests on unknown concentrations of first rock, then coal, and finally coal and rock.

This report describes the outcome of the tests, some of the difficulties encountered, and the methods taken to circumvent these difficulties. All tests were carried out with the 12" sensor mounted horizontally in the horizontal (return) section of the SRC test loop.

One of the difficulties was related to behavior of the coal/rock slurry at low velocities, where very severe "duning" effects were observed with the SRC densitometers as well as the SAIC coal slurry concentration sensor. Only the latter, of course, could separate out the coal and rock concentrations in the different parts of the duning cycle (from almost complete blockage to almost complete water concentration). This provided a rare opportunity to observe the segregation of coal and rock in different phases of the "duning" mode of transport, since only the coal/rock/water concentration sensor has the ability to measure these three individual in-situ concentrations almost instantaneously. Consequently, "enrichment-in-coal-content" phenomenon was measured during a complete "duning cycle", and is presented below.

6.2 THE CALIBRATIONS AND BLIND TESTS: BACKGROUND INFORMATION

Before the tests began, it was learned that the mean slurry velocity in the 12-inch pipe section could not exceed about 12 feet/second because of slurry-pump limitations. The pump and test loop are 10-inch-pipe systems, the latter half of which was a spliced section of 12-inch pipe where the SAIC coal slurry concentration sensor was installed. Here, the SRC vertical-scanning densitometer was installed and calibrated on 100% water in the pipe. This traversing densitometer provides the vertical density distribution in the slurry haulage pipe, from which can be estimated the solids concentration for a single-solids-component slurry.

The limitation of 12 ft/sec was known to be severe in terms of producing a strong vertical density gradient, approaching saltation flow or even the sliding-bed slurry flow. The proposed solution was to add 0.3% to 0.6% bentonite, a very fine clay. This, we informed both the U.S. Bureau of Mines and the SRC staff, would foul up the conductivity-gauge filter (used on the reference cell to correct for changing conductivity of the water). We were told to go ahead with the tests, regardless, and did so with one necessary change. Finding, as we expected, that the bentonite completely fouled up the conductivity gauge, we reprogrammed the Coal Slurry Concentration Sensor to operate with only two of the three sensors, namely the neutron gauge and the gamma-ray gauge. Omitting one of the sensors, i.e., the conductivity gauge, made it necessary to obtain the densities of coal and rock to good accuracy. This we did with the able and generous assistance of the SRC facility staff. The densities were input to the software, the software appropriately modified by Dr. Cassapakis, and the gauge was then applied to the calibration/blind test procedures laid out cooperatively by U.S. Department of Interior (Mr. Richard Wang), Canada Centre for Mineral and Energy Technology (Mr. L. B. Geller), SRC facility (Mr. Randy Gilles), and SAIC (Dr. Victor Verbinski and Dr. Costa Cassapakis).

There was, incidentally, a rewarding consequence of successfully operating the Coal Slurry Concentration Sensor as a two-component gauge. The neutron and gamma gauges are simple clamp-on, completely non-intrusive gauges

having proven stability, reliability and accessibility (freedom from breakdown).

6.3 TEST RESULTS

Both the calibration and the blind-test types of measurements are presented in Table 6.1 and Figures 6.1 through 6.12. After calibrating on rock (sand) alone, then sand plus bentonite, the blind tests were carried out. The accuracy of the U.S. Bureau of Mines/SAIC Coal Slurry Concentration Sensor is shown to be significantly better for rock than for coal. This arises from the much larger differential density of rock in water (the order of 1.65 versus about 0.35 for coal).

For the rock (sand) unknown, the SAIC Sensor results agreed with the SRC vertical density scan results within 0.3% to 1.3%. This is close to the estimated uncertainty for both methods of measurement.

For the coal unknown, the two methods agreed within 0.9% to 2.0%. This is again quite close to the combined uncertainties in the SRC and SAIC methods of measuring slurry concentrations for a single solid component and of known density.

For the coal/rock slurry, the SRC vertical scanning densitometer cannot be used to measure slurry concentrations, unless (1) the ratio of coal to rock loading is known, (2) the two components are present in the same fixed ratio everywhere (i.e., they maintain the same ratio throughout the vertical density scan, which can only hold true, in general, if there is no vertical profile; i.e., if there is completely turbulent flow), and (3) there is no selective segregation in the holding tank.

Of the above three conditions, only (1) applied with great certainty. Therefore, in line 18 of Table 6.1, the "SRC Estimate" of 25.1% coal and 10.0% rock (by volume) is not an accurate measurement, but an estimate. It was clearly a very good estimate at the highest pump speed, i.e., 12 ft/sec.; here, it was in good agreement with the SAIC Coal/Rock/Water Concentration Sensor result (24.57 $\pm$ 2.24% coal and 10.6 $\pm$ 0.73% rock). In this case, there was

TABLE 6.1 - Test results, in-situ concentrations

	Type of Run	Velocity (fps)	SRC Estimate Coal(Vol.%)	SRC Estimate Rock(Vol.%)	SAIC Sensor Coal(Vo.%)	SAIC Sensor Rock(Vol.%)
1.	Calibration, Rock	12.1	0	15.1	--	--
2.	Calibration, Rock	12.2	0	15.4	--	--
3.	Unknown: Add Bentonite	12.0	0	15.7	0	15.71 ± 0.26
4.		10.75	0	15.7	0	15.61 ± 0.27
5.		9.5	0	15.8	0	15.64 ± 0.23
6.	First Unknown, Rock	11.9	0	21.8	0	22.63 ± 0.30
7.		10.1	No Measurement Made		0	22.11 ± 0.21
8.		8.2	0	22.3	0	22.59 ± 0.22
9.	Second Unknown	11.4	0	26.9	0	28.13 ± 0.24
10.		9.4	0	22.3	0	27.76 ± 0.20
11.		7.2	0	26.7	0	28.08 ± 0.19
12.	Calibration, Coal	11.8	13.0	0	--	--
13.	Calibration, Coal	9.5	No Measurement Made		--	--
14.	Calibration, Coal	7.9	12.1	0	--	--
15.	First Unknown, Coal	11.8	25.5	0	27.52 ± 1.6	0
16.	First Unknown, Coal	8.0	26.8	0	25.9 ± 1.79	0
17.	First Unknown, Coal	9.7	23.9	0	25.43 ± 1.71	0
18.	Unknown, Coal and Sand	12.0	25.1 (EST)	10.0 (EST)	24.57 ± 2.24	10.6 ± 0.73
19.	Unknown, Coal and Sand	10.0	No Measurement Possible		Time Dependent:	See Figure 6.13.

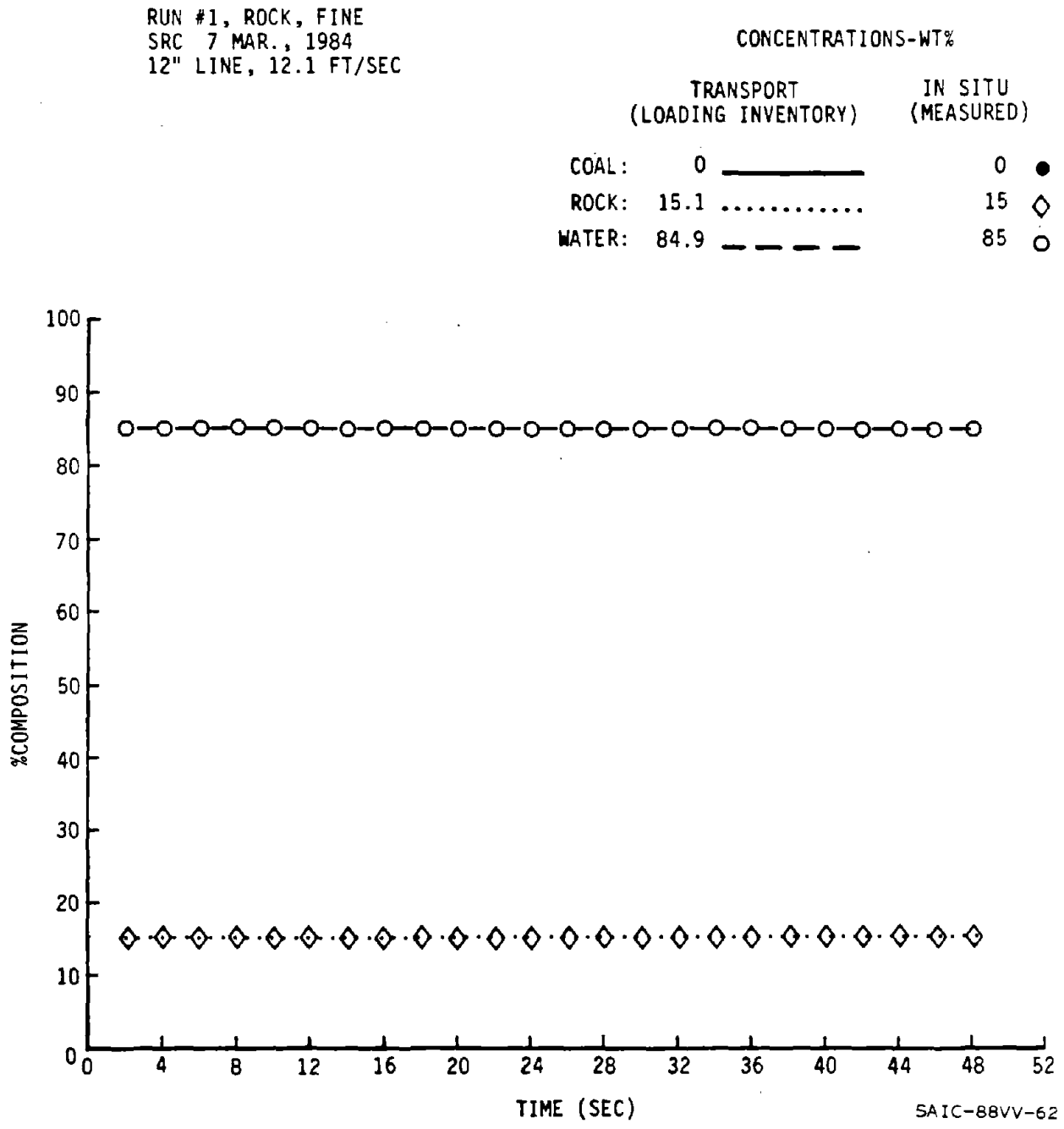
RUN #1, ROCK, FINE
SRC 7 MAR., 1984
12" LINE, 12.1 FT/SEC
CONCENTRATIONS-WT%
TRANSPORT (LOADING INVENTORY)
IN SITU (MEASURED)
COAL: 0 0
ROCK: 15.1 15
WATER: 84.9 85
%COMPOSITION
TIME (SEC)
0 4 8 12 16 20 24 28 32 36 40 44 48 52
0 10 20 30 40 50 60 70 80 90 100
SAIC-88VV-62

FIGURE 6.1.

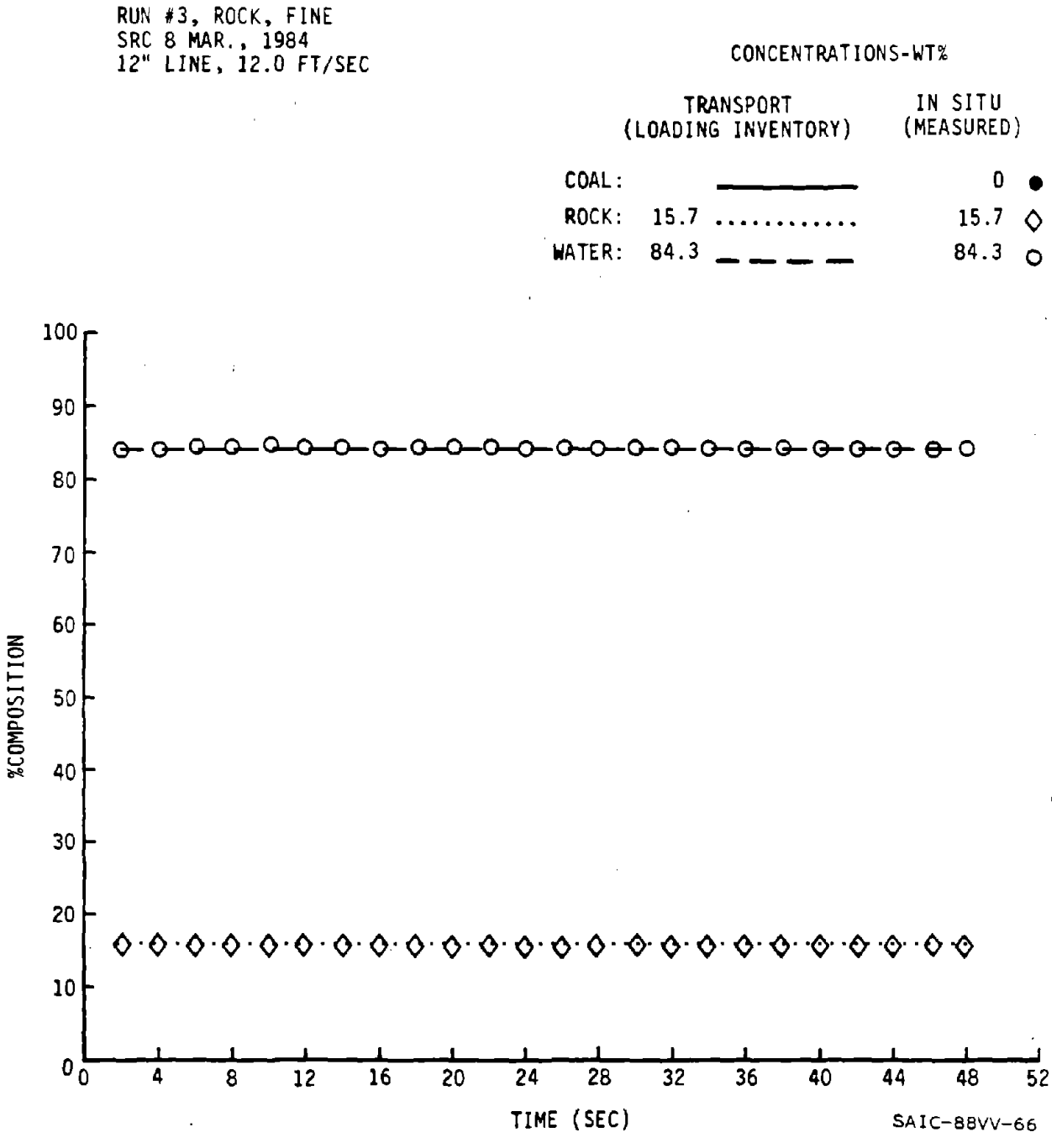
RUN #3, ROCK, FINE
SRC 8 MAR., 1984
12" LINE, 12.0 FT/SEC
CONCENTRATIONS-WT%
TRANSPORT (LOADING INVENTORY)
IN SITU (MEASURED)
COAL: 0
ROCK: 15.7 15.7
WATER: 84.3 84.3
%COMPOSITION
TIME (SEC)
SAIC-88VV-66

FIGURE 6.2.

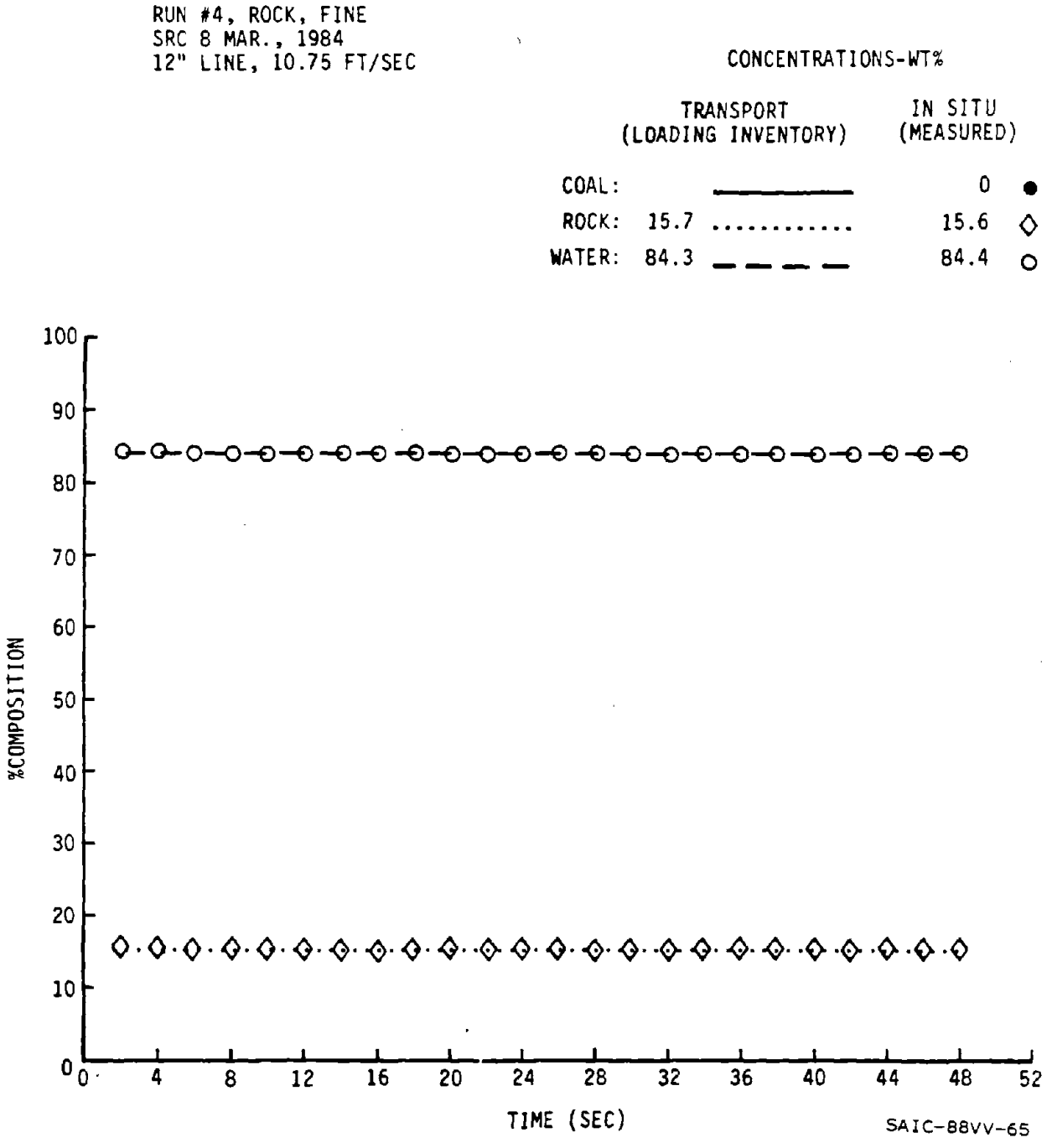
RUN #4, ROCK, FINE
SRC 8 MAR., 1984
12" LINE, 10.75 FT/SEC
CONCENTRATIONS-WT%
TRANSPORT (LOADING INVENTORY)
IN SITU (MEASURED)
COAL: 0
ROCK: 15.7 15.6
WATER: 84.3 84.4
%COMPOSITION
TIME (SEC)
SAIC-88VV-65

FIGURE 6.3.

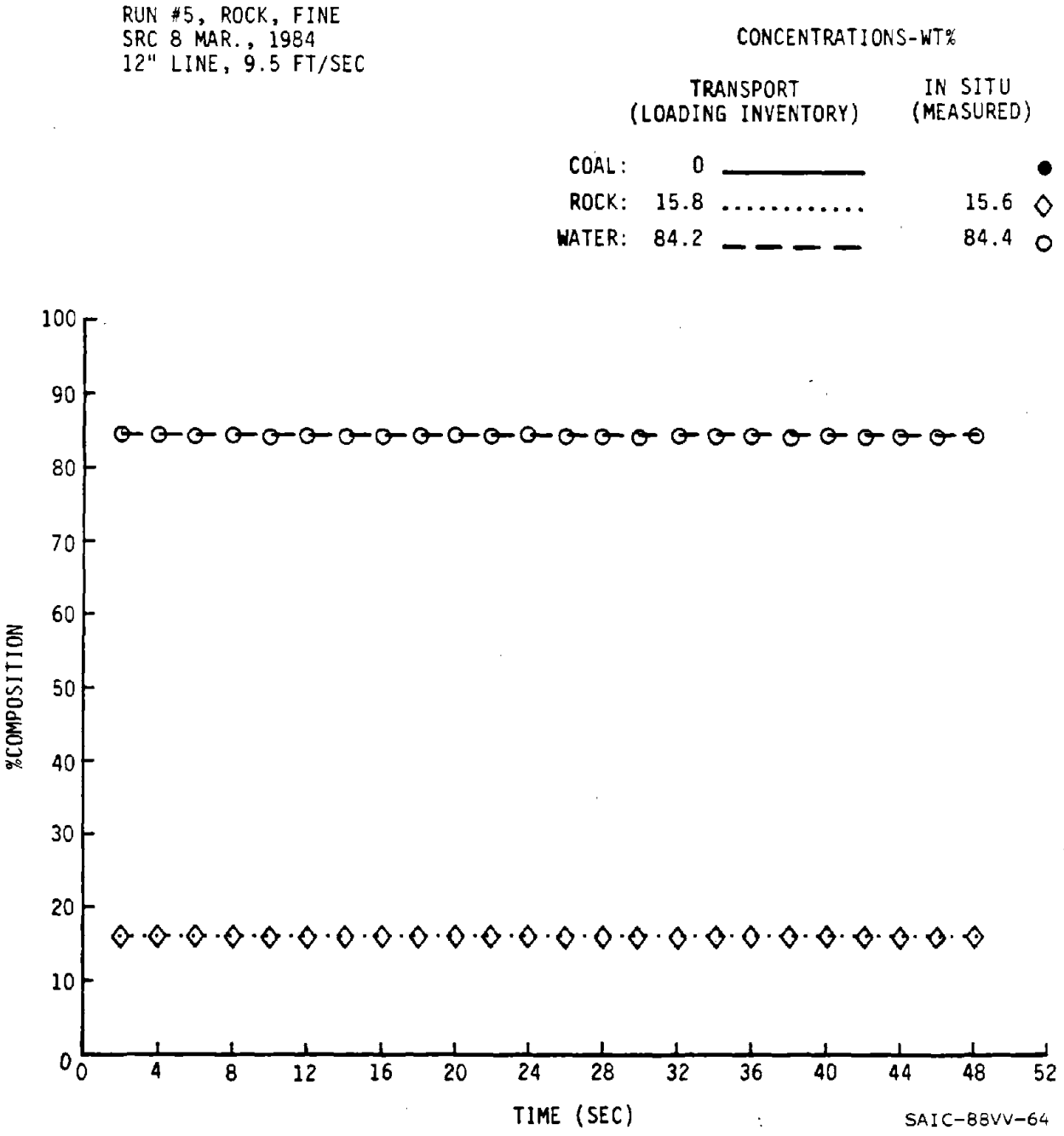
RUN #5, ROCK, FINE
SRC 8 MAR., 1984
12" LINE, 9.5 FT/SEC
CONCENTRATIONS-WT%
TRANSPORT (LOADING INVENTORY)
IN SITU (MEASURED)
COAL: 0
ROCK: 15.8
WATER: 84.2
15.6
84.4
%COMPOSITION
TIME (SEC)
SAIC-88VV-64

FIGURE 6.4.

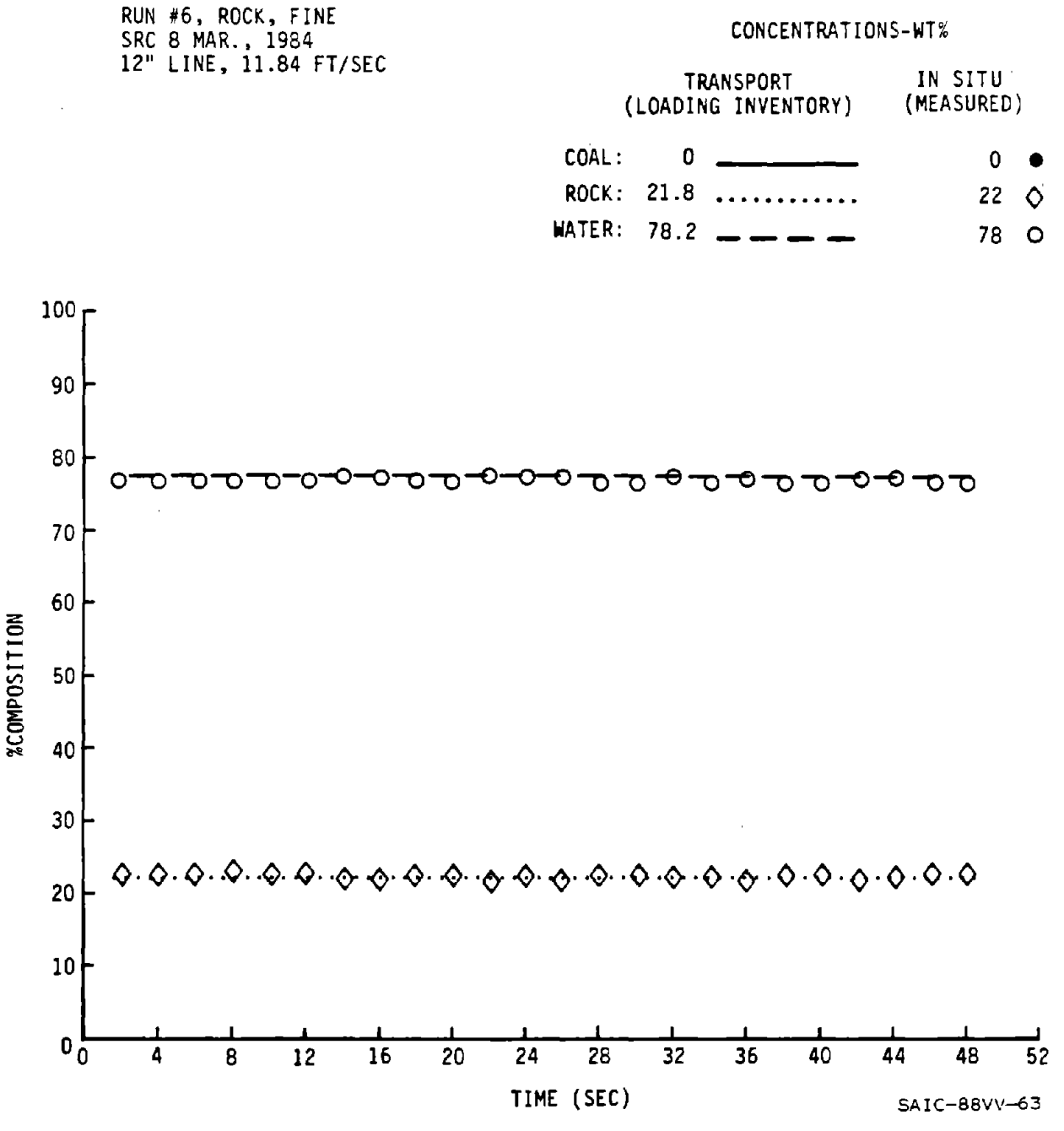
RUN #6, ROCK, FINE
SRC 8 MAR., 1984
12" LINE, 11.84 FT/SEC
CONCENTRATIONS-WT%
TRANSPORT (LOADING INVENTORY)
IN SITU (MEASURED)
COAL: 0
0
ROCK: 21.8
22
WATER: 78.2
78
%COMPOSITION
TIME (SEC)
SAIC-88VV-63

FIGURE 6.5.

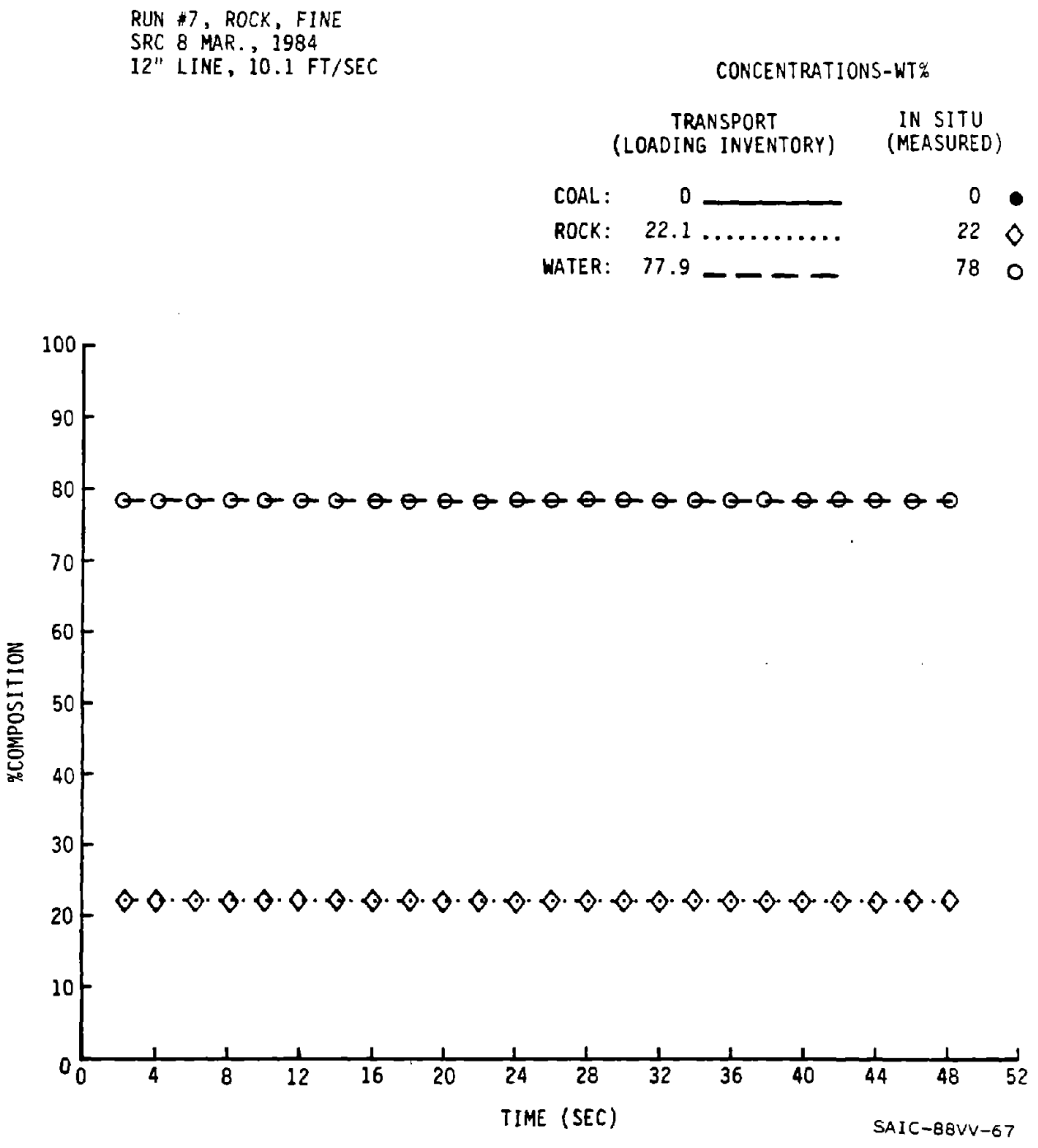
RUN #7, ROCK, FINE
SRC 8 MAR., 1984
12" LINE, 10.1 FT/SEC
CONCENTRATIONS-WT%
TRANSPORT (LOADING INVENTORY)
IN SITU (MEASURED)
COAL: 0
0
ROCK: 22.1
22
WATER: 77.9
78
%COMPOSITION
TIME (SEC)
0
10
20
30
40
50
60
70
80
90
100
0
4
8
12
16
20
24
28
32
36
40
44
48
52
SAIC-88VV-67

FIGURE 6.6.

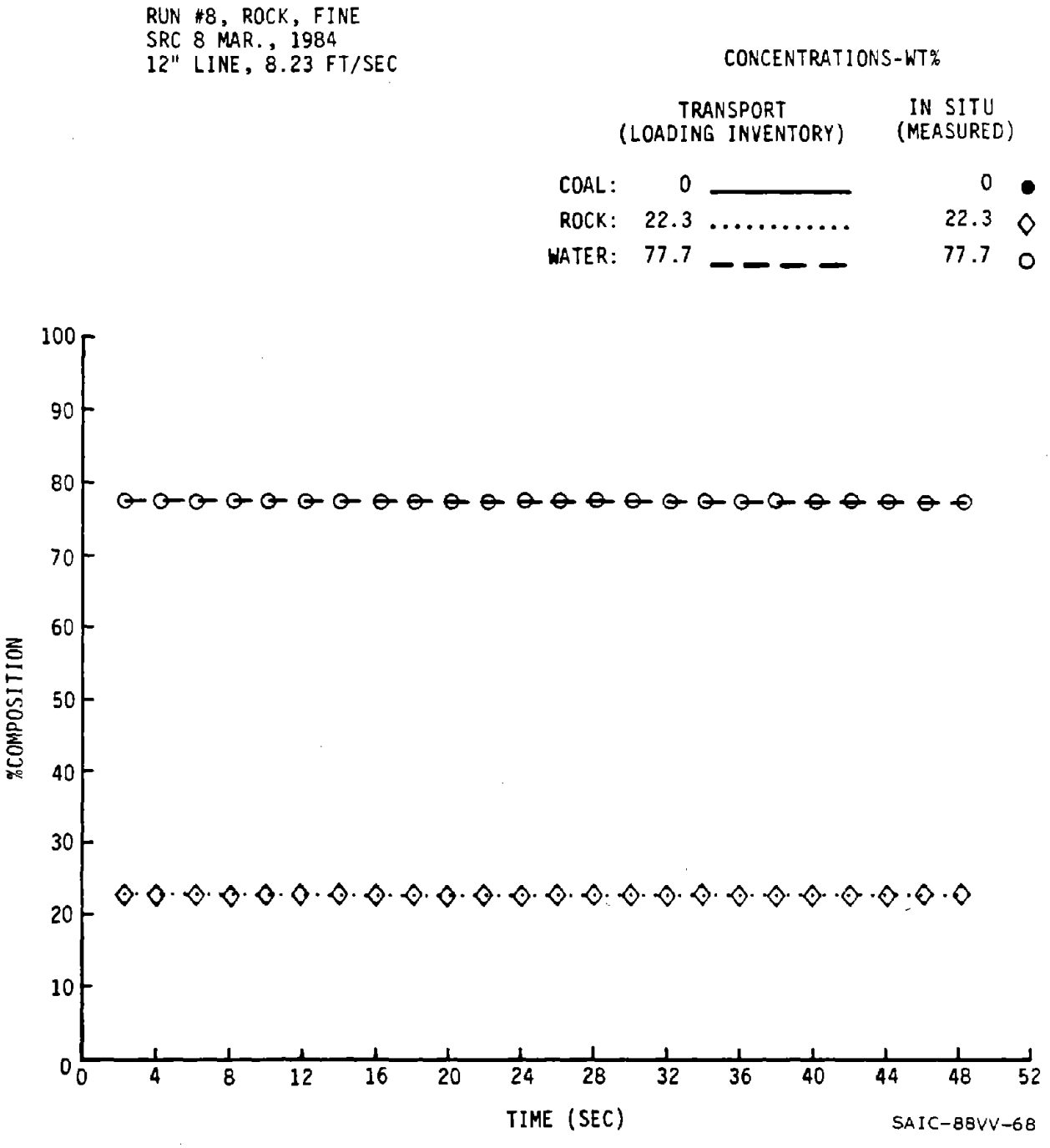
RUN #8, ROCK, FINE
SRC 8 MAR., 1984
12" LINE, 8.23 FT/SEC
CONCENTRATIONS-WT%
TRANSPORT (LOADING INVENTORY)
IN SITU (MEASURED)
COAL: 0 0
ROCK: 22.3 22.3
WATER: 77.7 77.7
%COMPOSITION
TIME (SEC)
0 4 8 12 16 20 24 28 32 36 40 44 48 52
0 10 20 30 40 50 60 70 80 90 100
SAIC-88VV-68

FIGURE 6.7.

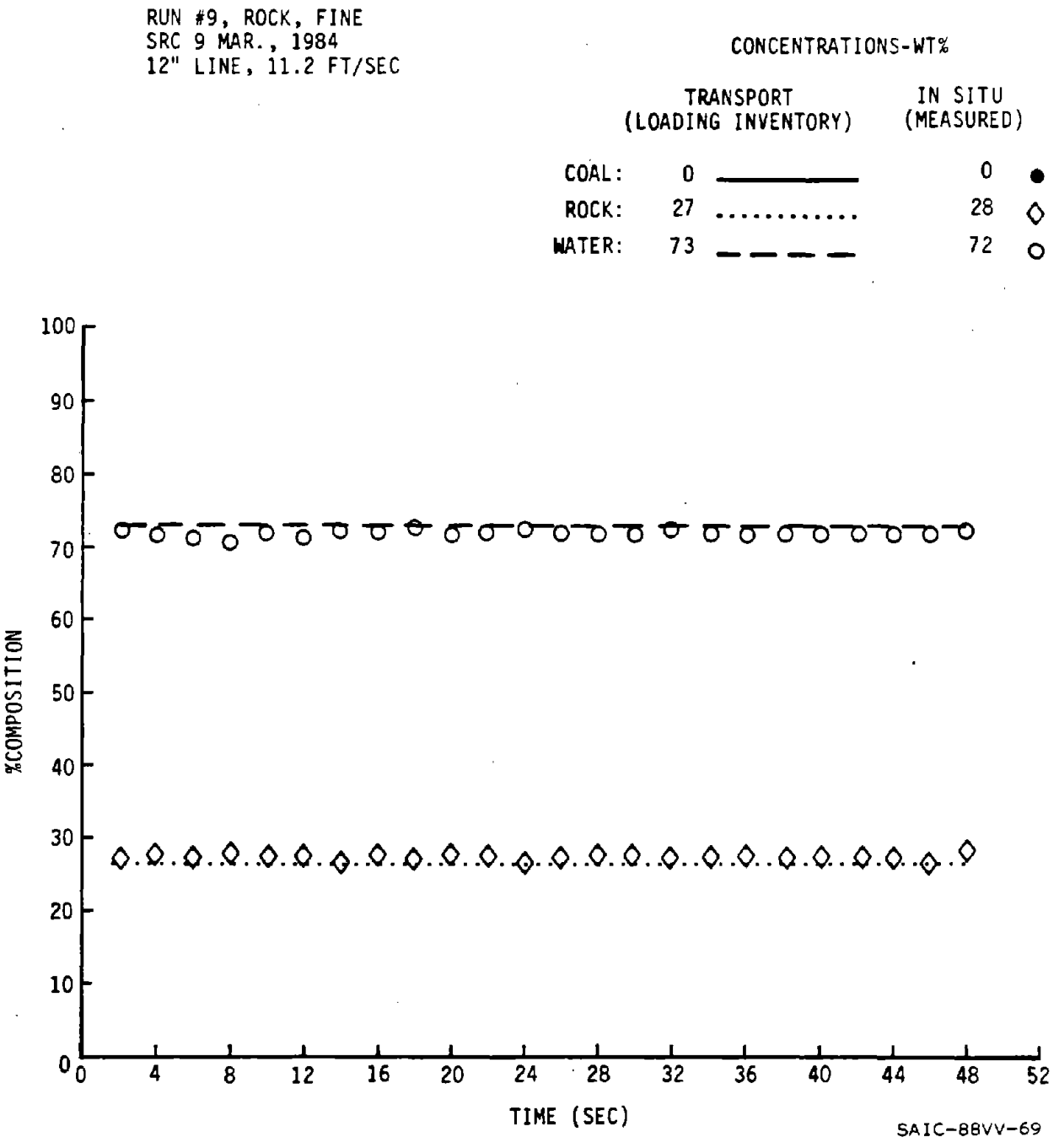
RUN #9, ROCK, FINE
SRC 9 MAR., 1984
12" LINE, 11.2 FT/SEC
CONCENTRATIONS-WT%
TRANSPORT (LOADING INVENTORY)
IN SITU (MEASURED)
COAL: 0 0
ROCK: 27 28
WATER: 73 72
%COMPOSITION
TIME (SEC)
0 4 8 12 16 20 24 28 32 36 40 44 48 52
10 20 30 40 50 60 70 80 90 100
SAIC-88VV-69

FIGURE 6.8.

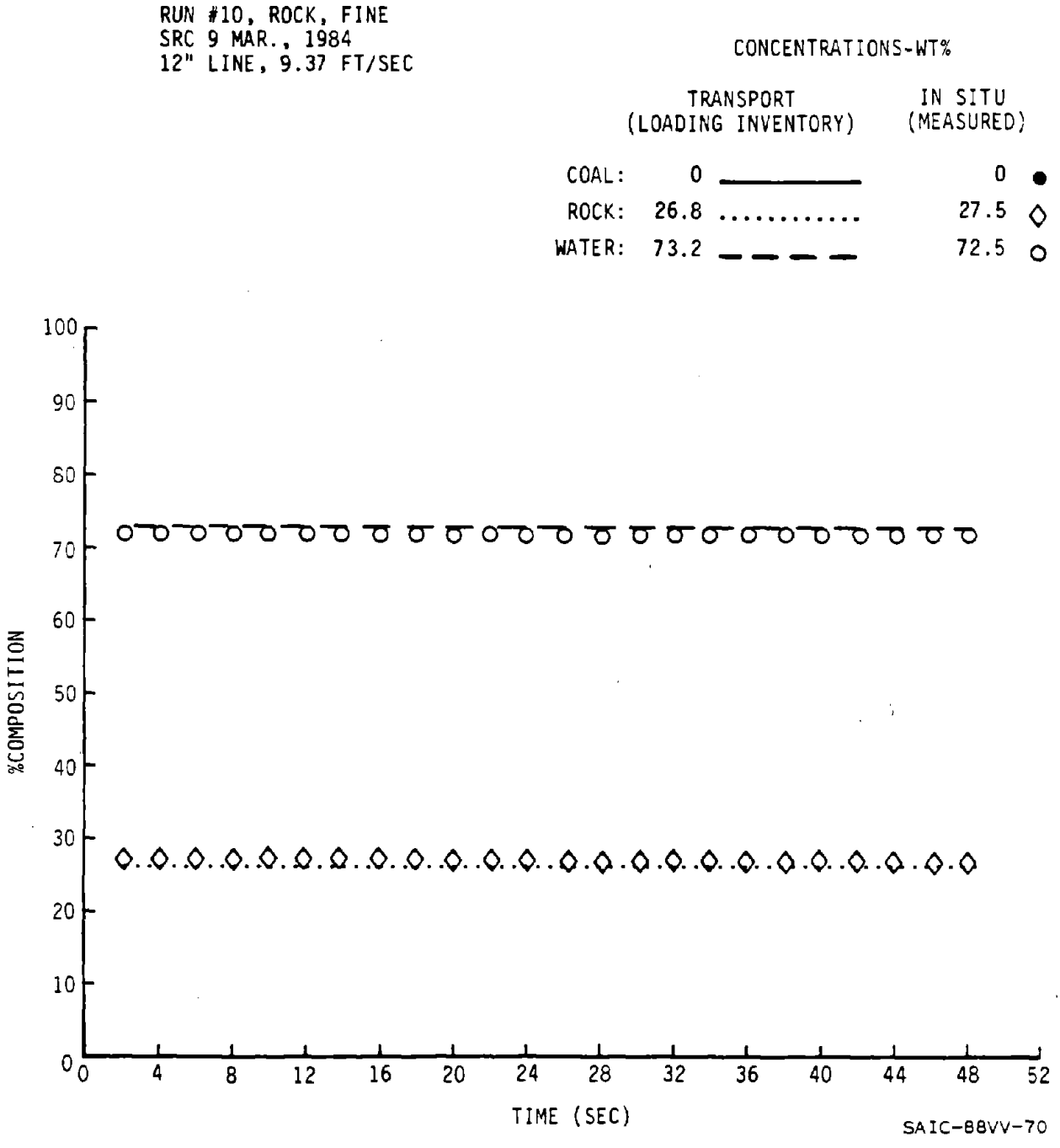
RUN #10, ROCK, FINE
SRC 9 MAR., 1984
12" LINE, 9.37 FT/SEC
CONCENTRATIONS-WT%
TRANSPORT (LOADING INVENTORY)
IN SITU (MEASURED)
COAL: 0 0
ROCK: 26.8 27.5
WATER: 73.2 72.5
%COMPOSITION
TIME (SEC)
0 4 8 12 16 20 24 28 32 36 40 44 48 52
0 10 20 30 40 50 60 70 80 90 100
SAIC-88VV-70

FIGURE 6.9.

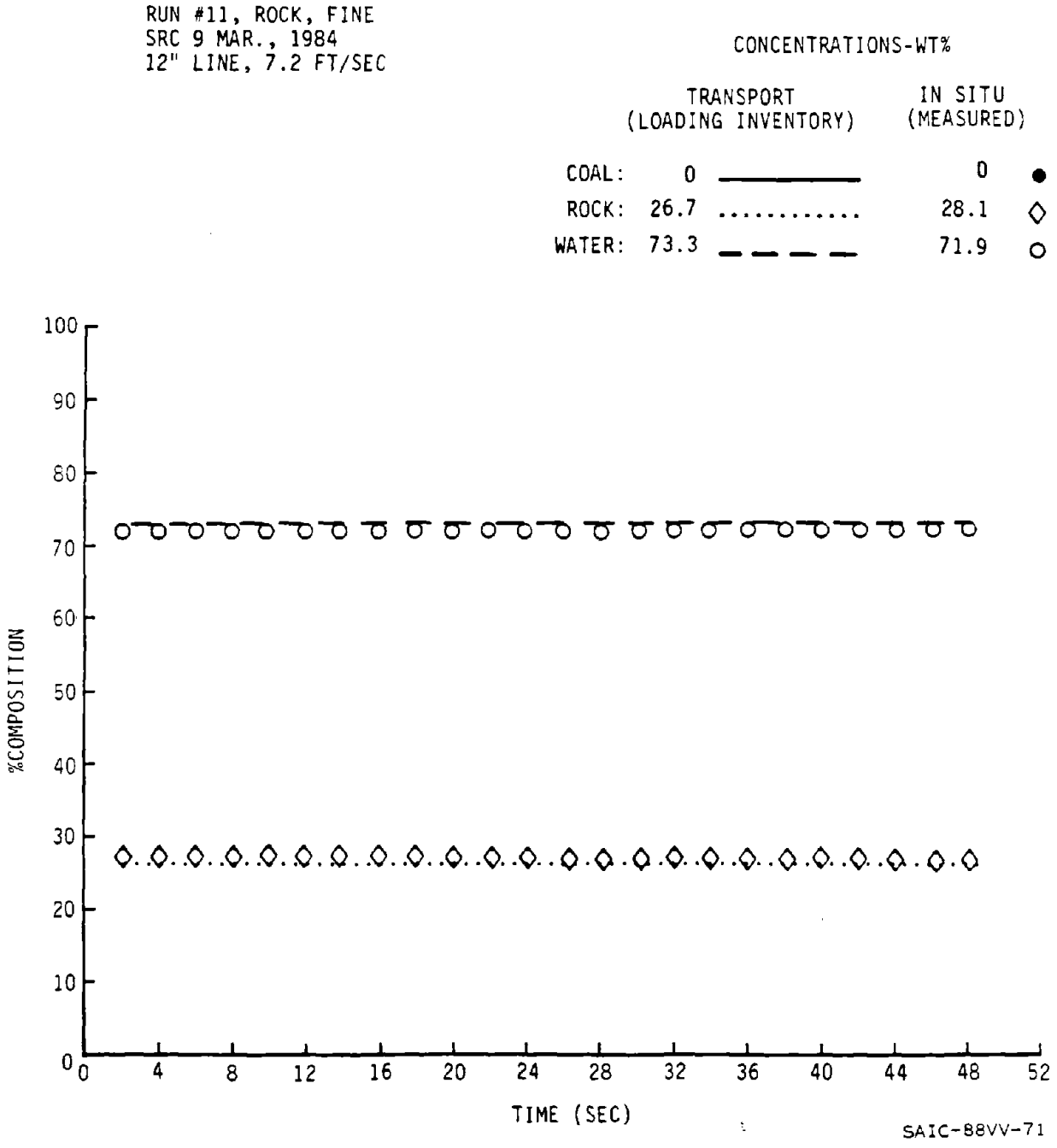
RUN #11, ROCK, FINE
SRC 9 MAR., 1984
12" LINE, 7.2 FT/SEC
CONCENTRATIONS-WT%
TRANSPORT (LOADING INVENTORY)
IN SITU (MEASURED)
COAL: 0 0
ROCK: 26.7 28.1
WATER: 73.3 71.9
%COMPOSITION
TIME (SEC)
0 4 8 12 16 20 24 28 32 36 40 44 48 52
0 10 20 30 40 50 60 70 80 90 100
SAIC-88VV-71

FIGURE 6.10.

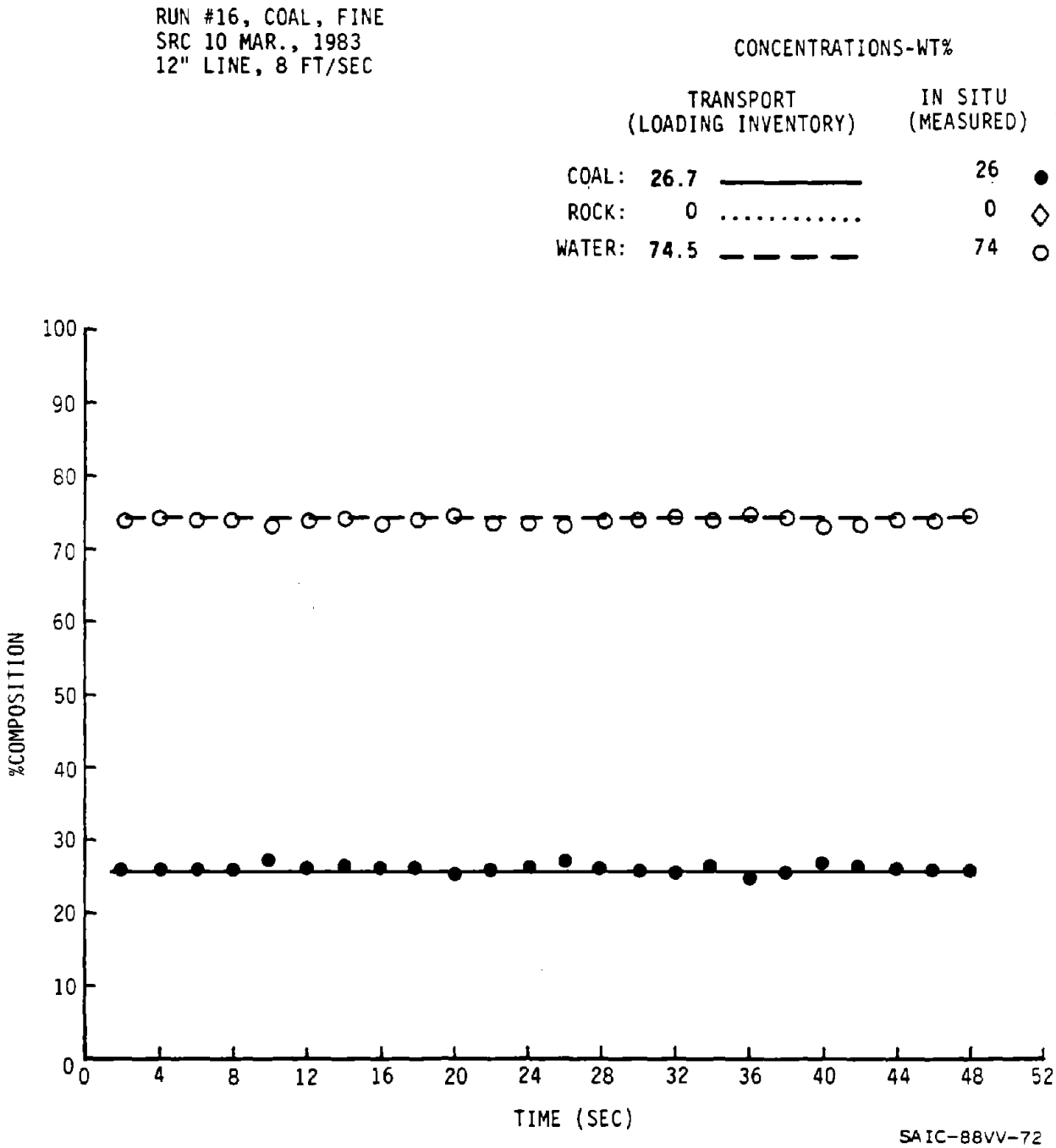
RUN #16, COAL, FINE
SRC 10 MAR., 1983
12" LINE, 8 FT/SEC
CONCENTRATIONS-WT%
TRANSPORT (LOADING INVENTORY)
IN SITU (MEASURED)
COAL: 26.7
26
ROCK: 0
0
WATER: 74.5
74
%COMPOSITION
TIME (SEC)
0
10
20
30
40
50
60
70
80
90
100
0
4
8
12
16
20
24
28
32
36
40
44
48
52
SAIC-88VV-72

FIGURE 6.11.

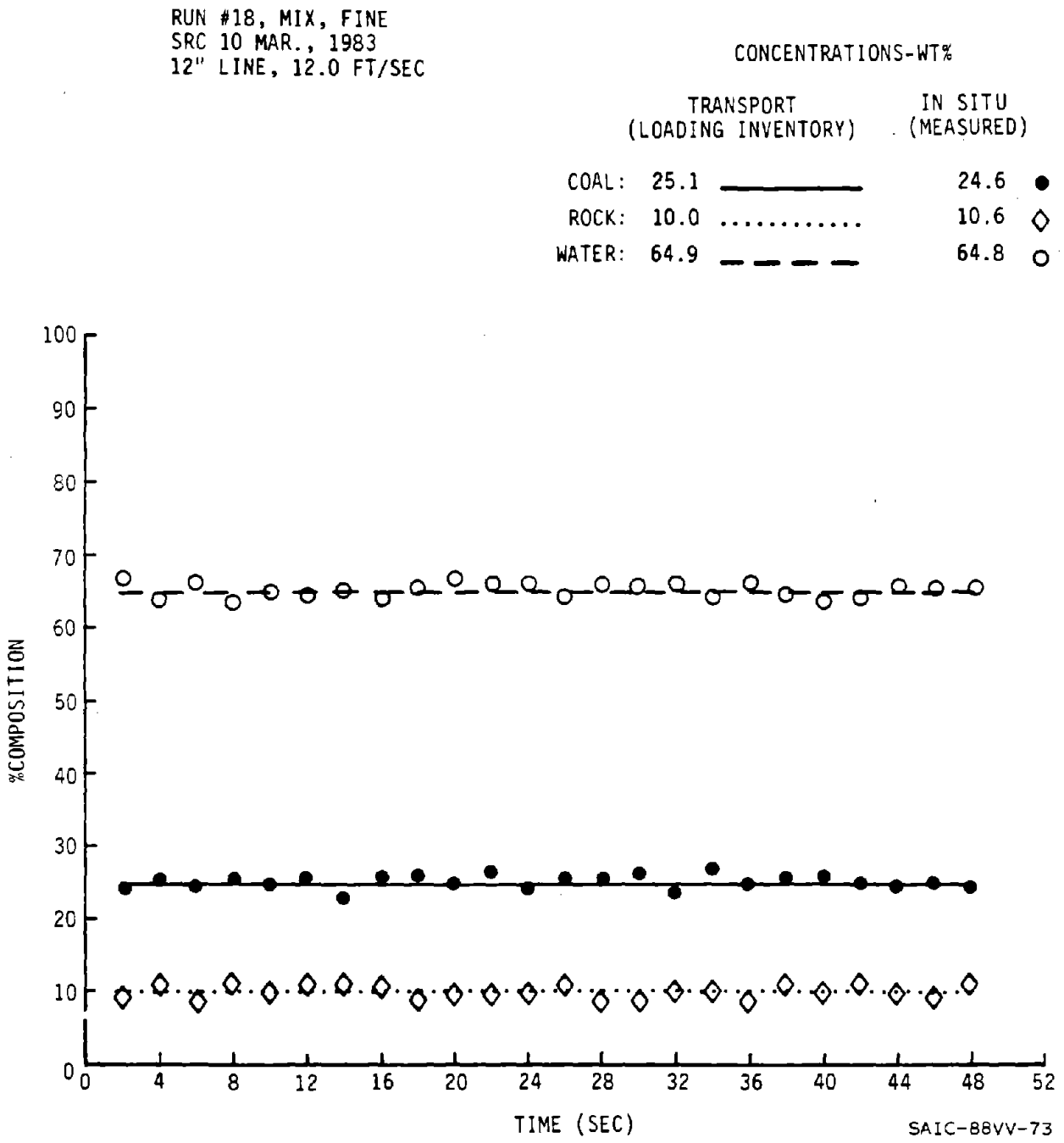
RUN #18, MIX, FINE
SRC 10 MAR., 1983
12" LINE, 12.0 FT/SEC
CONCENTRATIONS-WT%
TRANSPORT (LOADING INVENTORY)
IN SITU (MEASURED)
COAL: 25.1
24.6
ROCK: 10.0
10.6
WATER: 64.9
64.8
%COMPOSITION
TIME (SEC)
SAIC-88VV-73

FIGURE 6.12.

violent mixing in the holding tank, which mitigated against a disproportionately high water inventory in the holding tank (which normally occurs at lower pump speeds due to settling of the solids "into the pump inlet").

When the slurry velocity was reduced to 10 feet/second, "duning" occurred. The SAIC Sensor results are of great use in this case because the Sensor measures the separate coal and rock concentrations, and it does at a rate fast enough to follow such effects as "duning."

The in-situ concentrations of coal and rock during the occurrence of "duning" (i.e., a pile-up of solids almost to the point of blockage), from the peak to the trough of the dune, is shown in Figure 6.13 as a function of time. It is interesting to note that during the peak of the dune, there is nearly complete solids contents (which occurs at an estimated 65-70% by volume), with the water "filling in the cracks." Furthermore, at the peak, the rock is almost 100% displaced; an interesting sort of coal/rock separation system thus occurs at the peak of the dune. In the valley, the rock to coal volume concentrations have reversed. The weight concentrations even more dramatically show a high rock content at the valley.

6.4 CONCLUSIONS

It is clear that the Coal Slurry Concentration Sensor will not operate as a three-component gauge when bentonite is added. Bentonite is an absorptive and colloidal clay mineral used as a filler in paper or a carrier (as of drugs). It is possibly one of the worst conceivable additives to add to a slurry where a sintered metal filter of 0.5 micron pore size is used. It apparently acts as a carrier for materials that highly influence the conductivity of the slurry water (such as ionic salts), and is not dislodged from the pores of the filter. Nearly one week of constant flushing would not clear the filter to the point where the reference cell would give a stable reading through the pump/back-flush cycle.

As a two-component gauge, it works acceptably well and also makes possible a configuration that is relatively simple, extremely stable, and reliable for mine-environment applications for which it was originally designed.

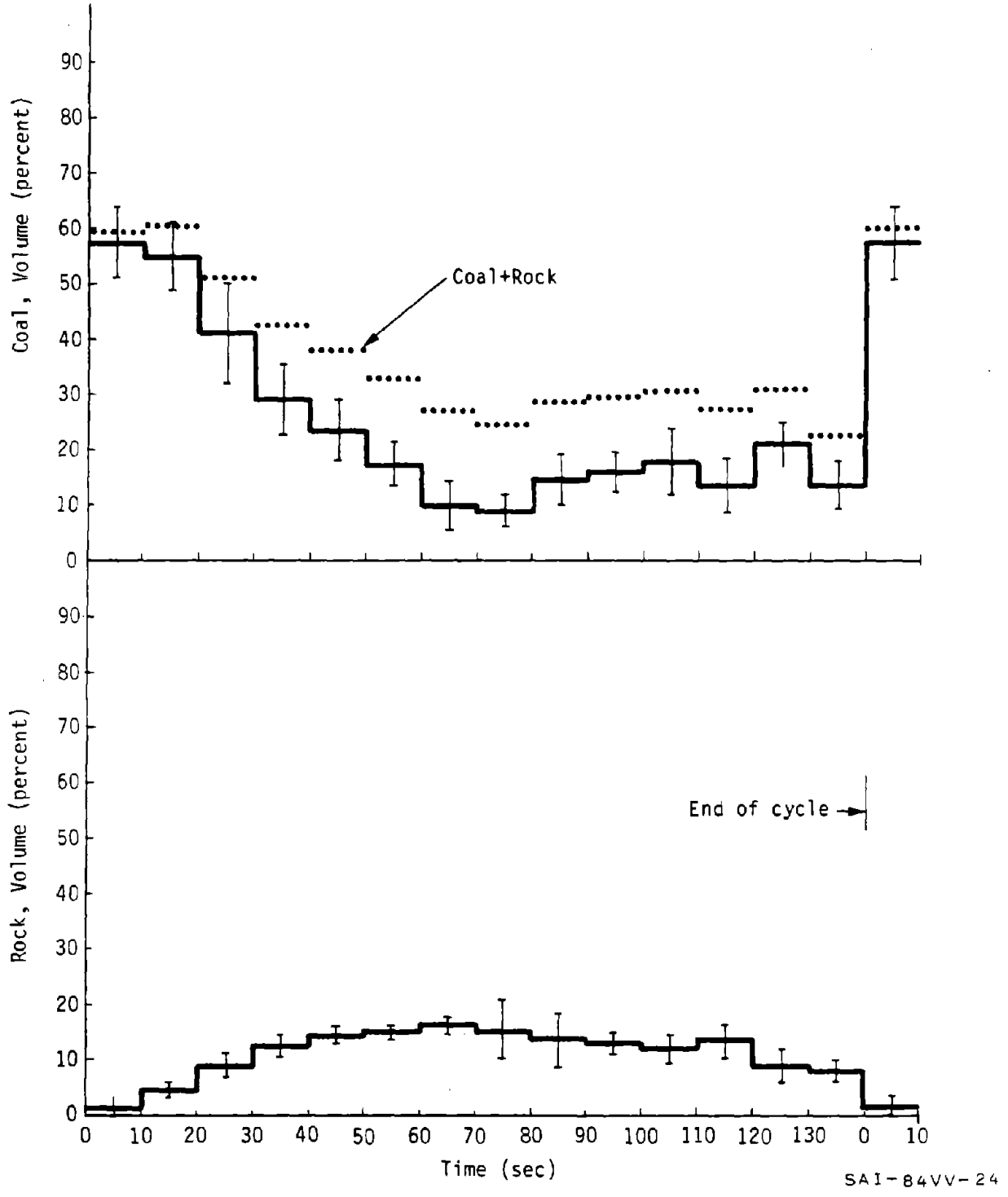

FIGURE 6.13. - Time dependence of coal/sand concentration during "duning" average over six "cycles"; velocity = 10.0 feet/sec. Note how the rock concentration in "duning", peaks at the valley of the lower (specific) density coal; an unusual hydrotransport behavior.

7.0 StBV TESTS: ESSEN, FEDERAL REPUBLIC OF GERMANY

The 6-inch coal slurry concentration sensor was shipped to StBV (Steinkohlenbergbauverein in Essen, West Germany (FRG)) for test and evaluation as part of the international test effort funded in part by the U.S. Bureau of Mines (Department of Interior) and coordinated by the Canadian Centre for Mineral and Energy Technology.

The 6-inch sensor was previously used at the Pittsburgh Research Center HTRF (Hydraulic Transport Research Facility) where it was tested on Pittsburgh seam coal. It had been previously calibrated on Pittsburgh seam coal at the CSMRI (Colorado School of Mines Research Institute) test loop, where a recirculating system (i.e., a test-loop) was used. It operated successfully at both places so that the tests in Essen were looked at as an interesting part of an international three-laboratory test series with the same instrument.

The coal in Essen was quite different from the Pittsburgh seam coal used in the earlier tests at CSMRI and PRC. Thus, the neutron and the gamma-ray sensors had to be calibrated carefully with the West German coal. This was done by recirculating the coal, and later the refuse, in the test loop until nearly all of it was broken down into fines.

The German coal, much like the Canadian coal, had a very fine clay component. This created havoc with the conductivity gauge because the very fine clay lodged itself in the sintered metal filter of the conductivity gauge, where it continually added solubles at a slow rate, to the reference-gauge water. This raised the reference-cell-water conductivity above that for the water in the main slurry line, and did so in an unpredictable manner. As a result of this, the conductivity gauge was a source of inaccuracy and therefore could not be used.

Subsequently, we obtained good samples of the Essen coal and rock and carefully measured the density of both. These densities were used as required

input to the coal slurry concentration sensor for the sensor to operate as a two-component system; i.e., neutron and gamma-ray gauge system.

The tests, reported in Appendix A, were all carried out with only the neutron and gamma-ray gauges. This two-component sensor is not as inherently accurate as the three-component sensor (when the conductivity gauge is functioning properly).

The measurements reported in Appendix A were made with the SAIC two-component sensor placed in the horizontal section of the StBV test loop and with a Cs-137 (BF) densitometer placed in a vertical section of the 6-inch test loop. At very low slurry velocities (see data presented in the tables of Appendix A), the flow varied from stationary-bed flow to sliding-bed flow as the velocities increased. Therefore, at these lowest velocities, the concentrations measured in the horizontal section (SAIC instrument) were much higher than those measured in the vertical section with the StBV densitometer (BF). At much higher slurry velocities, above 3.5 m/sec, turbulent flow set in. The SAIC and StBV (BF) readings were comparable at these velocities. At the highest velocities, the SAIC sensor could be evaluated by comparison with StBV sensor.

These data are plotted in the figures of Appendix A and are consistent with about a 3.5% accuracy of the SAIC two-component sensor. This includes an allowance for some error (about 2% in the BF readings due to drifts in the instrument and to varying coal and rock inventories in the header tank: the BF gauge (Cs-137) measures only total slurry density, and the coal and rock concentrations are calculated by utilizing the known coal and rock loadings in the test loop. The SAIC sensor, of course, provides coal/rock/water concentrations without knowledge of these loading inventories (i.e., without knowledge of the coal-to-rock loading ratios). Therefore, at lower slurry velocities where the hydraulic slippage is large, the rock concentration in the vertical section (upward flow) will be disproportionately higher than that for coal. Thus the BF (Cs-137) gauge data presented in Appendix A for velocities below, say, 3.5 m/sec, will be very inaccurate; completely so at the lowest velocities (stationary-bed and sliding-bed flow).

8.0 RESULTS AND CONCLUSIONS

The coal slurry concentration sensor program was initiated with the design goals as set out in Table 8.1 by the Pittsburgh Research Center (PRC), Bureau of Mines. The sensor was eventually to operate in mine environments where it would have to be rugged, almost maintenance free, and very easy to calibrate (i.e., on 100% water) on a day-to-day basis. The basic design would have to be applicable to measuring coal/refuse/water concentrations in haulage pipes varying from 6" to 24" in diameter and for pressures of up to 1,000 psig.

A three-component sensor was designed and fabricated for 6", 10", 12" and 18" lines for use at the HTRF and also in an international test series. This utilized a completely non-intrusive (clamp-on type) neutron and gamma-ray gauge, as well as an intrusive (requiring a special pipe section) conductivity gauge. The uncertainty of the sensor on the 6" line was the order of 2% and degraded to about 6% for the 18" line.

Problems were encountered with the conductivity gauge from the onset of the program. It was eventually designed to work up to about the 150 psig pressure limit for the research center and was utilized successfully on tests at the HTRF in Pittsburgh on both the 6" and 18" diameter haulage lines. Long term reliability was always a problem, however.

But when tests were carried out at the SRC test loop (Saskatoon, Saskatchewan, Canada) and the StBV test loop (Essen, Federal Republic of Germany), the refuse in both places contained a very fine clay that lodged itself in the interstices of the sintered-metal filter of the conductivity gauge reference cell, making the conductivity gauge completely inoperative at both places.

Therefore, the SAIC sensor was operated as a two-component sensor at these laboratories, with the on-line computer reprogrammed to operate with only the neutron and gamma-ray gauges.

Table 8.1 - Concentration sensor design specifications

Factor	Research Sensor	Commercial Sensor	Control Sensor
Accuracy			
Wt. concentration of coal	1.0%	2.0%	3.0%
Wt. Concentration of refuse	1.0%	2.0%	3.0%
Response time, sec.	0.5	1	2
Range			
Ambient temperature, ^{o}F	-20---+120	+20---+80	+20---+80
Water temperature, ^{o}F	+35---+80	+35---+80	+35---+80
Pipeline diameter, in.	6---18	6---24	6---24
Top size of coal, in.	2---6	2---6	2---6
Top size of refuse, in.	2---6	2---8	2---8
Pipeline pressure, psig	50---150	50---1,000	50---1,000
Flow velocity, ft/sec	4---20	4---20	4---20
Water condition, pH	3.5---8	3.5---8	3.5---8
Specific gravity of coal	1.2---1.6	1.2---1.6	1.2---1.6
Specific gravity of refuse	2.3---3.1	2.3---3.1	2.3---3.1
Wt. concentration of coal, %	0---80	5---70	10---60
Wt. concentration of refuse, %	0---80	5---50	10---50
Coal/refuse proportion	0/100---100/0	0/100---100/0	0/100---100/0
Water source	Fresh	Fresh---Brackish	Fresh---Brackish
Cost, desirable, $	7,000---10,000	6,000---9,000	3,000---5,000
Fluctuation (% of Factor)			
Pipeline pressure	20	10	10
Flow velocity	5	5	5
Specific gravity of coal	15	15	15
Specific gravity of refuse	15	15	15

In order for a two-component sensor to work successfully on a three-component slurry, additional data must be available; namely, the coal and rock densities. These densities were accurately measured for carefully selected test samples of coal and rock, and the density values were entered as inputs to the on-line computer.

The two-component sensor utilizing the measured coal and rock densities was seen to fluctuate nearly twice as much as the three-component sensor. The estimated accuracies for the two and three-component sensors are presented in Figure 8.1 for 6", 10", 12", 18" and 24" haulage lines.

While the two-component sensor is not as accurate under the best of conditions, it is, nevertheless, eminently well-suited for deep-mine coal haulage. First, both the neutron and gamma-ray gauges were improved in long-term counting stability, wherein the count rates at CSMRI varied over the period of about one month by not more than 1-2%. This was for conditions varying from direct afternoon sunlight to a snowstorm. Second, day-to-day (or week-to-week) calibrations are easily carried out. Simply pump 100% water (no solids) for a few seconds. Third, both radiation gauges are completely non-intrusive. They can be clamped on to any high pressure (up to 1000 psig) line and quickly calibrated on 100% water in the line.

An estimate of the SAIC/PRC coal slurry sensor accuracy as a function of pipe diameter is presented in Figure 8.1, both for the two-component and three-component sensors. It is evident that the coal slurry concentration sensor for Pittsburgh seam coal (where the three-component sensor can be used) meets virtually all the requirements set out in Table 8.1 by the U.S. Bureau of Mines. The two-component sensor is somewhat less accurate, but has many redeeming features such as non-intrusiveness, adaptability to very high pressure lines, stability, ease of calibration and useable with 6" to 24" lines. This is the only known three-component-slurry sensor that will operate with larger than 6" lines and with high pressure lines.

The only other three-component-slurry sensor known is the German sensor that utilizes a soft (60 keV Am-241) gamma ray and a hard gamma-ray source (662 KeV Cs-137). The count rate and stability requirements for this

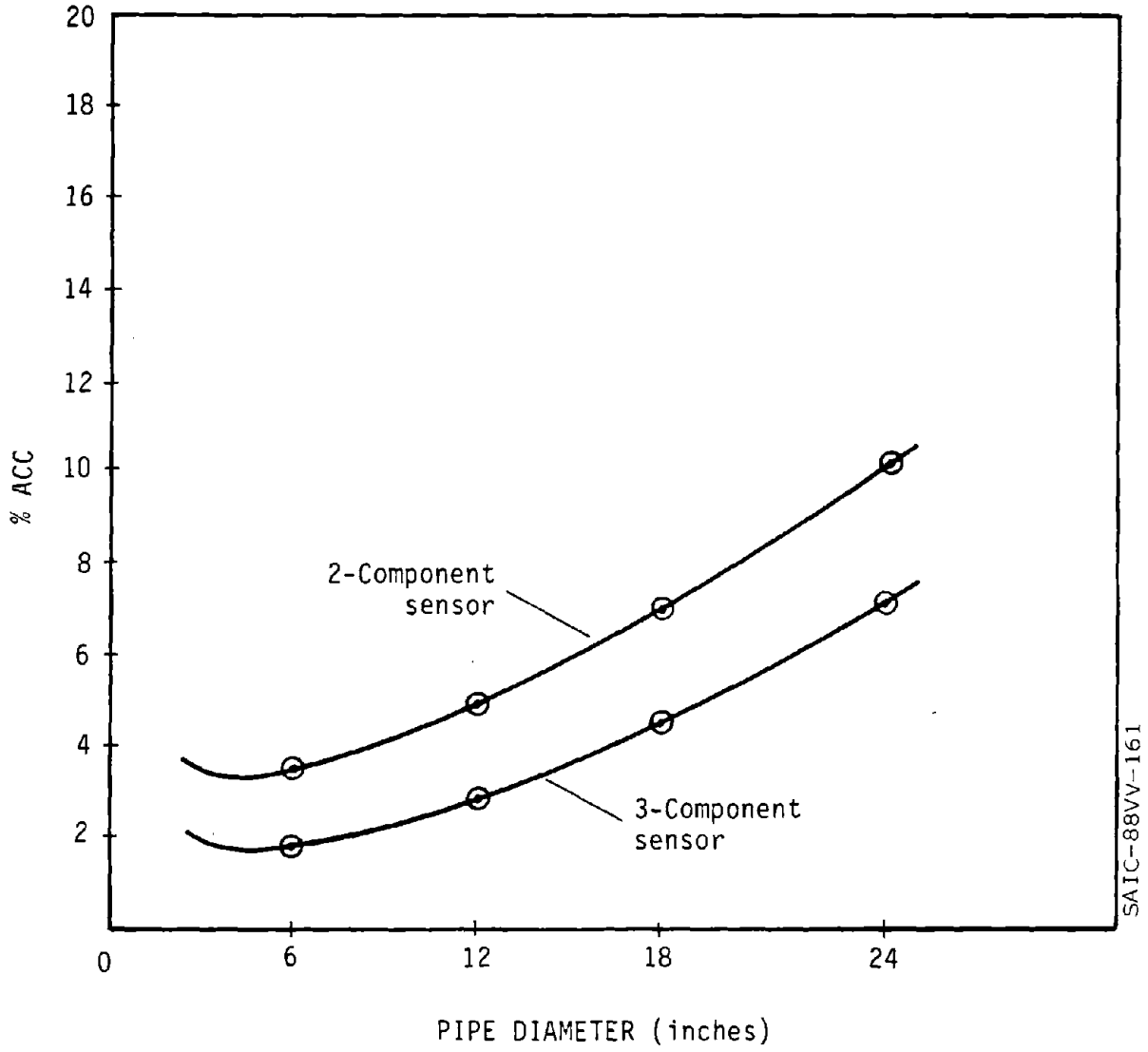

FIGURE 8.1. - Coal slurry concentration sensor accuracy versus pipe diameter for 2- and 3-component sensors.

sensor are extremely high because the two gamma rays do not give much different responses to coal, rock and water, whereas the responses are very suitably different for the SAIC/PRC neutron/gamma-ray sensor. Also, the soft, 60 KeV gamma-ray gauge will produce erroneous results for large lumps of coal or rock, where the "streaming" effect (i.e., nonlinearity in attenuation) is severe. In addition, small changes in the iron and calcium content of coal and rock produce very large errors in the German sensor because of the very high cross sections of these elements to the soft, 60 keV gamma ray. This soft gamma ray will not penetrate larger diameter slurries than 6", and the pipe walls must be thinned for the 6" line, for the 60 keV gammas to prenetrate the iron pipe. Thus, use of the two-gamma-gauge German sensor with high-pressure haulage pipes is not feasible, leaving the SAIC/PRC neutron-gamma-ray sensor the only known sensor suitable for deep mine hydraulic haulage with 6" to 24" haulage lines.

As a research sensor, the SAIC/PRC coal slurry concentration sensor is useful in following rapid changes in coal/rock/water concentration in the HTRF once-through system, where rapid changes in line-concentration (in solids-loading rate) are the norm rather than the exception: concentration measurements are made in the order of one-second intervals. In contrast, the vertical-scan densitometer at SRC (which provides interesting data on a horizontal haulage line) required a measurement time interval that was orders of magnitude longer. Furthermore, it provided only total-density data, whereas the SAIC/PRC concentration sensor was able to follow the individual coal and rock concentrations, providing the unique "duning" data presented in Section 6. There, it was seen that the peak in the coal concentration, in the dune, actually corresponded to a valley, a minimum, in the rock concentration; a most interesting hydraulic-flow phenomenon.

Another unique research application of the SAIC/PRC coal slurry concentration sensor is the study of coal and rock degradation. The sensor will provide an accurate, independent measure of coal and rock concentrations for a slurry with large chunks of coal and rock as well as for a slurry with fines. The German sensor (the only other three-component sensor in existence) cannot do this even for 6" haulage lines. In a recirculating system (a "test-loop"), the slurry velocity could be kept constant and the degradation could be measured indirectly, in a vertical pipe section, by observing the

reduction in "slippage" as the mean particle size becomes smaller with recirculating time. For the almost instant degradation of 80% to 90% of the rock associated with Pittsburgh seam coal, this could be followed by placing two or more SAIC/PRC coal slurry concentration sensors several yards apart in the long HTRF vertical section. As the degradation proceeds, the slippage decreases and the in-situ concentrations will be seen to decrease.

For either horizontal or vertical pipe orientations, the vertical (for horizontal pipes) or radial (for vertical pipes) density distributions can be measured with a gamma-ray tomography system, utilizing a multiple-detector arrangement. The source and detectors can be made small, providing the coal and/or rock density profile with a spatial resolution that is the order of inches, or even centimeters with added effort. A gamma-ray tomography system would look much like the SAIC/PRC gamma gauge, but for a larger number of (smaller) detectors, and some collimation of both source and detectors.

The tomography system can, in principle, be extended to the neutron system as well so that not only density but separate coal and rock concentrations are measured. However, the slowed-down neutrons that are now measured with a bank of He-3 counters surrounded by a neutron moderator (used for slowing down the neutrons), could not be used since they have lost their spatial "memory"; i.e., they tend to act as a gas undergoing diffusion. The slow-neutron counters would be simply replaced by fast-neutron counters, since the fast neutrons possess directional information if used with a collimator preceding the fast-neutron detector: the fast-neutron-detection system was not utilized for the concentration-sensor system designed for eventual use in mining environments, where the excellent stability provided by the "slowed-neutron" detectors was considered to be very important. Nevertheless, for a research system, these fast-neutron detectors can be used, thus opening the way for a combination gamma-neutron tomography system.

APPENDIX A

TESTS AT STBV, ESSEN, WEST GERMANY (FRG)

TABLE OF CONTENTS

APPENDIX

I. INTRODUCTION

The SAIC Coal Slurry Concentration Sensor was installed in the test facility for hydraulic transport of Bergbau-Forschung GmbH in Essen (FRG) in August 1984. First calibration tests were carried out under assistance of Dr. Verbinski and Dr. Cassapakis (SAIC) in September 1984. In the course of normal tests with raw coal, the sensor should be tested under regular conditions.

But after closing of the hydromine "HANSA" in Dortmund we were forced to reduce our efforts in hydraulic transport of coarse coal and to attend to other problems. So only during the last nine test runs with raw coal could the sensor be tested. In the meantime, all work on coarse coal transportation was stopped. The Coal Slurry Concentration Sensor was shipped back to SAIC in August 1985.

II. DESCRIPTION OF THE TEST FACILITY AND THE TEST PROCEDURE

Figure 1 shows the schematic layout of the test rig. In a screening plant, the raw feed coal is classified into the fractions 0-1 mm, 1-3 mm, 3-10 mm, 10-30 and 30-60 mm. The different grain fractions are fed onto a feed-regulating belt according to the desired grain composition of the slurry to be tested. To this purpose, the individual fractions are emptied into a metering car. This car can be moved above the feed-regulating belt to distribute the solids equally over the total length of the feed regulating belt (dosing belt). (See Figure 1.)

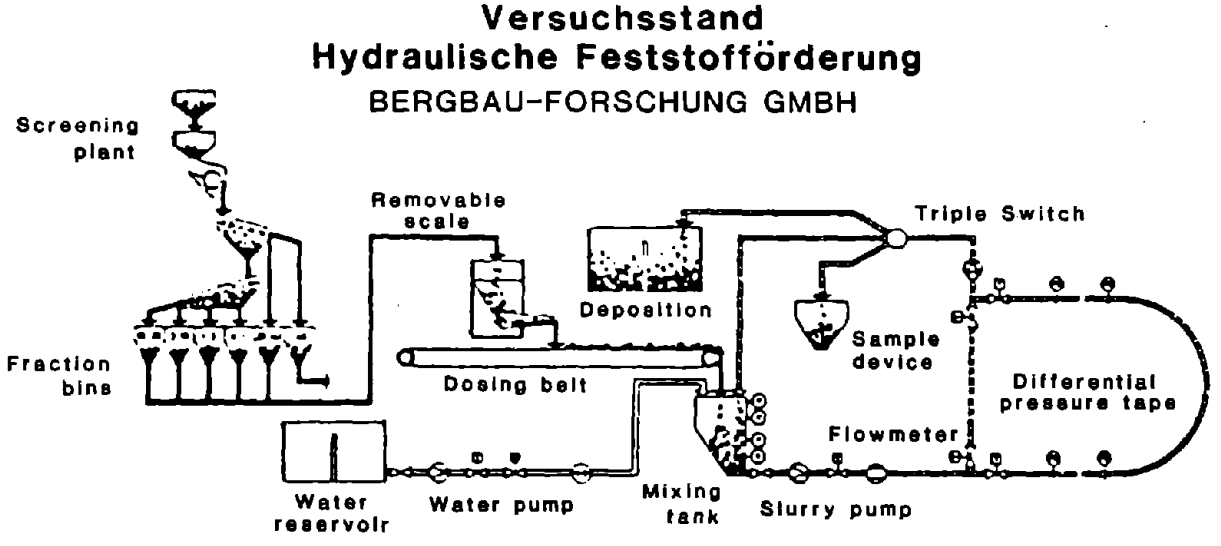

Technical Data		Slurry Pump	
Solids:	Coal, Dirt	Flow Rate:	Max. 1 200 M^3/H
Particle Size:	Max. 100 MM	Pressure:	Max. 8 Bar
Solids Concentration:	Max. 40 % by Volume	Total Power:	388 kW
Velocity:	1.0 - 7.0 M/S	Rotation Speed:	Infinitely Variable Thyristor
Length Short Loop:	57 M		
Length Long Loop:	235 M		
Pipe Diameter:	DN 150 and DN 250		

FIGURE 1. Schedule layout of the test rig.

The feed-regulating belt does not run during the metering process. It is 25m long and 1400 mm wide, so that approximately 7 m3 of solids can be metered out. This equals a solids concentration of 40% by volume in the slurry.

During the metering process a representative sample is taken to determine the particle size distribution as well as the mean density of the raw feed coal. To this purpose a part of the coal sample is ground and put in a Beckman helium pycnometer.

The feed-regulating belt is thyristor-controlled, thus allowing a stepless regulating of the speed, according to the desired solids concentration. The solids are discharged into the 8 m3 capacity feed hopper which is at the same time provided with clean water. The slurry pump sucks the slurry from the feed hopper and presses it into the pipeline. The pump, too, is driven by a thyristor-controlled motor, so that the speed and the flow rate of the slurry in the pipeline can be varied from 1 m/s to 7 m/s any time.

The end of the pipeline is provided with a triple switch allowing either a closed circuit operation, discharge of the slurry into a flow tank after test conclusion or sampling from the flowing slurry stream over a period of 2 - 4 s to determine delivered concentration and other values.

All measured data are stored on magnetic tape according to the PCM method for evaluation in numerical and graphical form by a digital computer.

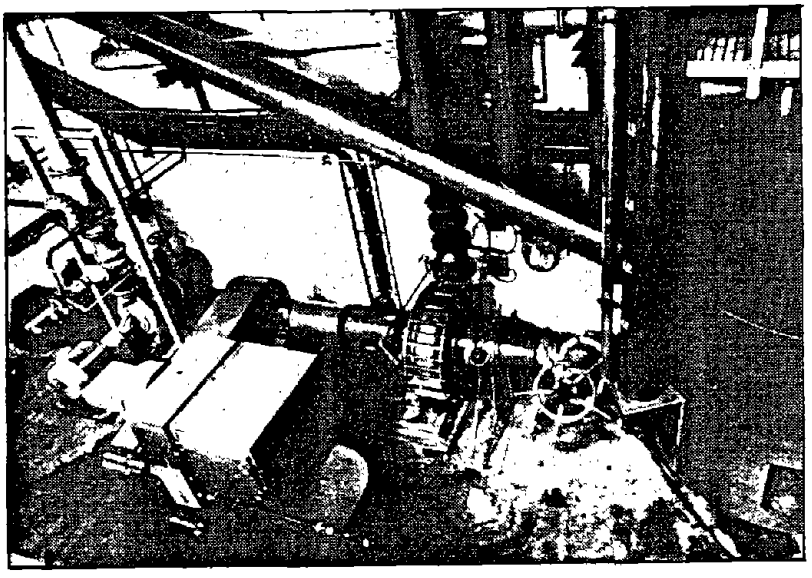

FIGURE 2. - Pump station with feed hopper.

FIGURE 2. - Shows the pump station with the centrifugal pump, dc-motor and feed hopper (on the right) while in FIGURE 3. the 235 m long test pipelines DN150 (6 inch) and DN250 (10 inch) can be seen.

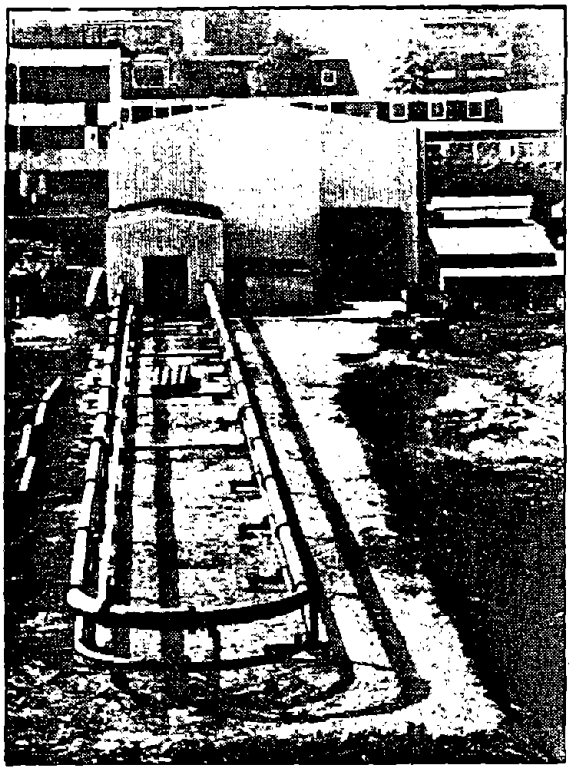

FIGURE 3: Test pipeline DN150 and DN250.

The SAI Coal Slurry Concentration Sensor was installed in the horizontal section of the pipeline. About four meters after the sensor a gamma ray densitometer (Cs-137,250 mCi) was mounted to measure the mean density of the coal-water-slurry (fig. 4).

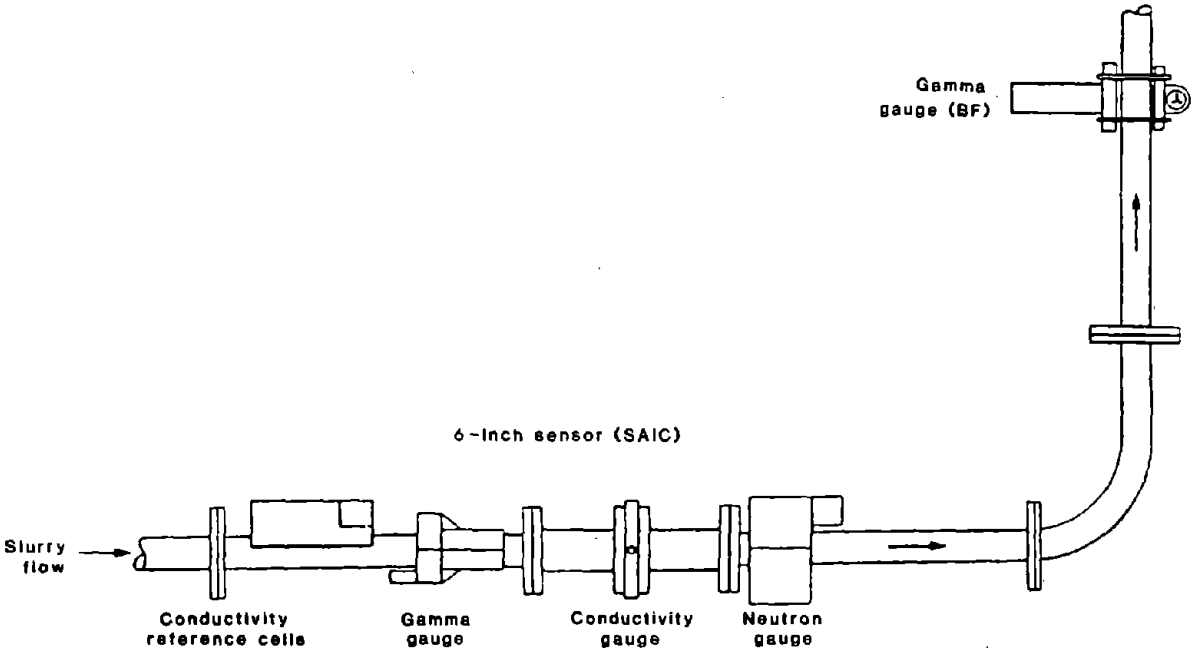

FIGURE 4: Location of the SAIC coal slurry contration sensor.

III. AVERAGE SOLIDS PROPERTIES

The tests were carried out with a long-flame coal from LOHBERG colliery in Dinslaken. The density of the clean coal part and the rock particles are determined to:

Density of clean coal ρ_C = 1330 kg/m3

Density of clean rock ρ_R = 2683 kg/m3

The other properties are shown in fig. 5.

TEST-NO	DENSITY (kg/m3)	CONTENT OF ROCK (Weight-%)	PARTICLE SIZE MAX (mm)	PARTICLE SIZE AVERAGE (mm)	TOTAL CONCENTRATION (Volume-%)
C/1	1677	41.1	31.5	5.644	12.7
C/2	1677	41.1	31.5	5.644	23.1
C/3	1677	41.1	31.5	5.644	30.2
D/1	1704	43.5	31.5	7.349	11.9
D/2	1704	43.5	31.5	7.349	24.1
D/3	1704	43.5	31.5	7.349	28.1
E/1	1743	47.0	31.5	8.732	12.2
E/2	1743	47.0	31.5	8.732	23.9
E/3	1743	47.0	31.5	8.732	30.7

Figure 5: Average solids properties

With the knowledge of the density of the raw feed coal and the density of the included clean coal and clean rock the content of clean coal and clean rock can be evaluated according to the following equations (1) - (4):

Content of rock:

$$C_{RV} = \frac{\rho_{RC} - \rho_C}{\rho_R - \rho_C} \cdot 100 \ (\%) \qquad (1)$$

and

$$C_{RW} = C_{RV} \cdot \frac{\rho_R}{\rho_{RC}} \qquad (2)$$

Content of coal:

$$C_{CV} = 100 - C_{RV} \qquad (3)$$

and

$$C_{CW} = 100 - C_{RW} \qquad (4)$$

where

C_{CV} , C_{RV} = Concentration by volume (coal,rock)

C_{CW} , C_{RW} = Concentration by weight (coal,rock)

ρ_{RC} = Density of raw feed coal

In fig. 5 the average particle size is the weighted mean value and the total solids concentration is the ratio between the input solids volume and the total volume of the test rig. In dependence of the particle size distribution and the mean density of the solids this concentration may differ from the in situ concentration in the pipe.

IV. TEST RESULTS

The test result are submitted in different way:

----- In two volumes of computer printouts

----- In several tables

----- In several diagramms.

In the printout volume 1 there are the results of the tests LOHBERG C/1 - C/3 and LOHBERG D/1 - D/3 while in volume 2 the these of LOHBERG E/1 - E/3 and the clean water tests. In each volumes both the printouts of the 2-component program and the printouts of the statistical programm are compiled.

In the annex of this volume the tables and diagrams are enclosed. Besides the results of the SAI Coal Concentration Sensor the measurements of BF densitometer are listed too.

In the diagrams only the measured values for slurry velocities higher then Vm = 3.5 m/s are plotted because at these flow rates it is guaranteed that there is the same concentration distribution both in the horizontal and in the vertical pipe section. At lower velocities there are sliding beds and even stationary depositions on the bottom of the horizontal pipe. It can bee seen that with decreasing velocities the solids concentration in the vertical pipe section (BF-Densitometer) is decreasing too while in the horizontal pipe section the solids concentration (SAI-Sensor) is increasing. This is caused by the enlargement of the slip between the solids and the carrier fluid.

The total solids concentration from the BF densitometer is calculated in according to the following equation (5):

$$C_{RCV} = \frac{\rho_M - \rho_F}{\rho_{RC} - \rho_F} \cdot 100 \ (\%) \qquad (5)$$

where

ρ_M = Mean slurry density

ρ_F = Water density

With the knowlegde of the composition of the raw coal (listed in the tables) the components coal and rock can be calcutated. The results are also listed in the tables

V. DISCUSSION OF THE TEST RESULTS

The time between the the tests with raw coal and the calibration tests was about five months. Therefore the counts specially of neutron sources were lower with clean water (fig. 6).

GAMMAS		NEUTRONS	
OLD	NEW	OLD	NEW
20001	19653	9176	8233

Figure 6: Old and new counts for gammas and neutrons.

Several partial calibrations with clean water were carried out to get new intercepts. -It must be said that the measurements were enforced with the two component program without the conductivity gauge. During the tests LOHBERG C/1 and LOHBERG C/2 the measured values for the mean slurry density was nearly the same as measured with the BF-Densitometer but the concentration as well as the components were very bad: Too high total solids concentration and specially too low values for the coal.

But the comparision between the densities of coal and rock used during the calibration tests and those used now have shown a difference (fig. 7).

	CALIBRATION TESTS	NORMAL TESTS
COAL	1314	1330
ROCK	2641	2683

Figure 8: Densities (kg/m3) used in the calibration tests and normal tests.

So the assumption was that the cross sections didn't match. At the end of LOHBERG C/2 the slurry velocity was rised up to Vm ≈ 4.5 m/s and referring to the BF-densitometer the cross sections were manually changed until the sensor gave good values for the components. These cross section were used in the next test and the aggreement between the analysis and the measurements were good. The used intercepts and cross sections are listed in the computer printouts.

All tests were run with a response time (input cycle time) of

10 seconds. After test LOHBERG E/3 at a constant speed of Vm = 4.00 m/s the cycle time was varied in 8, 4, 2 and 1 seconds. The tests LOHBERG D/3 and LOHBERG E/3 were carried in such a way that the raw feed coal was added in steps of 10 % by volume. Therefore the test-nos. are LOHBERG D/3-1 and so on.

VI. REMARKS TO THE COMPUTER PROGRAMS

To make the operation of the computer as easy as possible for german people some modifications were made on the computer programs for data aquisition and statistical analysis. The printouts of this programs are in german language and therefore following a small dictionary to understand the programs and printouts.

Data aquisition programm (2-Component program):

Hauptprogramm	= Mainprogram
Seite	= Page
Uhrzeit	= Time
Datum	= Date
Nr.	= No. eq. run number
Kohle	= Coal
Berge	= Rock, dirt, refuse
Wasser	= Water
Dichte	= Density
Cw	= Concentration by weight
Cv	= Concentration by volume
Vol.-%	= Total solids concentration in the slurry (means rock+coal) in percentage of volume

Statistical analysis program:

Datei	= Name of the file containing data from 2-Component program
Beginn	= First run no.
Ende	= Last run no.
Anzahl Werte	= Numbers of runs (cycles)
Mittelwerte	= Average (mean) values
Abweichung	= Deviation
Feststt.=Feststoff	= Solids (rock and coal)

Some more information can get from the remarks on the program listings.

The program listing is presented in Appendix E of the Operation/Service Manual.

TABLES

TEST-NO.:	SOLIDS:	DENSITY (kg/m3)			COMPOSITION (WEIGHT-%)	
LOHBERG C/1	RAW COAL	COAL:	REFUSE:	ROM:	COAL:	REFUSE:
		1 330	2 683	1 677	58,9	41,1

No.	v_m (m/s)	SLURRY-DENSITY (kg/m3)		TOTAL SOLIDS CONCENTRATION (Volume-%)		(Weight-%)		COAL (Weight-%)		REFUSE (Weight-%)	
		BF	SAI	BF	SAI	BF	SAI	BF	SAI	BF	SAI
1	4,94	1 085	1 093	12,7	6,5	19,1	14,0	11,2	1,6	7,9	12,4
2	4,47	1 085	1 101	12,7	6,5	19,1	14,3	11,2	1,5	7,9	12,8
3	3,94	1 085	1 096	12,7	6,9	19,1	15,0	11,2	1,8	7,9	13,2
4	3,53	1 084	1 106	12,4	6,6	19,1	14,8	11,3	1,2	7,9	13,6
5	2,97	1 081	1 101	12,0	7,8	18,6	16,0	11,0	2,9	7,6	13,1
6	2,48	1 077	1 102	11,5	9,2	17,9	17,6	10,5	4,6	7,4	13,0
7	2,21	1 073	1 129	10,8	13,9	16,9	23,6	10,0	9,4	6,9	14,2
8	1,96	1 0 3	1 144	9,4	14,0	14,8	23,7	8,7	8,9	6,1	14,8
9	1,73	1 053	1 127	7,9	17,5	12,6	27,0	7,4	16,7	5,2	10,3
10	1,46	1 045	1 135	6,7	12,6	10,8	22,6	6,4	7,0	4,4	15,6
11	3,94	1 083	1 091	12,3	6,8	19,1	14,3	11,2	2,3	7,9	12,0
12											

TEST-NO.:	SOLIDS:	DENSITY (kg/m3)			COMPOSITION (WEIGHT-%)	
LOHBERG C/2	RAW COAL	COAL:	REFUSE:	ROM:	COAL:	REFUSE:
		1 330	2 683	1 677	58,9	41,1

No.	v_s (m/s)	SLURRY-DENSITY (kg/m3)		TOTAL SOLIDS CONCENTRATION (Volume-%)		(Weight-%)		COAL (Weight-%)		REFUSE (Weight-%)	
		BF	SAI	BF	SAI	BF	SAI	BF	SAI	BF	SAI
1	4,90	1 164	1 152	24,3	12,3	35,0	23,9	20,6	4,7	14,4	19,2
2	4,37	1 164	1 154	24,3	13,6	35,0	25,1	20,6	6,4	14,4	18,7
3	3,90	1 163	1 158	24,1	14,7	34,8	26,3	20,5	7,6	14,3	18,7
4	3,40	1 160	1 157	23,7	15,6	34,3	27,1	20,2	9,0	14,1	18,1
5	2,91	1 155	1 161	23,0	16,0	33,4	27,7	19,7	9,2	13,7	18,5
6	2,42	1 145	1 162	21,4	18,4	31,4	29,8	18,5	12,5	12,9	17,3
7	2,16	1 125	1 158	18,6	23,3	27,7	33,8	16,3	19,8	11,4	14,0
8	1,91	1 117	1 205	17,3	21,3	26,0	34,7	15,3	12,6	10,7	22,1
9	1,67	1 104	1 201	15,5	20,8	23,5	34,1	13,8	12,2	9,7	21,9
10	1,39	1 089	1 217	13,2	18,9	20,3	33,3	12,0	8,2	8,3	25,1
11	3,87	1 154	1 147	22,8	13,2	33,1	24,3	19,5	6,5	13,6	17,8
12											

TEST-NO.:	SOLIDS:	DENSITY (kg/m3)			COMPOSITION (WEIGHT-%)	
LOHBERG C/3	RAW COAL	COAL:	REFUSE:	ROM:	COAL:	REFUSE:
		1 330	2 683	1 677	58,9	41,1

No.	v_m (m/s)	SLURRY-DENSITY (kg/m3)		TOTAL SOLIDS CONCENTRATION (Volume-%)		(Weight-%)		COAL (Weight-%)		REFUSE (Weight-%)	
		BF	SAI	BF	SAI	BF	SAI	BF	SAI	BF	SAI
1	4,92	1 223	1 215	33,0	30,95	45,2	43,1	26,6	24,7	18,6	18,4
2	4,40	1 216		31,9		44,0		25,9		18,1	
3	3,89	1 199	1 199	29,5	30,0	41,3	41,6	24,3	25,2	17,0	16,5
4	3,40	1 198	1 201	29,3	31,5	41,0	43,0	24,1	26,9	16,9	16,0
5	2,90	1 208	1 214	30,8	33,9	42,8	45,5	25,2	28,9	17,6	16,6
6	2,65	1 210	1 220	31,0	34,7	43,0	46,5	25,3	29,3	17,7	17,1
7	2,41	1 207	1 223	30,4	36,0	42,3	47,7	24,9	30,9	17,4	16,8
8	2,15	1 198	1 231	29,4	40,9	41,1	52,0	24,2	36,6	16,9	15,4
9	1,89	1 185	1 276	27,5	46,6	38,9	58,2	22,9	39,2	16,0	18,9
10	1,64	1 165	1 285	24,4	46,8	35,1	58,6	20,7	38,5	14,4	20,2
11	1,39	1 151	1 281	22,3	48,6	32,5	59,9	19,1	41,3	13,4	41,3
12	3,90	1 195	1 201	28,9	29,0	40,5	40,8	23,9	23,5	16,6	17,3

TEST-NO.:	SOLIDS:	DENSITY (kg/m3)			COMPOSITION (WEIGHT-%)	
LOHBERG D/1 (1)	RAW COAL	COAL:	REFUSE:	ROM:	COAL:	REFUSE:
		1330	2683	1704	56,48	43,52

No.	v_m (m/s)	SLURRY-DENSITY (kg/m3)		TOTAL SOLIDS CONCENTRATION (Volume-%)		(Weight-%)		COAL (Weight-%)		REFUSE (Weight-%)	
		BF	SAI	BF	SAI	BF	SAI	BF	SAI	BF	SAI
1	5,43	1 095	1 107	13,6	13,4	21,2	21,7	12,0	10,6	9,2	11,2
2	4,96	1 094	1 107	13,4	14,0	20,9	22,3	11,8	11,4	9,1	11,0
3	4,48	1 094	1 111	13,4	14,3	20,9	22,8	11,8	11,4	9,1	11,4
4	4,01	1 091	1 110	13,1	14,7	20,5	23,2	11,6	12,1	8,9	11,0
5	3,50	1 091	1 113	13,1	16,1	20,5	24,6	11,6	13,9	8,9	10,6
6	3,24	1 091	1 114	12,9	16,5	20,2	25,1	11,4	14,5	8,8	10,6
7	3,02	1 087	1 114	12,5	16,1	19,6	24,7	11,1	13,9	8,5	10,8
8	2,75	1 086	1 111	12,4	16,5	19,5	24,8	11,0	14,8	8,5	10,1
9	2,47	1 082	1 116	11,8	18,0	18,6	26,5	10,5	16,4	8,1	10,1
10	2,24	1 078	1 128	13,3	21,8	17,9	30,7	10,1	21,0	7,8	9,7
11	2,02	1 067	1 153	9,7	23,8	15,5	33,9	8,6	21,0	6,7	12,9
12	1,75	1 054	1 139	7,8	21,2	12,6	30,8	7,1	18,7	5,5	12,1

TEST-NO.:	SOLIDS:	DENSITY (kg/m3)			COMPOSITION (WEIGHT-%)	
LOHBERG D/1	RAW COAL	COAL:	REFUSE:	ROM:	COAL:	REFUSE:
(2)		1330	2683	1704	56,48	43,52

No.	v_s (m/s)	SLURRY-DENSITY (kg/m3)		TOTAL SOLIDS CONCENTRATION (Volume-%)		(Weight-%)		COAL (Weight-%)		REFUSE (Weight-%)	
		BF	SAI	BF	SAI	BF	SAI	BF	SAI	BF	SAI
13	1,54	1 047	1 138	6,8	20,1	11,1	29,8	6,3	17,3	4,8	12,4
14	4,0	1 087	1 103	12,5	14,3	19,6	22,3	11,1	12,3	8,5	10,0
15	4,0	1 066	1 079	9,6	11,2	15,3	10,7	8,6	9,9	6,7	7,7

TEST-NO.:	SOLIDS:	DENSITY (kg/m3)			COMPOSITION (WEIGHT-%)	
LOHBERG D/2	RAW COAL	COAL:	REFUSE:	ROM:	COAL:	REFUSE:
(1)		1330	2683	1704	56,48	43,52

No.	v_s (m/s)	SLURRY-DENSITY (kg/m3)		TOTAL SOLIDS CONCENTRATION (Volume-%)		(Weight-%)		COAL (Weight-%)		REFUSE (Weight-%)	
		BF	SAI	BF	SAI	BF	SAI	BF	SAI	BF	SAI
1	5,48	1 190	1 194	27,0	25,8	38,7	37,9	21,9	19,9	16,8	18,0
2	5,00	1 185	1 194	26,4	25,9	38,0	38,0	21,5	20,0	16,5	18,0
3	4,48	1 184	1 196	26,3	26,9	37,8	38,9	21,3	21,1	16,5	17,7
4	4,02	1 179	1 196	25,6	27,3	37,0	39,3	20,9	21,7	16,1	17,6
5	3,50	1 179	1 197	25,5	28,3	36,9	40,1	20,8	23,0	16,1	17,1
6	2,97	1 176	1 197	25,0	29,5	36,2	41,1	20,4	24,6	15,8	16,5
7	2,73	1 151	1 181	21,6	27,5	32,0	38,6	18,1	23,5	13,9	15,1
8	2,49	1 149	1 181	21,3	28,0	31,6	39,1	17,8	24,2	13,8	14,9
9	2,25	1 146	1 185	20,8	32,8	30,9	43,2	17,5	30,4	13,4	12,8
10	1,98	1 135	1 204	19,2	36,0	28,8	46,8	16,3	32,9	12,5	13,9
11	1,76	1 127	1 201	18,2	39,3	27,5	49,4	15,5	37,8	12,0	11,5
12	3,99	1 172	1 185	24,6	25,6	35,8	37,1	20,2	20,3	15,6	16,8

TEST-NO.:	SOLIDS:	DENSITY (kg/m3)			COMPOSITION (WEIGHT-%)	
LOHBERG D/2 (2)	RAW COAL	COAL:	REFUSE:	ROM:	COAL:	REFUSE:
		1330	2683	1704	56,48	43,52

No.	v_m (m/s)	SLURRY-DENSITY (kg/m3)		TOTAL SOLIDS CONCENTRATION (Volume-%)		(Weight-%)		COAL (Weight-%)		REFUSE (Weight-%)	
		BF	SAI	BF	SAI	BF	SAI	BF	SAI	BF	SAI
13	3,98	1 148	1 159	21,1	21,6	31,3	32,4	17,7	17,3	13,6	15,0

TEST-NO.:	SOLIDS:	DENSITY (kg/m3)			COMPOSITION (WEIGHT-%)	
LOHBERG D/3-1	RAW COAL	COAL:	REFUSE:	ROM:	COAL:	REFUSE:
(1)		1330	2683	1704	56,48	43,52

No.	v_s (m/s)	SLURRY-DENSITY (kg/m3)		TOTAL SOLIDS CONCENTRATION (Volume-%)		(Weight-%)		COAL (Weight-%)		REFUSE (Weight-%)	
		BF	SAI	BF	SAI	BF	SAI	BF	SAI	BF	SAI
1	5,51	1 077	1 083	11,0	10,3	17,4	17,2	9,8	8,3	7,6	9,0
2	5,01	1 075	1 084	10,8	11,3	17,1	18,2	9,7	9,6	7,4	8,6
3	4,50	1 072	1 082	10,4	11,0	16,5	17,8	9,3	9,4	7,2	8,3
4	4,01	1 077	1 080	9,7	11,5	15,5	18,0	8,8	10,3	6,7	7,7
5	3,51	1 062	1 074	8,9	10,3	14,3	16,5	8,1	9,1	6,2	7,4
6	3,24	1 060	1 072	8,7	10,5	14,0	16,5	7,9	9,6	6,1	6,8
7	3,00	1 058	1 070	8,6	10,5	13,9	16,3	7,9	9,8	6,0	6,5
8	2,73	1 055	1 070	8,0	10,4	12,9	16,2	7,3	9,6	5,6	6,5
9	2,52	1 052	1 067	7,4	10,1	12,9	15,8	7,3	9,6	5,6	6,2
10	2,25	1 050	1 065	7,3	10,6	11,8	16,0	6,7	10,4	5,1	5,5
11	2,00	1 044	1 060	6,4	12,2	10,4	17,2	5,9	13,5	4,5	3,7
12	1,75	1 041	1 072	5,9	14,3	9,7	20,0	5,5	15,5	4,2	4,5

TEST-NO.:	SOLIDS:	DENSITY (kg/m3)			COMPOSITION (WEIGHT-%)	
LOHBERG D/3-1 (2)	RAW COAL	COAL:	REFUSE:	ROM:	COAL:	REFUSE:
		1330	2683	1704	56,48	43,52

No.	v_s (m/s)	SLURRY-DENSITY (kg/m3)		TOTAL SOLIDS CONCENTRATION (Volume-%)		(Weight-%)		COAL (Weight-%)		REFUSE (Weight-%)	
		BF	SAI	BF	SAI	BF	SAI	BF	SAI	BF	SAI
13	1,49	1 034	1 069	5,0	14,6	8,2	20,1	4,6	16,2	3,7	3,9

TEST-NO.:	SOLIDS:	DENSITY (kg/m3)			COMPOSITION (WEIGHT-%)	
LOHBERG D/3-2 (1)	RAW COAL	COAL:	REFUSE:	ROM:	COAL:	REFUSE:
		1330	2683	1704	56,48	43,52

No.	v_s (m/s)	SLURRY-DENSITY (kg/m3)		TOTAL SOLIDS CONCENTRATION (Volume-%)		(Weight-%)		COAL (Weight-%)		REFUSE (Weight-%)	
		BF	SAI	BF	SAI	BF	SAI	BF	SAI	BF	SAI
1	5,54	1 132	1 135	18,8	18,4	28,3	28,1	16,0	15,2	12,3	13,0
2	5,01	1 132	1 135	18,8	18,6	28,3	28,3	16,0	15,3	12,3	12,9
3	4,52	1 130	1 139	18,6	19,5	28,0	29,3	15,8	16,2	12,2	13,1
4	4,02	1 129	1 138	18,4	19,7	27,8	29,4	15,7	16,7	12,1	12,7
5	3,53	1 127	1 139	18,2	20,8	27,5	30,5	15,5	18,2	12,0	12,2
6	3,24	1 125	1 141	17,9	20,8	27,1	30,6	15,3	18,1	11,8	12,5
7	3,00	1 123	1 142	17,6	21,6	26,7	31,4	15,1	19,1	11,6	12,3
8	2,76	1 119	1 143	17,1	22,1	26,0	31,8	14,7	19,7	11,3	12,1
9	2,48	1 105	1 135	15,1	21,4	23,3	30,7	13,2	19,4	10,1	11,3
10	2,24	1 100	1 132	14,3	24,1	22,1	33,0	12,5	23,8	9,6	9,2
11	1,99	1 091	1 170	13,1	29,4	20,5	39,7	11,6	27,3	8,9	12,4
12	1,74	1 080	1 181	11,5	29,0	18,1	39,9	10,2	25,5	7,9	14,4

TEST-NO.:	SOLIDS:	DENSITY (kg/m3)			COMPOSITION (WEIGHT-%)	
LOHBERG D/3-2 (2)	RAW COAL	COAL:	REFUSE:	ROM:	COAL:	REFUSE:
		1330	2683	1704	56,48	43,52

No.	v_m (m/s)	SLURRY-DENSITY (kg/m3)		TOTAL SOLIDS CONCENTRATION (Volume-%)		(Weight-%)		COAL (Weight-%)		REFUSE (Weight-%)	
		BF	SAI	BF	SAI	BF	SAI	BF	SAI	BF	SAI
13	1,48	1 068	1 182	9,8	30,2	15,6	40,9	8,8	27,2	6,8	13,7

TEST-NO.:	SOLIDS:	DENSITY (kg/m3)			COMPOSITION (WEIGHT-%)	
LOHBERG D/3-3 (1)	RAW COAL	COAL:	REFUSE:	ROM:	COAL:	REFUSE:
		1330	2683	1704	56,48	43,52

No.	v_s (m/s)	SLURRY-DENSITY (kg/m3)		TOTAL SOLIDS CONCENTRATION (Volume-%)		(Weight-%)		COAL (Weight-%)		REFUSE (Weight-%)	
		BF	SAI	BF	SAI	BF	SAI	BF	SAI	BF	SAI
1	5,53	1 222	1 209	31,7	31,2	44,2	43,1	25,0	25,7	19,2	17,4
2	5,01	1 220	1 210	31,3	32,2	43,7	44,0	24,7	27,0	19,0	17,0
3	4,51	1 218	1 210	31,1	32,3	43,5	41,1	24,6	27,1	18,9	17,0
4	4,01	1 216	1 211	30,8	32,6	43,1	44,3	24,3	27,4	18,8	17,0
5	3,52	1 213	1 213	30,4	33,8	42,7	45,4	24,1	28,9	18,6	16,5
6	3,24	1 209	1 211	29,8	34,0	42,0	45,5	23,7	29,3	18,3	16,2
7	3,01	1 207	1 213	29,5	34,4	41,6	46,0	23,5	29,7	18,1	16,3
8	2,75	1 203	1 211	28,9	34,7	40,9	46,1	23,1	30,3	17,8	15,7
9	2,53	1 173	1 199	24,6	32,9	35,7	44,0	23,1	29,1	15,5	14,8
10	2,27	1 171	1 187	24,4	31,9	35,5	42,6	20,1	28,9	15,4	13,7
11	1,99	1 166	1 204	23,7	40,6	34,6	50,7	19,5	39,3	15,1	11,4
12	1,72	1 152	1 214	21,5	41,8	31,8	51,9	18,0	39,8	13,8	12,1

TEST-NO.:	SOLIDS:	DENSITY (kg/m3)			COMPOSITION (WEIGHT-%)	
LOHBERG D/3-3 (2)	RAW COAL	COAL:	REFUSE:	ROM:	COAL:	REFUSE:
		1330	2683	1704	56,48	43,52

No.	v_s (m/s)	SLURRY-DENSITY (kg/m3)		TOTAL SOLIDS CONCENTRATION (Volume-%)		(Weight-%)		COAL (Weight-%)		REFUSE (Weight-%)	
		BF	SAI	BF	SAI	BF	SAI	BF	SAI	BF	SAI
13	4,01	1 206	1 193	29,4	30,2	41,5	41,5	23,4	26,1	18,1	15,4
14	4,00	1 148		21,1		31,3		17,7		13,6	

TEST-NO.:	SOLIDS:	DENSITY (kg/m3)			COMPOSITION (WEIGHT-%)	
LOHBERG E/1 (1)	RAW COAL	COAL:	REFUSE:	ROM:	COAL:	REFUSE:
		1330	26,83	1743	53,02	46,98

No.	v_s (m/s)	SLURRY-DENSITY (kg/m3)		TOTAL SOLIDS CONCENTRATION (Volume-%)		(Weight-%)		COAL (Weight-%)		REFUSE (Weight-%)	
		BF	SAI	BF	SAI	BF	SAI	BF	SAI	BF	SAI
1	4,80	1 102	1 118	13,8	15,5	21,8	24,4	11,6	12,5	10,2	11,8
2	4,33	1 101	1 118	13,7	15,6	21,7	24,5	11,5	12,6	10,2	11,8
3	3,96	1 099	1 118	13,4	15,7	21,3	24,6	11,3	12,9	10,0	11,8
4	3,52	1 095	1 116	12,9	16,2	20,5	24,9	10,9	13,8	9,6	11,1
5	3,04	1 092	1 115	12,5	16,4	20,0	25,0	10,6	14,1	9,4	10,9
6	2,77	1 091	1 115	12,3	17,0	19,7	25,6	10,4	15,1	9,3	10,5
7	2,51	1 087	1 114	11,8	17,2	18,9	25,6	10,0	15,4	8,8	10,2
8	2,27	1 081	1 110	11,0	17,7	17,7	25,8	9,4	16,7	8,3	9,1
9	2,03	1 072	1 105	9,9	17,9	16,1	25,7	8,5	17,4	7,6	8,3
10	1,76	1 067	1 112	9,1	24,1	14,9	31,7	7,9	26,1	7,0	5,6
11	1,51	1 053	1 113	7,2	21,5	11,9	28,8	6,3	22,5	5,6	6,3
12	4,01	1 092	1 089	12,5	11,6	20,0	18,8	10,6	9,6	9,4	9,2

TEST-NO.:	SOLIDS:	DENSITY (kg/m3)			COMPOSITION (WEIGHT-%)	
LOHBERG E/1 (2)	RAW COAL	COAL:	REFUSE:	ROM:	COAL:	REFUSE:
		1330	2683	1743	53,02	36,98

No.	v_m (m/s)	SLURRY-DENSITY (kg/m3)		TOTAL SOLIDS CONCENTRATION (Volume-%)		(Weight-%)		COAL (Weight-%)		REFUSE (Weight-%)	
		BF	SAI	BF	SAI	BF	SAI	BF	SAI	BF	SAI
13	4,01	1 078	1 097	10,7	12,7	13,3	20,5	9,2	10,5	8,1	10,0

TEST-NO.:	SOLIDS:	DENSITY (kg/m3)			COMPOSITION (WEIGHT-%)	
LOHBERG E/2	RAW COAL	COAL:	REFUSE:	ROM:	COAL:	REFUSE:
(1)		1330	26,83	1743	53,02	46,98

No.	v_s (m/s)	SLURRY-DENSITY (kg/m3)		TOTAL SOLIDS CONCENTRATION (Volume-%)		(Weight-%)		COAL (Weight-%)		REFUSE (Weight-%)	
		BF	SAI	BF	SAI	BF	SAI	BF	SAI	BF	SAI
1	5,02	1 200	1 204	27,0	29,3	39,2	41,3	20,8	23,6	18,4	17,7
2	4,51	1 195	1 203	26,4	29,7	38,5	41,6	20,4	24,4	18,1	17,2
3	4,01	1 189	1 199	25,6	30,3	37,5	41,9	19,9	25,4	17,6	16,4
4	3,50	1 185	1 198	25,0	31,0	36,8	42,5	19,5	26,6	17,3	15,9
5	3,01	1 180	1 186	24,4	30,6	36,0	41,5	19,1	27,3	16,9	14,2
6	2,74	1 155	-	20,9	-	31,6	-	16,8	-	14,8	-
7	2,48	1 152	1 169	20,6	27,4	31,2	37,9	16,5	24,6	14,6	13,3
8	2,25	1 149	1 179	20,2	29,3	30,6	40,0	16,2	26,2	14,4	13,8
9	2,01	1 143	1 170	19,3	30,7	29,4	40,7	15,6	29,1	13,8	11,7
10	1,76	1 132	1 189	17,8	33,6	27,4	46,5	14,5	35,4	12,9	11,1
11	1,49	1 113	1 137	15,3	33,6	24,0	41,5	12,7	37,1	11,3	4,4
12	4,02	1 176	1 164	23,8	24,9	35,3	35,4	18,7	21,5	16,6	13,9

TEST-NO.:	SOLIDS:	DENSITY (kg/m3)			COMPOSITION (WEIGHT-%)	
LOHBERG E/2 (2)	RAW COAL	COAL:	REFUSE:	ROM:	COAL:	REFUSE:
		1330	2683	1743	53,02	46,98

No.	v_s (m/s)	SLURRY-DENSITY (kg/m3)		TOTAL SOLIDS CONCENTRATION (Volume-%)		(Weight-%)		COAL (Weight-%)		REFUSE (Weight-%)	
		BF	SAI	BF	SAI	BF	SAI	BF	SAI	BF	SAI
13	4,02	1 153	1 160	20,7	23,6	31,3	34,1	16,6	20,0	14,7	14,1

TEST-NO.:	SOLIDS:	DENSITY (kg/m3)			COMPOSITION (WEIGHT-%)	
LOHBERG E/3-2	RAW COAL	COAL:	REFUSE:	ROM:	COAL:	REFUSE:
		1330	2683	1743	53,02	46,98

No.	v_m (m/s)	SLURRY-DENSITY (kg/m3)		TOTAL SOLIDS CONCENTRATION (Volume-%)		(Weight-%)		COAL (Weight-%)		REFUSE (Weight-%)	
		BF	SAI	BF	SAI	BF	SAI	BF	SAI	BF	SAI
1	4,99	1 151	1 168	20,3	21,6	30,7	32,9	16,3	16,5	14,4	16,4
2	4,52	1 149	1 168	20,0	22,3	30,3	33,5	16,1	17,5	14,2	16,6
3	4,01	1 147	1 168	19,8	22,9	30,1	34,0	16,0	18,2	14,1	15,7
4	3,50	1 142	1 166	19,1	23,4	29,2	34,3	15,5	19,2	13,7	15,1
5	3,00	1 138	1 166	18,5	24,5	28,3	35,3	15,0	20,8	12,3	14,5
6	2,76	1 134	1 166	18,1	24,9	27,8	35,5	14,7	21,4	13,1	14,2
7	2,49	1 131	1 166	17,6	25,2	27,1	35,8	14,4	21,8	12,7	14,0
8	2,25	1 105	1 144	14,1	26,0	22,2	35,3	11,8	25,2	10,4	10,1
9	1,97	1 101	1 153	13,6	29,2	21,5	38,5	11,4	28,9	10,1	9,6
10	1,72	1 094	1 188	12,7	33,7	20,2	44,0	10,7	31,5	9,5	12,5
11	3,88	1 136	1 145	18,3	20,0	28,1	30,1	14,9	16,4	13,2	13,6
12											

TEST-NO.:	SOLIDS:	DENSITY (kg/m3)			COMPOSITION (WEIGHT-%)	
LOHBERG E/3-3	RAW COAL	COAL:	REFUSE:	ROM:	COAL:	REFUSE:
		1330	2683	1743	53,02	46,98

No.	v_s (m/s)	SLURRY-DENSITY (kg/m3)		TOTAL SOLIDS CONCENTRATION (Volume-%)		(Weight-%)		COAL (Weight-%)		REFUSE (Weight-%)	
		BF	SAI	BF	SAI	BF	SAI	BF	SAI	BF	SAI
1	4,97	1 244	1 238	32,9	35,3	46,1	47,7	24,4	28,2	21,7	19,5
2	4,53	1 240	1 236	32,4	35,7	45,5	48,0	24,1	29,1	21,4	18,9
3	4,02	1 238	1 237	32,1	35,7	45,2	48,0	24,0	28,9	21,2	19,1
4	3,50	1 229	1 235	30,9	36,4	43,8	48,5	23,2	30,0	20,6	18,5
5	3,00	1 228	1 238	30,8	37,6	43,7	49,6	23,2	31,3	20,5	18,3
6	2,75	1 196	1 209	26,5	33,5	38,6	44,9	20,5	28,8	18,1	16,1
7	2,54	1 191	1 204	25,8	33,3	37,8	44,6	20,0	29,2	17,8	15,4
8	2,24	1 188	1 210	25,4	34,4	37,3	45,8	19,8	30,0	17,5	15,7
9	2,01	1 184	1 216	24,9	39,1	36,7	49,9	19,5	35,7	17,2	14,1
10	1,74	1 172	1 216	23,2	43,1	34,5	53,1	18,3	41,3	16,2	11,9
11	4,04	1 224	1 209	30,2	32,2	43,0	43,9	22,8	27,1	20,2	16,8
12											

DIAGRAMS

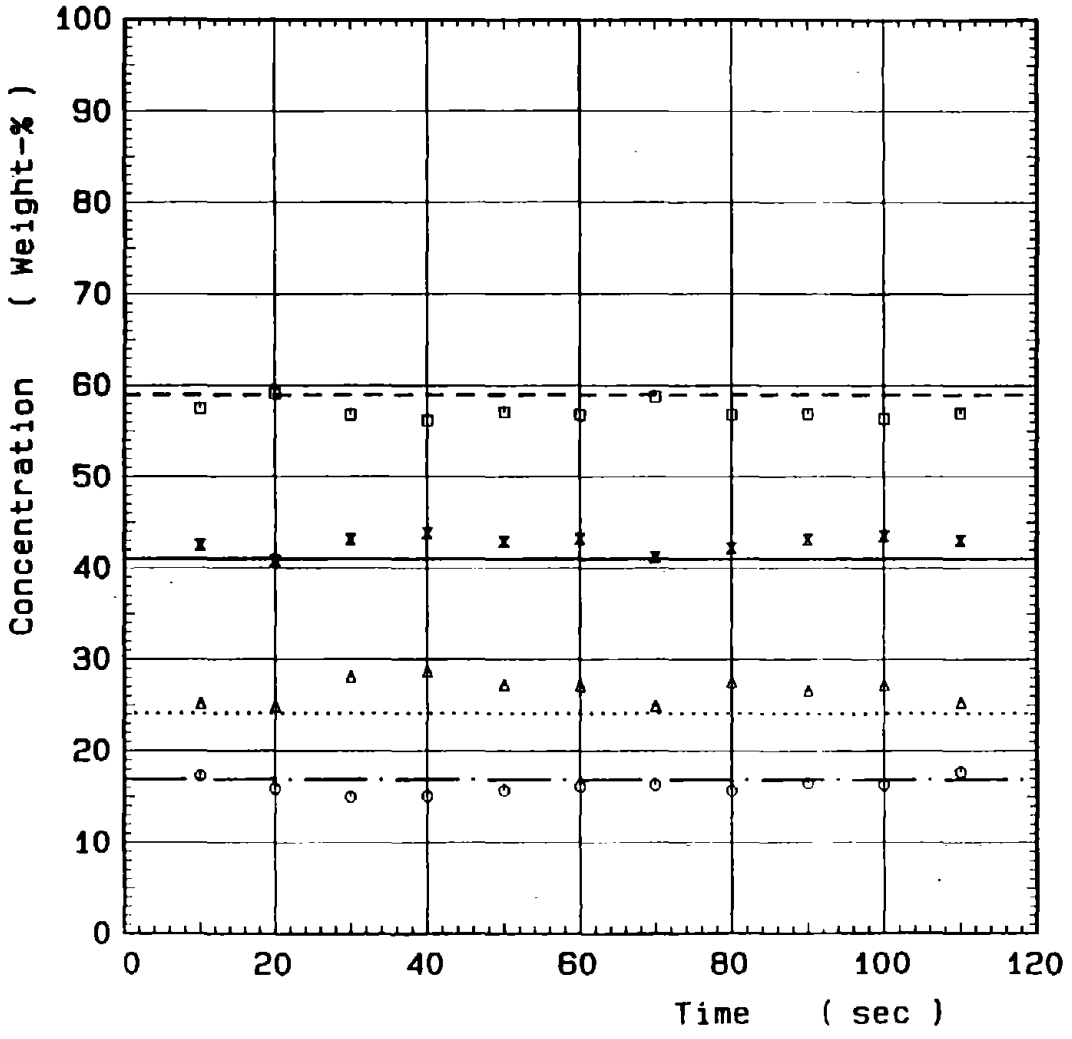

LOHBERG C/3

v = 3.5 m/s

	BF	SAI
Total	41.0 %	43.0 ± 0.9 %
Water	59.0 %	57.0 ± 0.9 %
Coal	24.1 %	26.9 ± 1.4 %
Refuse	16.9 %	16.0 ± 0.9 %

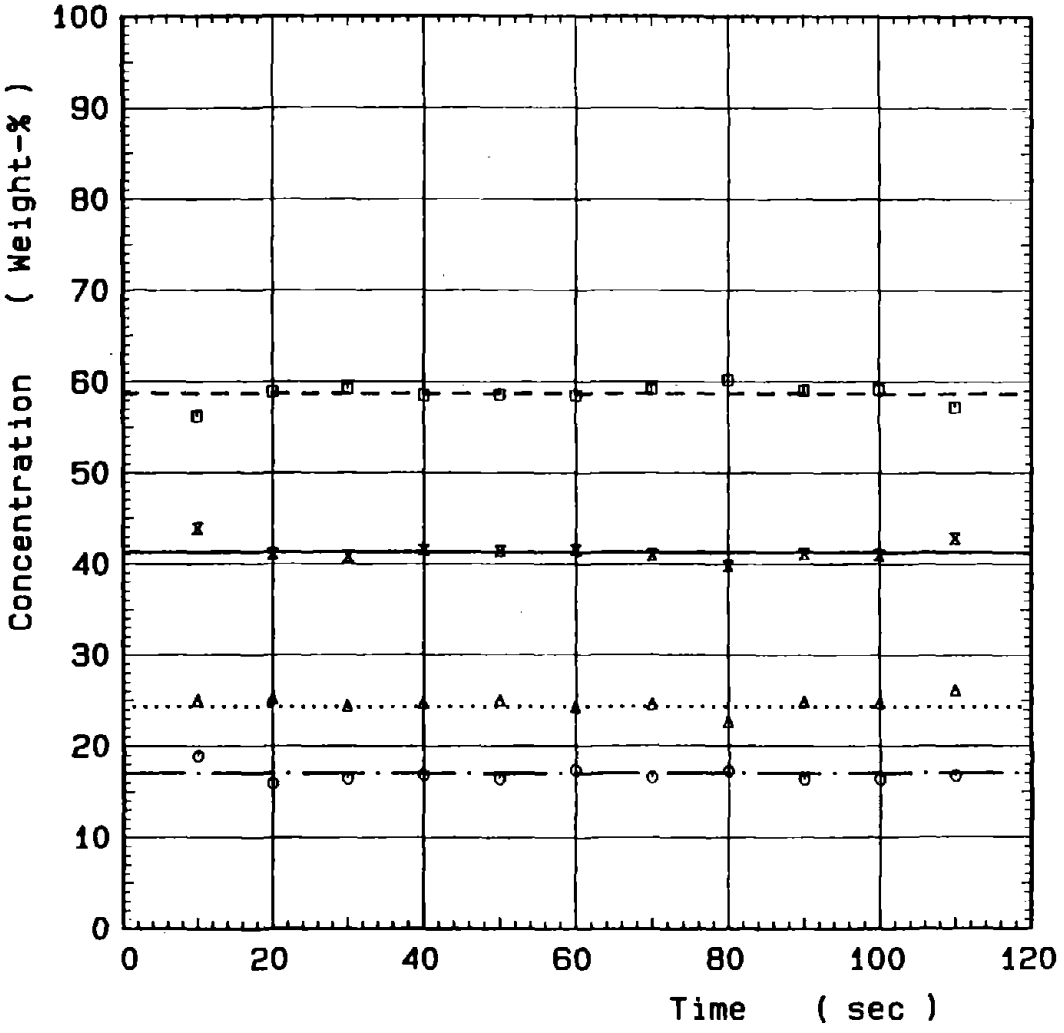

LOHBERG C/3

v = 4.0 m/s

	BF	SAI
Total	41.3 %	41.6 ± 1.2 %
Water	58.7 %	58.4 ± 1.2 %
Coal	24.3 %	25.2 ± 1.5 %
Refuse	17.0 %	16.5 ± 0.8 %

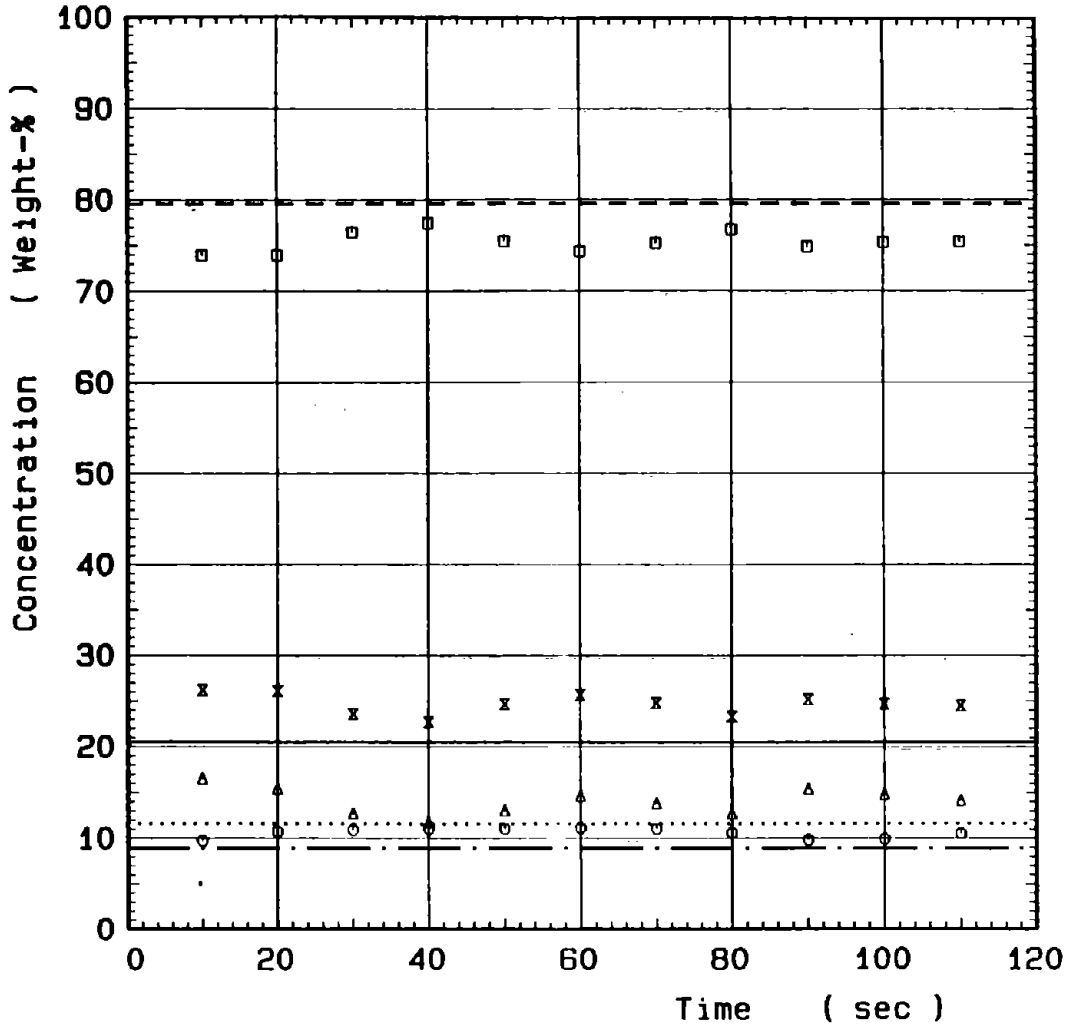

LOHBERG D/1

v = 3.5 m/s

		BF	SAI
Total	20.5 %	———	24.6 ± 1.0 %
Water	79.5 %	- - - - - -	75.4 ± 1.0 %
Coal	11.6 %	·····	13.9 ± 1.1 %
Refuse	8.9 %	—·—	10.6 ± 0.4 %

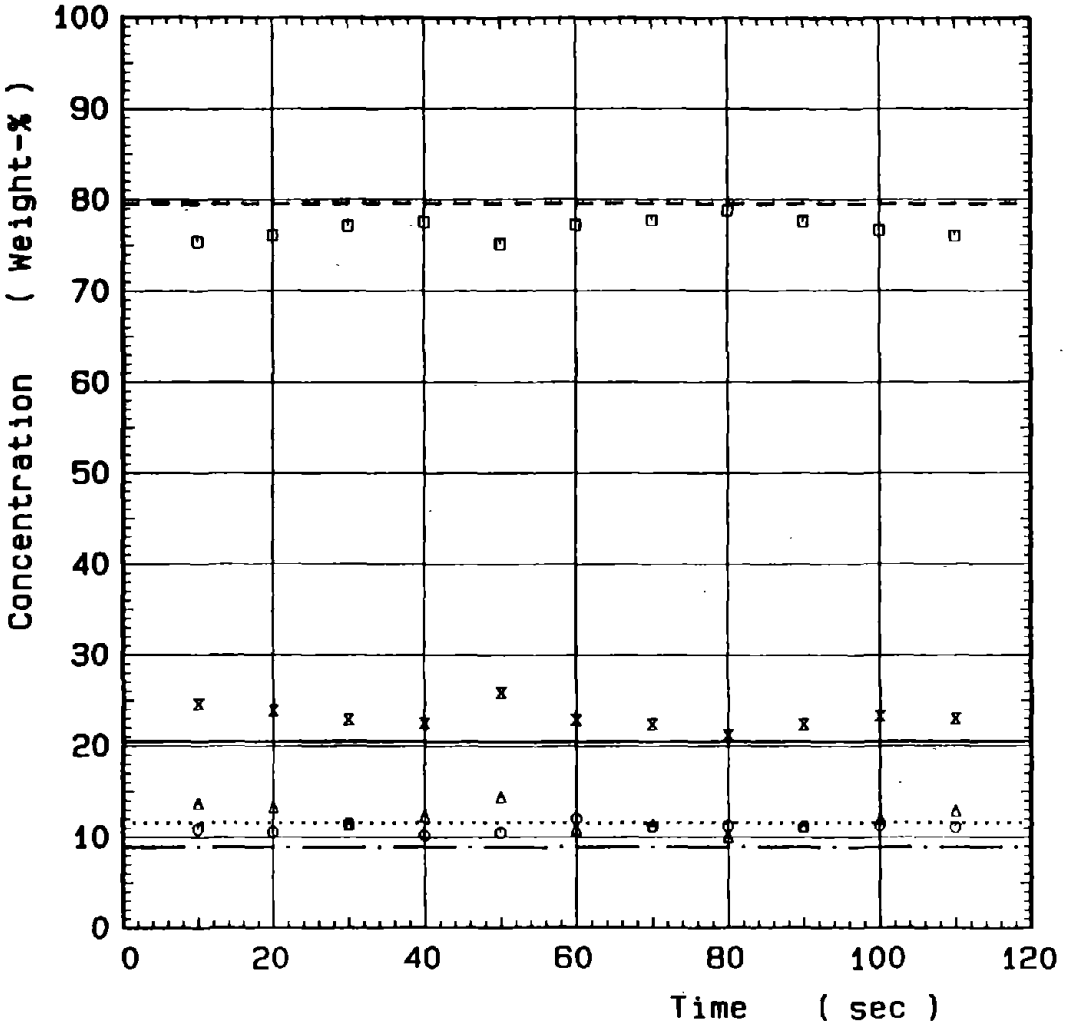

LOHBERG D/1

v = 4.0 m/s

		BF	SAI
Total	20.5 %	———	23.2 ± 1.0 %
Water	79.5 %	– – – – –	76.8 ± 1.0 %
Coal	11.6 %	·····	11.6 ± 1.3 %
Refuse	8.9 %	——·——	11.0 ± 0.5 %

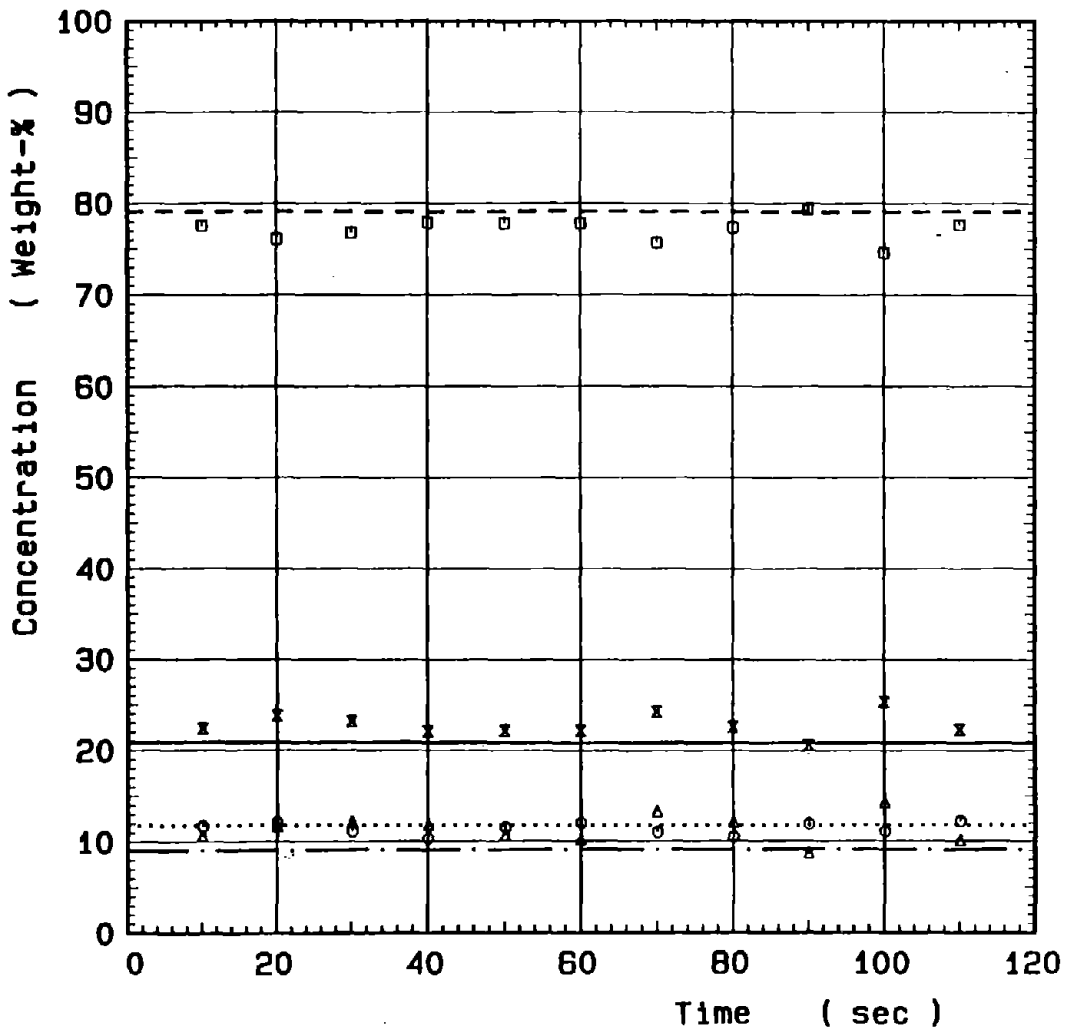

LOHBERG D/1

v = 4.5 m/s

	BF		SAI
Total	20.9 %	⧗	22.8 ± 1.2 %
Water	79.1 %	⧈	77.2 ± 1.2 %
Coal	11.8 %	△	11.4 ± 1.5 %
Refuse	9.1 %	⊙	11.4 ± 0.6 %

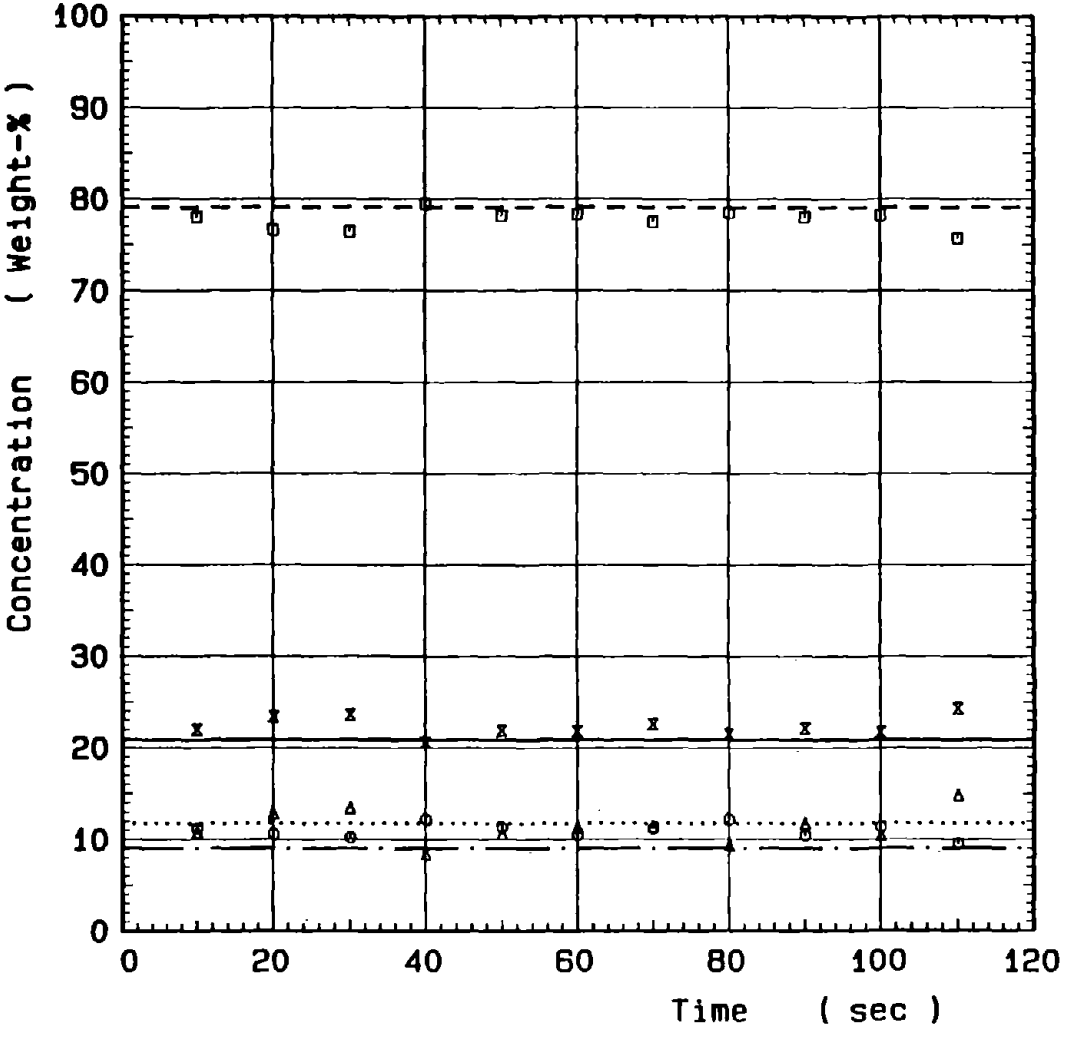

LOHBERG D/1

v = 5.0 m/s

		BF		SAI
Total	20.9 %	———	x	22.3 ± 1.0 %
Water	79.1 %	– – – –	□	77.7 ± 1.0 %
Coal	11.8 %	·····	△	11.4 ± 1.7 %
Refuse	9.1 %	—·—	○	11.0 ± 0.8 %

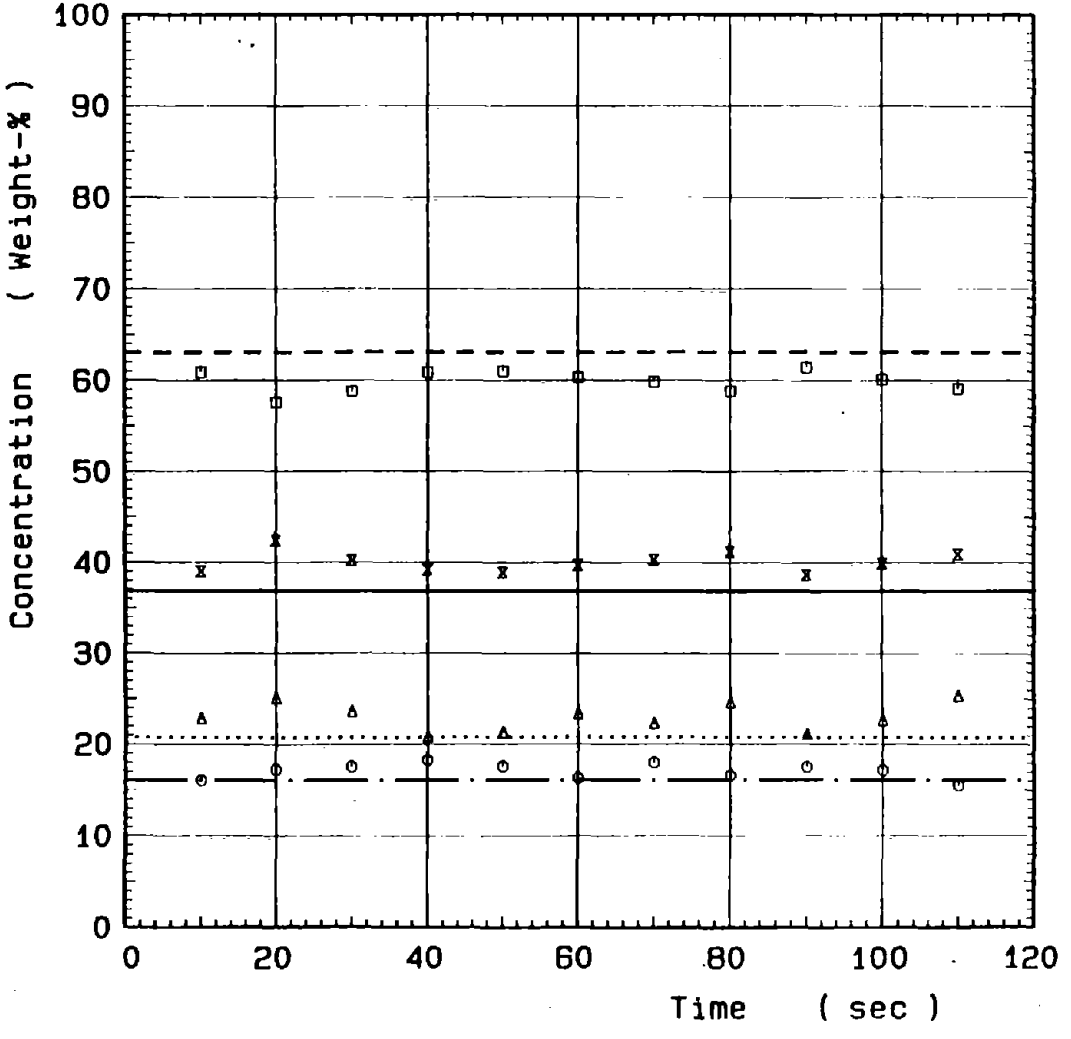

LOHBERG D/2

v = 3.5 m/s

	BF	SAI
Total	36.9 %	40.1 ± 1.1 %
Water	63.1 %	59.9 ± 1.1 %
Coal	20.8 %	23.0 ± 1.5 %
Refuse	16.1 %	17.1 ± 0.8 %

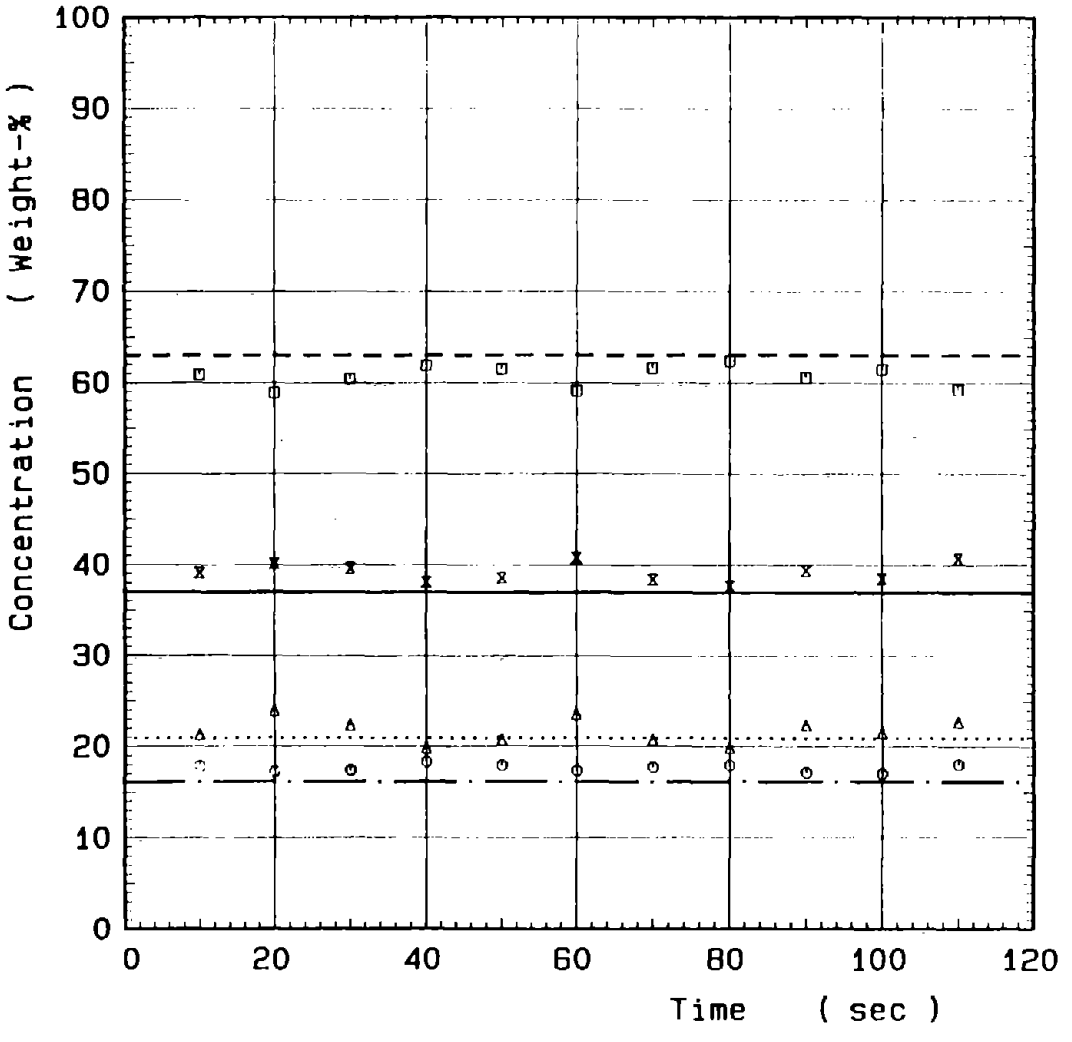

LOHBERG D/2

v = 4.0 m/s

	BF	SAI
Total	37.0 %	39.3 ± 1.1 %
Water	63.0 %	60.7 ± 1.1 %
Coal	20.9 %	21.7 ± 1.3 %
Refuse	16.1 %	17.6 ± 0.4 %

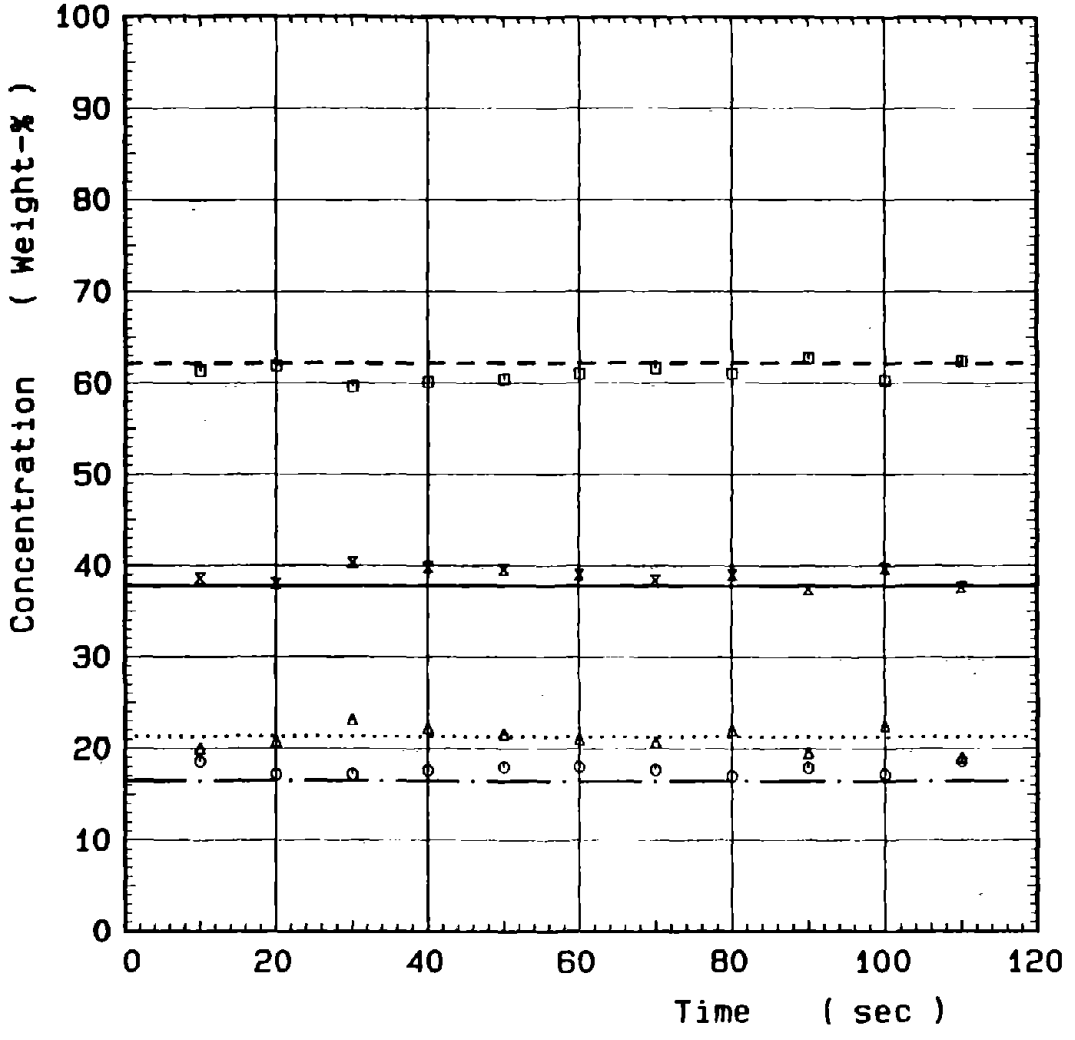

LOHBERG D/2

v = 4.5 m/s

	BF	SAI
Total	37.8 %	38.9 ± 0.9 %
Water	62.2 %	61.1 ± 0.9 %
Coal	21.9 %	21.1 ± 1.2 %
Refuse	16.5 %	17.7 ± 0.5 %

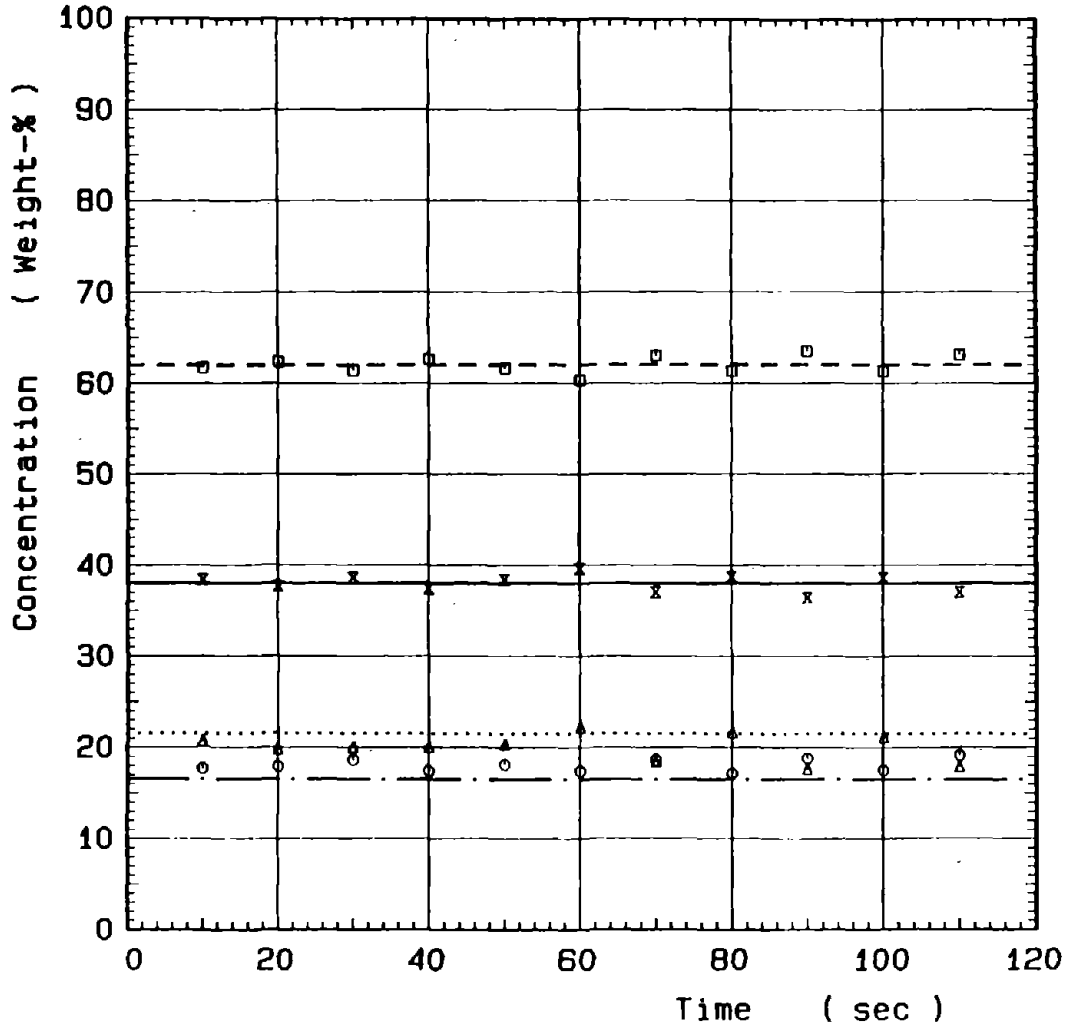

LOHBERG D/2

v = 5.0 m/s

	BF	SAI
Total	38.0 %	38.0 ± 0.9 %
Water	62.0 %	62.0 ± 0.9 %
Coal	21.5 %	20.0 ± 1.4 %
Refuse	16.5 %	18.0 ± 0.6 %

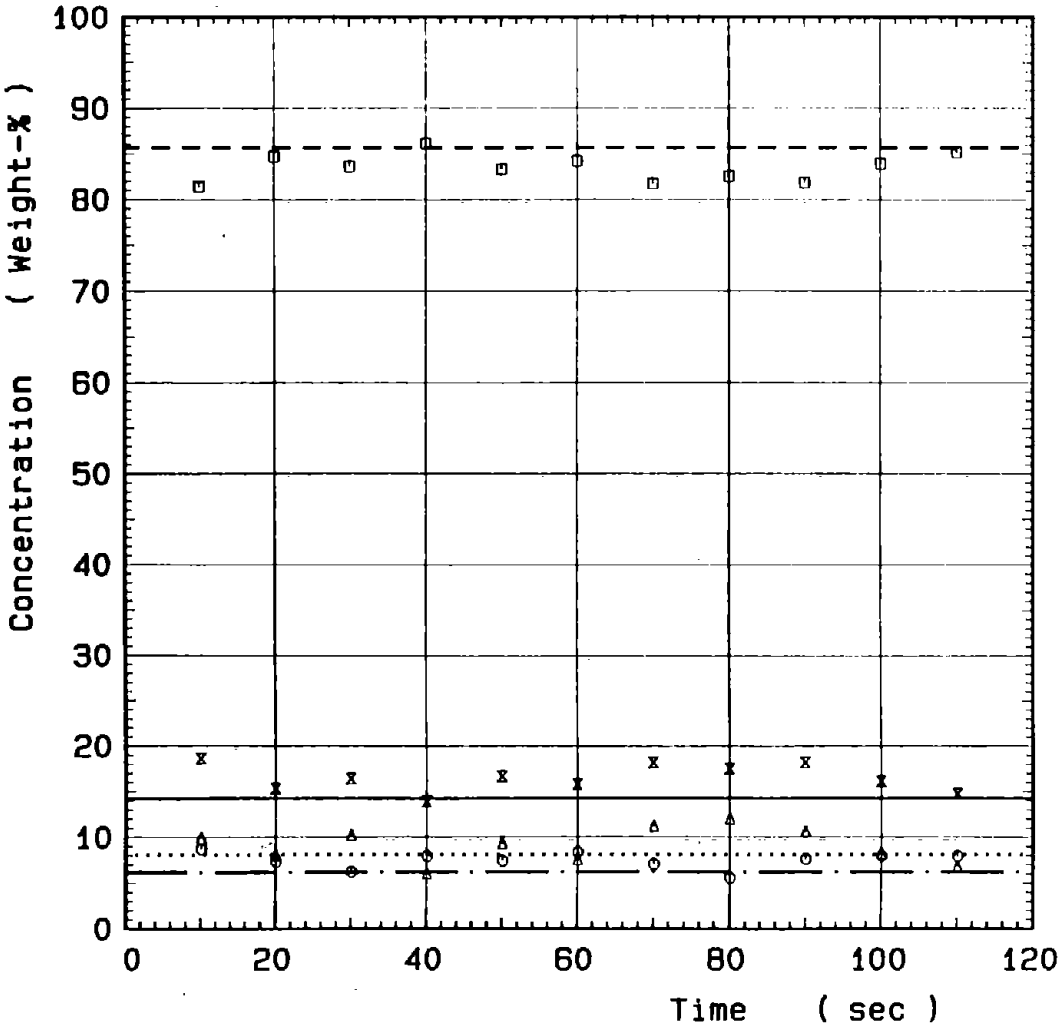

LOHBERG D/3-1

v = 3.5 m/s

		BF		SAI
Total	14.3 %	———	⧗	16.5 ± 1.5 %
Water	85.7 %	- - - - -	□	83.5 ± 1.5 %
Coal	8.1 %	·····	△	9.1 ± 1.8 %
Refuse	6.2 %	——·——	○	7.4 ± 0.9 %

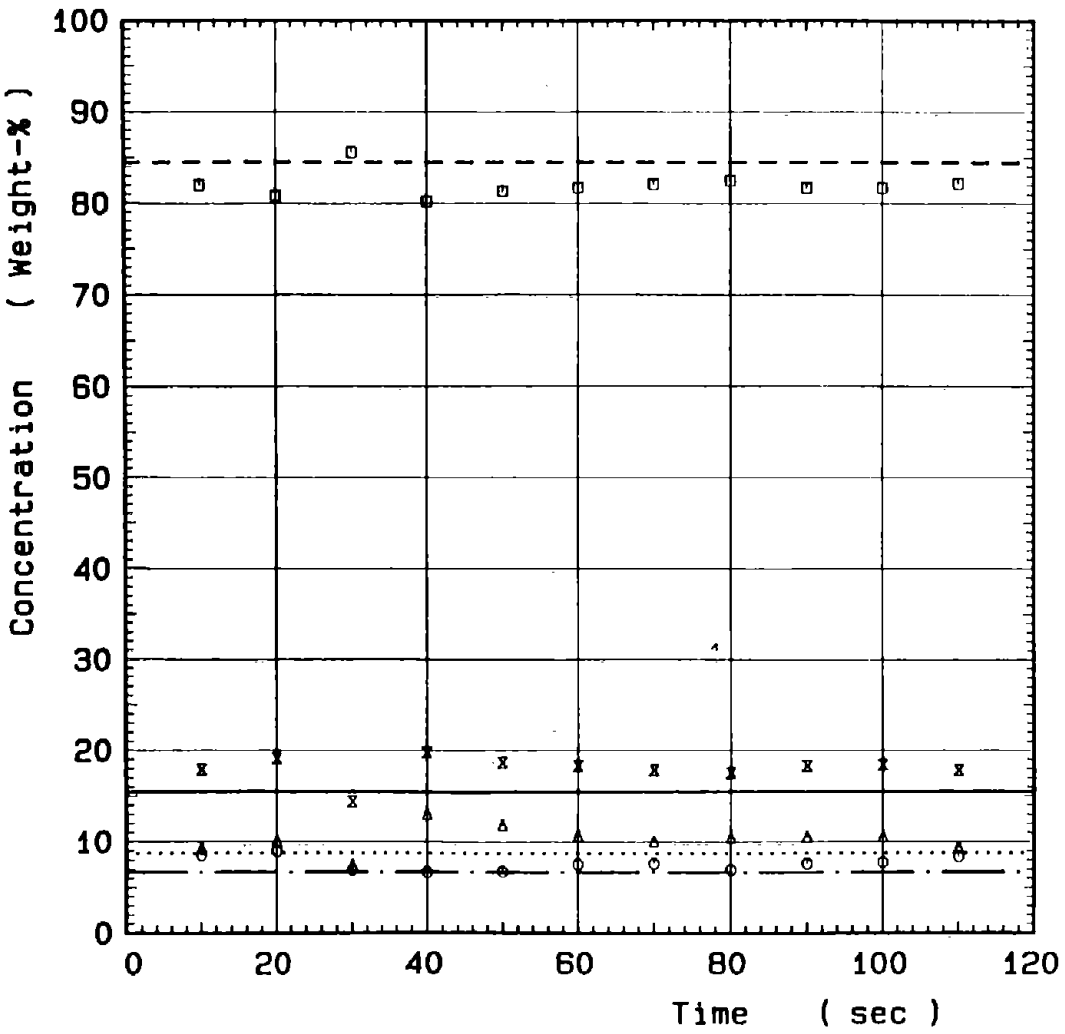

LOHBERG D/3-1

v = 4.0 m/s

	BF		SAI
Total	15.5 %	———	18.0 ± 1.3 %
Water	84.5 %	- - - - -	82.0 ± 1.3 %
Coal	8.8 %	·····	10.3 ± 1.4 %
Refuse	6.7 %	—·—	7.7 ± 0.7 %

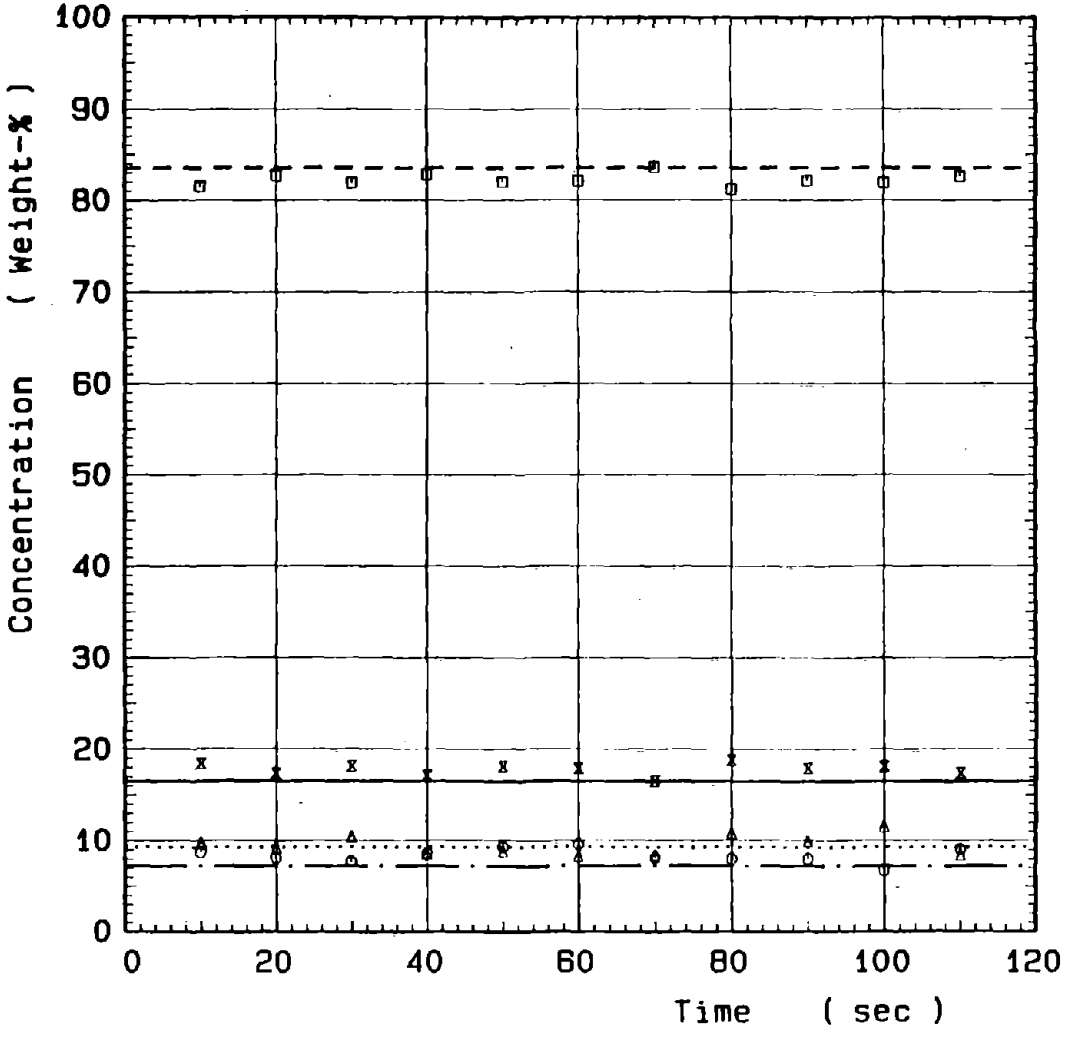

LOHBERG D/3-1

v = 4.5 m/s

	BF		SAI
Total	16.5 %	———	17.8 ± 0.6 %
Water	83.5 %	- - - - -	82.2 ± 0.6 %
Coal	9.3 %	·····	9.4 ± 1.1 %
Refuse	7.2 %	——·——	8.3 ± 0.8 %

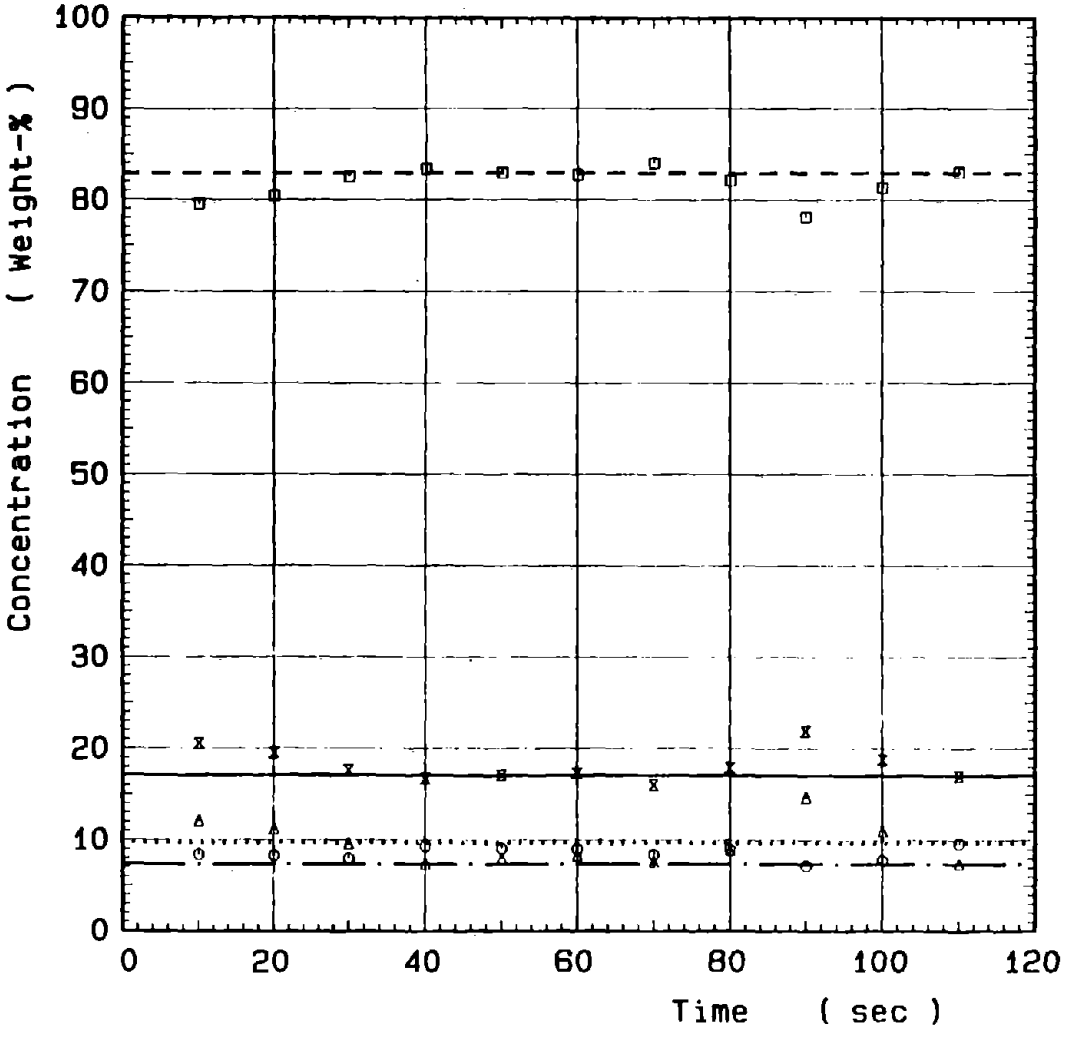

LOHBERG D/3-1

v = 5.0 m/s

	BF	SAI
Total	17.1 %	18.2 ± 1.7 %
Water	82.9 %	81.8 ± 1.7 %
Coal	9.7 %	9.6 ± 2.2 %
Refuse	7.4 %	8.6 ± 0.7 %

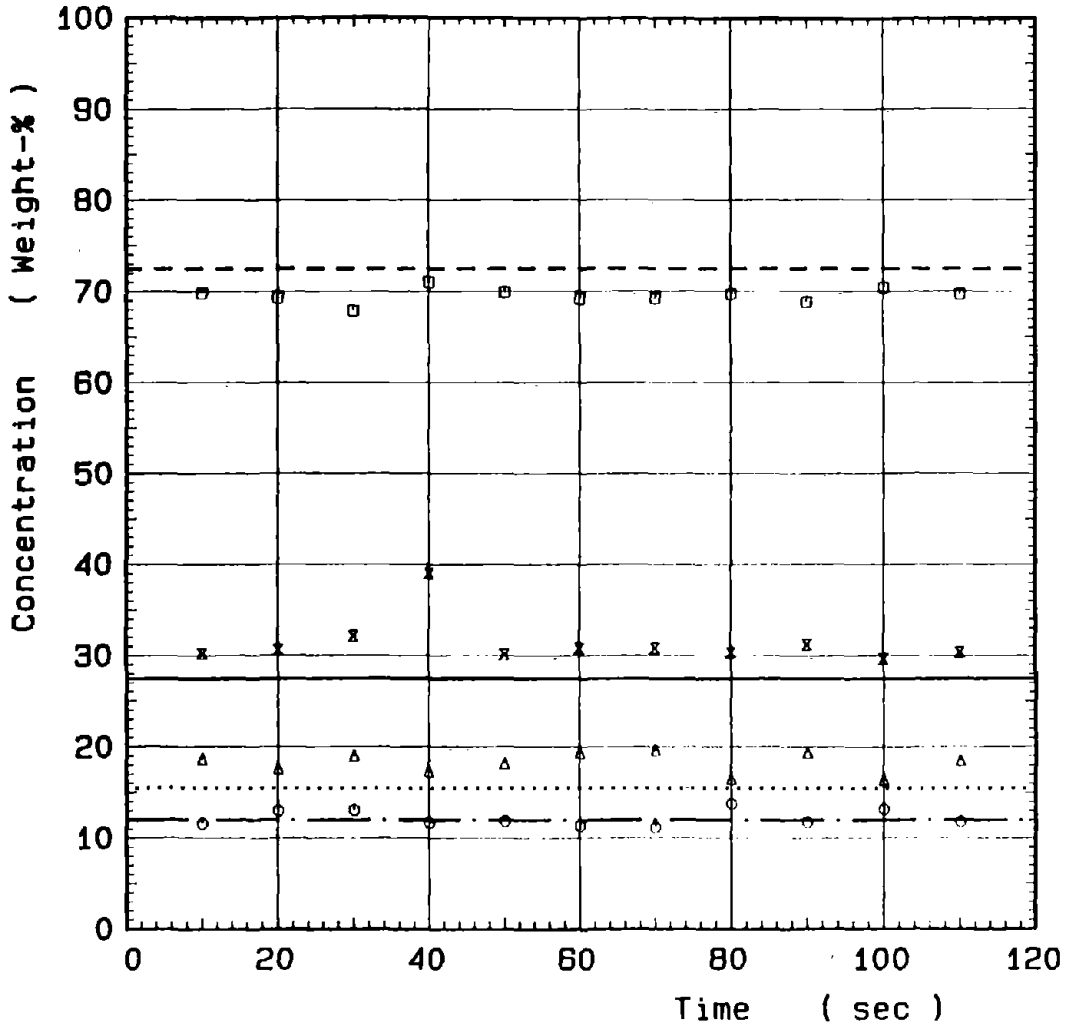

LOHBERG D/3-2

v = 3.5 m/s

		BF	SAI
Total	27.5 %	———	30.5 ± 0.8 %
Water	72.5 %	- - - - -	69.5 ± 0.8 %
Coal	15.5 %	·····	18.2 ± 1.1 %
Refuse	12.0 %	——·——	12.2 ± 0.8 %

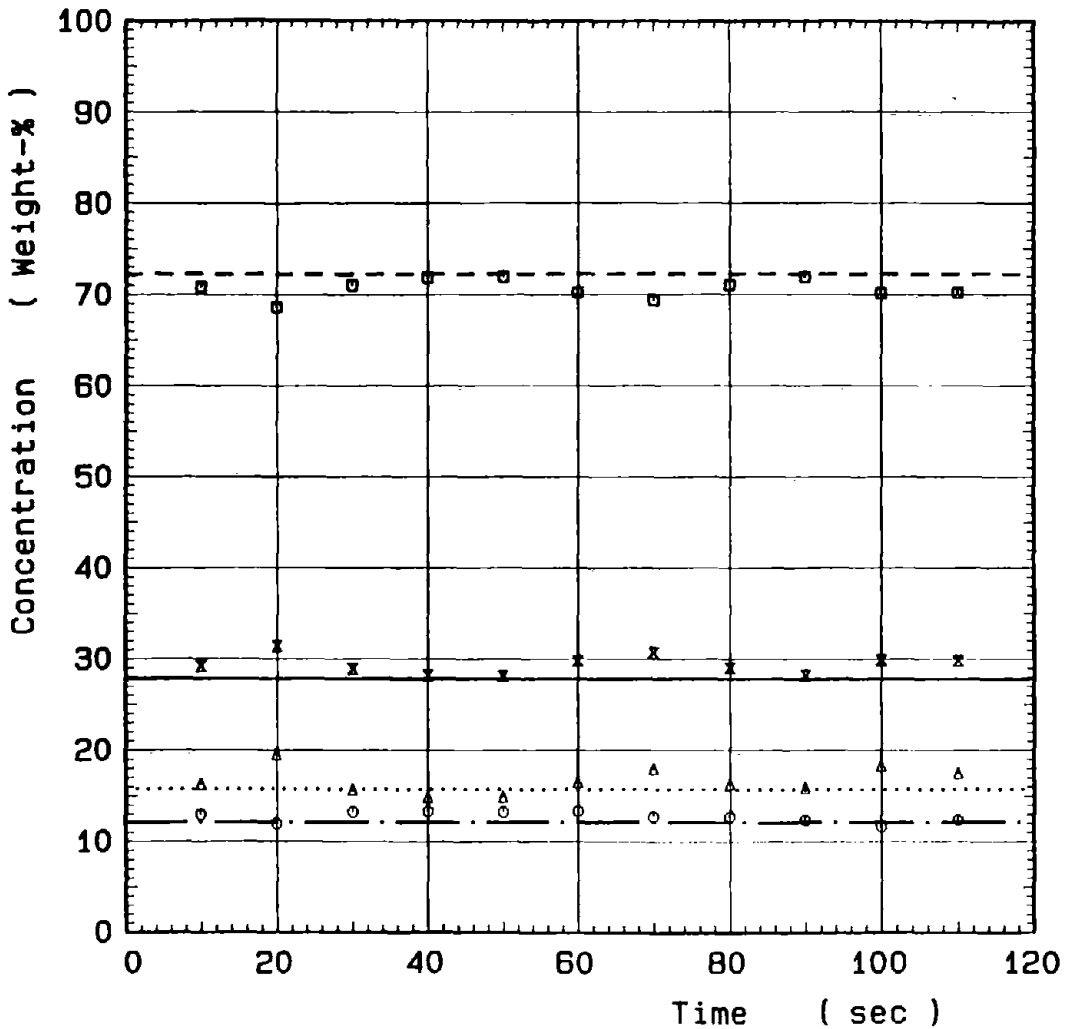

LOHBERG D/3-2

v = 4.0 m/s

		BF	SAI
Total	27.8 %	———	29.4 ± 1.0 %
Water	72.2 %	- - - - -	70.6 ± 1.0 %
Coal	15.7 %	·····	16.7 ± 1.4 %
Refuse	12.1 %	——·——	12.7 ± 0.6 %

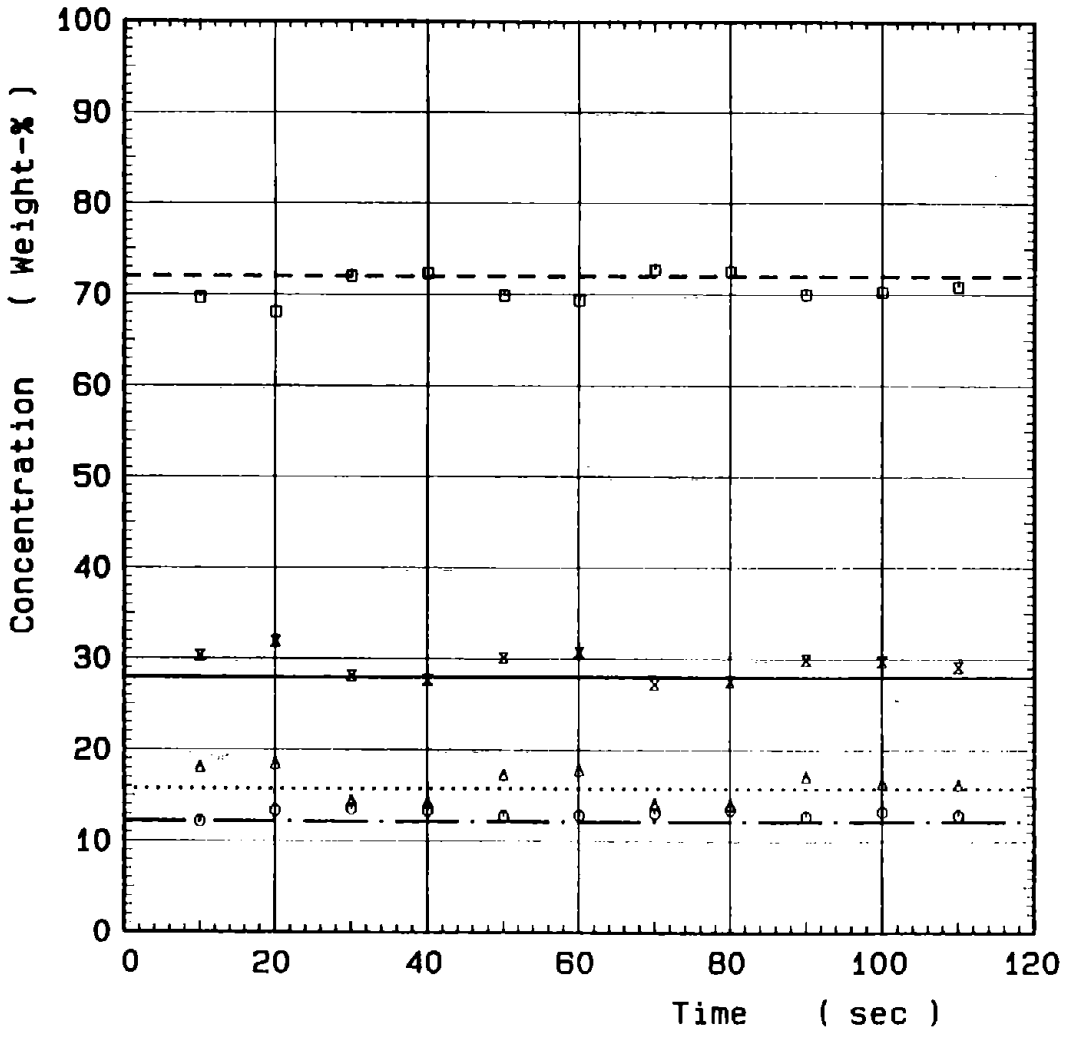

LOHBERG D/3-2

v = 4.5 m/s

	BF		SAI
Total	28.0 %	———	29.3 ± 1.4 %
Water	72.0 %	– – – –	70.7 ± 1.4 %
Coal	15.8 %	·····	16.2 ± 1.6 %
Refuse	12.2 %	——·——	13.1 ± 0.4 %

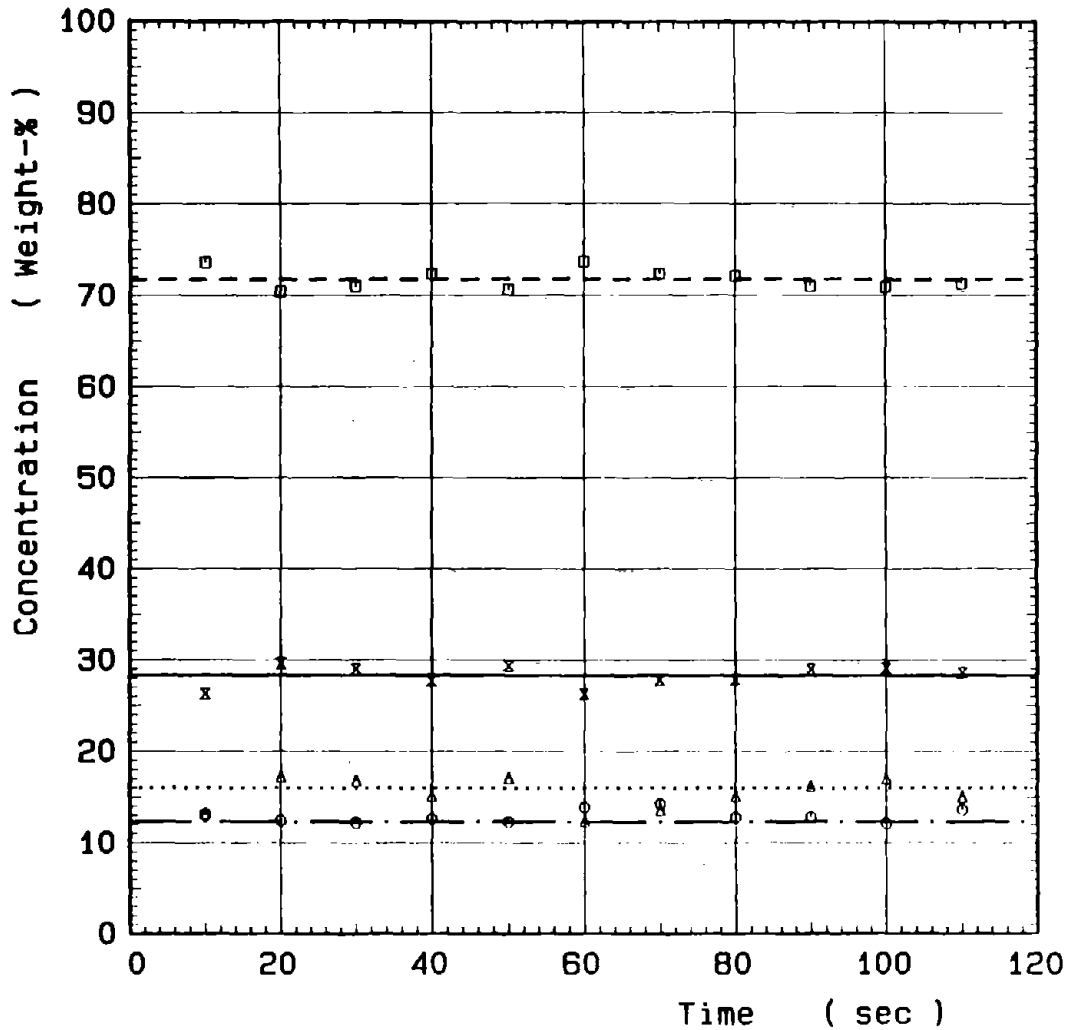

LOHBERG D/3-2

v = 5.0 m/s

		BF	SAI
Total	28.3 %	———	28.3 ± 1.1 %
Water	71.7 %	- - - - -	71.7 ± 1.1 %
Coal	16.0 %	·····	15.3 ± 1.6 %
Refuse	12.3 %	——·——	12.9 ± 0.7 %

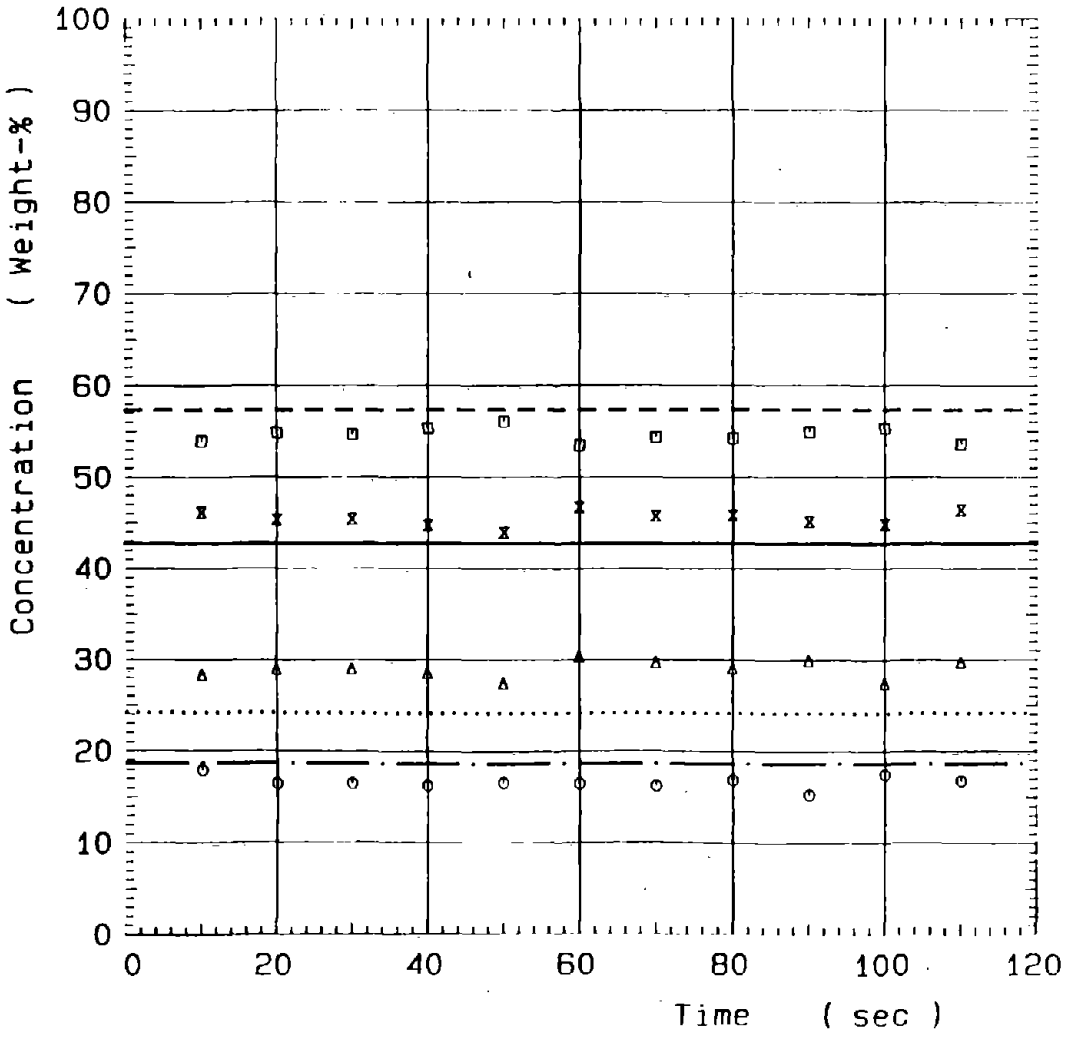

LOHBERG D/3-3

v = 3.5 m/s

		BF		SAI
Total	42.7 %	———	x	45.4 ± 0.8 %
Water	57.3 %	- - - - - -	□	54.6 ± 0.8 %
Coal	24.1 %	.....	△	28.9 ± 0.9 %
Refuse	18.6 %	—— · ——	○	16.5 ± 0.6 %

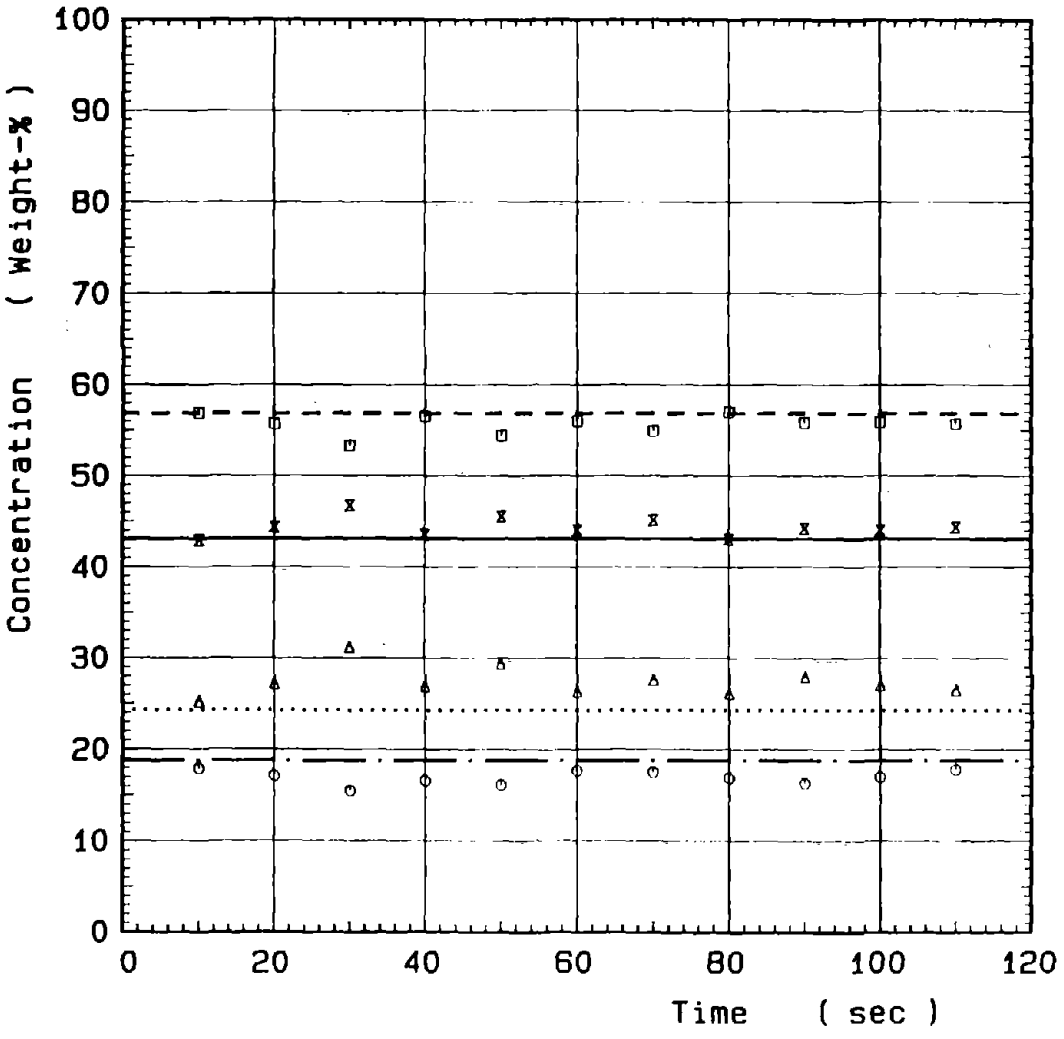

LOHBERG D/3-3

v = 4.0 m/s

	BF		SAI
Total	43.1 %	⧗	44.3 ± 1.0 %
Water	56.9 %	⧉	55.7 ± 1.0 %
Coal	24.3 %	△	27.6 ± 1.6 %
Refuse	18.8 %	⧉	17.0 ± 0.7 %

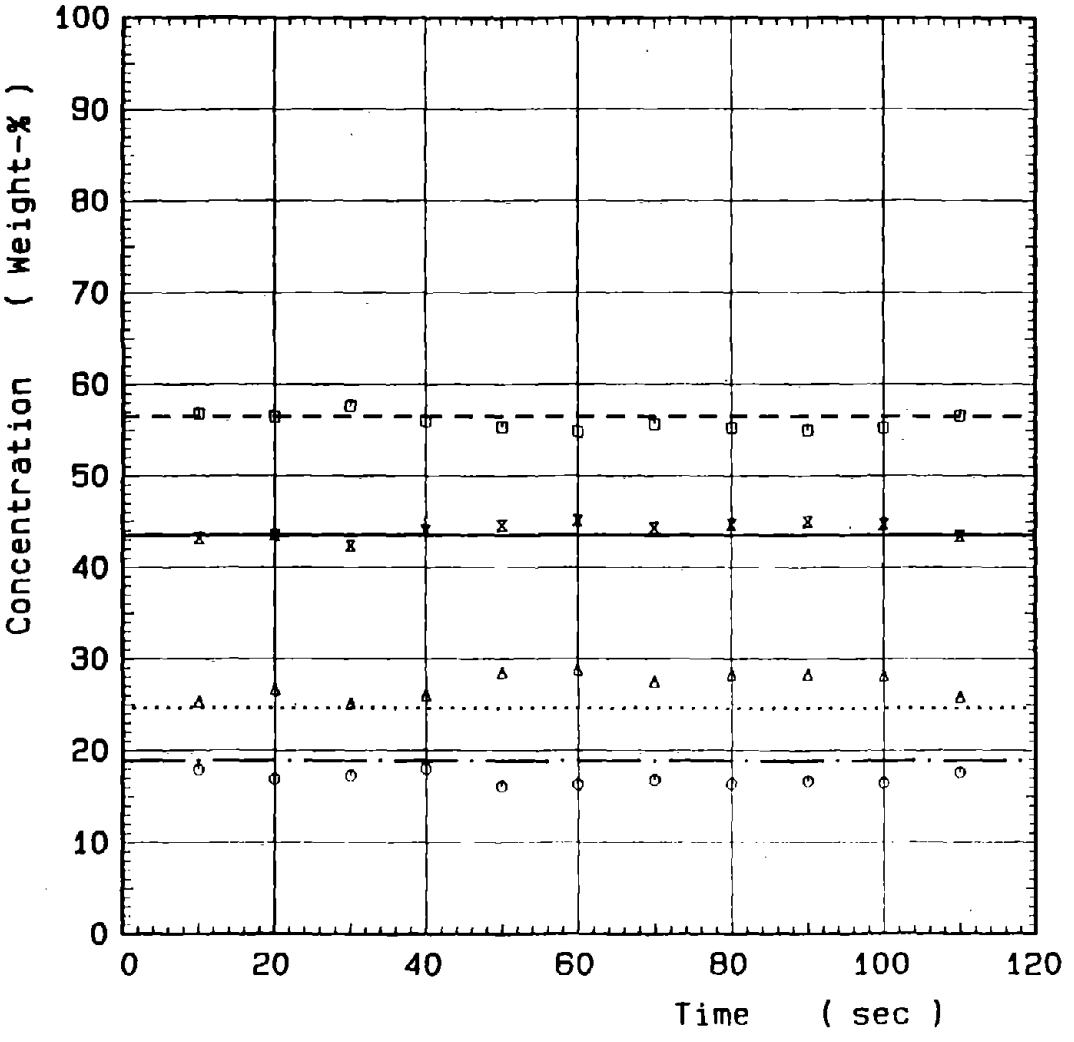

LOHBERG D/3-3

v = 4.5 m/s

	BF		SAI
Total	43.5 %	———	44.1 ± 0.8 %
Water	56.5 %	- - - - -	55.9 ± 0.8 %
Coal	24.6 %	·····	27.1 ± 1.3 %
Refuse	18.9 %	——·——	17.0 ± 0.6 %

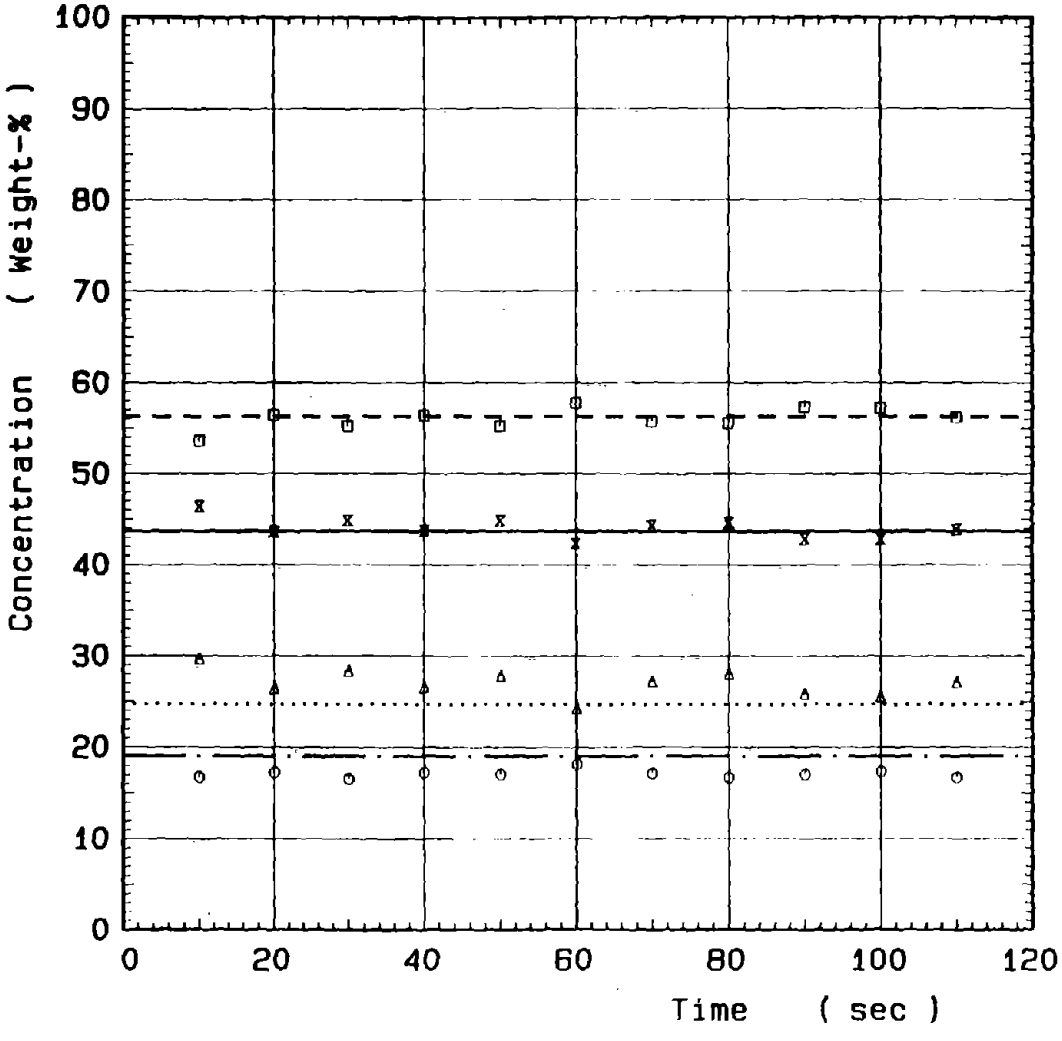

LOHBERG D/3-3

v = 5.0 m/s

		BF	SAI
Total	43.7 %	———	44.0 ± 1.1 %
Water	56.3 %	- - - - - -	56.0 ± 1.1 %
Coal	24.7 %	.....	27.0 ± 1.4 %
Refuse	19.0 %	—— ——	17.0 ± 0.4 %

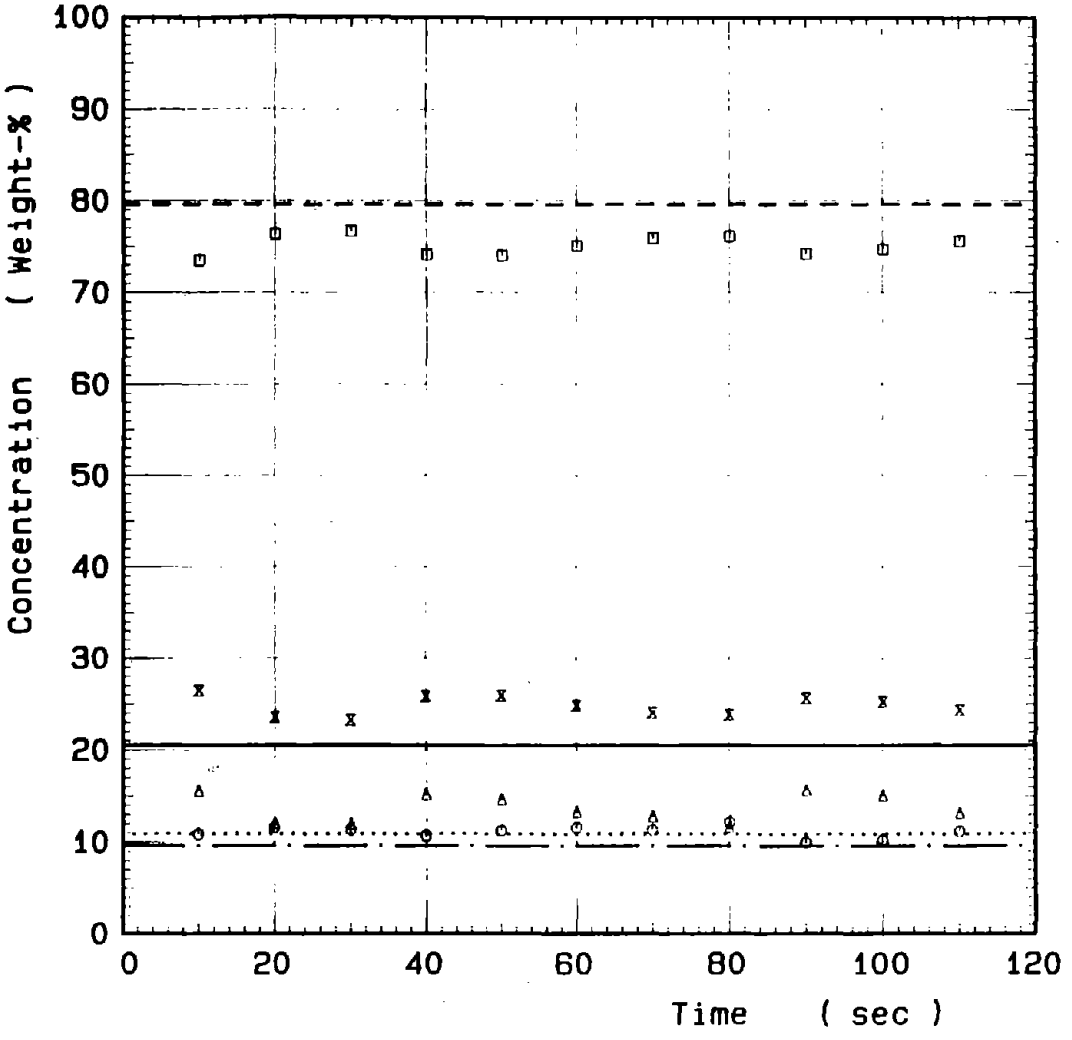

LOHBERG E/1

v = 3.5 m/s

		BF	SAI
Total	20.5 %	——·——·——	24.9 ± 1.0 %
Water	79.5 %	– – – – –	75.1 ± 1.0 %
Coal	10.9 %	· · · · ·	13.8 ± 1.5 %
Refuse	9.6 %	—— · ——	11.1 ± 0.6 %

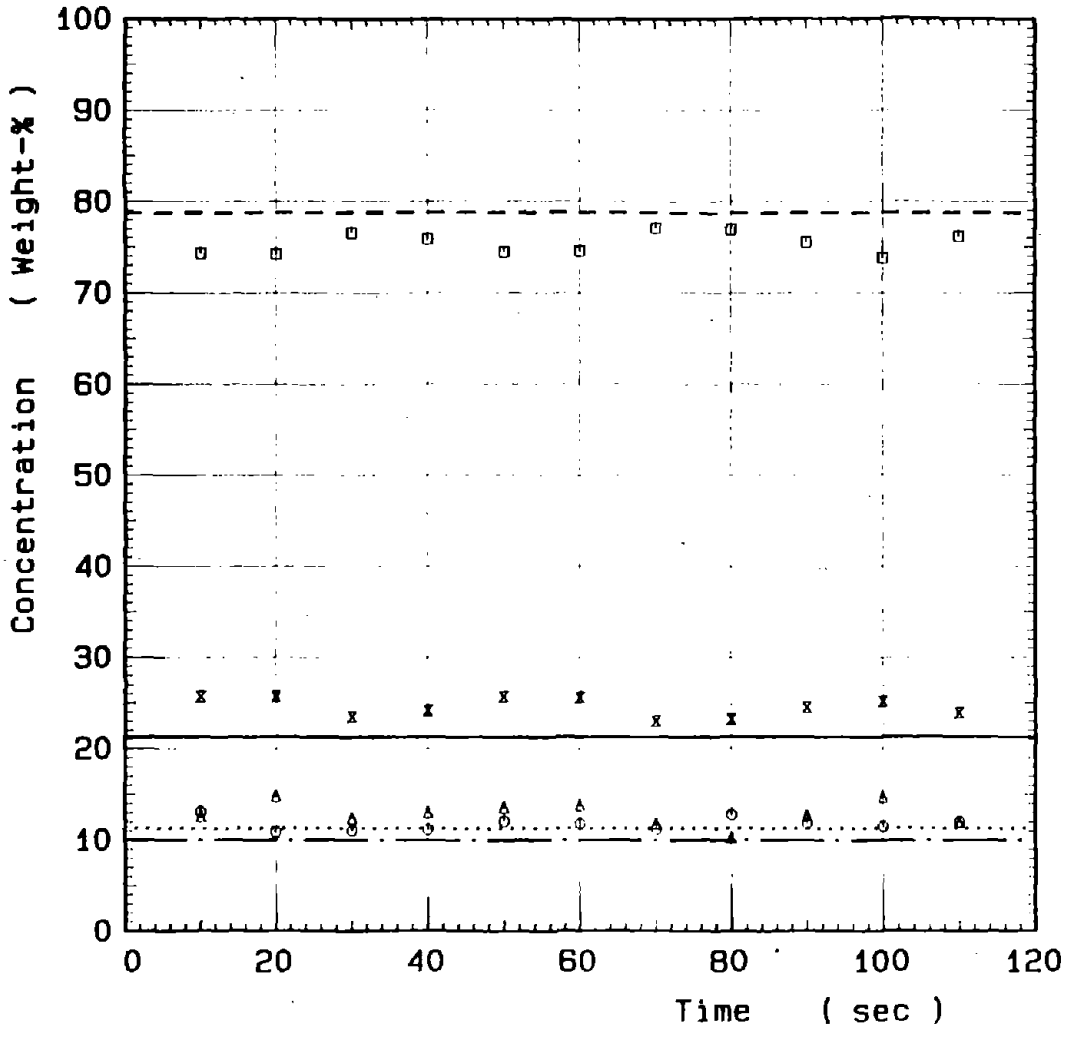

LOHBERG E/1
v = 4.0 m/s

		BF	SAI
Total	21.3 %	——— ———	24.6 ± 1.1 %
Water	78.7 %	– – – – – –	75.4 ± 1.1 %
Coal	11.3 %	· · · · · ·	12.9 ± 1.3 %
Refuse	10.0 %	——— · ——— ·	11.8 ± 0.6 %

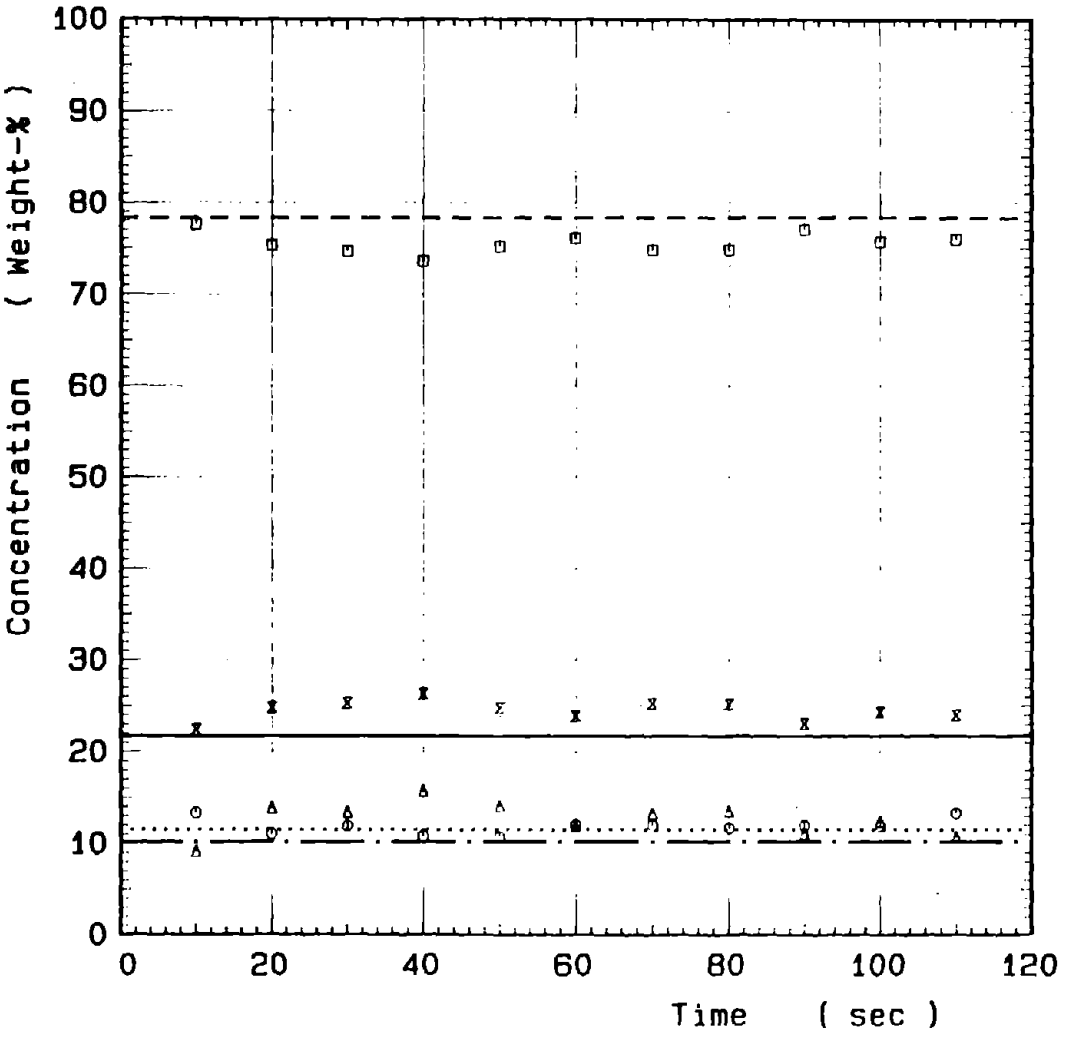

LOHBERG E/1

v = 4.5 m/s

	BF	SAI
Total	21.7 %	24.5 ± 1.1 %
Water	78.3 %	75.5 ± 1.1 %
Coal	11.5 %	12.6 ± 1.7 %
Refuse	10.2 %	11.8 ± 0.8 %

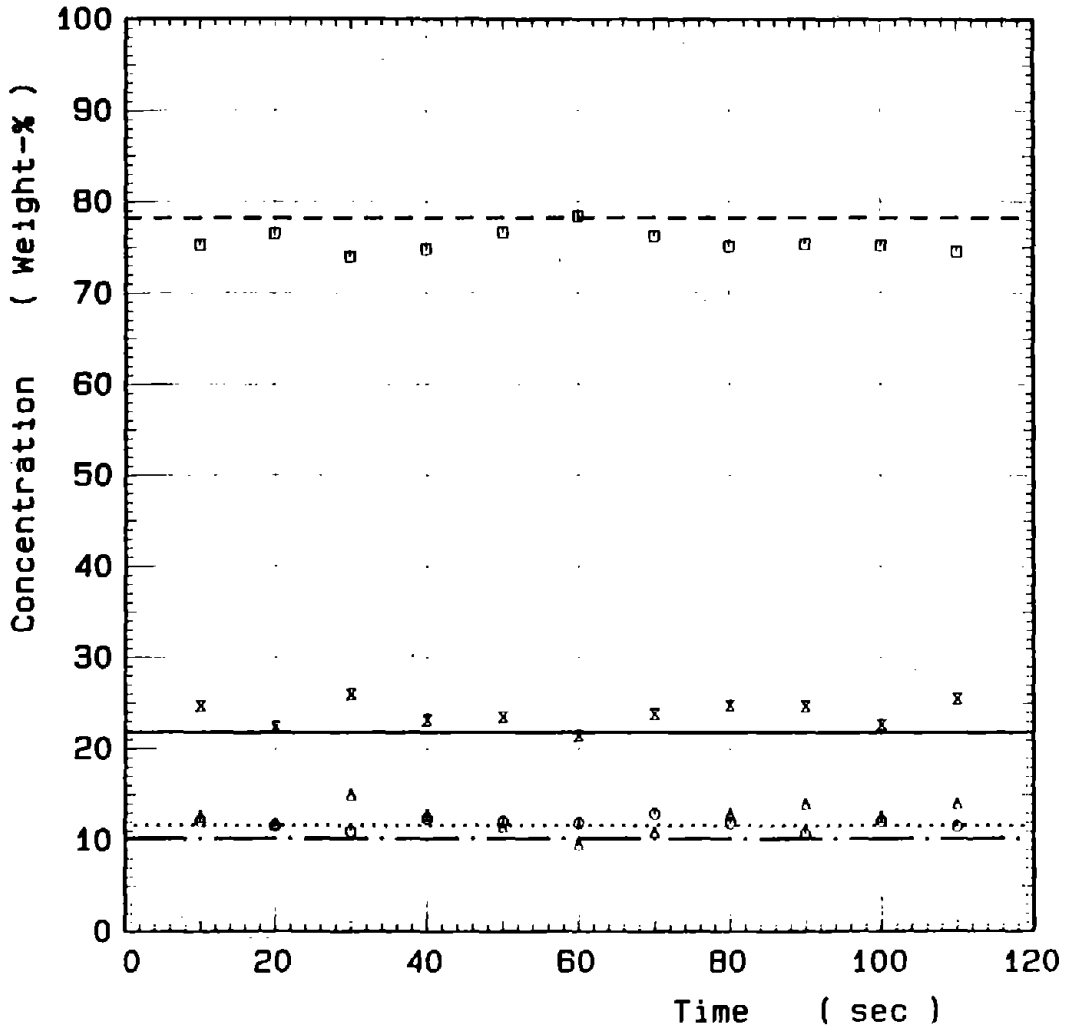

LOHBERG E/1

v = 5.0 m/s

		BF	SAI
Total	21.8 %	——	24.4 ± 1.2 %
Water	78.2 %	- - - - - -	75.6 ± 1.2 %
Coal	11.6 %	· · · · · ·	12.5 ± 1.5 %
Refuse	10.2 %	—— · ——	11.8 ± 0.6 %

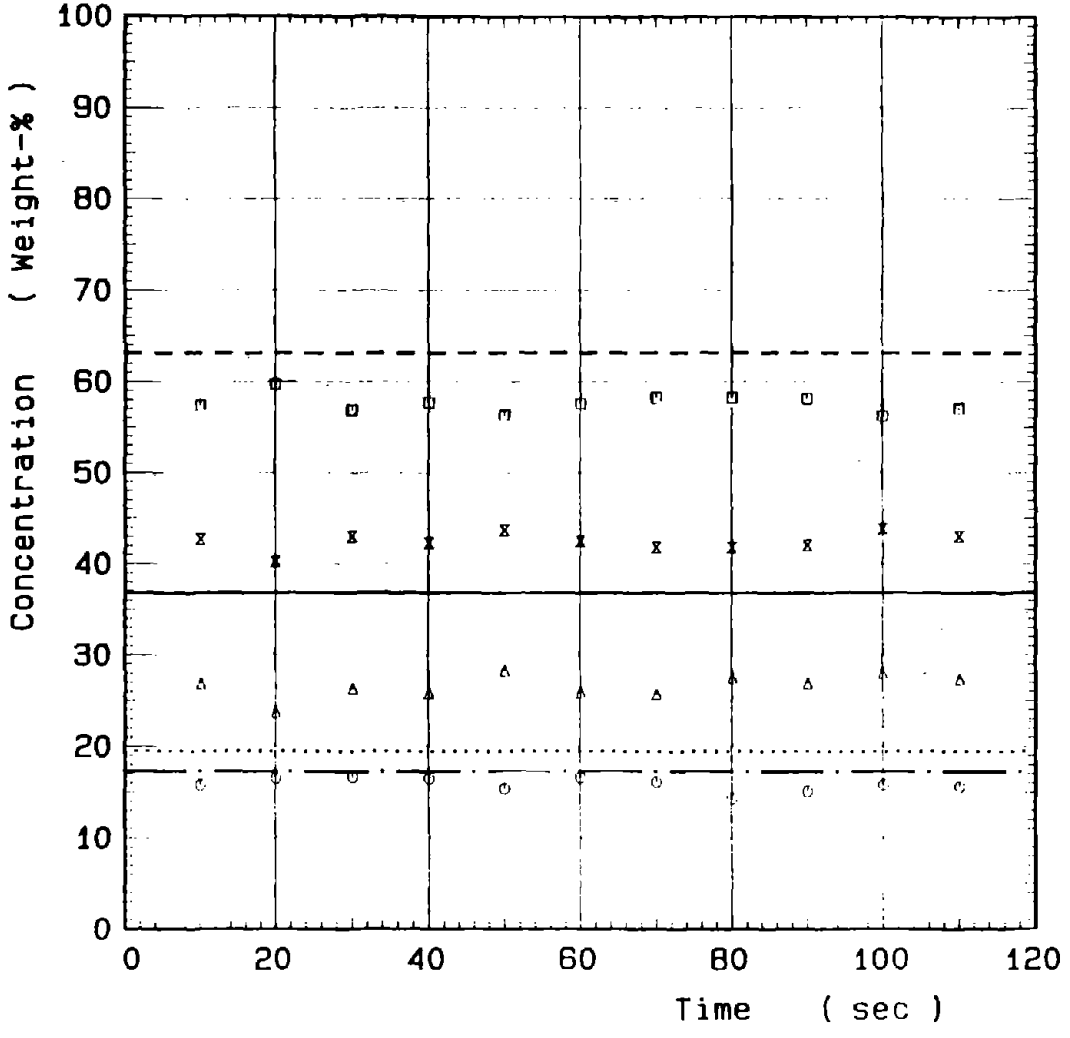

LOHBERG E/2
v = 3.5 m/s

		BF		SAI
Total	36.8 %	——— ··· ———	x	42.5 ± 1.0 %
Water	63.2 %	– – – – – –	□	57.5 ± 1.0 %
Coal	19.5 %	· · · · · ·	△	26.6 ± 1.2 %
Refuse	17.3 %	—·— ———	○	15.9 ± 0.7 %

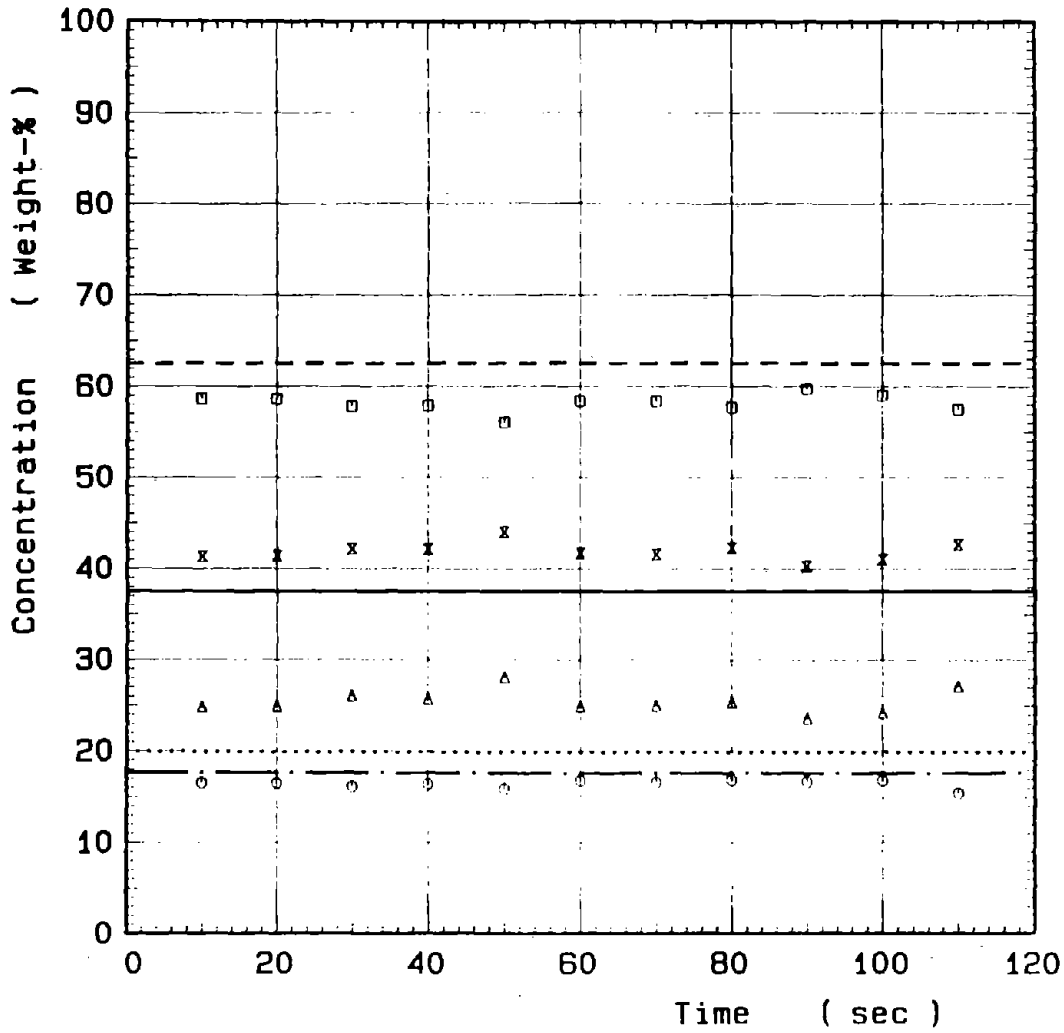

LOHBERG E/2
v = 4.0 m/s

		BF	SAI
Total	37.5 %		41.9 ± 0.9 %
Water	62.5 %		58.1 ± 0.9 %
Coal	19.9 %		25.4 ± 1.2 %
Refuse	17.6 %		16.4 ± 0.4 %

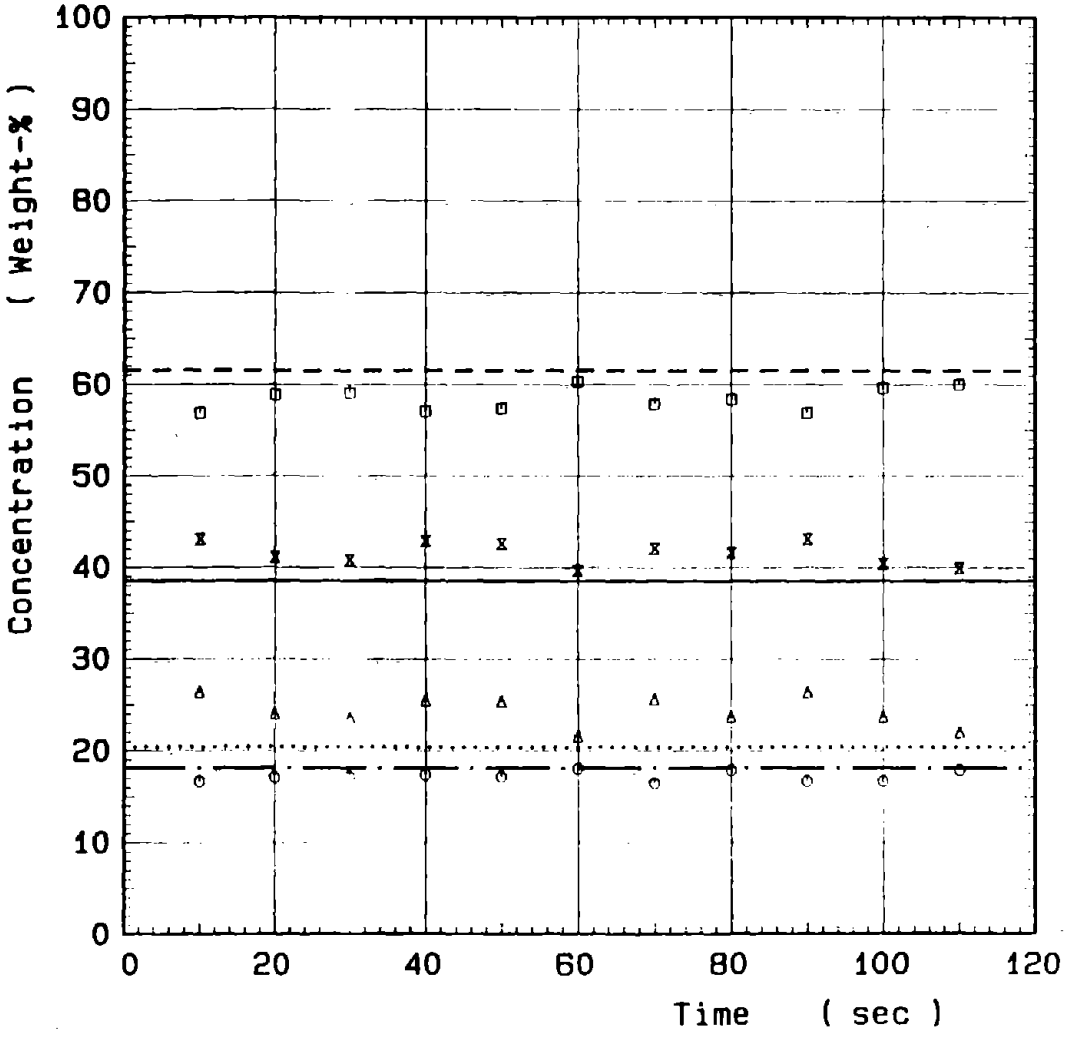

LOHBERG E/2

v = 4.5 m/s

	BF		SAI
Total	38.5 %	⧗	41.6 ± 1.2 %
Water	61.5 %	▯	58.4 ± 1.2 %
Coal	20.4 %	△	24.4 ± 1.6 %
Refuse	18.1 %	○	17.2 ± 0.5 %

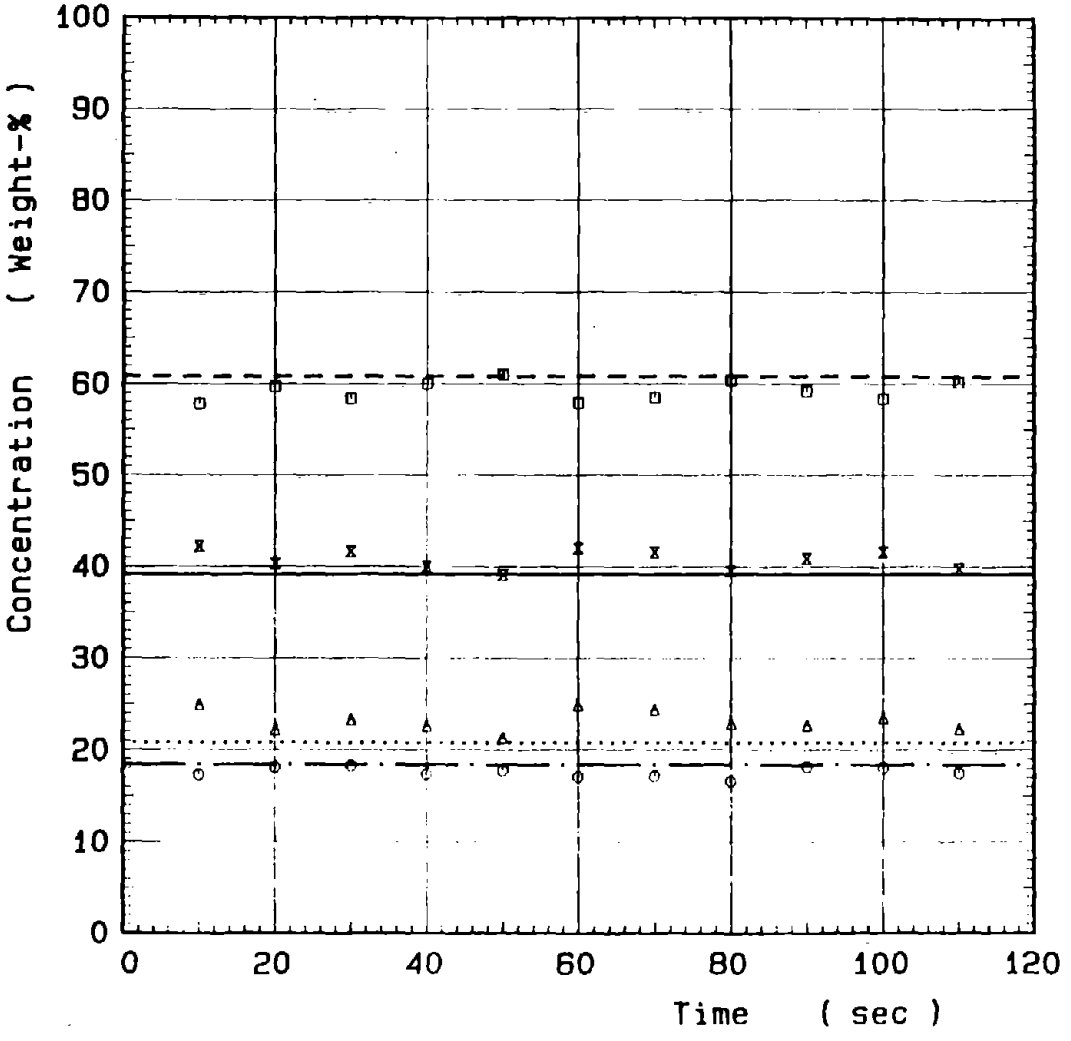

LOHBERG E/2
v = 5.0 m/s

		BF	SAI
Total	39.2 %		41.3 ± 1.3 %
Water	60.8 %		56.7 ± 1.3 %
Coal	20.8 %		23.6 ± 1.4 %
Refuse	18.4 %		17.7 ± 0.7 %

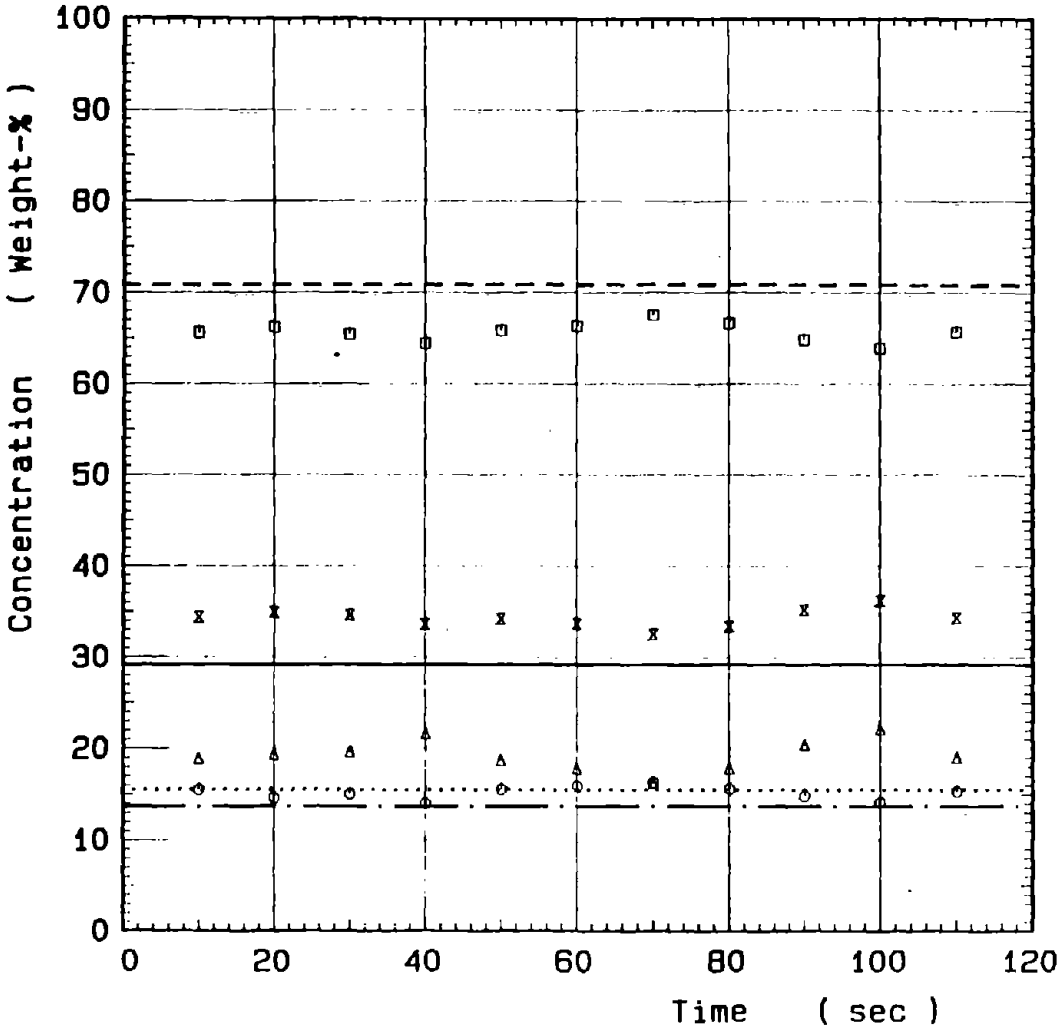

LOHBERG E/3-2

v = 3.5 m/s

	BF		SAI
Total	29.2 %	———	34.3 ± 1.0 %
Water	70.8 %	- - - - - -	65.7 ± 1.0 %
Coal	15.5 %	·····	19.2 ± 1.6 %
Refuse	13.7 %	——·——	15.1 ± 0.7 %

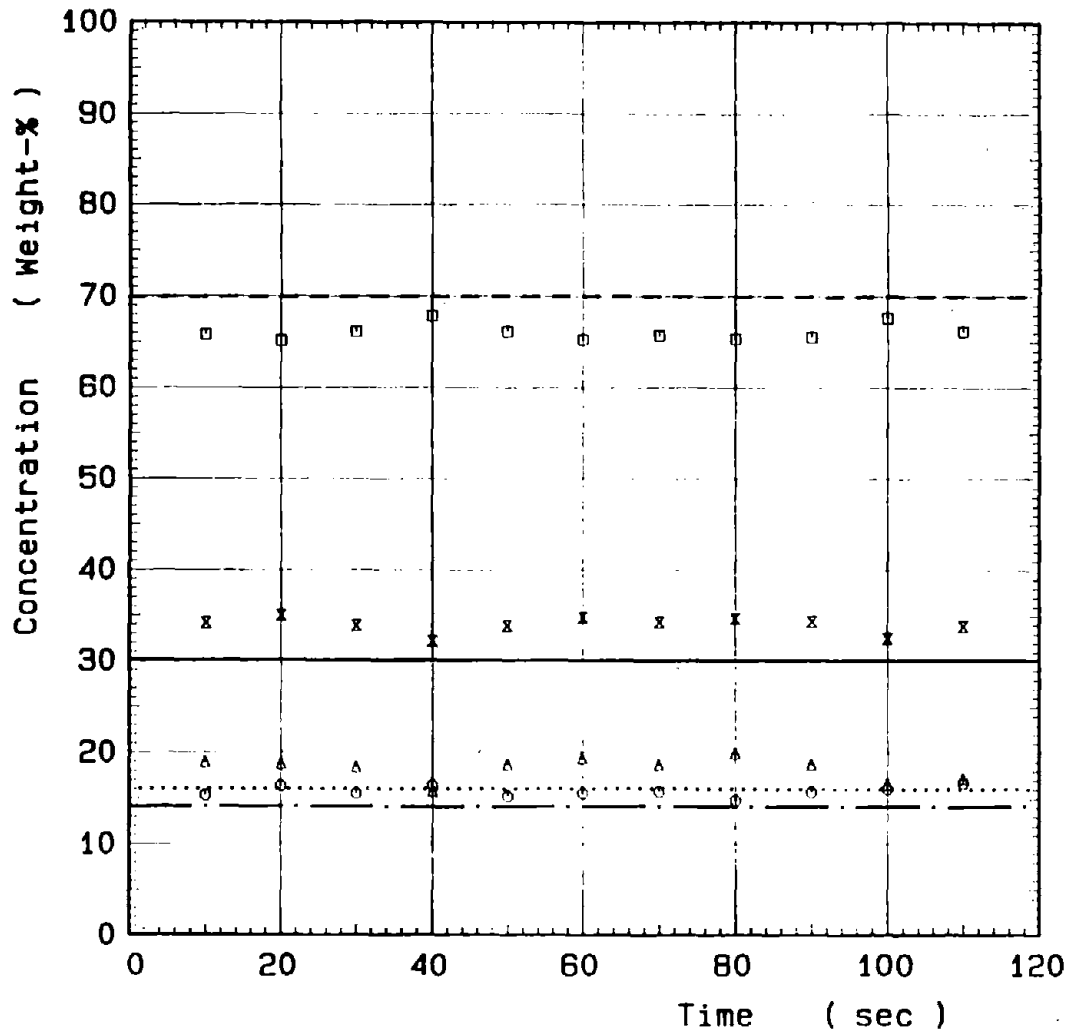

LOHBERG E/3-2

v = 4.0 m/s

		BF	SAI
Total	30.1 %	———	34.0 ± 0.9 %
Water	69.9 %	- - - - -	66.0 ± 0.9 %
Coal	16.0 %	·····	18.2 ± 1.2 %
Refuse	14.1 %	—— ——	15.7 ± 0.5 %

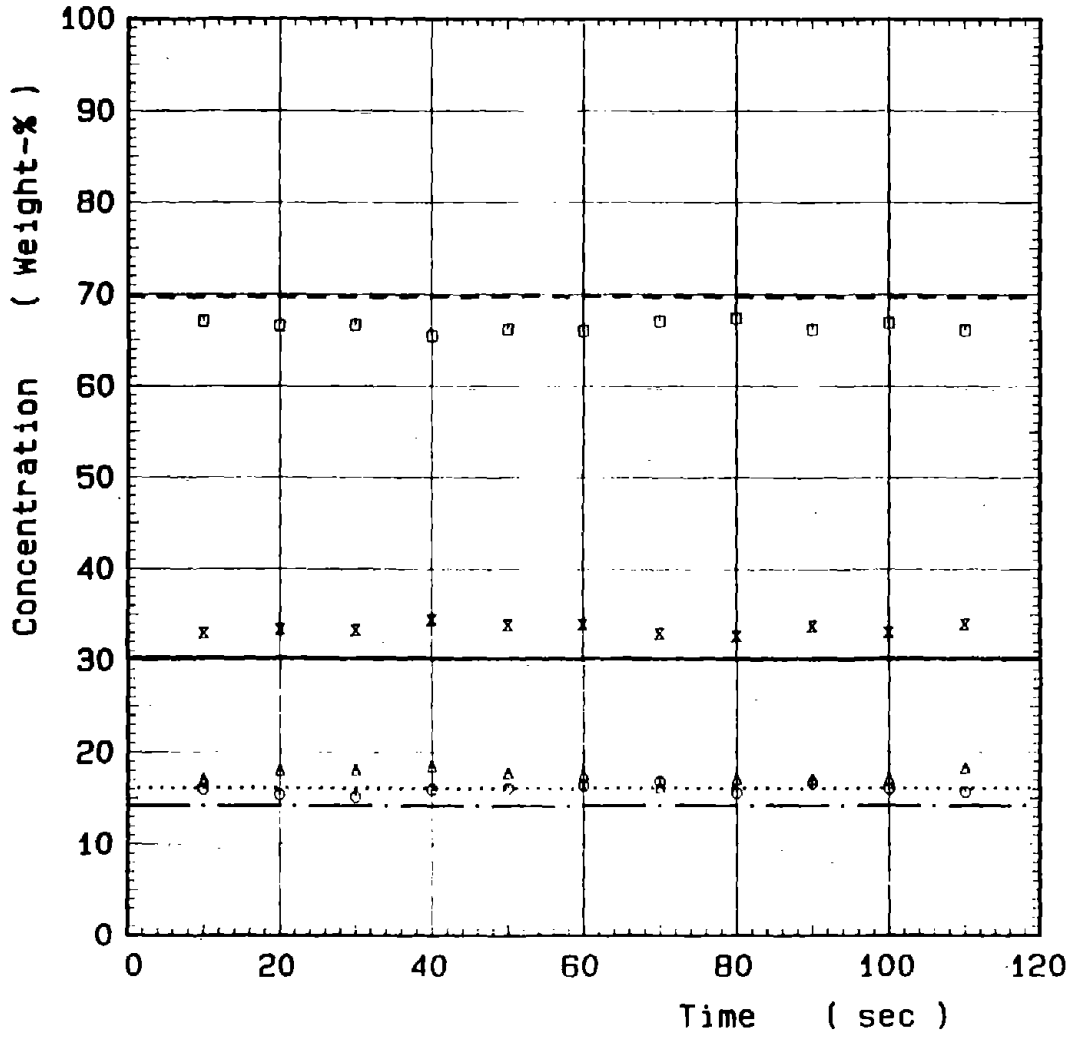

LOHBERG E/3-2

v = 4.5 m/s

		BF	SAI
Total	30.0 %	———	33.5 ± 0.5 %
Water	69.7 %	– – – –	66.5 ± 0.5 %
Coal	16.1 %	·····	17.5 ± 0.7 %
Refuse	14.2 %	——·——	16.0 ± 0.5 %

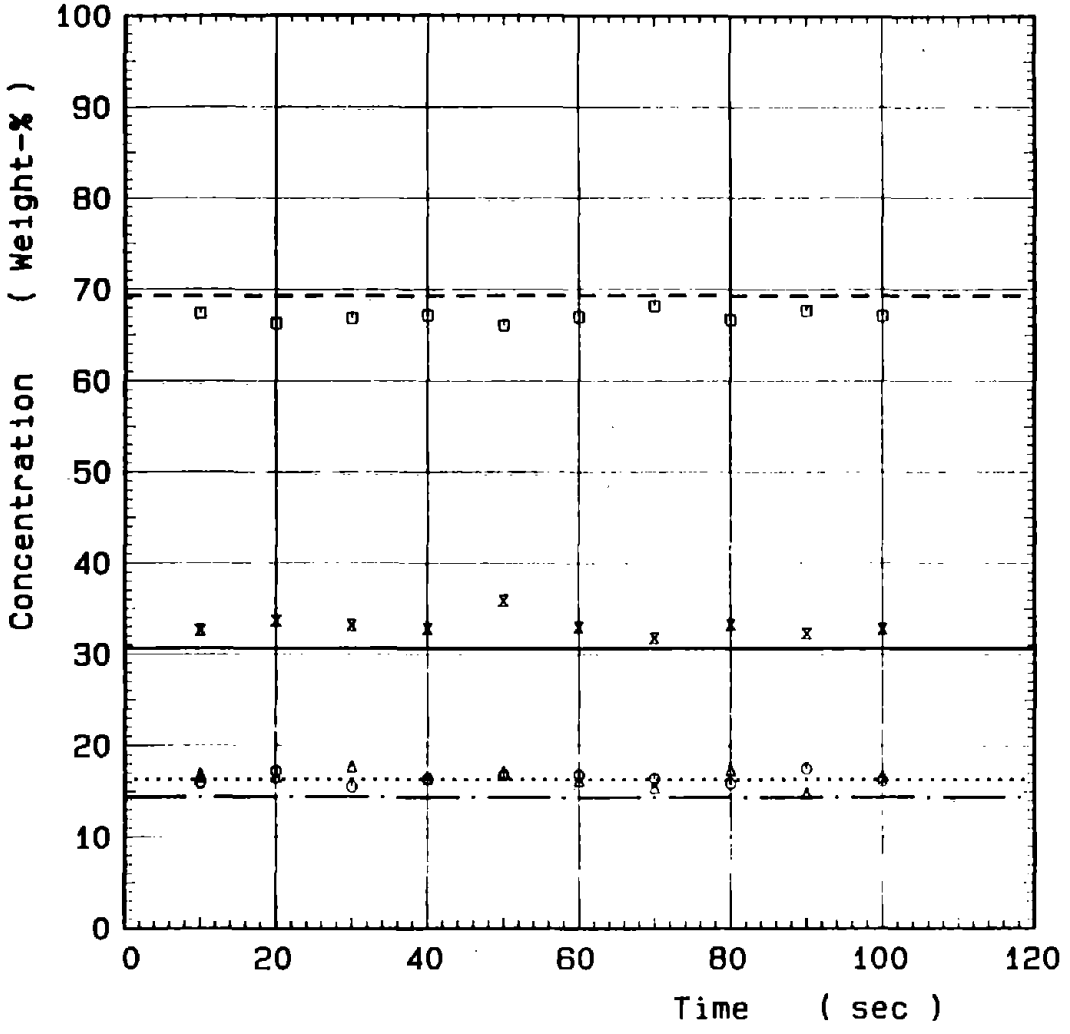

LOHBERG E/3-2

v = 5.0 m/s

	BF	SAI
Total	30.7 %	32.9 ± 0.6 %
Water	69.3 %	67.1 ± 0.6 %
Coal	16.3 %	16.5 ± 0.8 %
Refuse	14.4 %	16.4 ± 0.6 %

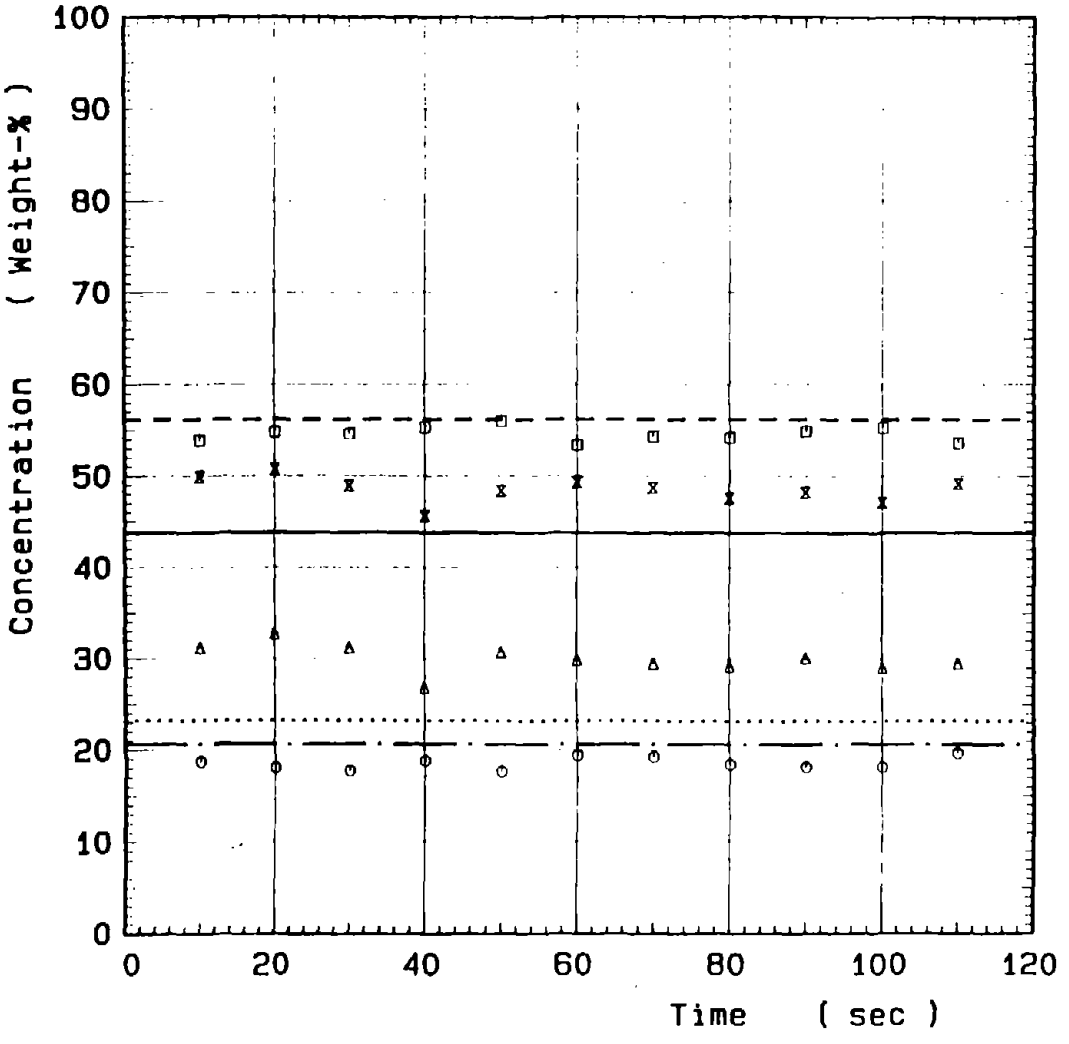

LOHBERG E/3-3

v = 3.5 m/s

	BF	SAI
Total	43.8 %	48.5 ± 1.3 %
Water	56.2 %	51.5 ± 1.3 %
Coal	23.2 %	30.0 ± 1.4 %
Refuse	20.6 %	18.5 ± 0.8 %

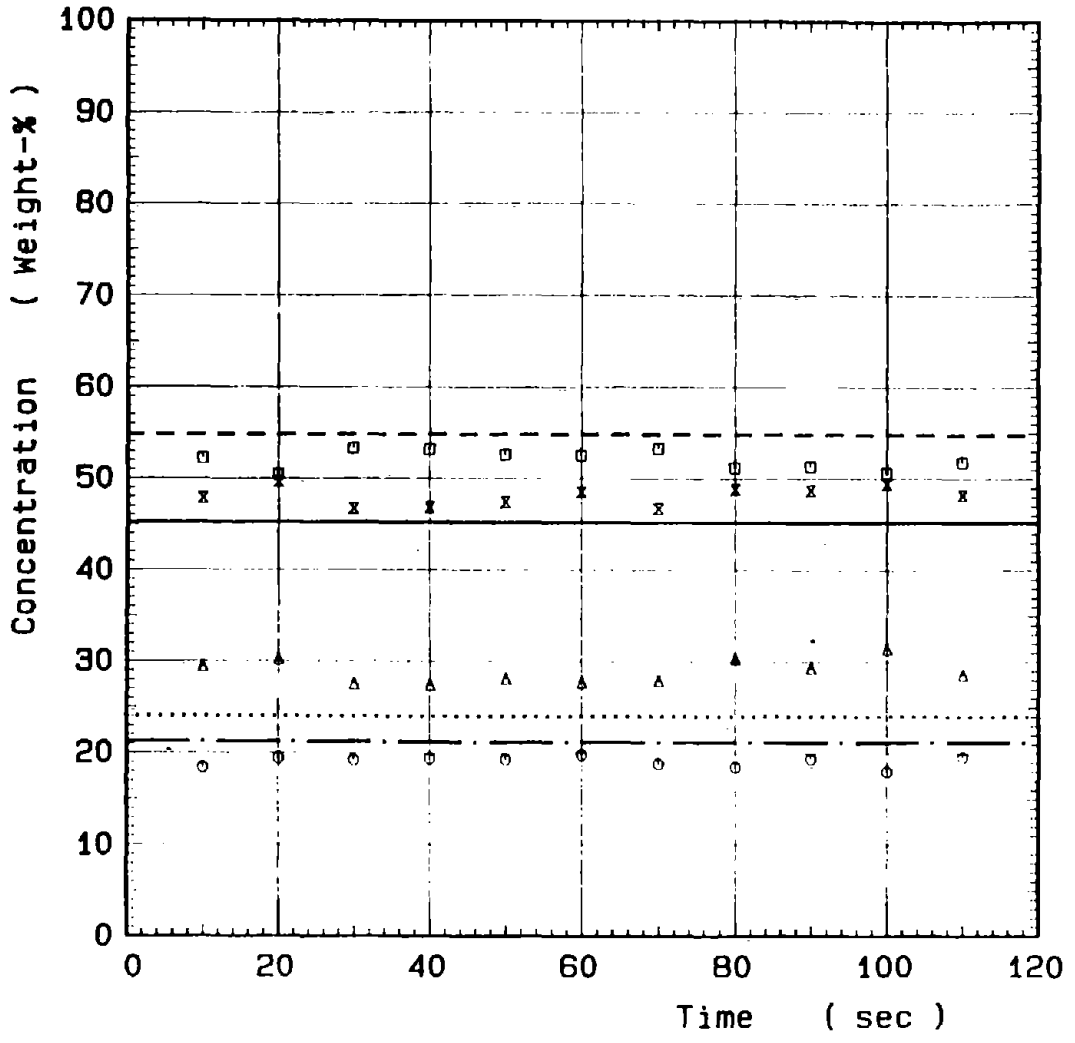

LOHBERG E/3-3

v = 4.0 m/s

		BF		SAI
Total	45.2 %	——	⧗	48.0 ± 1.0 %
Water	54.8 %	- - -	⧈	52.0 ± 1.0 %
Coal	24.0 %	·····	△	28.9 ± 1.3 %
Refuse	21.2 %	—·—	⊙	19.1 ± 0.5 %

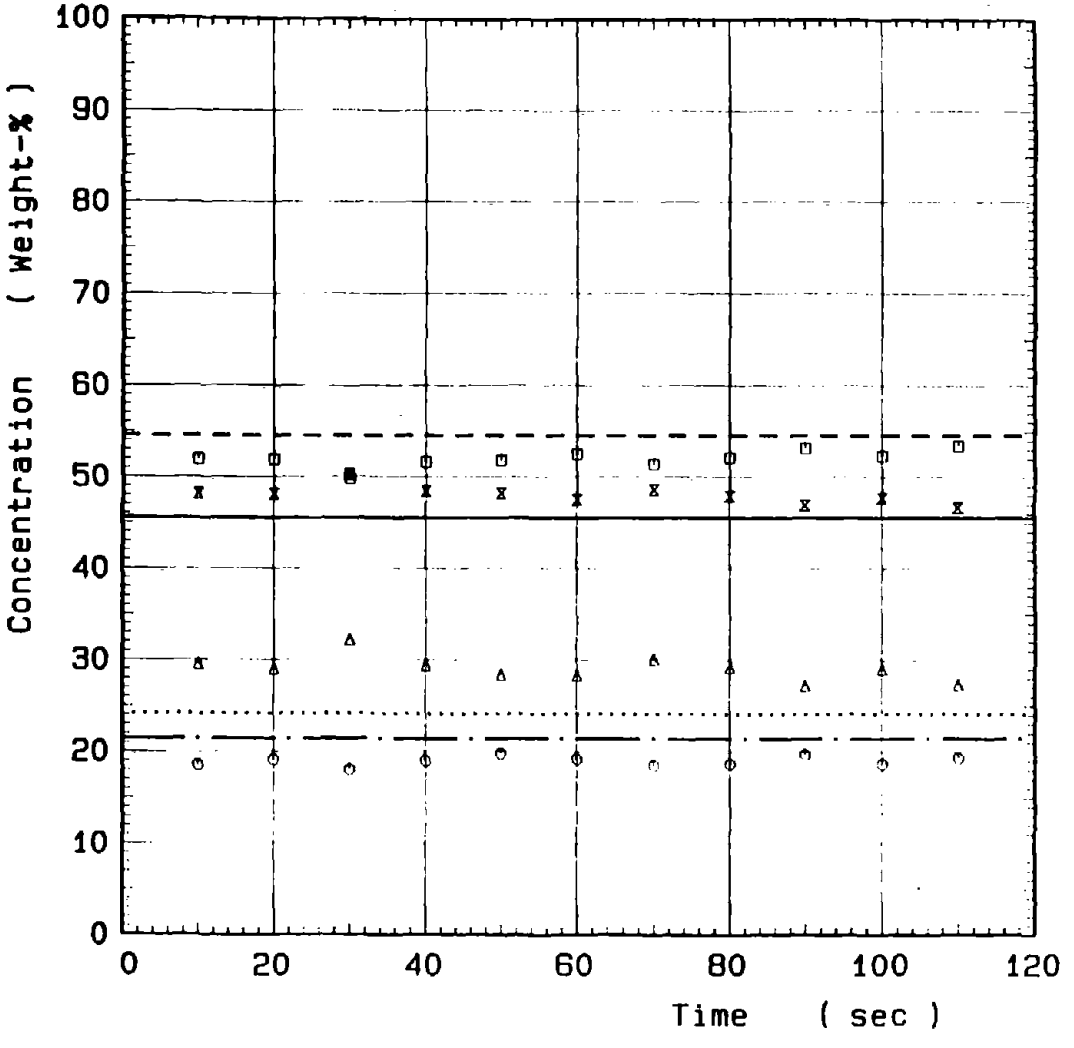

LOHBERG E/3-3

v = 4.5 m/s

		BF	SAI
Total	45.5 %	———	48.0 ± 0.9 %
Water	54.5 %	– – – – –	52.0 ± 0.9 %
Coal	24.1 %	·····	29.1 ± 1.3 %
Refuse	21.4 %	—— ——	18.9 ± 0.5 %

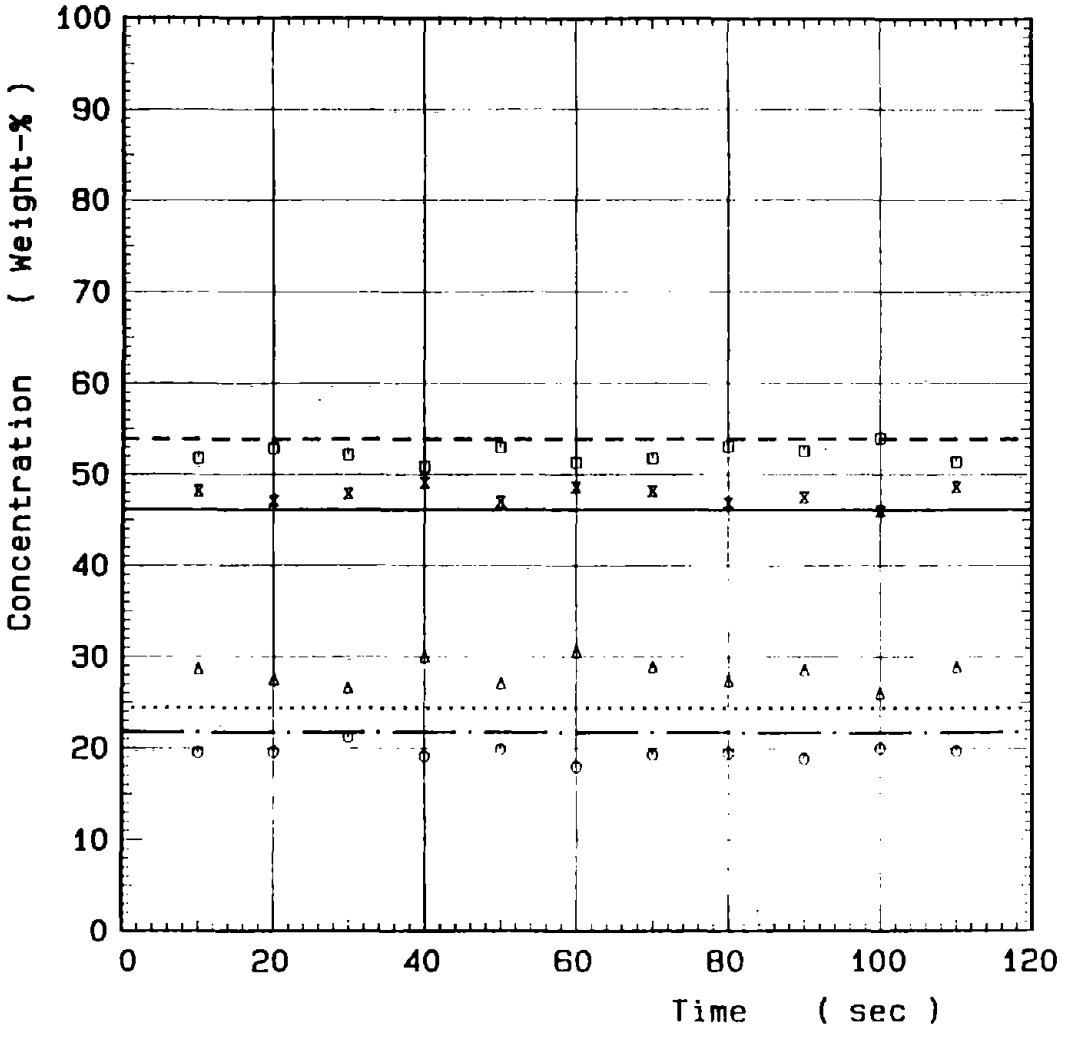

LOHBERG E/3-3

v = 5.0 m/s

	BF		SAI
Total	47.7 %	⧗	47.7 ± 0.9 %
Water	53.9 %	□	52.3 ± 0.9 %
Coal	24.4 %	△	28.2 ± 1.4 %
Refuse	21.7 %	○	19.5 ± 0.8 %

APPENDIX B

COAL/ROCK/WATER SLIPPAGE CALCULATIONS
(SLIPPAGE VERSUS PARTICLE SIZE AND SLURRY VELOCITY)

OBJECTIVE

The objective of this study is to predict the extent of measurement error inherent in a slurry flowmeter due to slippage between the conveying fluid and the solids being transported. Specifically, the conditions which were investigated were limited to upward vertical flow with coal/water and rock/water slurries.

Pipe diameters of 6 and 18 inches were specified. However, the slippage velocity is independent of pipe diameter and the calculated results should be valid for any pipe size with one proviso. Pipe diameter must be at least ten times greater than the largest particle size to avoid significant "wall effect." This constraint is of no concern for the operating conditions in this case.

Slurry concentration is a parameter of interest because the relationship between mean slurry velocity and mean solids velocity (or liquid velocity) is affected by the relative concentration of the solid and liquid components of the slurry. Results for slurry concentrations ranging from 10 to 50 wt % are presented in this report.

Nominal slurry velocities of 5, 10, 15, and 20 feet per second were used for both the coal and rock slurries. Specific gravities of 1.35 for coal and 2.75 for rock were assumed.

RESULTS

The calculated particle diameters for 1% and 2% error are given in Tables 1 and 2. Table 1 considers the more probable condition where the flowmeter measures solids velocity. The error exists because the mean slurry velocity always exceeds the measured solids velocity.

TABLE 1

PARTICLE SIZE WHICH YIELDS 1 % AND 2 % ERROR IN SLURRY VELOCITY

Mean Slurry Velocity Less Mean Velocity of Solids

$$(\bar{V} - V_s)/\bar{V}$$

Slurry Concentration, wt %	Slurry Velocity, ft/sec	Mean Particle Diameter, d, mm			
		1 % error		2 % error	
		coal	rock	coal	rock
10	5	0.365	0.147	0.610	0.230
	10	0.610	0.230	1.14	0.396
	15	0.870	0.310	1.74	0.580
	20	1.14	0.396	2.45	0.770
20	5	0.395	0.153	0.660	0.240
	10	0.660	0.240	1.24	0.420
	15	0.950	0.325	1.92	0.608
	20	1.24	0.420	2.73	0.820
30	5	0.420	0.160	0.725	0.252
	10	0.725	0.252	1.40	0.448
	15	1.06	0.346	2.23	0.660
	20	1.40	0.448	3.20	0.890
40	5	0.460	0.171	0.810	0.273
	10	0.810	0.273	1.61	0.492
	15	1.20	0.380	2.59	0.740
	20	1.61	0.492	3.82	1.00
50	5	0.615	0.185	0.925	0.300
	10	0.925	0.300	1.88	0.555
	15	1.38	0.425	3.06	0.840
	20	1.88	0.555	4.60	1.16

TABLE 2

PARTICLE SIZE WHICH YIELDS 1 % AND 2 % ERROR IN SLURRY VELOCITY

Mean Liquid Velocity Less Mean Slurry Velocity

$$(V_l - \overline{V}) / \overline{V}$$

Slurry Concentration, wt %	Slurry Velocity, ft/sec	Mean Particle Diameter, d, mm			
		1 % error		2 % error	
		coal	rock	coal	rock
10	5	4.35	2.63	>10	7.50
	10	>10	7.50	>10	>10
	15	>10	>10	>10	>10
	20	>10	>10	>10	>10
20	5	1.75	0.980	4.18	2.28
	10	4.18	2.28	>10	6.25
	15	7.60	4.00	>10	>10
	20	>10	6.25	>10	>10
30	5	1.10	0.560	2.32	1.18
	10	2.32	1.18	5.95	2.82
	15	3.95	1.93	>10	5.20
	20	5.95	2.82	>10	8.40
40	5	0.800	0.390	1.62	0.750
	10	1.62	0.750	3.80	1.68
	15	2.60	1.18	6.75	2.85
	20	3.80	1.68	>10	4.35
50	5	0.650	0.295	1.23	0.540
	10	1.23	0.540	2.75	1.12
	15	1.95	0.810	4.80	1.82
	20	2.75	1.12	7.30	2.66

Table 2 considers the less probable condition where the flowmeter measures liquid velocity. In this case the error exists because the mean slurry velocity is always less than the measured liquid velocity.

DISCUSSION

The slip velocity of a slurry in vertical flow is a result of two opposing forces. For a slurry with solids which are denser than the conveying liquid, there exists a downward acting gravitational force on the solid particles. At the same time there is an upward force exerted on the particles due to their drag in the upward flowing liquid stream. At some liquid velocity these forces cancel each other and the solids remain suspended. This velocity is the slip velocity. As liquid velocity is increased, the solids are transported upwards. The liquid velocity will always exceed the solids velocity by the slip velocity to maintain the force balance.

The gravitational force on a sphere is defined as follows:

$$F_g = \pi d^3 g (\rho_s - \rho_l) / 6$$

where d = particle diameter

g = gravitational acceleration

ρ_s = solids density

ρ_l = liquid density

The drag force on a sphere is defined as follows:

$$F_d = \pi d^2/4 \times C_d \times \rho_l V^2/2$$

where C_d = drag coefficient

V = relative liquid velocity

When solids are being transported vertically by the liquid the relative

liquid velocity is the slip velocity, $V_l - V_s$,

where V_l = liquid velocity

V_s = solids velocity

Combining equations:

$$(V_l - V_s)^2 = \frac{4\,g\,d}{3\,C_d} \times (\rho_s - \rho_l / \rho_l)$$

For particles other than spheres a shape factor is introduced to the equation. This adjustment factor has been ignored. Thus the calculated particle diameters in this report are effective spherical diameters.

The drag coefficient, C_d, is a function of the particle Reynolds number.

$$N_{re} = d\,\rho_l\,(V_l - V_s) / \mu$$

where μ = liquid viscosity

For small particles, Stokes law applies while for large particles, Newtons law is dominant. For the conditions of this study, neither law can be ignored and the subsequent transition region is best described by several empirical equations:

For N_{re} less than 500; $C_d = 24/N_{re}\,(1 + .15\,N_{re}^{.687})$

For N_{re} between 500 and 10^5; $C_d = 24/N_{re}\,(1 + .15\,N_{re}^{.687}) + \frac{.42}{1 + 42500\,N_{re}} - 1.16$

These equations have been used to generate Table 3 and Figure 1. The only other equation needed to compare the liquid velocity, V_l and the solid velocity, V_s, to the mean slurry velocity, $\bar{V}$, is the continuity equation:

$\bar{V}$ = (V_s x (vol. frac. solids in slurry)) + (V_l x (vol. frac. liquid in slurry))

where $\bar{V}$ = mean slurry velocity

The equations used to calculate slip velocity do not address particle size distribution. These equations assume a uniform or weight mean diameter as the representative particle diameter. The weight mean diameter

TABLE 3

PARTICLE SIZES FOR VARIOUS SLIP VELOCITIES

SOLIDS: COAL; ρ_s = 1.35 g/ml

ROCK: ρ_s = 2.75 g/ml

LIQUID: WATER; ρ_l = 1.0 g/ml

μ = 1.0 cps

	SOLID					
	COAL			ROCK		
$V_l - V_s$, ft/sec	N_{re}	C_d	d, mm	N_{re}	C_d	d, mm
0.001	0.01	1980	0.040	0.01	4410	0.018
0.005	0.14	180	0.091	0.06	398	0.040
0.01	0.40	64.7	0.131	0.18	142	0.058
0.05	5.2	6.75	0.342	2.2	13.9	0.142
0.10	17	2.84	0.576	6.8	5.50	0.223
0.50	451	0.59	2.96	143	0.93	0.941
1.0	2430	0.39	7.98	652	0.53	2.14
5.0	---	---	---	75900	0.49	49.8

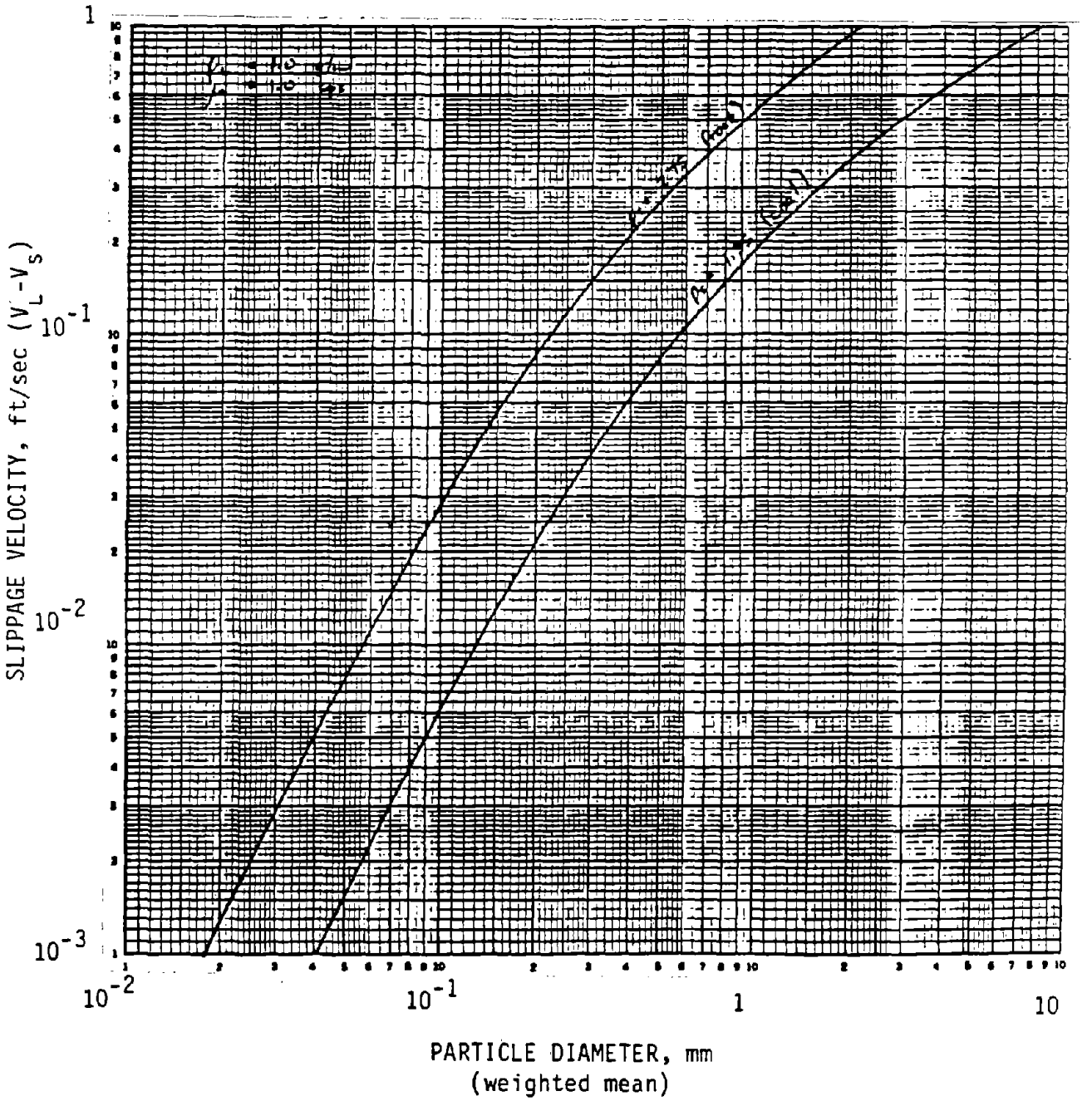

FIGURE 1. - Slip velocities as a function of particle size.

is defined as follows:

$$d = \Sigma(\text{particle diameter}_i \times \text{weight fraction}_i)$$

Thus the calculated slip velocity for a slurry with a typical broad size distribution is no different than for a slurry with a uniform particle diameter equal to the weight mean diameter of the broad sized distribution.

As an example, from Table 1, for a 30 wt % coal slurry at 15 ft/sec, a 1 % error exists between the mean slurry velocity, $\bar{V}$, and the mean solids velocity, V_s, if the particle diameter is 1.06 mm. A slurry with the following size distribution has a 1.06 mm weight mean diameter and would meet the 1 % error criterion:

Mesh size	Wt % retained
4	3.0
8	9.0
16	22.0
35	30.0
100	16.0
200	9.0
325	7.0
pan	4.0
	100.0

weight mean diameter = 1.06 mm

For a flowmeter which measures the mean velocity of the solids in a slurry, V_s, the mean slurry velocity, $\bar{V}$, is greater and the meter error is as follows:

$$\% \text{ error} = 100 \left(\frac{\bar{V} - V_s}{\bar{V}} \right)$$

The results of these calculations are in Figures 2 and 3. Note that for a given velocity and particle size the error decreases with increasing slurry concentration.

If a flowmeter which measures mean liquid velocity were used, the slurry velocity would be less than the measured velocity. The error

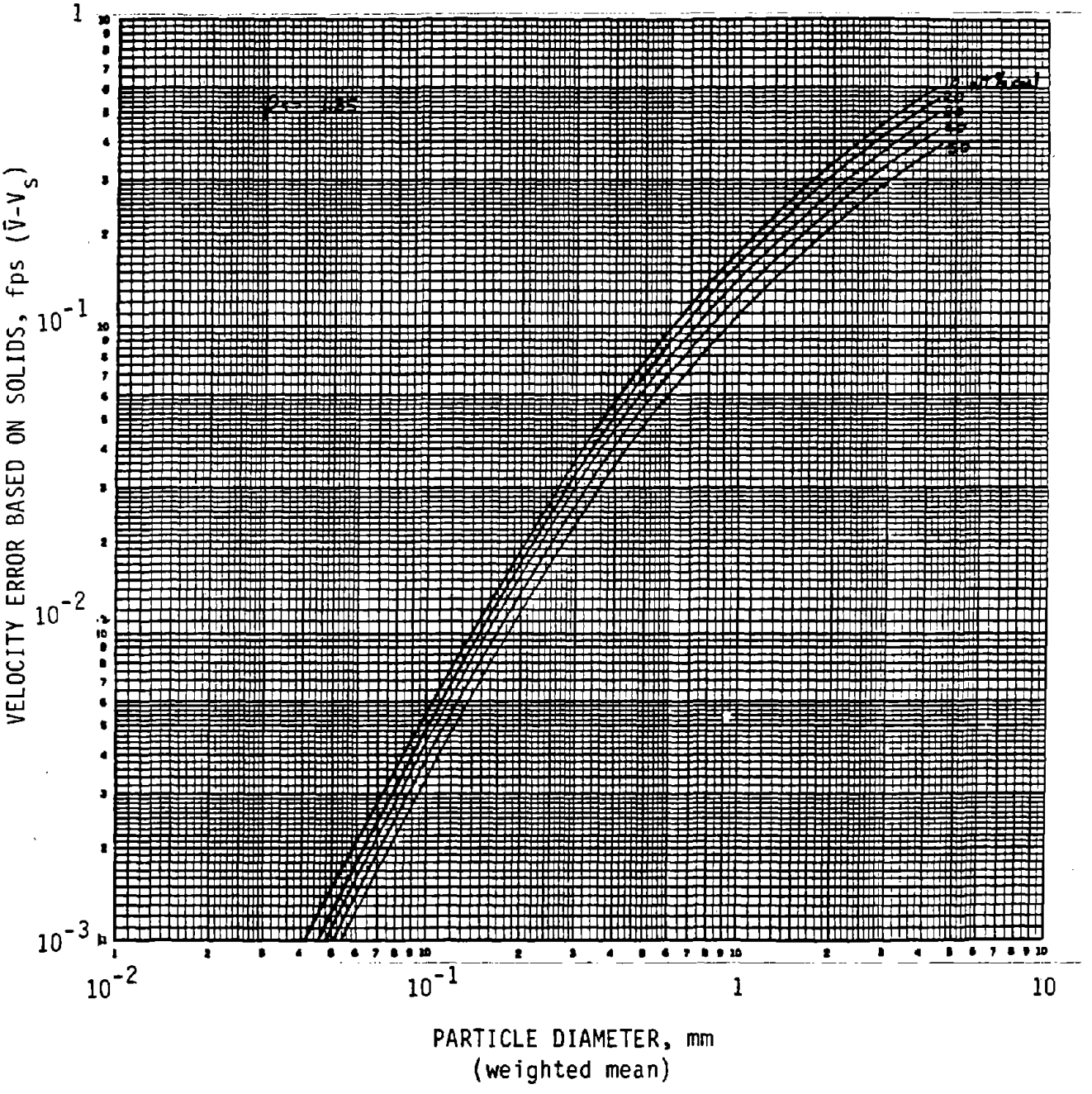

FIGURE 2. - Slurry velocity error based on solids velocity coal slurry.

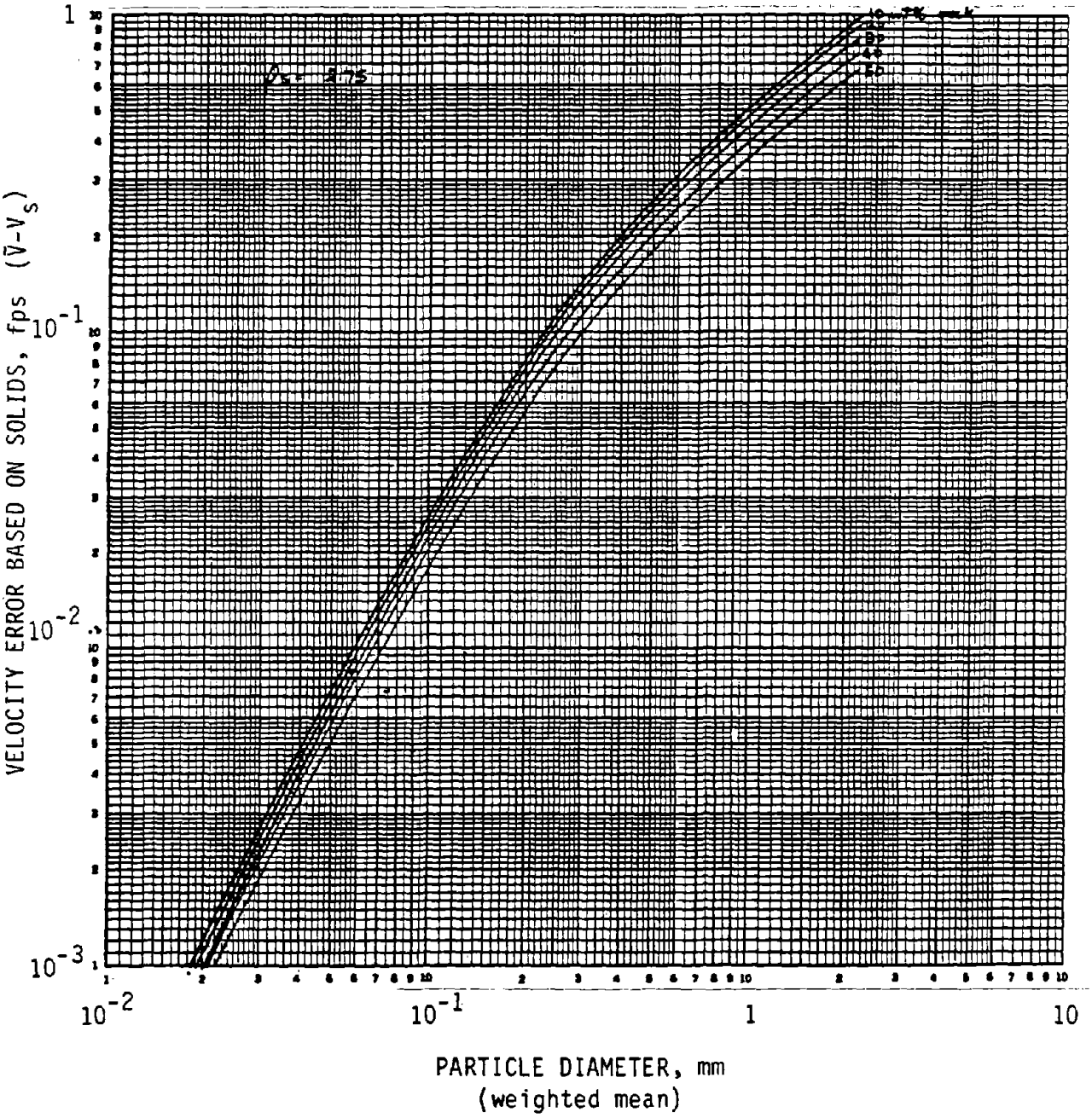

FIGURE 3. - Slurry velocity error based on solids velocity rock slurry.

would be as follows:

$$\% \text{ error} = 100 \left(\frac{V_1 - \bar{V}}{\bar{V}} \right)$$

The results of these calculations are in Figures 4 and 5. Note that for this case the effect of slurry concentration is reversed. That is, for a given velocity and particle size the error increases with increasing slurry concentration.

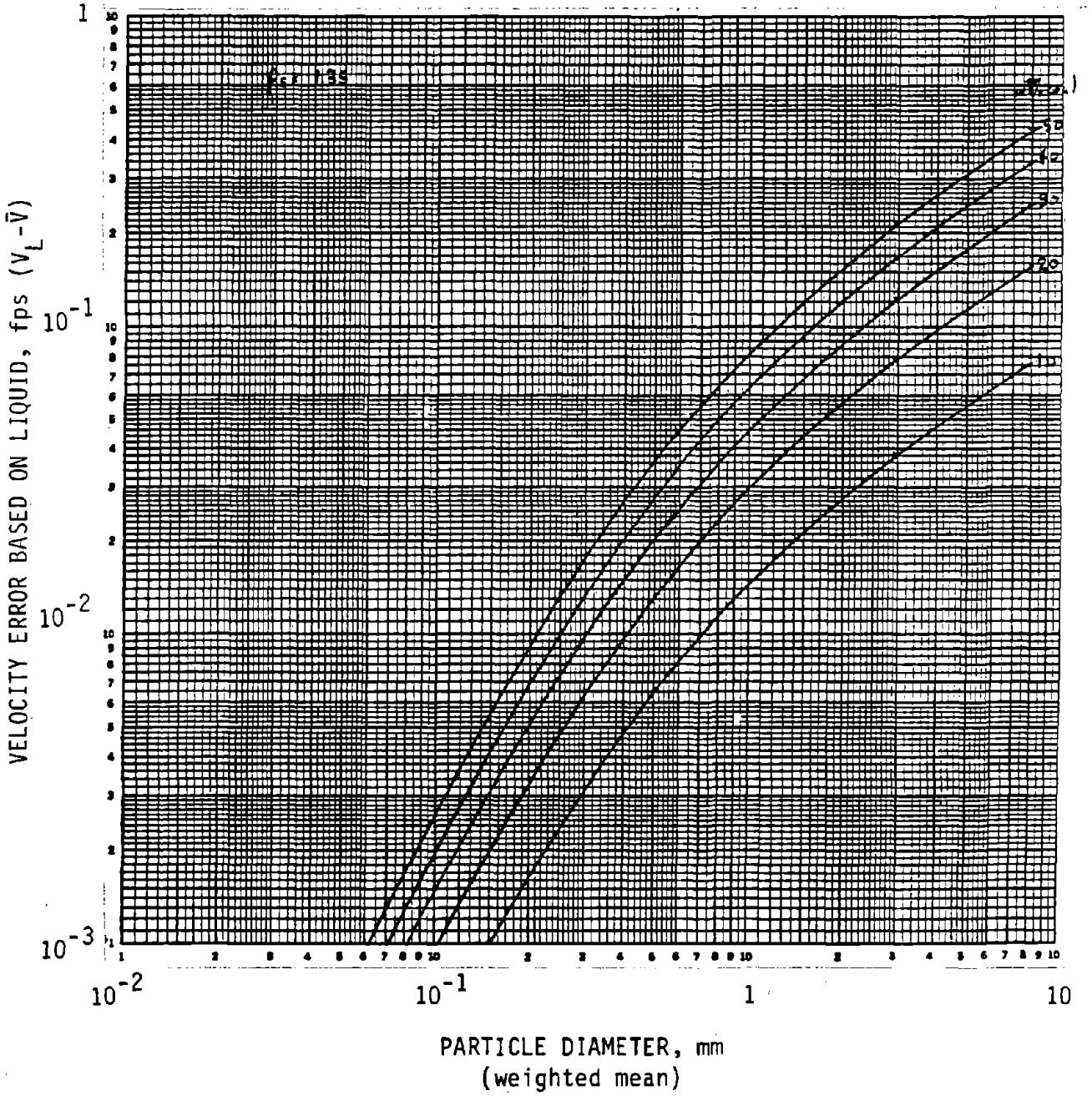

FIGURE 4. - Slurry velocity error based on liquid velocity coal slurry.

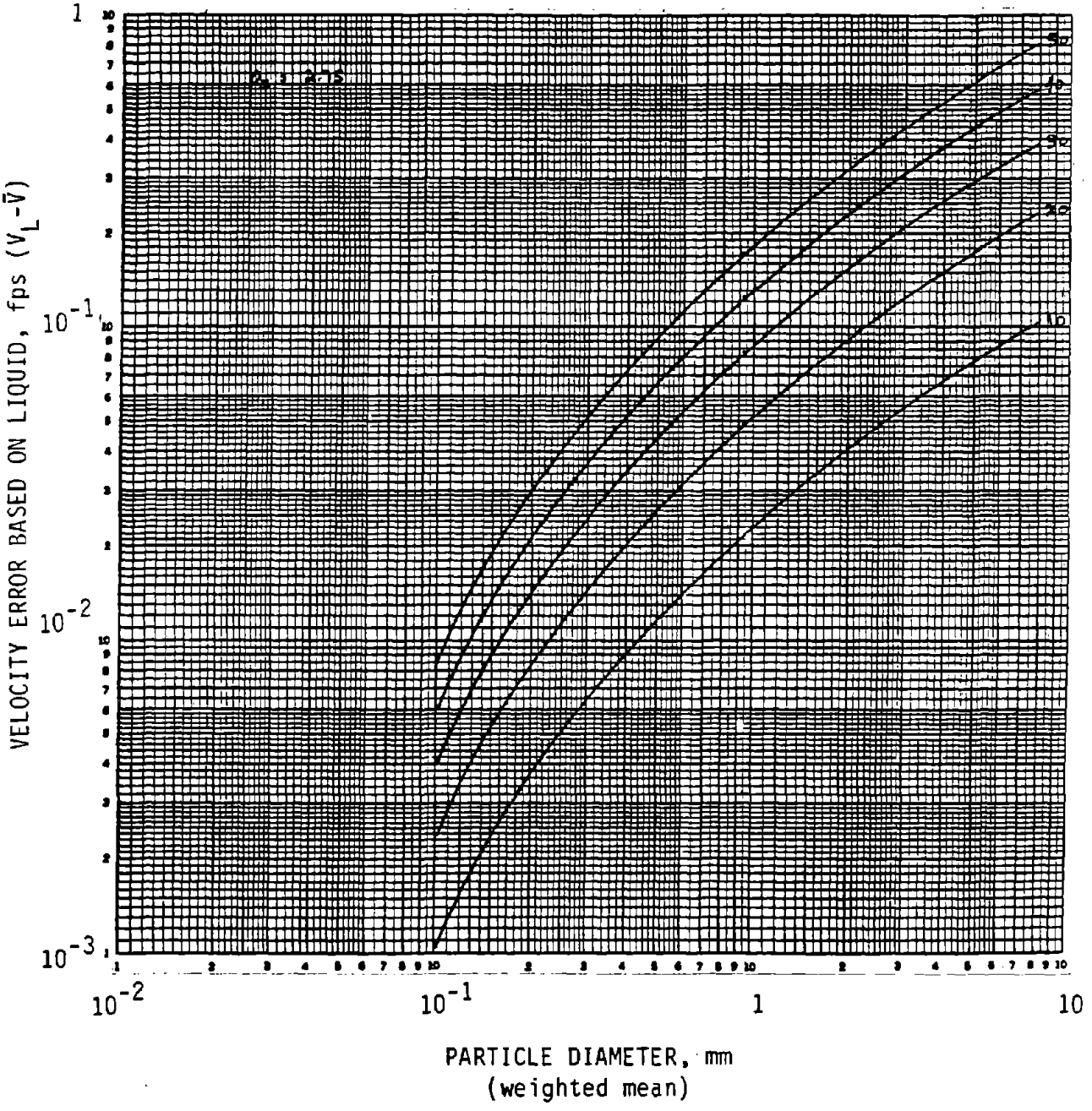

FIGURE 5. - Slurry velocity error based on liquid velocity rock slurry.

February 22 1982

6025 S. Meadowbrook Drive
Morrison CO 80465

Dr. Victor Verbinski
Science Applications Inc.
10401 Roselle St.
San Diego CA 92121

Dear Vic:

As per our phone conversation I have prepared an addendum to my report of January 29 1982 on particle slippage calculations. Specifically I have addressed two problems:

1. Convert solid/liquid slippage velocities to errors in measured slurry concentration.

2. Correlate crushed coal particle size distributions data to define any relationship between weight mean particle diameter and maximum particle size.

Table 4 summarizes the calculated weight mean particle diameter for 1 % and 2 % error in measured slurry concentration. Both absolute and relative errors have been considered. As before, slurry concentrations range from 10 to 50 wt %, and liquid velocities of 5, 10, 15, and 20 ft/sec are used. The relative error functions are presented graphically in Figure 6 for coal and Figure 7 for rock. The absolute error functions are presented in Figures 8 and 9 for coal and Figures 10 and 11 for rock.

Further to the discussion presented in my earlier report, the following equations are utilized to calculate errors in measured slurry concentration based on particle slippage:

$$C_v = \frac{V_s\ C_{iv}}{V_s\ C_{iv} + V_l(1-C_{iv})}$$

where C_v = volumetric concentration of solids delivered (actual concentration)

C_{iv} = volumetric concentration of solids in-situ (measured concentration)

Note that when $V_s = V_l$, the equation reduces to $C_v = C_{iv}$.

To convert volumetric concentrations to gravimetric concentrations the following equation is required:

$$C_w = \frac{C_v \rho_s}{C_v \rho_s + (1-C_v) \rho_l}$$

where C_w = gravimetric concentration of solids delivered.

The corresponding equation is used for the in-situ weight concentration, C_{iw}. Because of particle slippage, the in-situ solids concentration (measured value) always exceeds the actual delivered concentration. This error can be expressed as an absolute error, $(C_{iw} - C_w) \times 100$, or relative error, (absolute error)/C_w .

I have reviewed several projects involving crushed minerals and offer several observations. The particle size distribution for a crushed mineral sample is affected by the nature of the mineral and the method of crushing. Surprisingly, the shape of a particle size distribution curve as shown in Figure 12 is relatively independent of grinding method. The degree of grinding affects the mean particle size, but does little to alter the breadth of the distribution. In terms of Figure 12, further grinding will shift the curve to the left, but will not materially change the slope of the curve.

The slope of the curve is more a function of the mineral than the method of grinding. Thus the slope for crushed coal could be noticeably different than for crushed rock, even if both were crushed simultaneously using the same equipment.

Based on this generalization, it is possible to predict the maximum particle size based on weight mean particle size or any other similar measure, for a given mineral. Table 5 lists the particle size distribution data shown in Figure 12. These data are for a western coal. Based on the identical slope of these curves it can be predicted that the maximum particle size is approximately 5 times the weight mean diameter. In this case, the maximum particle size is defined as the size for which 2 wt % of a sample is retained (98 % of the sample passes the screen).

Thus the mean diameter given in Table 4 can be multiplied by 5 to convert each of them to maximum particle diameter. The factor of 5 could be somewhat different for other coals. It is quite likely that the factor would be different for rock. Grinding data on the samples to be used at the HTRF would be required to better define the factor between mean particle diameter and maximum particle diameter.

I will review the report you mailed to me and will contact you shortly regarding the problem of entrained air at the HTRF.

Sincerely,

George Fouska

TABLE 4

PARTICLE SIZE WHICH YIELDS 1 % AND 2 % ERROR IN SLURRY CONCENTRATION

Measured Slurry Conc.,wt%	Liquid Velocity ft/sec	Mean Particle Diameter, mm.* 1% rel. error coal	1% rel. error rock	2% rel. error coal	2% rel. error rock	1% abs. error coal	1% abs. error rock	2% abs. error coal	2% abs. error rock
10	5	0.37	0.15	0.63	0.24	3.32	1.02	9.0	2.35
	10	0.63	0.24	1.17	0.41	9.0	2.40	>10	8.00
	15	0.88	0.33	1.78	0.61	>10	4.80	>10	>10
	20	1.15	0.41	2.53	0.82	>10	8.05	>10	>10
20	5	0.40	0.16	0.68	0.26	1.70	0.57	3.85	1.15
	10	0.69	0.26	1.32	0.46	3.90	1.15	>10	2.75
	15	0.99	0.36	2.05	0.68	7.30	1.94	>10	5.50
	20	1.32	0.46	2.92	0.93	>10	2.80	>10	9.00
30	5	0.44	0.18	0.77	0.29	1.24	0.44	2.67	0.85
	10	0.77	0.29	1.50	0.52	2.70	0.87	7.30	1.95
	15	1.12	0.40	2.40	0.78	4.80	1.38	>10	3.60
	20	1.51	0.52	3.47	1.06	7.30	1.95	>10	5.60
40	5	0.49	0.20	0.88	0.33	1.08	0.39	2.26	0.74
	10	0.88	0.33	1.78	0.60	2.30	0.75	5.85	1.63
	15	1.31	0.46	2.90	0.90	3.88	1.15	>10	2.70
	20	1.78	0.61	4.28	1.26	5.90	1.66	>10	4.70
50	5	0.57	0.22	1.04	0.37	1.04	0.37	2.12	0.71
	10	1.06	0.38	2.20	0.71	2.20	0.71	5.40	1.53
	15	1.58	0.55	3.70	1.10	3.70	1.10	10.0	2.60
	20	2.22	0.73	5.60	1.35	5.60	1.55	>10	4.30

* Relative error: $((C_{iw} - C_w)/C_w) \times 100$

Absolute error: $(C_{iw} - C_w) \times 100$

TABLE 5

TYPICAL PARTICLE SIZE DISTRIBUTION FOR CRUSHED WESTERN COAL

Tyler Mesh Size	Coal C* Wt% retained	Coal C* Cumulative Wt% retained	Coal D* Wt% retained	Coal D* Cumulative Wt% retained
6	0.59	0.59	0.91	0.91
8	0.81	1.40	1.13	2.04
14	3.16	4.56	3.80	5.84
20	3.84	8.40	6.78	12.62
28	5.01	13.41	8.69	21.31
35	8.28	21.69	14.41	35.72
48	10.49	32.18	13.33	49.05
65	12.85	45.03	11.77	60.82
100	12.88	57.91	9.39	70.21
150	8.81	66.72	5.94	76.15
200	9.52	76.24	7.56	83.71
270	5.31	81.55	3.57	87.28
325	3.22	84.77	0.95	88.23
pan	15.22	99.99	11.77	100.00

weight mean diameter, mm	0.338	0.451
d_{50}, mm	0.184	0.288
particle diameter for which 2% of sample is greater in size, mm	1.80	2.30
size factor	1.80/0.338 = 5.3	2.30/0.451 = 5.1

* Coal crushed in a Cage Paktor mill.

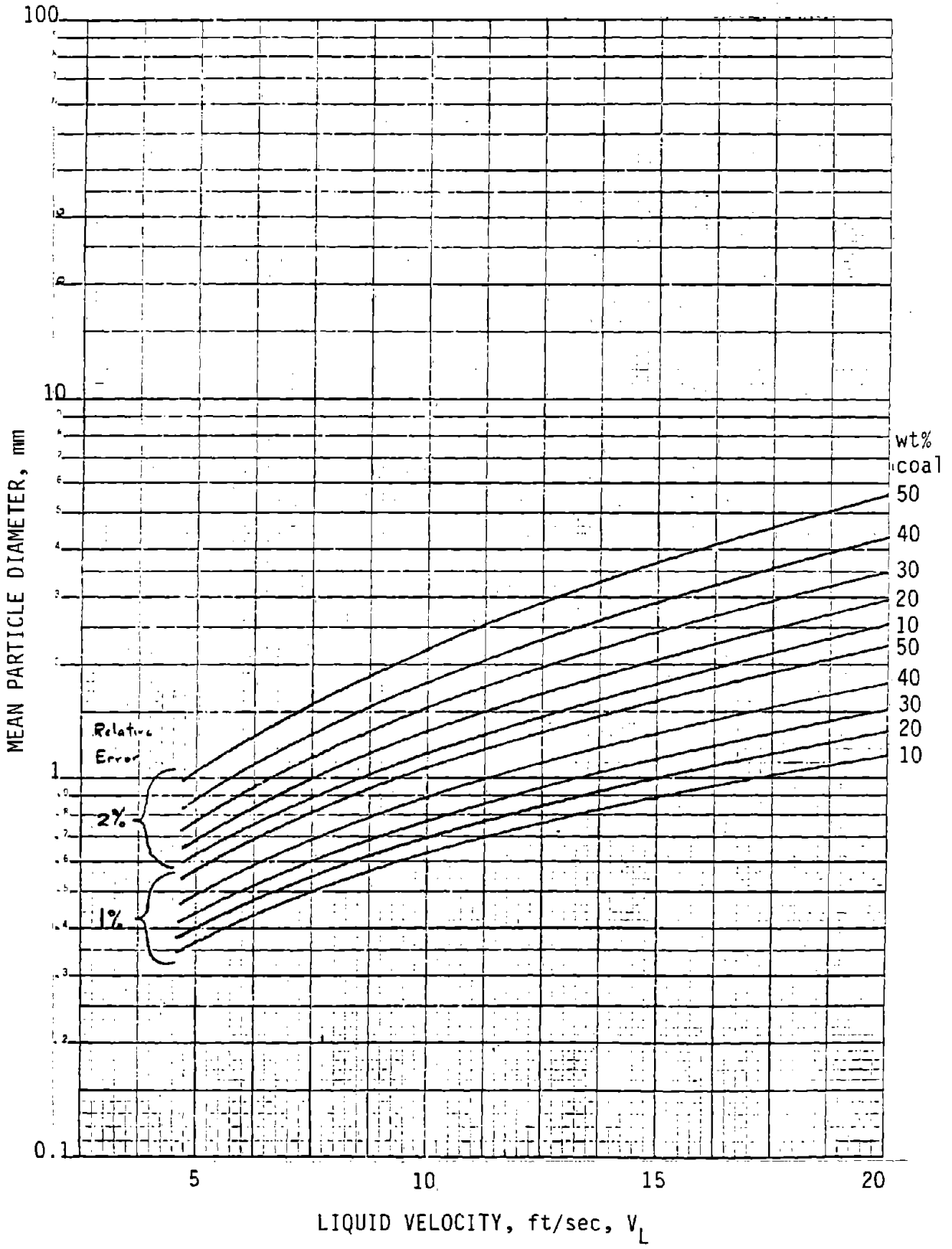

FIGURE 6. - Relative error in measured coal slurry concentration.

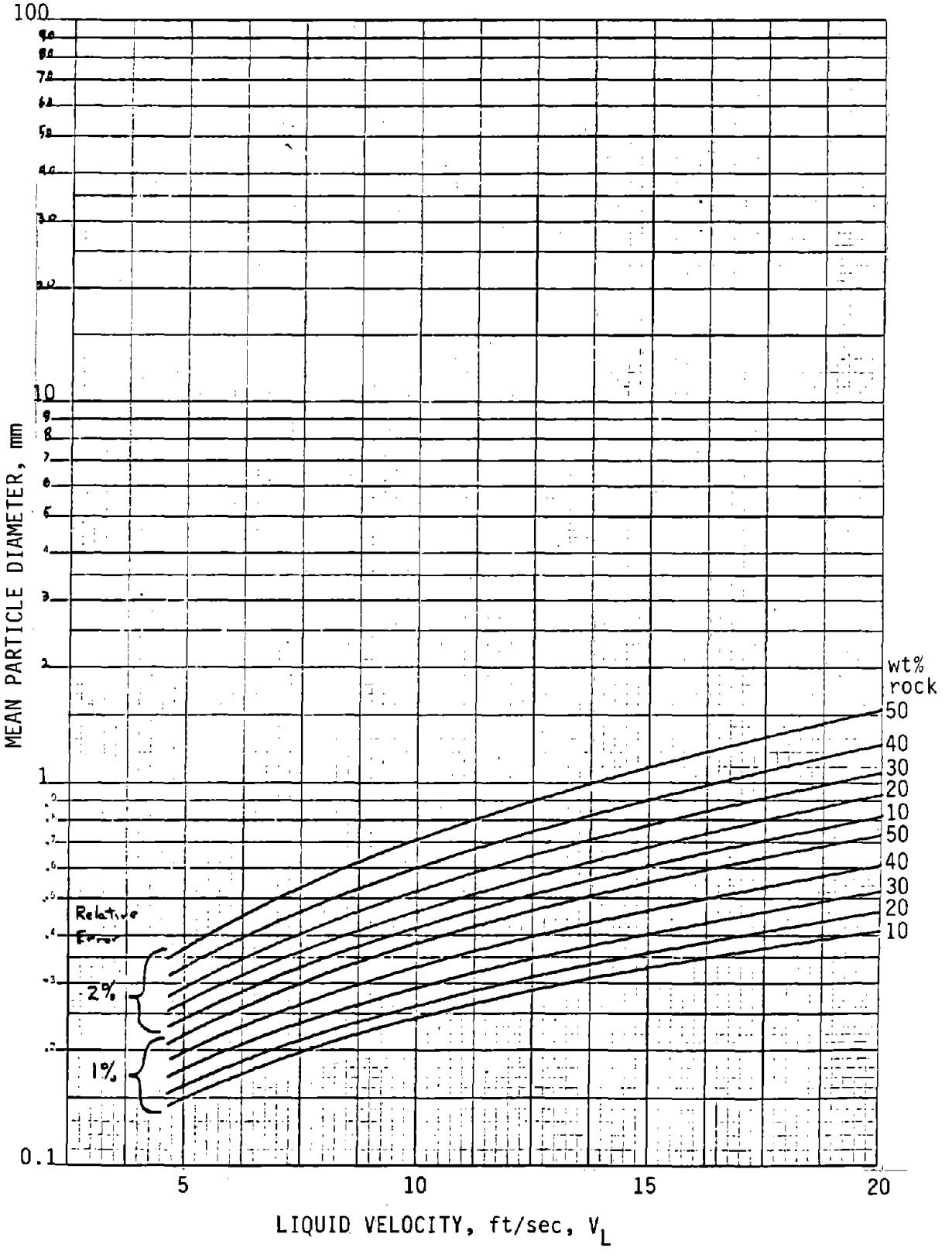

FIGURE 7. - Relative error in measured rock slurry concentration.

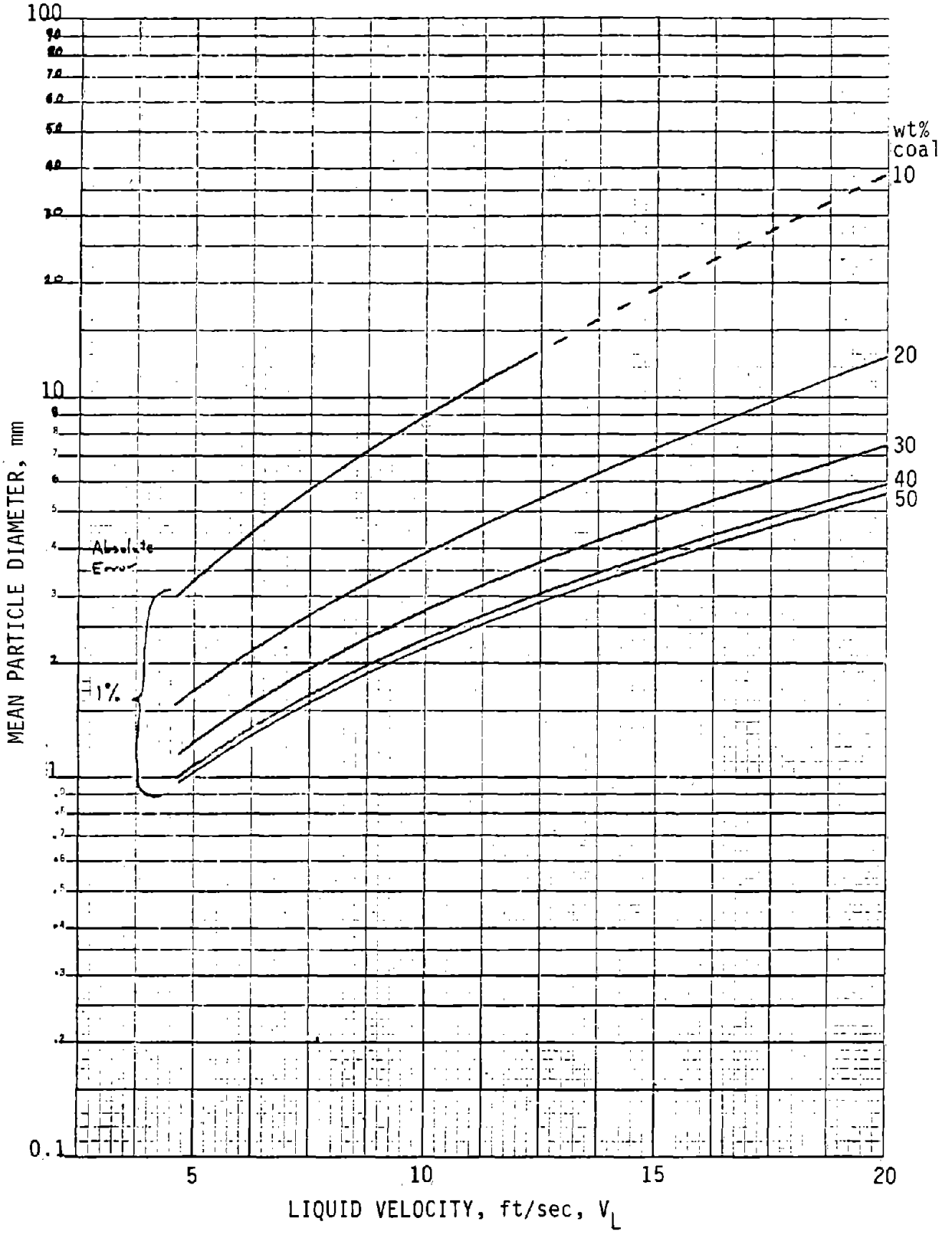

FIGURE 8. - Absolute error in measured coal slurry concentration.

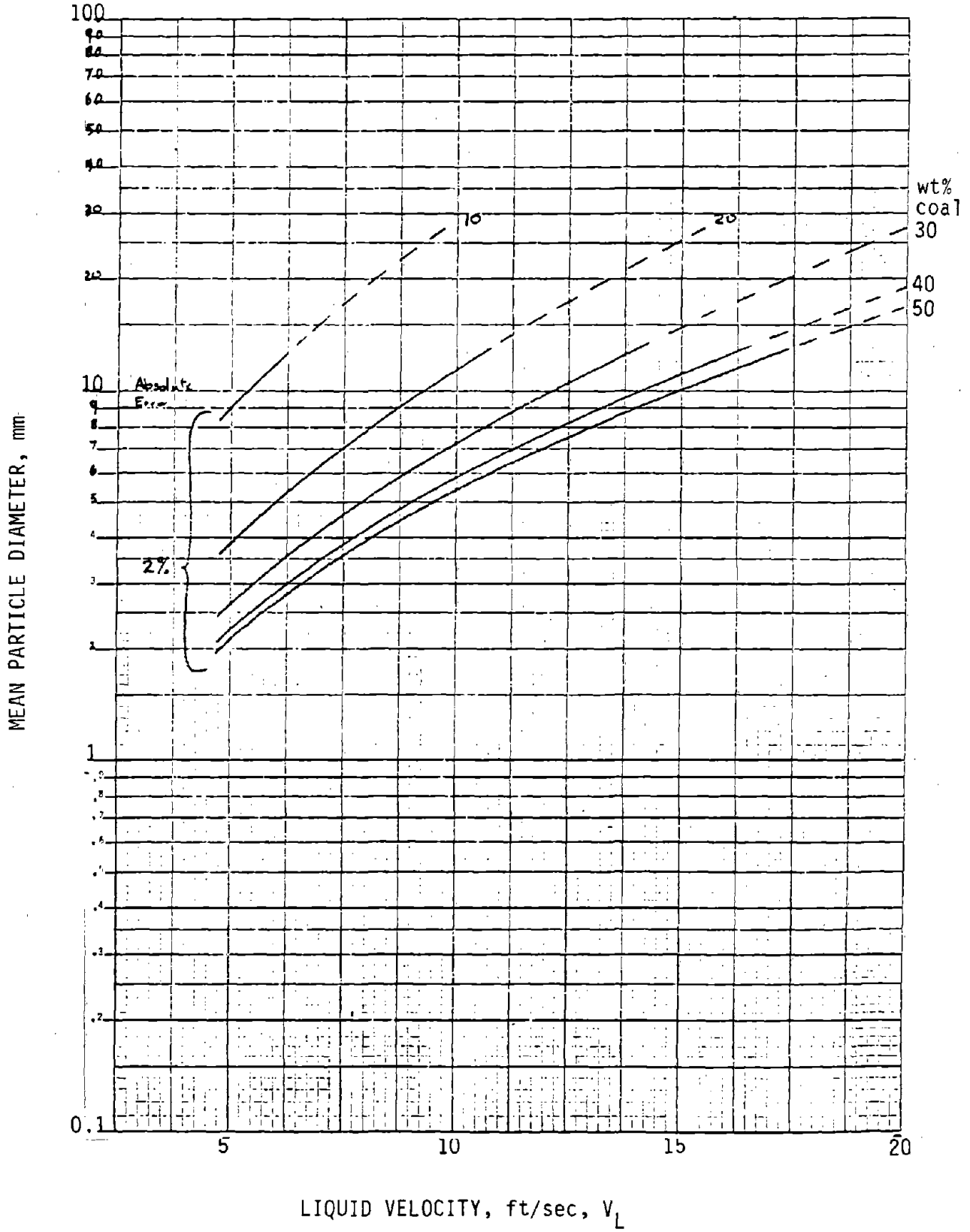

FIGURE 9. - Absolute error in measured coal slurry concentration.

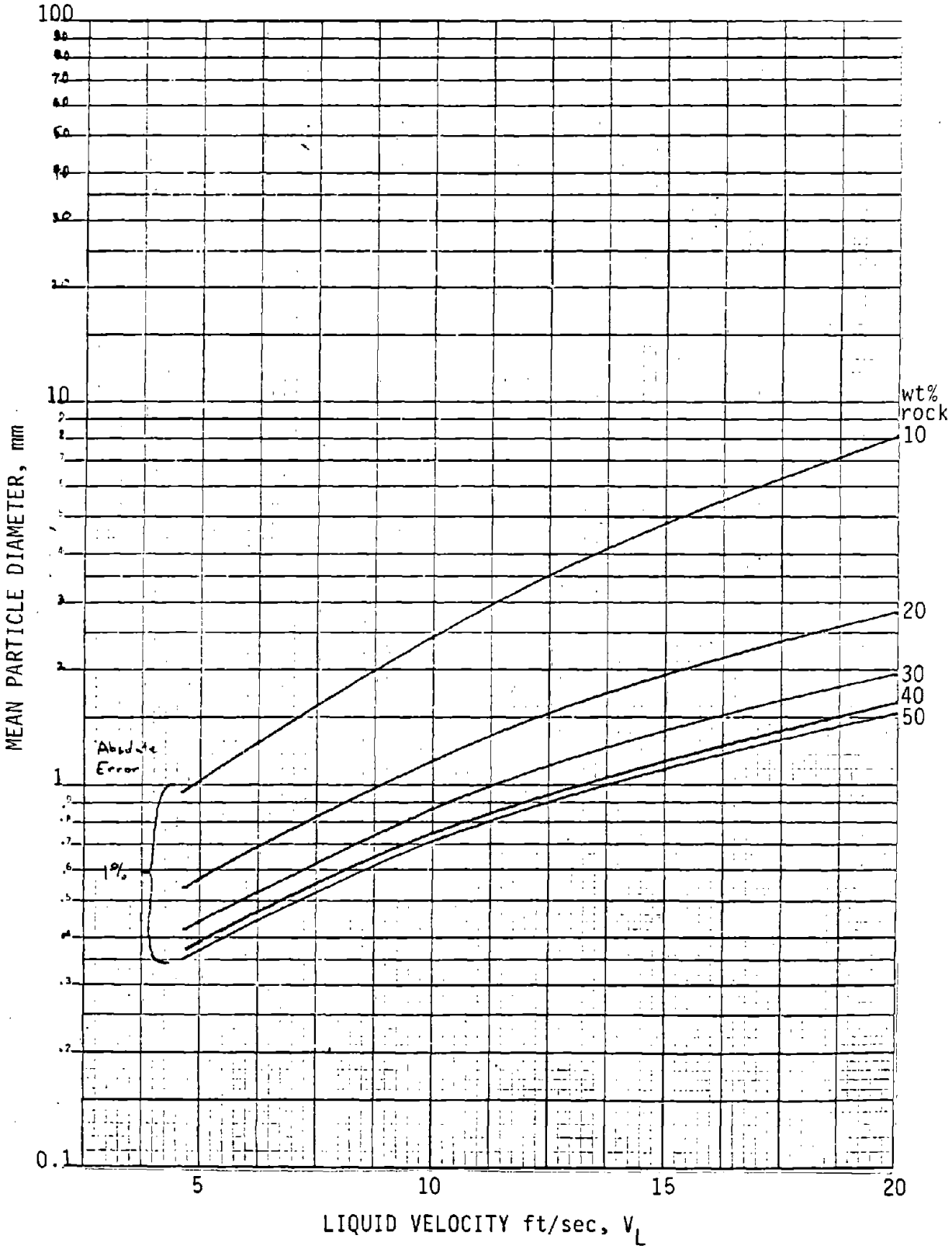

FIGURE 10. - Absolute error in measured rock slurry concentration.

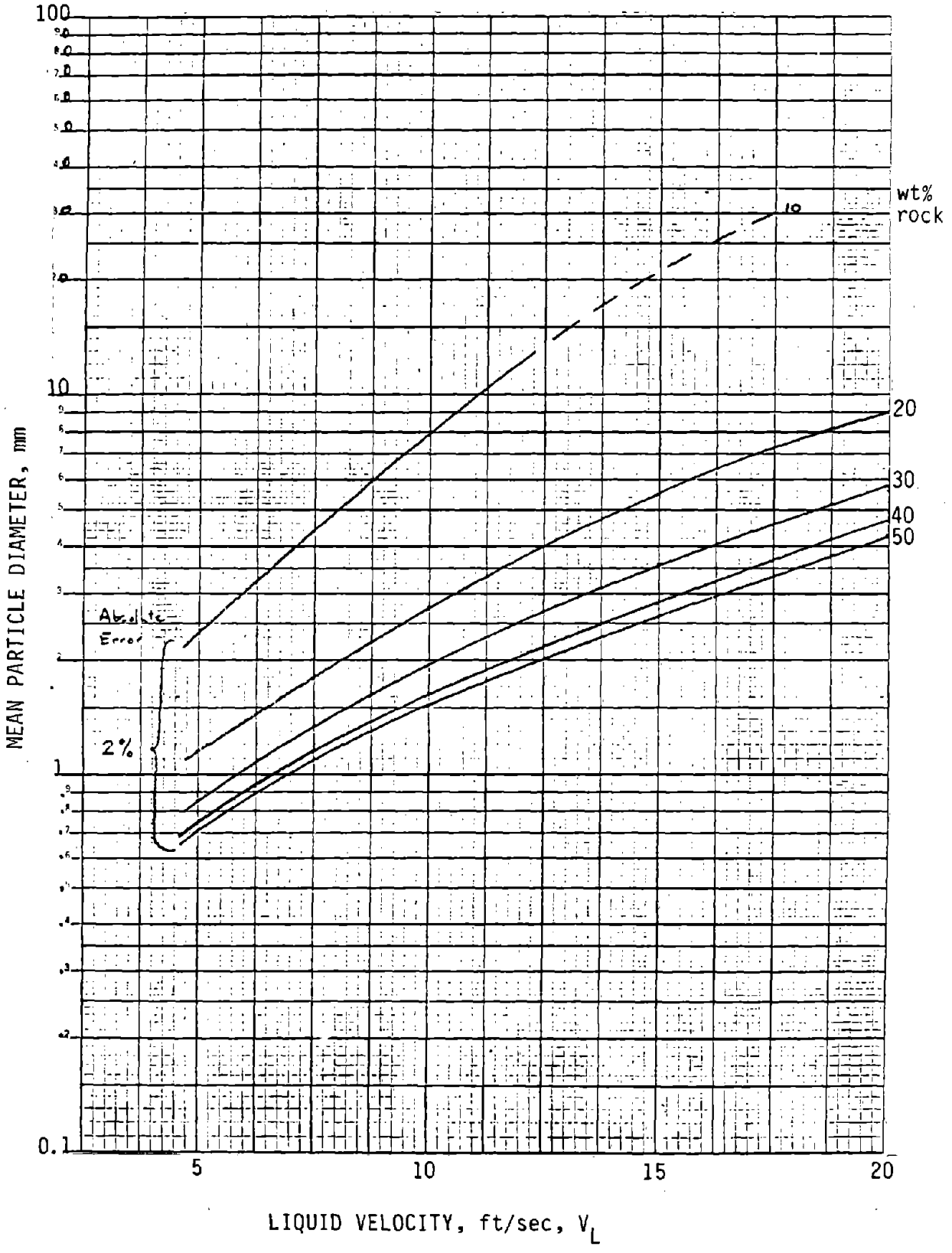

FIGURE 11. - Absolute error in measured rock slurry concentration.

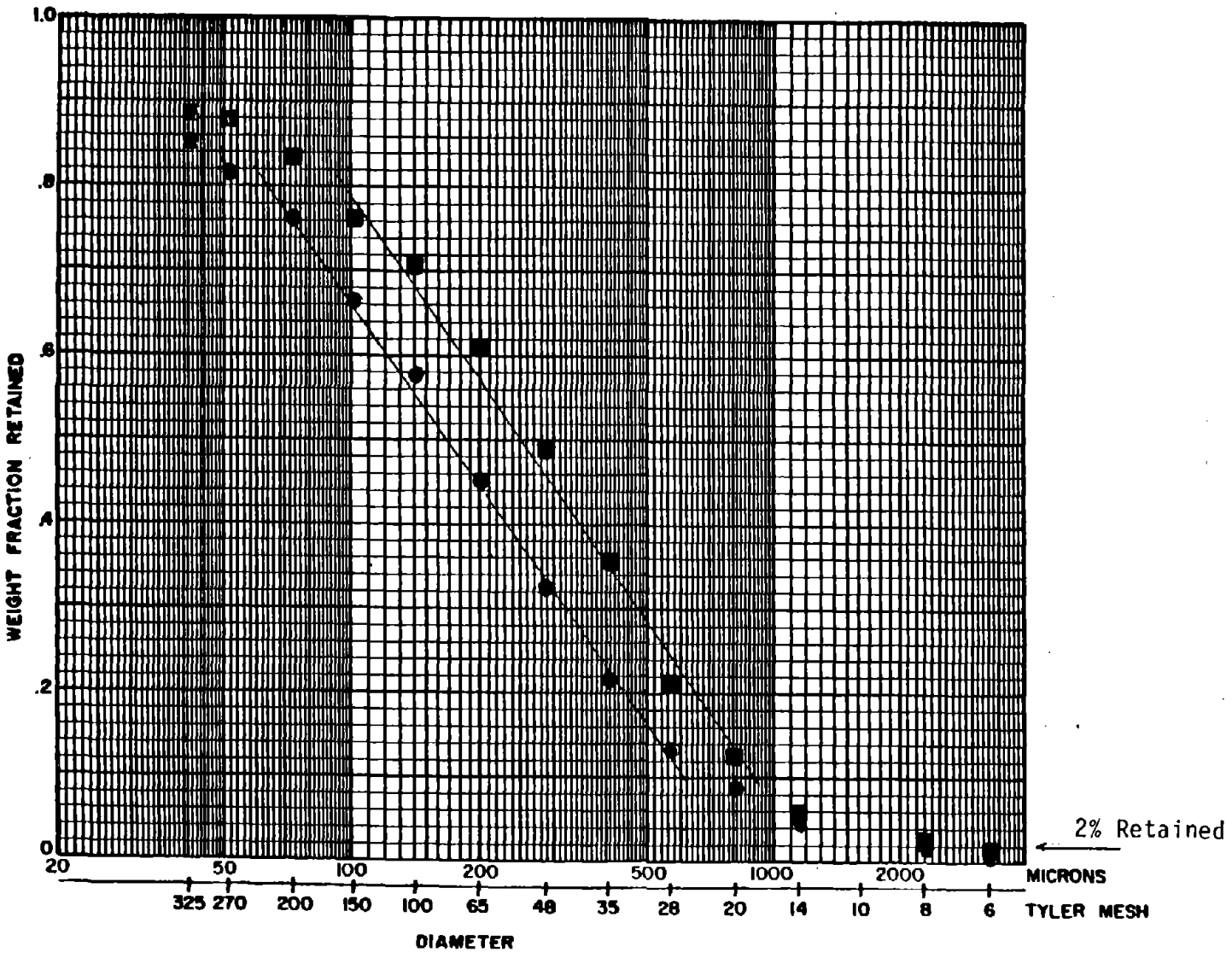

FIGURE 12. - Particle size distributions for crushed coal.